RCA Victor Research Report 7-801-35

SATELLITE CYCLOTRON HARMONIC RESONANCES

I.P. Shkarofsky
T.W. Johnston

MARCH 1965

Fields and Plasma Branch
GODDARD SPACE FLIGHT CENTER
NATIONAL AERONAUTICS AND SPACE ADMINISTRATION
Greenbelt, Maryland

Prepared Under Contract No. NASw-957
with
NASA, Washington, D.C. 20546

RCA VICTOR COMPANY, LTD.
RESEARCH LABORATORIES
MONTREAL, CANADA

THE DIELECTRIC TENSOR NEAR CYCLOTRON HARMONICS

I.P. Shkarofsky

RCA Victor Co. Ltd.
Research Laboratories
Montreal, Canada

- ABSTRACT -

The relativistic expression for the dielectric tensor obtained by Trubnikov is simplified in the very weakly relativistic limit at and near electron cyclotron harmonics. Wave numbers parallel to magnetic field are included, leading to relativistic damping when this wave number is zero and to cyclotron damping when it is sufficiently large. The transition is shown. Collisional damping is neglected. The dielectric elements given here are also applicable to cases of complex ω and real k. This situation arises in Alouette reception since we are concerned with an initial time value problem. For this application, we provide the analytic continuation of a complicated function and investigate the tracks where it is real for complex ω.

Research Laboratories
RCA Victor Company, Ltd.
Montreal, Canada

Satellite Cyclotron Harmonic Resonances

Prepared by I.P. Shkarofsky
I.P. Shkarofsky

Prepared by T.W. Johnston
T.W. Johnston

Approved by
Director, Microwave & Plasma Physics

Approved by
Director of Research

RCA ~~Victor~~ Research Report
7-801-35
March 1965

Prepared under Contract NASw-957 with the National Aeronautics and Space Administration, Washington, D.C. 20546.

PREFACE

This report contains the following, entitled:

General Introduction:

Part 1: The Dielectric Tensor Near Cyclotron Harmonics.

Part 2: The Dispersion of Waves in Cyclotron Harmonic Resonance Regions with Application to the Alouette.

Part 3: Time Decay for Cyclotron Harmonics.

Part 4: Alouette Cyclotron Harmonics: Observations and Results

Appendix: Critique of Theoretical Work on Topside Sounder Resonances

GENERAL INTRODUCTION

I. CYCLOTRON HARMONICS AND THE IONOSPHERE

This report in four parts summarizes the productive theoretical work on the problem of the cyclotron harmonic ringing or resonance in the upper ionosphere as observed by the Alouette swept-frequency topside sounder satellite and also by the fixed frequency S-48 satellite.

The Alouette sounder operates by generating a short ($\sim 100\,\mu$ sec) pulse every 15 milliseconds at some frequency between .5 and 12 Mc, 100 μ sec. after which a receiver is turned on for 14.6 milliseconds to listen for echoes from the upper ionosphere below the sounder. The cyclotron harmonic ringing is observed when the sounder receiver frequency is within say 60 kc of a harmonic of the electron cyclotron frequency(evaluated at the satellite) which is typically .5 to 1 Mc. When a resonance occurs in addition to the usual noise observed immediately after the receiver is turned on, there is a strong signal (at times, for the second harmonic, enough to block the receiver) which dies away with persistance times of from .5 to 2 or more milliseconds. Collisional effects are easily shown to be negligible for these times of interest. For more details see Lockwood (1963)(1964), Warren (1963) Johnston and Nuttall (1964) and Part 4.

The object of this work was to explain and predict the features of this interaction with a view to assessing the suitability of the phenomenon as a magnetic field diagnostic.

Preliminary Considerations

Because the cyclotron harmonic values fitted the satellite value of magnetic field within .5%, the effect was not due to plasma very far from the satellite (a minimum distance of 30 km) where the magnetic field would change by more than .5%. On the other hand this same agreement indicated that if plasma waves were involved the Doppler shift was small so the wave phase velocity had to be at least 200 times the relevant component of the satellite velocity and hence much greater than the electron thermal velocity. The wavelength thus had to be much larger than the electron gyro-radius or Debye length.

An initial attempt was made to see if the self-consistent field of the electrons could be neglected as in Lockwood's (1963) discussion. The conclusion was reached that the self-consistent field was vital and that self-consistent analysis had to be used. With the present state of theory the only tractable dynamic problem using the collisionless plasma (Vlasov) equation for the velocity distribution function is the perturbation of a uniform medium.

The Alouette problem thus reduced itself to the following: explain the Alouette cyclotron harmonic results using the Vlasov equation in its perturbation form for a uniform plasma.

For those unfamiliar with the Vlasov equation analysis in its perturbation form we give an outline of the basic theory next in this introduction.

Report Layout

The four parts to this report give the analysis and the results.

Part 1: From the basic theory the first requirement is the so-called Vlasov plasma dielectric tensor. This is the subject of Part 1. It proves necessary to obtain the tensor in the relativistic form; the instructive comparison with the nonrelativistic form is also discussed.

Part 2: Having obtained the dielectric tensor the next order of business is the dispersion equation whose roots are vital to the problem: this is the topic of Part 2.

Part 3: We are then in a position to calculate interesting features of the resonant or singular time behaviour done in Part 3, using a fairly new mathematical technique based on "pinches" by poles of integration contours in complex planes, essentially the same as that used by Nuttall (1965).

Part 4: The foregoing parts are highly mathematical and so in Part 4 the essential features and results are indicated with a minimum of mathematics as applied to the Alouette results. Discussions and suggestions for future work and verification of the present results are also presented. There is also a critique of other theoretical work on the problem.

The reading order suggested is the Introduction and perhaps the Basic Theory and Part 4 at first and then, in depth, the Basic Theory section and Parts 1, 2 and 3. While the results and discussion of Part 4 can be understood without the second reading, following the derivation of the results requires the careful second reading.

II. BASIC THEORY

The theoretical problem equivalent to the Alouette situation is the following: "A certain electromagnetic source in a warm uniform plasma runs for some time and then is turned off. What is the electric field afterward as a function of time and space? More particularly, how does the largest-lived part of field vary in the vicinity of the source as seen by a slowly moving (at the satellite velocity) receiver?"

In view of the fact that the phenomena of interest are observed involve local values of electron cyclotron frequency the initial assumptions are those of a uniform infinite plasma and of small perturbations. (The last cannot be correct very near the antenna. The Alouette near field is of order 36/r volts/meter (r in meters)).

The standard technique for this kind of problem of a uniform dispersive medium with some arbitrary source is that of a Green's function or its transformed equivalent obtained from the time-Laplace and space-Fournier transformed Maxwell equations and those for the medium.

The transforms will be distinguished where confusion might arise by their argument, e.g. for electric field $\underset{\sim}{E}(\underset{\sim}{r},t)$ its frequency transform is

$$\underset{\sim}{E}(\underset{\sim}{r},\omega) = \int_0^\infty dt\, e^{i\omega t}\, \underset{\sim}{E}(\underset{\sim}{r},t)$$

and the combined frequency and wave number or plane wave transform is

$$\underset{\sim}{E}(\underset{\sim}{k},\omega) = \int d^3\underset{\sim}{k} \int_0^\infty dt\, e^{i(\omega t - \underset{\sim}{k}\cdot\underset{\sim}{r})}\, \underset{\sim}{E}(\underset{\sim}{r},t)$$

The time and space integrals are thus defined for $I_m \omega > 0$ and Im $\underset{\sim}{k}\cdot\underset{\sim}{r} < 0$ and may require analytic continuation away from the region of validity for the integral definition.

The two relevant Maxwell equations in rationalized M.K.S. units are:

$$\nabla \times \underset{\sim}{E}(\underset{\sim}{r},t) = - \mu_o \frac{\partial \underset{\sim}{H}(\underset{\sim}{r},t)}{\partial t} \tag{1a}$$

$$\nabla \times \underset{\sim}{H}(\underset{\sim}{r},t) = \varepsilon_o \frac{\partial \underset{\sim}{E}(\underset{\sim}{r},t)}{\partial t} + \underset{\sim}{J}(\underset{\sim}{r},t) + \underset{\sim}{J}_e(\underset{\sim}{r},t) \tag{1b}$$

where $\underset{\sim}{J}_e$ is an external current and $\underset{\sim}{J}$ is the plasma convection current.

The Fourier-Laplace transform version of these is

$$+ j\underset{\sim}{k} \times \underset{\sim}{E}(\underset{\sim}{k},\omega) = + j\omega\mu_o \underset{\sim}{H}(\underset{\sim}{k},\omega) + \mu_o \underset{\sim}{H}(\underset{\sim}{k}, t = 0) \tag{2a}$$

$$+ j\underset{\sim}{k} \times \underset{\sim}{H}(\underset{\sim}{k},\omega) = - j\omega\varepsilon_o \underset{\sim}{E}(\underset{\sim}{k},\omega) + \underset{\sim}{J}(k,\omega) + \underset{\sim}{J}_e(k,\omega)$$

$$- \varepsilon_o \underset{\sim}{E}(\underset{\sim}{k},\ t = 0) \tag{2b}$$

The plasma current $\underset{\sim}{J}$ will be given in terms of $\underset{\sim}{E}(\underset{\sim}{k},\omega)$ so eliminating $\underset{\sim}{H}(\underset{\sim}{k},\omega)$ gives

$$- \underset{\sim}{k} \times \underset{\sim}{k} \times \underset{\sim}{E}(\underset{\sim}{k},\omega) - \frac{\omega^2}{c^2}\left(\underset{\sim}{E}(\underset{\sim}{k},\omega) - \frac{j\underset{\sim}{J}(\underset{\sim}{k},\omega)}{\omega\varepsilon_o}\right) \tag{3}$$

$$= j\mu_o \underset{\sim}{k} \times \underset{\sim}{H}(\underset{\sim}{k},\ t = 0) - \frac{j\omega}{c^2} \underset{\sim}{E}(\underset{\sim}{k},\ t = 0) + j\omega\mu_o \underset{\sim}{J}_e(\underset{\sim}{k},\omega)$$

From some plasma equation one can write $\underset{\sim}{J}(\underset{\sim}{k},\omega)$ in terms of $\underset{\sim}{E}(\underset{\sim}{k},\omega)$ and some initial conditions and we will then be able to get a solution for $\underset{\sim}{E}(\underset{\sim}{k},\omega)$. The general nonrelativistic Vlasov plasma solution has been given by Sitenko and Stepanov (1956) and by Bernstein (1958) and the relativistic problem has been discussed by Trubnikov(1958). The relativistic result is

$$f_1(\underset{\sim}{k},\omega,\underset{\sim}{u}) = \frac{1}{\omega_b}\int_{-\infty}^{\phi} d\phi' G\left[f_1(k,t=0,\underset{\sim}{u}') + \frac{e}{m}\underset{\sim}{E}(\underset{\sim}{k},\omega)\cdot\frac{u'_4\partial f_0(u')}{c\partial\underset{\sim}{u}'}\right] \quad (4)$$

where $f_1(\underset{\sim}{k},\omega,\underset{\sim}{u})$ is the distribution function plane wave transform and

$f_1(\underset{\sim}{k}, t = 0, \underset{\sim}{u})$ is the spatial Fournier transform at time $t = 0$

$f_0(\underset{\sim}{u})$ is the undisturbed distribution as a function of

$\underset{\sim}{u}$ which is the spatial part of the four-velocity $v(1 - v^2/c^2)^{-\frac{1}{2}}$ while

u_4 component is $c(1 - v^2/c^2)^{-\frac{1}{2}} = c(1 + u^2/c^2)^{1/2}$

$\omega_b = eB/m$ where m is the rest mass

$$G = \exp\left[-\int_{\phi'}^{\phi} d\phi\left(i\left(\frac{\underset{\sim}{k}\cdot\underset{\sim}{u} - u_4\omega/c}{\omega_b}\right)\right)\right]$$

$$\underset{\sim}{u} = u_\perp(\underset{\sim}{i}_x\cos\phi + \underset{\sim}{i}_y\sin\phi) + u_z\underset{\sim}{i}_z$$

For the nonrelativistic case $\underset{\sim}{u}$, the four velocity, becomes $\underset{\sim}{v}$ the usual velocity much less than c and u_4 becomes 1.

The plasma current transform is given by

$$\underset{\sim}{J}(\underset{\sim}{k},\omega) = -e\int d^3u\,\frac{\underset{\sim}{u}c}{u_4} f_1(\underset{\sim}{k},\omega,\underset{\sim}{u})$$

$$= \underset{\sim}{J}_p(\underset{\sim}{k},\omega) - \frac{\underset{\sim}{J}_S}{j\omega}(\underset{\sim}{k}, t = 0) \quad (5)$$

where $J_S(\underset{\sim}{k}, t = 0)$ has the special initial terms $f_1(\underset{\sim}{k}, t = 0, \underset{\sim}{u}')$ and

$J_p(\underset{\sim}{k},\omega)$ the characteristic plasma term with $\underset{\sim}{E}_4(\underset{\sim}{k},\omega)\partial f/\partial \underset{\sim}{u}$. It proves convenient to group $\underset{\sim}{J}_p(\underset{\sim}{k},\omega)$ with the displacement current term to give

$$-\frac{\omega^2}{c^2}\left[\underset{\sim}{E}(\underset{\sim}{k},\omega) - j\frac{\underset{\sim}{J}_p(\underset{\sim}{k},\omega)}{\omega\varepsilon_o}\right] = -\frac{\omega^2}{c^2}\left[\underline{\underline{I}} + \frac{je^2}{\omega m\varepsilon_o}\int d^3u\,\frac{\underset{\sim}{u}c}{u_4}\,\frac{1}{\omega_b}\int_{-\infty} d\phi' G\,\underline{\underline{E}}\frac{\mu_4}{c}\frac{\partial f}{\partial \underset{\sim}{u}'}\right]\cdot\underset{\sim}{E}(k,\omega) \tag{6}$$

The term in square brackets is the plasma dielectric coefficient

$$\underline{\underline{\varepsilon}}(\underset{\sim}{k},\omega) = \underline{\underline{I}} + \frac{je^2}{\omega m\varepsilon_o}\int d^3u\,\frac{\underset{\sim}{u}}{\omega b}\,\frac{1}{\omega_b}\int_{-\infty}^{\phi} d\phi' G\,\frac{\partial f}{\partial \underset{\sim}{u}'} \tag{7}$$

The dependence on k,ω comes from G as well as the explicit ω term. The wave equation thus becomes

$$-\underset{\sim}{k}\times\underset{\sim}{k}\times\underset{\sim}{E}(\underset{\sim}{k},\omega) - \frac{\omega^2}{c^2}\,\underline{\underline{\varepsilon}}(\underset{\sim}{k},\omega)\cdot\underset{\sim}{E}(\underset{\sim}{k},\omega) = \underline{\underline{R}}(k,\omega)\cdot\underset{\sim}{E}(\underset{\sim}{k},\omega)/c^2 \tag{8}$$

or

$$\left(k^2\underline{\underline{I}} - \underset{\sim}{k}\,\underset{\sim}{k} - \frac{\omega^2}{c^2}\,\underline{\underline{\varepsilon}}(k,\omega)\right)\cdot\underset{\sim}{E}(\underset{\sim}{k},\omega)$$

$$= -j\frac{\omega}{c^2}\underset{\sim}{E}(\underset{\sim}{k},t=0) + j\mu_o\underset{\sim}{k}\times\underset{\sim}{H}(\underset{\sim}{k},t=0) + \frac{\underset{\sim}{J}(k,t=0)}{\varepsilon_o c^2}$$

$$+\frac{j\omega}{c^2\varepsilon_o}\,\underset{\sim}{J}_e(\underset{\sim}{k},\omega) = \underset{\sim}{S}/c^2$$

Thus $$\underline{\underline{R}}(\underset{\sim}{k},\omega)\cdot\underset{\sim}{E}(k,\omega) = \underset{\sim}{S} \tag{9}$$

Some controversy exists among Vlasov theorists as to the results and limits of permissible initial velocity distribution function perturbations. For a source problem, one avoids this by starting with only the

external source and allowing the distribution function to emerge naturally, that is $\underset{\sim}{S}$ is taken to be $j\omega\ \underset{\sim}{J}_e(\underset{\sim}{k},\omega)/\varepsilon_0$.

The formal solution for $\underset{\sim}{E}\ (\underset{\sim}{k},\omega)$ is then

$$\underset{\sim}{E}(\underset{\sim}{k},\omega) = \underset{\approx}{R}^{-1}(\underset{\sim}{k},\omega) \cdot \underset{\sim}{S}(\underset{\sim}{k},\omega) = \frac{j\omega}{\varepsilon_0}\ \underset{\approx}{R}^{-1}(k,\omega) \cdot \underset{\sim}{J}_e(\underset{\sim}{k},\omega) \tag{10}$$

where $$\underset{\approx}{R}^{-1}(k,\omega) = \frac{\underset{\approx}{R}_2(\underset{\sim}{k},\omega)}{R_3(\underset{\sim}{k},\omega)} \tag{11}$$

$\underset{\approx}{R}_2(\underset{\sim}{k},\omega)$ is the transpose of the cofactor matrix of $\underset{\approx}{R}(\underset{\sim}{k},\omega)$ and $R_3(\underset{\sim}{k},\omega)$ is the determinant of $\underset{\approx}{R}(\underset{\sim}{k},\omega)$. The subscripts are reminders of the order of the products in $\underset{\approx}{R}_2(\underset{\sim}{k},\omega)$ and $R_3(\underset{\sim}{k},\omega)$.

Since the $\underset{\approx}{R}$ elements have dimensions of frequency squared, it is often convenient to define a dimensionless function D such that

$$D = \omega^{-6} R_3 \tag{12}$$

One can perhaps appreciate the result more readily if one realized that the $\underset{\approx}{R}^{-1}(\underset{\sim}{k},\omega)$ is the Laplace—Fourier—transformed tensor Green's function $\underset{\approx}{G}'\ (\underset{\sim}{r},t)$ for the problem. This is evident since we have the following result on inverting the transforms of the equation for $\underset{\sim}{E}\ (\underset{\sim}{k},\omega)$ and using the convolution theorem for the $\underset{\approx}{R}^{-1}(\underset{\sim}{k},\omega) \cdot \underset{\sim}{S}(k,\omega)$ product:

$$\underset{\sim}{E}(\underset{\sim}{r},t) = \int_0^t dt' \int_V d^3r'\, \underset{\approx}{G}'(\underset{\sim}{r}-\underset{\sim}{r}',\ t-t') \cdot \underset{\sim}{S}(\underset{\sim}{r}',t')$$

where $\underset{\approx}{G}'(\underset{\sim}{r},t)$ is the transform inverse of $\underset{\approx}{R}^{-1}(k,\omega)$ and is evidently

the Green's function.

The $\underset{\approx}{\underset{\approx}{E}}$ Green's function or its transform evidently gives one the option of inserting arbitrary sources, providing the integration can be done.

If the behaviour of the antenna impedance is a factor (as it in practice) it is convenient to use the time-Laplace transformed Green's function $\underset{\approx}{\underset{\approx}{G}}(\underset{\sim}{r},\omega)$ since the impedance is given in terms of ω. The equivalent equation is as follows:

$$\underset{\sim}{E}(\underset{\sim}{r},\omega) = - \int d^3r \, \underset{\approx}{\underset{\approx}{G}}'(\underset{\sim}{r}-\underset{\sim}{r}', \omega) \cdot \underset{\sim}{S}(\underset{\sim}{r}',\omega)$$

Failing a more general solution of the problem, simply studying the form of $\underset{\approx}{\underset{\approx}{G}}'$ or $\underset{\approx}{\underset{\approx}{R}}$ is worth while.

Before discussing the behaviour of $\underset{\approx}{\underset{\approx}{G}}'$ or $\underset{\approx}{\underset{\approx}{R}}$ there is one question to settle.

An advantage of calculating $\underset{\approx}{\underset{\approx}{G}}(\underset{\sim}{r},\omega)$ or $\underset{\approx}{\underset{\approx}{G}}(\underset{\sim}{k},\omega)$ is that one can see when a singularity appears whose frequency is unlikely to be affected by the transmitter-receiver impedance (in contrast with a simple pole which is so affected). However the actual problem can only be solved by including in self-consistent manner the transmitter receiver impedance and the boundary and current field relations on and in the antenna as is done for free space antenna, well described by King (1956). In view of the intractability of the plasma problem this is far beyond the reach of current theory.

The problem is therefore limited to considering a source with a plausible specified current or charge distribution for excitation

(equivalent to a zero impedance source) with no boundary restriction and an ideal non-disturbing electric field measuring device (infinite impedance) as receiver (an ideal current density sensor (zero impedance) could also be considered). This procedure is, of course, inconsistent and unrealistic but is the only procedure likely to produce any answer, considering the present state of theory and the difficulty of the problem.

For the Maxwellian plasma the $\underset{\sim}{R}(\underset{\sim}{k},\omega)$ elements have no singularities in the finite complex plane of their argument in the region we explore. In general the only other singularities of $E(\underset{\sim}{k},\omega)$ for finite $\underset{\sim}{k},\omega$ values will be the zeros of $R_3(\underset{\sim}{k},\omega)$ i.e. of D. Setting D equal to zero is the dispersion equation and D is called the dispersion function. From it one can determine the characteristic behaviour of the medium. The study of the dispersion equation is the theme of Part 2.

The zeros of $D(\underset{\sim}{k},\omega)$ do not by themselves single out any particular frequency for attention, but relate ω to $\underset{\sim}{k}$. To obtain some particularly significant $\underset{\sim}{k}\omega$ combination an auxiliary condition is needed, indicating the likelihood of singular behaviour. The pinching or coalescing of singularities across the integration hypersurface in complex $\underset{\sim}{k}\omega$ (6-dimensional) space results in singularities which give the anticipated singular behaviour. [The Bromwich inversion line is on one side of the singularities for Laplace transform inversion and cannot be pinched. The k-pinch however introduces a different ω singularity from the usual simple poles in the ω plane.]

If one considers the $\underset{\sim}{k}$-derivative of $D(\underset{\sim}{k},\omega)=0$ equation the result is

$$\frac{\partial}{\partial \underset{\sim}{k}} D(\underset{\sim}{k},\omega) = 0 = \frac{\partial \omega}{\partial \underset{\sim}{k}} \frac{\partial D(\underset{\sim}{k},\omega)}{\partial \omega} + \frac{\partial D(\underset{\sim}{k},\omega)}{\partial \underset{\sim}{k}}$$

Now the conditions that two roots may coalesce is (part 3)

$$\frac{\partial D}{\partial \underset{\sim}{k}} (\underset{\sim}{k},\omega) = 0$$

So long as $\partial D(\underset{\sim}{k},\omega)/\partial\omega$ itself is not zero the singularities in the Green's function can occur at points where the group velocity is zero, i.e.

$$\frac{\partial \omega}{\partial \underset{\sim}{k}} = 0$$

For an observer moving at a nonrelativistic velocity $\underset{\sim}{v}$ the $\partial\omega/\partial\underset{\sim}{k} = 0$ condition in his frame of reference becomes

$$\frac{\partial \omega}{\partial \underset{\sim}{k}} - \underset{\sim}{V} = 0$$

in the plasma frame so the wave packet keeps step with the observer.

Hence one is led to examine the dispersion equation for these points of zero relative group velocity. [Strictly speaking, the concept of $\partial\omega/\partial\underset{\sim}{k}$ playing the role of the velocity of a wave pocket fails as other terms become more important, so in the vicinity of $\partial\omega/\partial\underset{\sim}{k} = 0$ the name "group velocity" is inappropriate, but is more convenient than inventing another title for $\partial\omega/\underset{\sim}{k}$.]

Since the satellite velocity is much less ($\sim 1/16$) than the electron thermal velocity and is very much less ($\sim 3\times10^{-5}$)than the velocity of light, a good beginning is to consider the points where the group velocity is low and can be equal to the satellite velocity. So far the approach is quite general. To proceed further one must get down to

particular dispersion equations and look for the interesting $\omega\underset{\sim}{k}$ combinations. These will be discussed in the part on Plasma Dispersion Equations (Part 2). There are collective plasma zero group velocity frequencies (i.e. explicitly dependent on electron density) at the plasma frequency (ω_p), near the transverse resonance frequency $(\omega_p^2 + \omega_b^2)^{\frac{1}{2}}$ (covered by Nuttall (1965)) and the left and right cut-off frequencies $\left(\left(\omega_p^2 + \frac{\omega_b^2}{4}\right)^{\frac{1}{2}} \pm \frac{\omega_b}{2}\right.$ discussed by Sturrock (1965)$\left.\right)$. These do not concern us directly here except for the connection (observed and very plausible from theory) between the transverse resonance frequency effect and that at twice the gyro frequency.

The behaviour near the cyclotron harmonic frequencies is much more difficult to follow and seems impossible to resolve without the relativistic formulation.

The general rationale for the layout of the report can be seen to follow from this outline of the basic theory. The elements of the $\underset{\approx}{R}(\underset{\sim}{k},\omega)$ tensor and its inverse are products of $\underset{\sim}{k}c$ and the elements of $\underset{\approx}{\varepsilon}(\underset{\sim}{k},\omega)\omega^2/c^2$. Hence the first step is the study and exposition of the relevant dielectric tensor elements. This one subject of Part 1. The dispersion equation ($R_3(\underset{\sim}{k},\omega) = 0$) is next taken up in Part 2. After a brief introduction (with an illustrative example) Part 3 discusses the pinch method and its application to the pinch of interest for the Alouette cyclotron harmonic. These three parts are fairly mathematical in nature and so Part 4 is a summary of the work without the mathematics, and with more emphasis on physics. It also contains the conclusions and suggestions for future work.

REFERENCES

Bernstein, I.B. (1958) - Phys. Rev. 109, 10 (1958).

Johnston, T.W., J. Nuttall (1964) - J. Geophys. Res. 69, 2305 (1964).

King, R.W.P. (1956) - The Theory of Linear Antennas, Harvard University Press (1956)

Lockwood (1963) - Can. J. Phys. 41, 190 (1963).

Lockwood (1965) - Can. J. Phys. 43, 291 (1965).

Nuttall, J. (1965) - Phys. Fluids 8, 286 (1965).

Sitenko, A.G., K.N. Stepanov (1956) - Zh. Exp. Th. Fiz. 31, 642(1956), Soviet Phys. JETP 4, 512 (1957).

Trubnikov, B.A. (1959) - Plasma Physics and the Problem of Controlled Thermonuclear Reactions, Vol. III, p 122 (editor M.A. Leontovich) Pergamon (1959). See also U.S. Atomic Energy Commission Translation AEC-tr-4073.

Warren, E.S. (1963) - Nature 197, 636 (1963).

I. INTRODUCTION

In this report (Part 1), we discuss and simplify the dielectric tensor of a plasma near electron cyclotron harmonics. A relativistic approach has to be used since the difference $\omega - n\omega_b$ (between angular frequency and cyclotron harmonic frequency) is less than v_t^2/c^2 in many wave number regions of interest. We restrict ourselves to small transverse wave numbers i.e. we take $\lambda \equiv k_\perp^2 v_t^2/\omega_b^2$ less than one. At first we consider general values for $k_{||}$ (wave number parallel to magnetic field) but later we consider only the region $k_{||}\, c^2/v_t\omega \ll 1$. It will be shown in Part 2 that with such small values of $k_{||}$, we can match satellite velocity to group velocity along the magnetic field.

A relativistic expression for the dielectric tensor ε of a plasma was obtained by Trubnikov (1959) which will not be rederived here. This expression is exceedingly complicated and simplification is necessary for further analysis of dispersion equations. For $k_{||} = 0$, Dnestrovskii et al (1964) have obtained such a simplification. Original contributions in this report are the inclusion of $k_{||}$ in the analysis and the derivation of the dielectric tensor elements for complex ω and real k rather than vice versa. The latter extension requires the analytic continuation of a complicated function.

In the analysis, we neglect collisional damping since it is negligible for the times of interest during which harmonics effects are measured on the Alouette.

II. GENERAL VALUES OF $k_{\parallel}$

Trubnikov's equation for the elements $\varepsilon_{\alpha\beta}$ of the tensor $\underset{\sim}{\varepsilon}$ is

$$\varepsilon_{\alpha\beta} - \delta_{\alpha\beta} = \frac{i\omega_p^2}{\omega\omega_b} \frac{c^4}{v_t^4 K_2\left(\frac{c^2}{v_t^2}\right)} \int_0^\infty d\xi \left\{ \frac{K_2(\sqrt{R})}{R} T_{\alpha\beta}^{(1)} - \frac{K_3(\sqrt{R})}{R^{3/2}} T_{\alpha\beta}^{(2)} \right\} \quad (1a)$$

where

$$T_{\alpha\beta}^{(1)} = \begin{pmatrix} \cos\xi & -\sin\xi & 0 \\ \sin\xi & \cos\xi & 0 \\ 0 & 0 & 1 \end{pmatrix} \quad (1b)$$

$$T_{\alpha\beta}^{(2)} = \frac{c^2}{\omega_b^2} \begin{pmatrix} k_\perp^2 \sin^2\xi & -k_\perp^2 \sin\xi(1-\cos\xi) & k_\perp k_{\parallel} \xi \sin\xi \\ k_\perp^2 \sin\xi(1-\cos\xi) & -k_\perp^2(1-\cos\xi)^2 & k_\perp k_{\parallel}\xi(1-\cos\xi) \\ k_\perp k_{\parallel}\xi \sin\xi & -k_\perp k_{\parallel}\xi(1-\cos\xi) & k_{\parallel}^2 \xi^2 \end{pmatrix} \quad (1c)$$

K_ν is a MacDonald function of order ν.

$$R = \left(\frac{c^2}{v_t^2} - i\xi\frac{\omega}{\omega_b}\right)^2 + 2\left(\frac{k_\perp c}{\omega_b}\right)^2 (1-\cos\xi) + \frac{k_{\parallel}^2 c^2 \xi^2}{\omega_b^2} \quad (1d)$$

$\omega_p = \sqrt{n_e e^2/\varepsilon_o m}$ is the plasma frequency, $\omega_b = eB/m$ is the angular cyclotron frequency, $v_t = \sqrt{\kappa T/m}$ is the thermal velocity and i, n_e, e, ε_o, m, B, c, κ, T and ω have their usual significance. The wave numbers perpendicular and parallel to the magnetic field are denoted as $k_\perp$ and $k_{\parallel}$ and taken along the x and z directions respectively. In the following, we denote by $\mu = c^2/v_t^2$, the square of the ratio of light to thermal velocity and let this be very large.

In the very weakly relativistic case ($\mu \gg 1$), the argument of K_ν is large, and the asymptotic expression

$$K_\nu(x) = \sqrt{\frac{\pi}{2x}}\, e^{-x}$$

applies. Thus we find

$$\varepsilon_{\alpha\beta} - \delta_{\alpha\beta} = \frac{i\omega_p^2}{\omega\omega_b}\,\mu^{5/2}\, e^{\mu} \int_0^\infty \frac{d\xi e^{-R^{1/2}}}{R^{5/4}}\, T_{\alpha\beta}^{(3)} \qquad (2a)$$

where $T_{\alpha\beta}^{(3)} =$

$$\begin{pmatrix} \cos\xi - \frac{k_\perp^2 c^2}{\omega_b^2\sqrt{R}}\sin^2\xi & -\sin\xi + \frac{k_\perp^2 c^2}{\omega_b^2\sqrt{R}}\sin\xi(1-\cos\xi) & -\frac{k_\perp k_\parallel c^2}{\omega_b^2\sqrt{R}}\,\xi\,\sin\xi \\ \sin\xi - \frac{k_\perp^2 c^2}{\omega_b^2\sqrt{R}}\sin\xi(1-\cos\xi) & \cos\xi + \frac{k_\perp^2 c^2}{\omega_b^2\sqrt{R}}(1-\cos\xi)^2 & -\frac{k_\perp k_\parallel c^2}{\omega_b^2\sqrt{R}}\,\xi(1-\cos\xi) \\ -\frac{k_\perp k_\parallel c^2}{\omega_b^2\sqrt{R}}\sin\xi & \frac{k_\perp k_\parallel c^2}{\omega_b^2\sqrt{R}}\,\xi(1-\cos\xi) & 1 - \frac{k_\parallel^2 c^2}{\omega_b^2\sqrt{R}}\xi^2 \end{pmatrix} \qquad (2b)$$

Next we simplify the expression for R by assuming $(k_\perp v_t/\omega_b)^2 \lesssim 1$, so that

$$\sqrt{R} = \mu\left[\left(1 - \frac{i\xi\omega}{\mu\omega_b}\right)^2 + \frac{k_\parallel^2 v_t^2}{\mu\omega_b^2}\,\xi^2\right]^{\frac{1}{2}} + \Lambda(1-\cos\xi) \qquad (3a)$$

where

$$\Lambda \equiv \frac{k_\perp^2 v_t^2}{\omega_b^2}\left[\left(1 - \frac{i\xi\omega}{\mu\omega_b}\right)^2 + \frac{k_{\parallel}^2 v_t^2 \xi^2}{\mu\omega_b^2}\right]^{-\frac{1}{2}} \tag{3b}$$

The above expression for $\sqrt{R}$ has to be used in the exponent. However in the $T_{\alpha\beta}^{(3)}$ matrix and in the $R^{5/4}$ factor, we can omit the $\Lambda(1 - \cos\xi)$ part of $\sqrt{R}$. Thus we see that $k_\perp^2 c^2/\omega_b^2\sqrt{R} \approx \Lambda$. A point to note is that the $k_{\parallel}$ part of Λ is multiplied by ξ^2 and ξ^2 varies from 0 to ∞, so that care must be exercised in any approximation for $k_{\parallel}$. At the moment, we leave the range of $k_{\parallel}$ arbitrary.

At this stage we can introduce the familiar modified Bessel function (I_n) expansion:

$$\exp(\Lambda \cos\xi) = \sum_{-\infty}^{\infty} I_n(\Lambda) \exp(-in\xi) \tag{4a}$$

Using Eq. (4a) we note that:

$$\sin\xi \exp(\Lambda\cos\xi) = -\frac{1}{\Lambda}\frac{d}{d\xi}\exp(\Lambda\cos\xi) = \sum \frac{in}{\Lambda} I_n e^{-in\xi} \tag{4b}$$

$$\cos\xi \exp(\Lambda\cos\xi) = \frac{d}{d\Lambda}\exp(\Lambda\cos\xi) = \sum I_n' e^{-in\xi} \tag{4c}$$

$$(\cos\xi - \Lambda\sin^2\xi)\exp(\Lambda\cos\xi) = -\frac{1}{\Lambda}\frac{d^2}{d\xi^2}\exp(\Lambda\cos\xi) = \sum \frac{n^2 I_n}{\Lambda} e^{-in\xi} \tag{4d}$$

$$\left[-\sin\xi + \Lambda\sin\xi(1-\cos\xi)\right]\exp(\Lambda\cos\xi) = \left(-\frac{d}{d\xi} + \frac{d}{d\xi}\frac{d}{d\Lambda}\right)\exp(\Lambda\cos\xi)$$

$$= \sum in(I_n - I_n')e^{-in\xi} \tag{4e}$$

$$\left[\cos\xi + \Lambda(1-\cos\xi)^2\right]\exp(\Lambda\cos\xi) = \left(\Lambda\frac{d}{d\Lambda^2} + (1-2\Lambda)\frac{d}{d\Lambda} + \Lambda\right)\exp(\Lambda\cos\xi)$$

$$= \sum\left[\frac{n^2 I_n}{\Lambda} + 2\Lambda\left(I_n - I_n'\right)\right]e^{-in\xi} \qquad (4f)$$

where $I_n' = dI_n(\Lambda)/d\Lambda$ and $I_n'' = -I_n'/\Lambda + (1 + n^2/\Lambda^2)I_n$.

Further observation shows that

$$\frac{\xi^2 k_n^2 c^2}{\omega_b\sqrt{R}} \approx k_n \frac{\partial}{\partial k_n} e^{-\sqrt{R}} \qquad (4g)$$

and changing variables to $t = \frac{\xi\omega}{\mu\omega_b}$, we find that $\xi = i\frac{\partial}{\partial n}e^{-in\xi}$ or

$$t = i\frac{\partial}{\partial\left(n\mu\frac{\omega_b}{\omega}\right)}\exp\left(-in\mu\frac{\omega_b}{\omega}t\right) \qquad (4h)$$

Hence the form for $\varepsilon_{\alpha\beta}$ becomes

$$\varepsilon_{\alpha\beta} - \delta_{\alpha\beta} = i\frac{\omega_p^2}{\omega^2}\mu\sum_{n=-\infty}^{\infty}\int_0^\infty \frac{dt\, e^{-\Lambda}\, T_{\alpha\beta}^{(4)}\exp\left\{\mu - \mu\left[(1-it)^2 + \frac{k_n^2c^2t^2}{\omega^2}\right]^{\frac{1}{2}} - in\mu\frac{\omega_b}{\omega}t\right\}}{\left[(1-it)^2 + \frac{k_n^2c^2t^2}{\omega^2}\right]^{1/4}} \qquad (5a)$$

with

$$T_{\alpha\beta}^{(4)} = \left[(1-it)^2 + \frac{k_n^2c^2t^2}{\omega^2}\right]^{\frac{1}{2}}\begin{pmatrix} \frac{n^2I_n}{\Lambda} & -in(I_n' - I_n) & 0 \\ in(I_n' - I_n) & \frac{n^2I_n}{\Lambda} + 2\Lambda(I_n - I_n') & 0 \\ 0 & 0 & I_n\left(1 + k_n\frac{\partial}{\partial k_n}\right) \end{pmatrix}$$

+

$$+\frac{k_\perp k_\parallel c^2}{\omega\omega_b}\begin{pmatrix} 0 & 0 & \frac{nI_n}{\Lambda} \\ 0 & 0 & i\left(I_n' - I_n\right) \\ \frac{nI_n}{\Lambda} & -i\left(I_n' - I_n\right) & 0 \end{pmatrix} \frac{\partial}{\partial\left(n\mu\frac{\omega_b}{\omega}\right)} \qquad (5b)$$

and

$$\Lambda = \lambda\left[(1-it)^2 + \frac{k_\parallel^2 c^2 t^2}{\omega^2}\right]^{-\frac{1}{2}}, \quad \lambda \equiv \frac{k_\perp^2 v_t^2}{\omega_b^2} \qquad (5c),(5d)$$

Let us now restrict ourselves to $\Lambda << 1$ rather than $\Lambda \sim 1$.

In this limit

$$\frac{n^2 I_n}{\Lambda} \approx \frac{n^2 I_n}{\Lambda} + \Lambda(I_n - I_n') \approx n\,(I_n' - I_n) \approx \frac{n^2\Lambda^{n-1}}{2^n n!} \qquad (6)$$

It is also proper to change the sum over n to start from 0. Note that $I_{-n} = I_n$ and the n = 0 term requires a $\left(1 - \frac{\delta(n)}{2}\right)$ factor since this term is included only once in the summation. Define furthermore a function $\mathcal{J}_q$ dependent on two dimensionless parameters $\mu\omega_b n/\omega$ and $k_\parallel c/\omega$ besides q.

$$\mathcal{J}_q\left(\frac{\mu n\omega_b}{\omega}, \frac{k_\parallel c}{\omega}\right) \equiv -i\int_0^\infty \frac{dt\,\exp\left\{\mu - \mu\left[(1-it)^2 + \frac{k_\parallel^2 t^2 c^2}{\omega^2}\right]^{\frac{1}{2}} - in\mu\frac{\omega_b}{\omega}\,t\right\}}{\left[(1-it)^2 + \frac{k_\parallel^2 c^2 t^2}{\omega^2}\right]^{q/2}} \qquad (7)$$

As a result writing $\mathcal{J}_q^{(a)}_{(b)} = \mathcal{J}_q\left(\mu\frac{n\omega_b}{\omega}, \frac{k_\parallel c}{\omega}\right) \pm \mathcal{J}_q\left(-\mu\frac{n\omega_b}{\omega}, \frac{k_\parallel c}{\omega}\right)$ we have for $\Lambda << 1$:

$$\varepsilon_{\alpha\beta} - \delta_{\alpha\beta} = -\frac{\omega_p^2}{\omega^2}\mu \sum_{n=0}^{\infty} \Bigg[\frac{n^2\lambda^{n-1}}{2^n n!} \begin{pmatrix} \mathcal{J}^{(a)}_{n+3/2} & -i\,\mathcal{J}^{(b)}_{n+3/2} & 0 \\ i\,\mathcal{J}^{(b)}_{n+3/2} & \mathcal{J}^{(a)}_{n+3/2} & 0 \\ 0 & 0 & 0 \end{pmatrix}$$

$$+ \frac{\lambda^n}{2^n n!} \begin{pmatrix} 0 & 0 & 0 \\ 0 & 0 & 0 \\ 0 & 0 & 1 \end{pmatrix} \frac{\partial}{\partial k_\parallel} \left(k_\parallel \mathcal{J}^{(a)}_{n+5/2} \right)$$

$$+ \frac{k_\perp k_\parallel c^2}{\omega\omega_b} \frac{n\lambda^{n-1}}{2^n n!} \frac{\partial}{\partial(n\mu\omega_b/\omega)} \begin{pmatrix} 0 & 0 & \mathcal{J}^{(a)}_{n+5/2} \\ 0 & 0 & i\,\mathcal{J}^{(b)}_{n+5/2} \\ \mathcal{J}^{(a)}_{n+5/2} & -i\,\mathcal{J}^{(b)}_{n+5/2} & 0 \end{pmatrix} \Bigg] \left(1 - \frac{\delta(n)}{2}\right) \tag{8}$$

Before proceeding with the analysis, it will be reassuring to show that we can obtain the non-relativistic dielectric tensor expression under appropriate conditions. Let us use the more general formula in (5a).

When $$\frac{\omega - n\omega_b}{\omega} \ll \frac{k_\parallel^2 c^2}{\omega^2} \quad \text{i.e.} \quad \frac{\omega - n\omega_b}{\sqrt{2}k_\parallel v_t} \equiv \zeta \ll \frac{k_\parallel c^2}{\omega v_t} \tag{9}$$

the main contribution from the integral arises from $t \ll 1$ (see Sec. VI), in which case,

$$\left[(1 - it)^2 + \frac{k_\parallel^2 c^2 t^2}{\omega^2} \right]^{\frac{1}{2}} \approx 1 - it + \frac{k_\parallel^2 c^2 t^2}{2\omega^2}$$

in the exponent and unity in the denomenator. Also $\Lambda \approx \lambda$. The integral we are left to evaluate is

$$\int_0^\infty dt \exp\left\{ i \mu t \left(1 - \frac{\omega_b}{\omega}\right) - \frac{\mu k_n{}^2 c^2 t^2}{2\omega^2} \right\} = e^{-\zeta^2} \int_{-\infty}^{i\zeta} e^{-x^2} dx \Big/ \left(\frac{k_n c^2}{\sqrt{2} v_t \omega} \right) = Z(\zeta) \left(\frac{v_t \omega}{\sqrt{2} i k_n c^2} \right) \tag{10a}$$

where

$$\zeta \equiv \frac{\omega - n\omega_b}{\sqrt{2} v_t k_n}, \quad x \equiv i\zeta - \frac{k_n{}^2 c^2 t^2}{\sqrt{2} v_t \omega} \tag{10b}$$

and the integral is given in terms of the "plasma dispersion function" (Fried and Conte 1961).

$$Z(\zeta) \equiv 2ie^{-\zeta^2} \int_{-\infty}^{i\zeta} e^{-x^2} dx \tag{10c}$$

Substituting these results into Eq. (5a) we obtain the well known expression for $\varepsilon_{\alpha\beta}$ (see Stix (1962) p. 188 or Fried and Conte (1961), for example):

$$\varepsilon_{\alpha\beta} - \delta_{\alpha\beta} = \frac{\omega_p{}^2 e^{-\lambda}}{\omega k_n v_t \sqrt{2}} \sum_{n=-\infty}^{\infty} \begin{pmatrix} \frac{n^2 I_n}{\lambda} Z & -in(I_n' - I_n) Z & \frac{-k_\perp v_t}{\sqrt{2}\omega_b} \frac{n I_n}{\lambda} Z' \\ in(I_n' - I_n) Z & \left[\frac{n^2 I_n}{\lambda} + 2\lambda(I_n - I_n') \right] Z & \frac{-ik_\perp v_t}{\sqrt{2}\omega_b} (I_n' - I_n) Z' \\ -\frac{k_\perp v_t}{\sqrt{2}\omega_b} \frac{n I_n}{\lambda} Z' & \frac{ik_\perp v_t}{\sqrt{2}\omega_b} (I_n' - I_n) Z' & -I_n \zeta Z' \end{pmatrix} \tag{11a}$$

where $Z' = dZ(\zeta)/d\zeta = -2(1 + \zeta Z)$ and noting that (11b)

$$\partial \Big/ \partial \left(n\mu \frac{\omega_b}{\omega} \right) = -\left(\frac{\omega v_t}{c^2 k_n \sqrt{2}} \right) \frac{d}{d\zeta} \quad \text{and} \quad \left(1 + k_n \frac{\partial}{\partial k_n} \right) \left(\frac{Z}{k_n} \right) = \frac{\partial}{\partial k_n} Z(\zeta) = -\frac{1}{k_n} \zeta Z'$$

Sometimes it is convenient to sum n from 0 to ∞ rather than $-\infty$ to ∞. If one changes n to - n, one notes that $I_{-n} = I_n$ whereas the argument of Z changes from $\zeta_a = (\omega - n\omega_b)/\sqrt{2}v_t k_\parallel$ to $\zeta_b = (\omega + n\omega_b)/\sqrt{2}v_t k_\parallel$. Since the n = 0 term is included only once, we require a $(1 - \delta(n)/2)$ factor. Thus writing $Z_a = Z(\zeta_a)$ and $Z_b = Z(\zeta_b)$,

$$\varepsilon_{\alpha\beta} - \delta_{\alpha\beta} = \frac{\omega_p^2 e^{-\lambda}}{\omega k_\parallel v_t \sqrt{2}} \sum_{n=0}^{\infty} \left(1 - \frac{\delta(n)}{2}\right) \times$$

$$\begin{pmatrix} \frac{n^2 I_n}{\lambda}(Z_a + Z_b) & -in(I_n' - I_n)(Z_a - Z_b) & \frac{-k_\perp v_t}{\sqrt{2}\omega_b}\frac{nI_n}{\lambda}(Z_a' - Z_b') \\ in(I_n' - I_n)(Z_a - Z_b) & \left[\frac{n^2 I_n}{\lambda} + 2\lambda(I_n - I_n')\right](Z_a + Z_b) & \frac{-ik_\perp v_t}{\sqrt{2}\omega_b}(I_n' - I_n)(Z_a' + Z_b') \\ \frac{-k_\perp v_t}{\sqrt{2}\omega_b}\frac{nI_n}{\lambda}(Z_a' - Z_b') & \frac{ik_\perp v_t}{\sqrt{2}\omega_b}(I_n' - I_n)(Z_a' + Z_b') & -I_n(\zeta_a Z_a' + \zeta_b Z_b') \end{pmatrix} \tag{12}$$

Finally we note that in the limit $\lambda << 1$ and subject to the conditions in (9), the relation between $\mathcal{F}$ and Z in simply

$$\mathcal{F} = -\left(\frac{v_t \omega}{\sqrt{2}k_\parallel c^2}\right) Z \tag{13}$$

III. THE CASE OF SMALL $k_\parallel$

By small $k_\parallel$, we mean

$$k_\parallel^2 \lesssim v_t^2 \omega^2 / c^4 \tag{14a}$$

This limit is of interest since it will be shown that the satellite velocity can be matched to the wave group velocity along the magnetic field for very small $k_{\parallel}$ values. Subject to (14a)

$$\mathcal{J}_q = -i \int_0^\infty \frac{dt}{(1-it)^q} \exp\left[i\mu\delta t - \frac{t^2 c^4 k_{\parallel}^2}{2v_t^2 \omega^2 (1-it)} \right] \tag{14b}$$

where $$\delta \equiv \frac{\omega - n\omega_b}{\omega} \tag{14c}$$

Note that in this relativistic approach, we are not faced with the "problem" of which is smaller $k_{\parallel} v_t \sqrt{2}$ or $\omega - n\omega_b$ in the ζ argument of the less exact Z function.

By further expansion, we can now relate the $\mathcal{J}$ function to a simpler one F, a function of one variable only. Define

$$F_q(\mu\delta) \equiv -i \int_0^\infty \frac{dt\, e^{i\mu\delta t}}{(1-it)^q} \tag{15}$$

Then from Eq. (7)

$$\mathcal{J}_q\left(\mu n \frac{\omega_b}{\omega}, \frac{k_{\parallel} c}{\omega}\right) = -i \int_0^\infty \frac{dt\, e^{i\mu\delta t}}{(1-it)^q} \left(1 - \frac{t^2 c^4 k_{\parallel}^2}{2v_t^2 \omega^2 (1-it)}\right) = F_q + \frac{c^4 k_{\parallel}^2}{2v_t^2 \omega^2} (F_{q-1} - 2F_q + F_{q+1}) \tag{16a}$$

using $-t^2 = (1-it)^2 - 2(1-it) + 1$. The same relation holds for $\mathcal{J}_q(-\mu n\omega_b/\omega, k_{\parallel} c/\omega)$, if we substitute $\mu(\omega + n\omega_b)/\omega$ for the argument of F_q. With this relation we find

$$\frac{\partial}{\partial k_{\parallel}} (k_{\parallel} \mathcal{J}_q) = F_q + \frac{3c^4 k_{\parallel}^2}{v_t^2 \omega^2} (F_{q-1} - 2F_q + F_{q+1}) \tag{16b}$$

$$\frac{\partial}{\partial\left(n\mu\frac{\omega_b}{\omega}\right)}\mathcal{J}_q\left(n\mu\frac{\omega_b}{\omega},\ \frac{k_n c}{\omega}\right) = -\frac{\partial}{\partial\mu\delta}\mathcal{J}_q \approx -\,i\int_0^\infty \frac{dt\ e^{i\mu\delta t}}{(1-it)^q}\left[(1-it)-1\right] = F_{q-1} - F_q \tag{16c}$$

Similarly $$\frac{\partial}{\partial\left(n\mu\frac{\omega_b}{\omega}\right)}\mathcal{J}_q\left(-\,n\mu\frac{\omega_b}{\omega},\ \frac{k_n c}{\omega}\right) = -\,F_{q-1} + F_q$$

As a result, one can write Eq. (8) as:

$$\begin{aligned}
\varepsilon_{\alpha\beta} - \delta_{\alpha\beta} = \frac{-\omega_p^2}{\omega^2}\,\mu \sum_{n=0}^{\infty}\Bigg\{ & \frac{n^2\lambda^{n-1}}{2^n n!}\begin{pmatrix}1&0&0\\0&1&0\\0&0&0\end{pmatrix}\left[F^{(a)}_{n+3/2} + \frac{k_n^2 c^4}{2v_t^2\omega^2}\left(F^{(a)}_{n+1/2} - 2F^{(a)}_{n+3/2} + F^{(a)}_{n+5/2}\right)\right] \\
& + \frac{n^2\lambda^{n-1}}{2^n n!}\begin{pmatrix}0&-i&0\\i&0&0\\0&0&0\end{pmatrix}\left[F^{(b)}_{n+3/2} + \frac{k_n^2 c^4}{2v_t^2\omega^2}\left(F^{(b)}_{n+1/2} - 2F^{(b)}_{n+3/2} + F^{(b)}_{n+5/2}\right)\right] \\
& + \frac{\lambda^n}{2^n n!}\begin{pmatrix}0&0&0\\0&0&0\\0&0&1\end{pmatrix}\left[F^{(a)}_{n+5/2} + \frac{3k_n^2 c^4}{2v_t^2\omega^2}\left(F^{(a)}_{n+3/2} - 2F^{(a)}_{n+5/2} + F^{(a)}_{n+7/2}\right)\right] \\
& + \frac{k_\perp k_n c^2}{\omega\omega_b}\frac{n\lambda^{n-1}}{2^n n!}\begin{pmatrix}0&0&1\\0&0&0\\1&0&0\end{pmatrix}\left[-F^{(b)}_{n+5/2} + F^{(b)}_{n+3/2}\right] \\
& + \frac{k_\perp k_n c^2}{\omega\omega_b}\frac{n\lambda^{n-1}}{2^n n!}\begin{pmatrix}0&0&0\\0&0&i\\0&-i&0\end{pmatrix}\left[-F^{(a)}_{n+5/2} + F^{(a)}_{n+3/2}\right]\Bigg\}\left(1-\frac{\delta(n)}{2}\right)
\end{aligned} \tag{17}$$

where $$F_q^{(a)}_{(b)} = F_q\left[\mu\left(\frac{\omega - n\omega_b}{\omega}\right)\right] \pm F_q\left[\mu\left(\frac{\omega + n\omega_b}{\omega}\right)\right]$$

The nonrelativistic limit can be shown to have some validity in this case if we assume that

$$\mu\delta \gg 1 \quad \text{or} \quad (\omega - n\omega_b)/\omega \gg v_t^2/c^2 \tag{18a}$$

Because of the condition (14a) on small $k_\parallel$, this implies that

$$\zeta = \frac{\omega - n\omega_b}{\sqrt{2}k_\parallel v_t} \gg \frac{\omega v_t}{k_\parallel c^2} > 1 \tag{18b}$$

Since (18b) contradicts the inequality in (9), we have to be careful in applying the Z-function unscrupulously. We now show that the Z and F functions give the same results provided we limit ourselves to Im $\omega > 0$. That is we shall not compare analytic continuations of these functions for Im $\omega < 0$ since they differ (see Sec. VI). Omission of the contribution arising from the analytic continuation (usually of exponential form) implies that for $k_\parallel \to 0$ we omit the contribution to $\mathcal{J}_q$ from the region $i\tau \approx 1$ (see Sec. V). In this case, the approximation in (10a) and Eq. (12) are valid. To summarize, when the analytic continuation of the Z function is not required (Im $\omega > 0$) and $\zeta > 1$ from Eq. (18b), we can expand the Z function in Eq. (12) for large arguments and indeed the exponential part of Z is zero. Thus

$$Z \approx -\frac{1}{\zeta}\left(1 + \frac{1}{2\zeta^2}\right) ; \; Z' \approx \frac{1}{\zeta^2} ; \; \zeta Z' \approx \frac{1}{\zeta^2}\left(1 + \frac{3}{2\zeta^2}\right) \tag{18c}$$

Noting as well that

$$Z_a + Z_b = -k_\parallel v_t\sqrt{2}\,\frac{2\omega}{\omega^2 - n^2\omega_b}(1+\alpha_1)\;;\quad Z_a - Z_b = -\,k_\parallel\,\frac{v_t\sqrt{2}\;2n\omega_b}{\omega^2 - n^2\omega_b}\,(1+\alpha_2)$$

$$Z'_a + Z'_b = k_\parallel{}^2 2v_t{}^2\,\frac{2(\omega^2 + n^2\omega_b{}^2)}{(\omega^2 - n^2\omega_b{}^2)^2}\;\cdot\;Z'_a - Z'_b = k_\parallel{}^2 2v_t{}^2\,\frac{4n\omega\omega_b}{(\omega^2 - n^2\omega_b{}^2)^2}$$

where

$$\alpha_1 = v_t{}^2 k_\parallel{}^2\left(\frac{\omega^2 + 3n^2\omega_b{}^2}{(\omega^2 - n^2\omega_b{}^2)^2}\right)\;;\quad \alpha_2 = v_t{}^2 k_\parallel{}^2\left(\frac{3\omega^2 + n^2\omega_b{}^2}{(\omega^2 - n^2\omega_b{}^2)^2}\right) \qquad (19a,b)$$

we derive from Eq. (12) that

$$\varepsilon_{\alpha\beta} - \delta_{\alpha\beta} = \omega_p{}^2 e^{-\lambda}\sum_{n=o}^{\infty}\frac{(\delta(n)-2)}{(\omega^2 - n^2\omega_b{}^2)}\;X$$

$$\begin{pmatrix}
(1+\alpha_1)\,\dfrac{n^2 I_n}{\lambda} & -i(1+\alpha_2)\,\dfrac{n^2\omega_b}{\omega}(I'_n - I_n) & \dfrac{k_\perp k_\parallel v_t{}^2}{\omega^2 - n^2\omega_b{}^2}\,\dfrac{2n^2 I_n}{\lambda} \\
i(1+\alpha_2)\dfrac{n^2\omega_b}{\omega}(I'_n - I_n) & (1+\alpha_1)\left[\dfrac{n^2 I_n}{\lambda} + 2\lambda(I_n - I'_n)\right] & \dfrac{ik_\perp k_\parallel v_t{}^2(\omega^2 + n^2\omega_b{}^2)}{(\omega^2 - n^2\omega_b{}^2)\omega\omega_b}(I'_n - I_n) \\
\dfrac{k_\perp k_\parallel v_t{}^2}{\omega^2 - n^2\omega_b{}^2}\,\dfrac{2n^2 I_n}{\lambda} & -\,ik_\perp k_\parallel v_t{}^2\,\dfrac{(\omega^2 + n^2\omega_b{}^2)}{(\omega^2 - n^2\omega_b{}^2)}\,\dfrac{}{\omega\omega_b}(I'_n - I_n) & (1+3\alpha_1)I_n
\end{pmatrix} \qquad (20)$$

For $\lambda << 1$, this reduces to

$$\varepsilon_{\alpha\beta}-\delta_{\alpha\beta} = \sum_{n=0}^{\infty} \frac{\omega_p^2(\delta(n)-2)}{(\omega^2 - n^2\omega_b^2)} \left[\frac{n^2\lambda^{n-1}}{2^n n!} \begin{pmatrix} 1+\alpha_1 & -i(1+\alpha_2)\frac{n\omega_b}{\omega} & 0 \\ i(1+\alpha_2)\frac{n\omega_b}{\omega} & 1+\alpha_1 & 0 \\ 0 & 0 & 0 \end{pmatrix} \right.$$

$$\left. + \frac{\lambda^n}{2^n n!} \begin{pmatrix} 0 & 0 & 0 \\ 0 & 0 & 0 \\ 0 & 0 & 1+3\alpha_1 \end{pmatrix} + \frac{k_\perp k_\parallel v_t^2}{(\omega^2 - n^2\omega_b^2)} \frac{2n^2\lambda^{n-1}}{2^n n!} \begin{pmatrix} 0 & 0 & 1 \\ 0 & 0 & i\frac{(\omega^2+n^2\omega_b^2)}{2n\omega_b\omega} \\ 1 & -i\frac{(\omega^2+n^2\omega_b^2)}{2n\omega_b\omega} & 0 \end{pmatrix} \right] \tag{21}$$

This latter result is identical to that obtained from Eq. (17), since for $\mu\delta >> 1$.

$$F_q(\mu\delta) = -i\int_0^\infty dt\, e^{i\mu\delta t} = (\mu\delta)^{-1} \quad \text{if} \quad \text{Im}\,\omega > 0. \tag{22a}$$

$$F_q - F_{q-1} \approx -(\mu\delta)^{-2} \quad \text{and} \quad F_{q-1} - 2F_q + F_{q+1} = 2(\mu\delta)^{-3} \tag{22b,c}$$

We have thus shown that for Im $\omega > 0$, the relativistic analysis reduces to the nonrelativistic one for $\mu\delta >> 1$ and $k_\parallel$ zero or very small.

Near the n th cyclotron harmonic ($n \neq 1$, see Sec. IX), $\pm\omega \approx n\omega_b$, $\alpha_1 \approx \alpha_2 = \alpha$ say, etc. Besides the n = 0 and n = 1 terms, we need to keep only the n th harmonic term. Then we can write $\underset{\sim}{\varepsilon} = \underset{\sim}{\varepsilon}_{cold} + \underset{\sim}{\varepsilon}_{warm}$ (23a)

where

$$(\varepsilon_{cold})_{\alpha\beta} = \begin{pmatrix} 1 - \frac{\omega_p^2}{\omega^2-\omega_b^2} & \frac{i\omega_p^2\omega_b}{\omega(\omega^2-\omega_b^2)} & 0 \\ \frac{-i\omega_p^2\omega_b}{\omega(\omega^2-\omega_b^2)} & 1 - \frac{\omega_p^2}{\omega^2-\omega_b^2} & 0 \\ 0 & 0 & 1 - \frac{\omega_p^2}{\omega^2} \end{pmatrix} \qquad (23b)$$

For the nonrelativistic case (Eq. (21)).

$$(\varepsilon_{warm})_{\alpha\beta} = -\frac{2\omega_p^2}{\omega^2-n^2\omega_b^2}\frac{n^2\lambda^{n-1}}{2^n n!}\begin{pmatrix} 1+\alpha & -i(1+\alpha) & \sqrt{\alpha\lambda}/n \\ i(1+\alpha) & 1+\alpha & i\sqrt{\alpha\lambda}/n \\ \sqrt{\alpha\lambda}/n & -i\sqrt{\alpha\lambda}/n & \lambda(1+3\alpha)/n^2 \end{pmatrix} \qquad (23c)$$

where $\sqrt{\alpha\lambda} = \frac{k_\perp k_\parallel v_t^2 2n}{\omega^2 - n^2\omega_b^2}$. For the warm terms, it is convenient to consider positive ω near $n\omega_b$ independently from negative ω near $n\omega_b$. When $\omega \approx n\omega_b$, the contribution from $-\omega$ is negligible of course and vice versa. For this reason we restrict ourselves in the following to positive ω bearing in mind that negative ω can be treated in a similar fashion. Thus in Eq. (23c) we can set $\omega^2-n^2\omega_b^2 \approx 2n\omega_b(\omega-\omega_b)$ if we wish. Similarly for the F function, we only consider arguments $(\omega-n\omega_b)\mu/\omega$. A general relation for complex ω is (Landau and Lifshitz (1960) Vol. 8, Sec. 62):

$$\varepsilon(-\omega^*) = \varepsilon^*(\omega) \qquad (23d)$$

Thus for the relativistic case (Eq. 17)

$$(\varepsilon_{warm})_{\alpha\beta} = -\frac{\omega_p^2}{\omega^2}\mu\frac{n^2\lambda^{n-1}}{2^n n!}\left\{\begin{pmatrix}1 & -i & 0\\ i & 1 & 0\\ 0 & 0 & 0\end{pmatrix}\left[F_{n+3/2} + \frac{k_\parallel^2 c^4}{2v_t^2\omega^2}\left(F_{n+1/2} - 2F_{n+3/2} + F_{n+5/2}\right)\right]\right.$$

$$+ \begin{pmatrix}0 & 0 & 0\\ 0 & 0 & 0\\ 0 & 0 & 1\end{pmatrix}\frac{\lambda}{n^2}\left[F_{n+5/2} + \frac{3k_\parallel^2 c^4}{2v_t^2\omega^2}\left(F_{n+3/2} - 2F_{n+5/2} + F_{n+7/2}\right)\right]$$

$$\left. + \frac{k_\perp k_\parallel c^2}{\omega\omega_b n}\begin{pmatrix}0 & 0 & 1\\ 0 & 0 & i\\ 1 & -i & 0\end{pmatrix}\left[-F_{n+5/2} + F_{n+3/2}\right]\right\} \qquad (23e)$$

IV. THE CASE OF $k_\parallel = 0$ AND THE F FUNCTION

For a wave propagating exactly perpendicular to the magnetic field, the warm elements of the dielectric tensor are for $\lambda \ll 1$ (see Eq. 23d):

$$\varepsilon_{11} = \varepsilon_{22} = i\varepsilon_{12} = -i\varepsilon_{21} = -\frac{\omega_p^2}{\omega^2}\mu\frac{n^2\lambda^{n-1}}{2^n n!}F_{n+3/2} \qquad (24a)$$

$$\varepsilon_{33} = -\frac{\omega_p^2}{\omega^2}\mu\frac{\lambda^n}{2^n n!}F_{n+5/2}; \quad \varepsilon_{13} = \varepsilon_{23} = \varepsilon_{31} = \varepsilon_{32} = 0 \qquad (24b)$$

where

$$F_q(\mu\delta) = -i\int_0^\infty \frac{dt}{(1-it)^q}e^{i\mu\delta t}, \quad \mu = \frac{c^2}{v_t^2}, \quad \delta = \frac{\omega - n\omega_b}{\omega} \qquad (25)$$

The above relations were first given by Dnestrovskii et al (1964) who also plotted the real and imaginary parts of the function for real ω and $n = 1,2,3$ (see Fig. 1). For real ω and $\omega \lesseqgtr n\omega_b$ (viz $\mu\delta \lesseqgtr 0$), Dnestrovskii et al also give the following expansion* for $F(\mu\delta < 0)$ written here in terms of the Gamma function Γ and an integral expressible in terms of the error function Φ.

---

* There is an error in Dnestrovskii et al (1964). The sign of the last term is negative as given here and not positive as given in their Eq. VIII.

$$F_q(z) = \sum_{p=0}^{q-3/2} |\mu\delta|^p \frac{\Gamma(q-1-p)}{\Gamma(q)} - \frac{|\mu\delta|^{q-1/2}\sqrt{\pi}}{\Gamma(q)} \int_0^1 \frac{e^{-|\mu\delta|t}}{(1-t)^{1/2}}\, dt - \frac{i\pi}{\Gamma(q)} |\mu\delta|^{q-1} e^{-|\mu\delta|} \tag{26a}$$

$$= \sum_{p=0}^{q-3/2} |\mu\delta|^p \frac{\Gamma(q-1-p)}{\Gamma(q)} - \frac{i\pi}{\Gamma(q)} |\mu\delta|^{q-1} e^{-|\mu\delta|} \left[1 - \Phi(i\sqrt{|\mu\delta|})\right] \tag{26b}$$

In Sec. V we shall prove this relation and also give a more general expression valid for complex ω.

Since we are dealing with a time decaying signal (after the satellite transmitter is shut off) or an initial value problem, we have to consider complex ω, rather than only real ω. The complex ω is an inherent feature of the inverse Laplace transform which gives the time decay of the signal. If we were dealing with a function which is real for real ω then it is simple to apply the same function for complex ω. However, since F is complex for real ω, the dispersion relation which includes F will require complex k. This situation is appropriate to a steady broadcasting transmitter with a decaying signal in space. For our situation however, we are interested in a space localized signal decaying in time, or real k and complex ω. Since we wish k to be real, F must be real and this can only be done if we let ω or $z = \mu\delta$, the argument of F, be complex. Furthermore, it turns out that we have to define F for both Imz (or Im ω) greater or less than zero. That is, F has to be continued into the lower half plane Im $z < 0$, although the original definition applies only to the upper half plane Im $z > 0$. When F is real, it is shown in Sec. VII that Im $z < 0$ (or Im $\omega < 0$).

In the inverse Laplace transform we integrate over $e^{-i\omega t}$ and we thus derive a time decaying exponential $e^{-\omega_i t}$. However we find in Sec.VII, Eq. (40d) that ω_i is of the order of $n\omega_b/\mu$ so that this relativistic exponential decay is negligible for our times of interest and the actual decay must arise from the other time-amplitude factors multiplying this exponential. Although the exponential decay factor is negligible, we still need a relativistic approach since the F function has to continued throughout the complex ω plane and be used in the region of $\mathrm{Re}(\omega - n\omega_b)/\omega < v_t^2/c^2$ within which most of the ω versus k variation occurs. The nonrelativistic approach is only applicable for $|\mu\delta| \gg 1$ and $\mathrm{Im}\,\omega > 0$, in which case $F \sim (\mu\delta)^{-1}$, as shown above in Sec.III.

V. ANALYSIS OF THE F_q FUNCTION AND ITS ANALYTIC CONTINUATION

Starting from

$$F_q(z) = -i \int_0^\infty \frac{e^{izt}\,dt}{(1-it)^q} \tag{27a}$$

where q is a half integer and assuming Im z > 0 for complex $z = \mu\delta$, we can integrate by parts a sufficient number of times until the power q is reduced to $\frac{1}{2}$. We obtain

$$F_q = \frac{1}{q-1} + \frac{(-z)}{(q-1)(q-2)} + \frac{(-1)^2 z^2}{(q-1)(q-2)(q-3)} + \cdots\cdots + \frac{(-1)^{q-3/2} z^{q-3/2}}{(q-1)\cdots 1/2}$$

$$+ \frac{i(-1)^{q-3/2} z^{q-1/2}}{(q-1)\cdots 1/2} \int_0^\infty \frac{e^{izt}\,dt}{(1-it)^{1/2}}$$

$$= \sum_{p=0}^{q-3/2} (-z)^p \frac{\Gamma(q-1-p)}{\Gamma(q)} + \frac{i(-1)^{q-3/2}\sqrt{\pi}}{\Gamma(q)} z^{q-1/2} \int_0^{\infty} \frac{e^{izt}dt}{(1-it)^{1/2}} \qquad (27b)$$

Now $$\int_0^{\infty} \frac{e^{izt}dt}{(1-it)^{1/2}} = i\sqrt{\frac{\pi}{z}} e^z \left[1 - \Phi(\sqrt{z})\right] \qquad (28a)$$

where Φ is the error function. (The above can be verified by defining a new variable of integration equal to $\sqrt{z(1-it)}$.) Furthermore we have the following equation for the Z function in terms of the error function:

$$Z(iy) = i\sqrt{\pi}\, e^{y^2}(1 - \Phi(y)) \qquad (28b)$$

As a result we can relate F_q to the Z function which is already tabulated, thus

$$F_q = \sum_{p=0}^{q-3/2} (-z)^p \frac{\Gamma(q-1-p)}{\Gamma(q)} + \frac{\pi}{\Gamma(q)} \frac{(-z)^{q-1/2} e^z}{\sqrt{z}} \left[1 - \Phi(\sqrt{z})\right] \qquad (29a)$$

$$= \sum_{p=0}^{q-3/2} (-z)^p \frac{\Gamma(q-1-p)}{\Gamma(q)} + \frac{\sqrt{\pi}}{\Gamma(q)} (-z)^{q-3/2} \left[i\sqrt{z}\, Z(i\sqrt{z})\right] \qquad (29b)$$

$$= \sum_{p=0}^{q-5/2} (-z)^p \frac{\Gamma(q-1-p)}{\Gamma(q)} - \frac{\sqrt{\pi}}{2\Gamma(q)} (-z)^{q-3/2} Z'(i\sqrt{z}) \quad \text{since}$$

$$Z'(i\sqrt{z}) = -2\left[1 + i\sqrt{z}\, Z(i\sqrt{z})\right] \qquad (29c)$$

When z is real and negative, $-z = |\mu\delta|$ and taking $\sqrt{-|\mu\delta|} = i\sqrt{|\mu\delta|}$ we see that Eq. (29a) assumes the form given in (26b) or given in Dnestrovskii et al (1964). The imaginary contribution in (26b) arises from the region

around it ≈ 1 as shown by Dnestrovskii et al who rotate the contour through 90°. Note also that for real z, F_q has an imaginary contribution only for $z < 0$ (see Fig. 1) since q is a half-integer.

To be of greater use, the $F_q(z)$ function defined above only for Im $z > 0$, has to be analytically continued for Im $z < 0$. Fortunately, we have succeeded in expressing F in terms of Z, a function whose analytic continuation has been considerably investigated (see Fried and Conte 1961). Thus we can allow Eqs. (29b,c) to be valid everywhere in the complex z plane using the proper continuation for Z.

The following expansions of $Z(\zeta)$ are valid throughout the complex ζ plane (c.f. Fried and Conte).

$$Z(\zeta) = i\sqrt{\pi}\ e^{-\zeta^2} - \zeta \sum_{l=0}^{\infty} (-\zeta^2)^l \sqrt{\pi}/\Gamma(l + 3/2) \tag{30a}$$

For $|\zeta| >> 1$ $$Z(\zeta) \simeq i\sqrt{\pi}\sigma\ e^{-\zeta^2} - \sum_{l=0}^{\infty} \zeta^{-(2l+1)} \Gamma(l + \tfrac{1}{2})/\sqrt{\pi} \tag{30b}$$

where $\sigma = 0,1,2$ for Im $\zeta > 0$, Im $\zeta = 0$, Im $\zeta < 0$ respectively. (30c)

Also $$Z'(\zeta) \approx -2i\sqrt{\pi}\sigma\zeta\, e^{-\zeta^2} + \frac{2}{\sqrt{\pi}} \sum_{l=0}^{\infty} \zeta^{-2(l+1)} \Gamma(l + 3/2) \tag{30d}$$

Let us now substitute Eq. (30a) into (29b). Using $q = n + 3/2$, we obtain

$$\Gamma(n+3/2)F_{n+3/2}(z) = \sum_{p=0}^{n}(-z)^p\Gamma(n-p+\tfrac{1}{2}) - \pi(-z)^n\sqrt{z}\,e^z - \pi(-z)^{n+1}\sum_{l=0}^{\infty} z^l/\Gamma(l+3/2)$$

Since $[\Gamma(l + 3/2)]^{-1} = \Gamma(-l-\tfrac{1}{2})\cos[\pi(l+1)]/\pi = (-1)^{l+1}\Gamma(-l-\tfrac{1}{2})/\pi$ (see Magnus and Oberhettinger 1949, p. 1), the last term becomes (after changing the summation index $l = p - n - 1$) $\sum_{p=n+1}^{\infty}(-z)^p\Gamma(n-p+\tfrac{1}{2})$.

This term completes the series given by the first term, so that the net result is

$$\Gamma(n+3/2)F_{n+3/2}(z) = \sum_{p=0}^{\infty}(-z)^p\Gamma(n-p+\tfrac{1}{2}) - \pi(-z)^n\sqrt{z}\,e^z \qquad (31a)$$

This form shows that F_q is composed of two confluent hypergeometric functions which are the two independent solutions of the Kummer differential equation:

$$z\frac{d^2F_q}{dz^2} + (2-q-z)\frac{dF_q}{dz} - F_q = 0 \qquad (31b)$$

The two independent solutions are (see Magnus and Oberhettinger 1948, p. 87)

$$_1F_1(1,\ 2-q,\ z) \quad \text{and} \quad z^{q-1}\,{}_1F_1(q,q,z) = z^{q-1}e^z \qquad (31c)$$

Note that

$$_1F_1(1,2-q,z) = \sum_{p=0}^{\infty}\frac{z^n\Gamma(2-q)}{\Gamma(2+p-q)} = 1 + \frac{z}{2-q} + \frac{z^2}{(2-q)(3-q)} + \ldots. \qquad (31d)$$

so that upon comparing (31c) with (31a) we see that

$$F_q(z) = \frac{1}{(q-1)}\ {}_1F_1(1,2-q,z) + \frac{(-1)^{q-\frac{1}{2}}\pi\left[z^{q-1}e^z\right]}{\Gamma(q)} \qquad (31e)$$

Besides Eq. (31b), one can readily prove using Eq. (27a) the following relations:

$$\frac{dF_q}{dz} = F_q - F_{q-1} \qquad (32a)$$

$$F_{q-1} = \frac{1}{z} - \frac{(q-1)}{z} F_q\ ;\ F_q(1-q+z) = zF_{q-1} - q\,F_{q+1} \qquad (32b,c)$$

$$z\frac{dF_q}{dz} + F_q(1-q) + q\,F_{q+1} = 0 \qquad (32d)$$

The above series expansions for F_q are especially useful in considering cases when $|z| \ll 1$.

For large arguments, $|z| \gg 1$, it is convenient to substitute Eq. (30d) into (29c). Using again $q = n+\frac{3}{2}$, we find

$$\Gamma(n+\tfrac{3}{2})F_{n+\frac{3}{2}}(z) \approx \sum_{p=0}^{n-1} (-z)^p\Gamma(n-p+\tfrac{1}{2}) - \pi\sigma(-z)^n\sqrt{z}\,e^z - \sum_{l=0}^{\infty}\Gamma(l+\tfrac{3}{2})(-z)^{n-l-1} \qquad (33a)$$

where $\sigma = 0, 1, 2$ for Im $i\sqrt{z}$ greater, equal or less than zero respectively. If we write $l = n-m-1$ in the last series, then it becomes

$$-\sum_{m=n-1}^{-\infty}(-z)^m\Gamma(n-m+\tfrac{1}{2}) = -\sum_{m=n-1}^{0}(-z)^m\Gamma(n-m+\tfrac{1}{2}) - \sum_{m=-1}^{-\infty}(-z)^m\Gamma(n-m+\tfrac{1}{2})$$

$$= -\sum_{p=0}^{n-1}(-z)^p\Gamma(n-p+\tfrac{1}{2}) - \sum_{p=0}^{\infty}(-z)^{-p-1}\Gamma(p+n+\tfrac{3}{2})$$

where m = p in first term and m = -p-1 in second term on right hand side. Combining this with the other terms in (33a), we obtain some cancellation with the result that

$$\Gamma(n+\tfrac{3}{2})F_{n+\frac{3}{2}}(z) = -\pi\sigma(-z)^n\sqrt{z}e^z - \sum_{p=0}^{\infty}\frac{\Gamma(p+n+\tfrac{3}{2})}{(-z)^{p+1}} \qquad (33b)$$

where $\sigma = \begin{pmatrix} 0 \\ 1 \\ 2 \end{pmatrix}$ for $\operatorname{Im} i\sqrt{z} \begin{matrix} > 0 \\ = 0 \\ < 0 \end{matrix}$

Before we investigate the complex values of z which make F real (see Sec. VII), let us briefly turn our attention to the $\mathcal{F}_q$ function and the variation with $k_{\parallel}$ of the second (exponential) term in Eq. (31a).

VI. PARTIAL ANALYSIS OF THE $\mathcal{F}_q$ FUNCTION

Previously we have shown in Eq. (31e) that F_q is composed of two hypergeometric functions. A similar analysis on $\mathcal{F}_q$ is very much more complex. Nonetheless, one of the functions comprising $\mathcal{F}_q$ can be investigated for various $k_{\parallel}$ values. This function corresponds for $k_{\parallel} = 0$ to the exponential term in (31e). It will be shown that as $k_{\parallel}$ ranges from 0 to above ω/v_t, the form changes from

$$\frac{(-1)^{q-\frac{1}{2}}\pi(\mu\delta)^{q-1}e^{\mu\delta}}{\Gamma(q)} \quad \text{to} \quad \frac{i\sqrt{\pi}\,e^{-\zeta^2}}{(-\sqrt{2}k_{\parallel}c^2/v_t\omega)}$$

the latter corresponding to part of the $Z(\zeta)$ function. Such an analysis will also prove the assertion in (9) on how large $k_{\parallel}$ has to be before nonrelativistic analysis becomes applicable.

To illustrate the change in $\mathcal{J}_q$ as $k_{\parallel}$ deviates from zero we use the form for $\mathcal{J}_q$ given in Eq. (14b) valid for

$$\sqrt{\mu}y = c^2k_{\parallel}/v_t\omega \lesssim 1 \quad \text{where } y \equiv k_{\parallel}\, c/\omega \tag{34}$$

Then since $\frac{-t^2c^4k_{\parallel}^2}{2v_t^2\omega^2(1-it)} = \frac{-\mu}{2}\left[y^2 + ity^2 - \frac{y^2}{1-it}\right]$

$$\mathcal{J}_q = -\,ie^{-\mu y^2/2}\int_0^\infty \frac{dt}{(1-it)^1}\exp\left[it\,\frac{\mu}{2}\,(2\delta - y^2) + \frac{\mu}{2}\,\frac{y^2}{(1-it)}\right]$$

Expanding $\exp\left(\frac{\mu y^2}{2(1-it)}\right) = \sum_p \frac{1}{\Gamma(p+1)}\left(\frac{\mu y^2}{2(1-it)}\right)^p$ we have

$$\mathcal{J}_q = -\,ie^{-\mu y^2/2}\sum_p\left(\frac{\mu y^2}{2}\right)^p\frac{1}{\Gamma(p+1)}\int_0^\infty \frac{dt}{(1-it)^{q+p}}\exp\left[\frac{it\mu}{2}\,(2\delta - y^2)\right]$$

$$= e^{-\mu y^2/2}\sum_p\left(\frac{\mu y^2}{2}\right)^p\frac{1}{\Gamma(p+1)}\;F_{q+p}\left(\frac{\mu}{2}\,(2\delta - y^2)\right) \tag{35a}$$

using the definition (15a) of the F function. Eq. (35a) is general in that it includes both solutions of the hypergeometric function. We now show

that the exponential part of F (see Eq. (31e)) can be summed. Denote this part of $\mathcal{F}_q$ by $\mathcal{F}_q^{(1)}$. Then, since $z = \frac{\mu}{2}(2\delta - y^2)$ here, we obtain

$$\mathcal{F}_q^{(1)} = \pi \exp[\mu(\delta - y^2)] \sum_p \frac{(-1)^{p+q-\frac{1}{2}}}{\Gamma(p+q)\Gamma(p+1)} \left(\mu\delta - \frac{\mu y^2}{2}\right)^{p+q-1} \left(\frac{\mu y^2}{2}\right)^p$$

$$= i\pi \exp[\mu(\delta - y^2)] \left(1 - \frac{2\delta}{y^2}\right)^{\frac{q-1}{2}} I_{q-1}\left[\mu\delta\sqrt{-2\delta + y^2}\right] \qquad \left(\text{valid for } \sqrt{\mu}\,y < 1\right)$$

where I is the modified Bessel function. Note that for real y and δ, $F_q^{(1)}$ is purely imaginary only for $-2\delta + y^2 > 0$ or $-2\mu\delta + \mu y^2 > 0$. Otherwise the I function converts to a J Bessel function, $-2\delta + y^2$ becomes $2\delta - y^2$, the i disappears and $F_q^{(1)}$ becomes real. (In particular for $y = 0$, we know from Fig. 1 that for real ω, F_q is complex only for $\delta < 0$.)

We now look at two limiting cases of Eq. (35b). For $\mu y|\delta|^{\frac{1}{2}} \ll 1$, the small argument expansion of I gives

$$\mathcal{F}_q^{(1)} = -ie^{\mu\delta}(-\mu\delta)^{q-1} \frac{\pi}{\Gamma(q)} \left\{1 - \frac{\mu y^2}{2}\left[2 + \frac{q-1}{\mu\delta} + \frac{\mu\delta}{q}\right]\right\} \qquad \begin{matrix}(\text{Valid for} \\ \sqrt{\mu}\,y < 1 \text{ and} \\ \mu\sqrt{|\delta|}\,y \ll 1)\end{matrix} \qquad (35c)$$

which is identical with Eq. (16a) in conjunction with (26a) or (31e). For $\mu y|\delta|^{\frac{1}{2}} \gg 1$, the large argument expansion of I yields

$$\mathcal{F}_q^{(1)} = -i\sqrt{\frac{\pi}{2\mu}} \frac{1}{y}\left(1 - \frac{2\delta}{y^2}\right)^{\frac{q}{2} - \frac{3}{4}} \exp\left\{-\frac{\mu}{2}\left[\sqrt{y^2 - 2\delta} - y\right]^2\right\} \qquad \left(\text{Valid for } \frac{1}{\sqrt{\mu}} > y > \frac{1}{\mu\sqrt{|\delta|}}\right) \qquad (35d)$$

We show later than this formula is actually valid for $\delta \gg y > \frac{1}{\mu\sqrt{|\delta|}}$

For larger values of y or k_n, the form for $\mathcal{J}_q$ in (14b) is invalid and we must use the original definition in Eq. (7). Let us make the transformation

$$it = \frac{1}{1-y^2}\left[1 - \frac{y(1-\delta)}{\sqrt{y^2+\delta^2-2\delta}}\right] + i\varepsilon$$

then $$[(1-it)^2 + y^2t^2] = \left[\frac{y}{[y^2+\delta^2-2\delta]^{\frac{1}{2}}} - i\varepsilon(1-\delta)\right]^2 + \varepsilon^2(y^2+\delta^2-2\delta)$$

The motivation for the above transformation is that, as we show below, first order ε terms cancel in the expansion of the exponential factor in $\mathcal{J}_q$ and only terms of order ε^2 or higher survive. We find

$$\mathcal{J}_q = -i\int_{ic}^{\infty} d\varepsilon \left\{\left[\frac{y}{\sqrt{y^2+\delta^2-2\delta}} - i\varepsilon(1-\delta)\right]^2 + \varepsilon^2(y^2+\delta^2-2\delta)\right\}^{-q/2}$$

$$\times \exp\left\{\frac{\mu(\delta-y^2)}{1-y^2} + \frac{\mu y(1-\delta)^2}{(1-y^2)\sqrt{y^2+\delta^2-2\delta}} - \mu(1-\delta)i\varepsilon - \mu\left[\left(\frac{y}{\sqrt{y^2+\delta^2-2\delta}} - i\varepsilon(1-\delta)\right)^2 + \varepsilon^2(y^2+\delta^2-2\delta)\right]^{\frac{1}{2}}\right\} \tag{36}$$

where $$c = \left[1 - \frac{y(1-\delta)}{\sqrt{y^2+\delta^2-2\delta}}\right] \Big/ (1-y^2)$$

The contribution $\mathcal{J}_q^{(1)}$ is obtained by taking the lower integral limit as zero, (i.e. subtracting of the o to ic contribution) and letting $\varepsilon \to 0$. Note that first order terms in ε cancel in the exponential. Thus

$$\mathcal{J}_q^{(1)} = -i\frac{(y^2+\delta^2-2\delta)^{q/2}}{y^q}\exp\left[\frac{\mu(\delta-y^2)+\mu y\sqrt{y^2+\delta^2-2\delta}}{1-y^2}\right]\int_0^\infty d\varepsilon \exp\left[\frac{-\mu\varepsilon^2}{2y}\left(y^2+\delta^2-2\delta\right)^{3/2}\right]$$

$$= -i\sqrt{\frac{\pi}{2\mu}}\frac{(y^2+\delta^2-2\delta)^{q/2-3/4}}{y^{q-\frac{1}{2}}}\exp\left[\frac{\mu(\delta-y^2)+\mu y\sqrt{y^2+\delta^2-2\delta}}{1-y^2}\right] \qquad \text{(Valid for } y \neq 0\text{)}$$

(36b)

For $y << \delta$ $(1-y^2 \approx 1)$ and neglecting δ^2 terms, Eq. (36b) reduces to (35d). Hence we can extend the range of validity of (35d) as we indicated. Also the lower limit of validity of (36b) is obviously $y > \frac{1}{\mu\sqrt{|\delta|}}$.

In the third limiting situation of $y^2 >> \delta$, we find from (36b) that

$$\mathcal{J}_q^{(1)} = -\frac{i}{y}\sqrt{\frac{\pi}{2\mu}}\left[1-\frac{\delta}{y^2}(q-3/2)\right]\exp\left[-\zeta^2\left(1+\frac{\delta}{y^2}\right)\right] \qquad \text{(Valid for } y^2 >> \delta\text{)}$$

(36c)

$$\approx \frac{i\sqrt{\pi}\, e^{-\zeta^2}}{(\sqrt{2k_\parallel c^2/\omega v_t})} \qquad \text{where } \zeta^2 = \frac{(\omega-n\omega_b)^2}{2k_\parallel{}^2 v_t{}^2} = \frac{\delta^2\mu}{2y^2} \tag{36d}$$

Since $i\sqrt{\pi}e^{-\zeta^2}$ is one of the parts of the Z function (see Eq. 30a) and recalling Eq. (13), we see that the transition of the $\mathcal{J}_q$ function to the Z function has been demonstrated at least for part of these functions. Comparing Eq. (36a) and (36d), we note that the Z function becomes valid only for $k_\parallel$ large enough that $y^2 >> \delta$ which is the condition given in (9).

VII. THE TRACK OF REAL F_q

As we indicated in Sec. (4) we are interested in the frequency track of real F_q i.e. in finding the values of real and imaginary ω for real F_q. Strictly speaking, we should actually be concerned with the function $\mathcal{F}_q$ rather than F_q. However, the previous section indicated the great difficulty in a complete analysis or expansion of $\mathcal{F}_q$. We restrict the analysis to small $k_{\parallel}$ values for which we get a substantial component of group velocity propagation perpendicular to the magnetic field lines, and then the damping of the wave (viz $\mathcal{F}_q^{(1)}$ in Sec. VI) is small. We are mainly concerned with $k_{\parallel}^2 < v_t^2\omega^2/c^4$ in which case Eq. (16a) applies to a first approximation and $\mathcal{F}_q \approx F_q$ to zero approximation. Hence the track of real F_q very nearly follows the track of real $\mathcal{F}_q$ for very small $k_{\parallel}$.

In a nonrelativistic treatment, $\frac{\omega}{\mu(\omega - n\omega_b)}$ is the real function that replaces F_q in the analysis. Thus nonrelativistically, the function goes to $\pm\infty$ as $\omega \to n\omega_b$. These are the dashed curves indicated in Fig. 1. Relativistically, we note that F_q remains real for $\omega > n\omega_b$ and is finite for $\omega = n\omega_b$. For real $\omega < n\omega_b$, F_q is complex and bounded. The track of real F_q to be found below is identical for $\omega > n\omega_b$ and ω is also real here. Beyond this $\omega = n\omega_b$ point on the track, we can expect the track for complex ω to yield larger and larger values of F_q as $|\mu\delta|$ increases and eventually F_q goes to $+\infty$. There is also a distinctly separate track for negative F_q for which F_q goes to $-\infty$. These tracks in some sense imitate the nonrelativistic behaviour.

The mathematical statement of the above is simple. We recall Eq. (33b) valid for large $|\mu\delta|$. The positive F_q track which follows the curve in Fig. 1 up to $\omega = n\omega_b$ is obtained by taking Im $i\sqrt{\mu\delta} > 0$ which is satisfied since $\mu\delta$ is real and positive here. Hence $\sigma = 0$ and for $\mu\delta >> 1$, F_q is a decreasing function behaving as $(\mu\delta)^{-1}$. However beyond the $\omega = n\omega_b$ point, we change to the lower sheet for which Im $\omega < 0$ or Im $i\sqrt{\mu\delta} < 0$. (See Figs. 2a,2b). Although the real part of ω initial dips below $n\omega_b$, it soon rises again above $n\omega_b$, so that the real part of $\mu\delta$ is positive and steadily increasing. Since $\sigma = 2$ in this case, F_q goes to infinity as $2\pi|\mu\delta|^{q-1}e^{|\mu\delta|}/\Gamma(q)$. Of course we cannot believe our analysis if δ is not small, but even for $\delta = 0.1$, $e^{\mu\delta}$ is an enormcus number.

The negative F_q track is also readily understood. The track always lies in the lower half plane. The initial part of the track follows the dashed curve in Fig. 1. Although for this track Im $i\sqrt{\mu\delta} < 0$ always, and $\sigma = 2$, we note that the real part of $z \equiv \mu\delta$ is negative and consequently, the exponential part in Eq. (33b) decays as $e^{-|z|}$ and F decreases as z^{-1} for large negative z. However, as ω_{real} increases, the real part of z becomes positive. Keeping ω_{imag} negative ($\sigma = 2$), F_q goes to minus infinity as $-2\pi|\mu\delta|^{q-1}e^{|\mu\delta|}/\Gamma(q)$ (see Figs. 2c,2d). Note that the singularity of $F_q(z)$ is located at Im $i\sqrt{z} = -\infty$ or $z = \infty$ on the lower sheet. The tracks one must take in either the z or $i\sqrt{z}$ planes to make F_q real are shown in Fig. 3. (If one follows the indicated ω points, one gets the tracks for real ω and complex F_q corresponding to the results in Fig. 1.)

A schematic plot of the real function F_q versus the real part of ω is shown in Fig. 4a and an expanded view of the region where $\delta < 1$ (the region where our analysis applies) is also shown in 4b. Below we

give equations for positive F_q valid in the regions AB, CD, EFG, and HI and for negative F_q in regions JK, and LM.

Let us look at the track for positive F_q. The region AB is simply that for which $\sigma = 0$ and $F_q(z) = z^{-1}$ for large z. The curve AC is identical to that plotted in Fig. 1. Past point C, z starts to become complex. Denote $z = |z|e^{i\theta}$ and note from Fig. 3 that $2\pi < \theta < \pi$ so that initially in CD, $\theta \approx \pi + \delta\theta$. Also since $|z|$ is small, we can write using Eq. (31a)

$$F_{n+\frac{1}{2}}(z) \approx \frac{1}{(n+\frac{1}{2})} - \frac{z}{(n^2-\frac{1}{4})} - \frac{\pi(-z)^{-n}\sqrt{z}\,e^{z}}{\Gamma(n+\frac{3}{2})}$$

$$= \frac{1}{(n+\frac{1}{2})} - \frac{|z|(\cos\theta + i\sin\theta)}{(n^2-\frac{1}{4})} - \frac{\pi|z|^{n+\frac{1}{2}}}{\Gamma(n+\frac{3}{2})} e^{|z|\cos\theta} e^{i|z|\sin\theta} e^{-i\pi n} e^{i\theta(n+\frac{1}{2})}$$

To make the imaginary part of F zero, we require

$$\frac{-|z|\sin\theta}{n^2-\frac{1}{4}} - \frac{\pi|z|^{n+\frac{1}{2}}e^{|z|\cos\theta}}{\Gamma(n+\frac{3}{2})} \sin\left[|z|\sin\theta + \theta(n+\tfrac{1}{2}) - \pi n\right] = 0$$

This is possible for $\theta = \pi + \Delta\theta$ with

$$\Delta\theta \approx \frac{(n^2-\frac{1}{4})}{\Gamma(n+\frac{3}{2})}\pi|z|^{n-\frac{1}{2}}e^{-|z|} \tag{37a}$$

Then

$$F_{n+\frac{3}{2}}(z) = \frac{1}{n+\frac{1}{2}} - \frac{z_r}{(n^2-\frac{1}{4})} \quad \text{where } z_r = \text{real part of } z \approx \left(\frac{\omega_r - n\omega_b}{\omega_r}\right)\mu \tag{37b}$$

It can also be easily shown how F is made real for large $|z|$ values. In this case we use Eq. (33b) with $\sigma = 2$.

$$F_{n+3/2}(z) \approx \frac{1}{z} - \frac{2\pi(-z)^n}{\Gamma(n+3/2)} \sqrt{z}\, e^z \tag{38a}$$

Writing again $z = |z|\, e^{i\theta}$ we see that

$$F_{n+3/2}(z) \approx \frac{(\cos\theta - i\sin\theta)}{|z|} + \frac{2\pi|z|^{n+\frac{1}{2}}}{\Gamma(n+3/2)} e^{|z|\cos\theta} e^{-i\pi(n+1)} e^{i(n+\frac{1}{2})\theta} e^{i|z|\sin\theta} \tag{38b}$$

To have real F, we require

$$-\frac{\sin\theta}{|z|} + \frac{2\pi|z|^{n+\frac{1}{2}}}{\Gamma(n+3/2)} e^{|z|\cos\theta} \sin\left[|z|\sin\theta + (n+\tfrac{1}{2})\theta - \pi(n+1)\right] = 0 \tag{38c}$$

Let us consider values of $2\pi \geq \theta \geq 3\pi/2$ for which $\cos\theta > 0$.

Since $|z|$ is large, $|z|^{n+\frac{1}{2}} e^{|z|\cos\theta}$ is very large so in order to satisfy the above equation, we require the argument of the sine function to be very near zero.

$$|z|\sin\theta + (n+\tfrac{1}{2})\theta - \pi(n+1) = 0 \tag{38d}$$

In this case

$$F_{n+3/2}(z) \approx \frac{\cos\theta}{|z|} + \frac{2\pi|z|^{n+\frac{1}{2}} e^{|z|\cos\theta}}{\Gamma(n+3/2)} \approx \frac{2\pi|z|^{n+\frac{1}{2}} e^{|z|\cos\theta}}{\Gamma(n+3/2)} \tag{38e}$$

This formula applies along the complete track beyond point E for which $\theta = 3\pi/2$. Provided $|z| \ll \mu$, the following approximations are valid

$$\frac{c^2}{v_t^2}\left(\frac{\omega_r - n\omega_b}{n\omega_b}\right) \approx |z|\cos\theta \quad \text{and} \quad \frac{c^2\omega_i}{v_t^2 n\omega_b} \approx |z|\sin\theta \tag{38f,g}$$

Near point E, $\theta = \frac{3\pi}{2} + \Delta\theta$ and Eq. (38d) gives

$$|z| = \left(\frac{n\pi}{2} - \frac{\pi}{4}\right) + \left(n + \tfrac{1}{2}\right)\Delta\theta \tag{39a}$$

so that

$$z_r = |z|\Delta\theta = \left(\frac{n\pi}{2} - \frac{\pi}{4}\right)\Delta\theta \quad \text{and} \quad z_i \approx -|z| \tag{39b,c}$$

Since $z_i = \mu\omega_i n\omega_b/|\omega|^2$ and $z_r = \mu\,[1 - \omega_r n\omega_b/|\omega|^2]$, one can solve for ω_r and ω_i in terms of $\Delta\theta$ to yield

$$\omega \approx n\omega_b\left[1 + \left(\frac{n\pi}{2} - \frac{\pi}{4}\right)\frac{\Delta\theta}{\mu} - \left(\frac{n\pi}{2} - \frac{\pi}{4}\right)^2 \frac{1}{\mu^2}\right] \tag{39d}$$

and

$$\omega_i \approx -\frac{n\omega_b}{\mu}\left[\frac{n\pi}{2} - \frac{\pi}{4} + \left(n + \frac{1}{2}\right)\Delta\theta\right] \tag{39e}$$

Exactly at point E, $\Delta\theta = 0$ and

$$\omega_r = n\omega_b\left[1 - \frac{v_t^2}{c^2}\left(\frac{n\pi}{2} - \frac{\pi}{4}\right)^2\right], \quad \omega_i \approx \frac{-v_t^2}{c^2}\, n\omega_b\left(\frac{n\pi}{2} - \frac{\pi}{4}\right) \tag{39f,g}$$

and Eq. (38e) reduces to

$$F_{n+\frac{3}{2}}(z) = \frac{2\pi}{\Gamma(n+\frac{3}{2})}\left[\frac{n\pi}{2} - \frac{\pi}{4}\right]^{n+\frac{1}{2}} \tag{39h}$$

Note that ω_r is slightly less than $n\omega_b$ at point E. Slightly further along the track at point F, ω_r is exactly equal to $n\omega_b$ again. Solving Eq. (39d) for $\Delta\theta$

$$\Delta\theta = \left(\frac{n\pi}{2} - \frac{\pi}{4}\right)\frac{1}{\mu} \quad \text{and} \quad \theta = \frac{3\pi}{2} + \left(\frac{n\pi}{2} - \frac{\pi}{4}\right)\frac{v_t^2}{c^2} \tag{39i}$$

Beyond point H, the angle θ is very nearly equal to 2π, say $\theta = 2\pi - \Delta\theta$. Eq. (38d) shows that $|z|\Delta\theta \approx \pi n$ or $z_i = |z| \sin\theta = -\pi n$ and $z_r = |z| \cos\theta \approx |z| = \pi n/\Delta\theta$. Since $z_i = \mu\omega_i n\omega_b/|\omega|^2$ and $z_r = \mu[\omega_r(\omega_r - n\omega_b) + \omega_i^2]/|\omega|^2$ we can solve for ω_r and ω_i in terms of $\Delta\theta$ to yield

$$\omega_r = \frac{\frac{\mu n\omega_b}{n\pi}\left(\frac{\mu}{n\pi} - \frac{1}{\Delta\theta}\right)}{1 + \left(\frac{\mu}{n\pi} - \frac{1}{\Delta\theta}\right)^2} \quad \text{and} \quad \omega_i = \frac{-\mu n\omega_b}{n\pi}\,\frac{1}{\left[1 + \left(\frac{\mu}{n\pi} - \frac{1}{\Delta\theta}\right)^2\right]} \tag{40a,b}$$

All the structure beyond point H shown in Fig. 4a can be described in terms of Eqs. (40a,b). However the validity of our analysis imposes the limits that $\Delta\theta > n\pi/\mu = n\pi v_t^2/c^2$. In this case, expanding Eqs. (40a,b) we get

$$\omega_r = n\omega_b\left(1 + \frac{v_t^2 n\pi}{c^2\Delta\theta}\right) \quad \text{and} \quad \omega_i = -n\omega_b\left(\frac{v_t^2 n\pi}{c^2}\right) \tag{40c,d}$$

For the times of interest in Alouette data, $\omega_r t \approx 10^4$ so that $\omega_i t$ is minute and cannot account for the time decay. Thus we see that ω_i is always negligible even with respect to $10^{-4} n\omega_b$, but ω_r can differ fractionally from $n\omega_b$. Also solving to first order Eq. (40a) for $\Delta\theta$ in terms of ω_r, we find that $|z| = \pi n/\Delta\theta \approx \mu(\omega_r - n\omega_b)/\omega_r$ which is the value for $|z|$ to be inserted in the following:

$$F_{n+3/2}(z) = 2\pi |z|^{n+\frac{1}{2}} e^{|z|} / \Gamma(n+3/2) \qquad (40e)$$

namely Eq. (38b) for $\theta \approx 2\pi$.

We can also investigate part of the track for negative F_q, namely regions JK and LM in both of which $|z|$ is large. Writing $z = |z| e^{i\theta}$, $\pi \leq \theta \leq 2\pi$, Eqs. (38a-c) apply. For region JK, $\theta \approx \pi + \Delta\theta$ and substituting this into Eq. (38c) we find

$$\Delta\theta = \frac{2\pi |z|^{n-\frac{1}{2}}}{\Gamma(n+\frac{1}{2})} e^{-|z|} \quad , \quad F = -\frac{1}{|z|} \quad \text{where } z \approx \mu\left(\frac{\omega_r - n\omega_b}{\omega_r}\right) \qquad (41a,b,c)$$

For region LM, we take $\theta \approx 2\pi - \Delta\theta$, but instead of taking the argument of the sine function equal to zero as before, we now equate it to $-\pi$. Instead of Eq. (38d), we have

$$|z| \sin\theta + (n+\tfrac{1}{2})\theta - \pi n = 0 \quad \text{or} \quad |z| \Delta\theta = (n+1)\pi \qquad (42a)$$

Equations (40a-d) apply here as well with $(n+1)\pi$ replacing $n\pi$. Also $|z| \approx \mu\ (\omega_r - n\omega_b)/\omega_r$ as before and

$$F_{n+3/2}(z) = \frac{\cos\theta}{|z|} + \frac{2\pi |z|^{n+\frac{1}{2}}}{\Gamma(n+3/2)} e^{|z|\cos\theta} \cos(-\pi) \approx -2\pi |z|^{n+\frac{1}{2}} e^{|z|} / \Gamma(n+3/2) \qquad (42b)$$

Note that $F_{n+3/2}$ has the same form as in (40e) but is of opposite sign. The above completes our investigation on the analytic continuation of the F function. This function will be used in Part 2 to obtain dispersion curves of frequency versus wave number.

VIII. CORRECTION TERMS TO THE DIELECTRIC TENSOR ELEMENTS FROM HIGHER λ POWERS

In certain cases in Part 2, we require higher order λ terms to the dielectric tensor elements. These terms will now be derived for $k_n = 0$ using Eq. (5b) and expanding $e^{-\Lambda} I_n(\Lambda)$ to two higher order terms. We have

$$e^{-\Lambda} I_n(\Lambda) = \frac{\Lambda^n}{n! 2^n}\left(1 - \Lambda + \frac{\Lambda^2}{4(n+1)} + \frac{\Lambda^2}{2}\right) \tag{43a}$$

$$e^{-\Lambda}(I_n' - I_n) = \frac{\Lambda^{n-1}}{n! 2^n}\left[n - \Lambda(1+n) + \Lambda^2\left(\frac{n+2}{4(n+1)} + 1 + \frac{n}{2}\right)\right] \tag{43b}$$

$$e^{-\Lambda}\left[\frac{-n^2 I_n}{\Lambda} + 2\Lambda(I_n - I_n')\right] = \frac{\Lambda^{n-1}}{n! 2^n}\left[n^2 - \Lambda(2n + n^2) + \Lambda^2\left(2 + \frac{n^2}{4(n+1)} + 2n + \frac{n^2}{2}\right)\right] \tag{43c}$$

In the manipulations yielding Eq. (8) from (5b), we note that every extra power of Λ raises the order of q in $\mathcal{F}_q$ (or F_q for $k_n = 0$) by one. Thus we obtain using Eq. (43a).

$$(\varepsilon_{11})_{warm} = -\mu \frac{\omega_p^2}{\omega^2} \frac{n^2}{2^n n!} \lambda^{n-1}\left[F_{n+3/2} - \lambda F_{n+5/2} + \lambda^2 F_{n+7/2}\left(\frac{1}{4(n+1)} + \frac{1}{2}\right)\right] \tag{44a}$$

$$(\varepsilon_{33})_{warm} = -\mu \frac{\omega_p^2}{\omega^2} \frac{\lambda^n}{2^n n!}\left[F_{n+5/2} - \lambda F_{n+7/2} + \lambda^2 F_{n+9/2}\left(\frac{1}{4(n+1)} + \frac{1}{2}\right)\right] \tag{44b}$$

using Eq. (43b)

$$(-i\varepsilon_{21})_{warm} = (i\varepsilon_{12})_{warm} = -\mu \frac{\omega_p^2}{\omega^2} \frac{n^2}{2^n n!} \lambda^{n-1} \left[F_{n+3/2} - \frac{\lambda(1+n)}{n} F_{n+5/2} \right.$$

$$\left. + \frac{\lambda^2}{n} \left(\frac{n+2}{4(n+1)} + 1 + \frac{n}{2} \right) F_{n+7/2} \right] \qquad (44c)$$

and using Eq. (43c)

$$(\varepsilon_{22})_{warm} = -\mu \frac{\omega_p^2}{\omega^2} \frac{n^2}{2^n n!} \lambda^{n-1} \left[F_{n+3/2} - \lambda \frac{(2+n)}{n} F_{n+5/2} + \frac{\lambda^2}{n^2} \left(2 + 2n + \frac{n^2}{4(n+1)} + \frac{n^2}{2} \right) F_{n+7/2} \right]$$

(44d)

The additional terms provide correction terms in the dispersion relations in the relativistic case. In the nonrelativistic limit, they however predict unrealistically, a completely new wave as is shown in part 2 .

IX. THE DIELECTRIC TENSOR FOR THE FUNDAMENTAL (n = 1) CYCLOTRON FREQUENCY

For the fundamental frequency, the "cold terms" in Eq. (23a) are incorrect. For the "cold terms", we allow only n = - 1 in $\varepsilon_{11}, \varepsilon_{12}$ and ε_{33}, keeping n = +1 for the "warm terms". Thus

$$(\varepsilon_{cold})_{\alpha\beta} = \begin{pmatrix} 1 - \frac{\omega_p^2}{2\omega(\omega + \omega_b)} & \frac{i\omega_p^2}{2\omega(\omega + \omega_b)} & 0 \\ \frac{-i\omega_p^2}{2\omega(\omega + \omega_b)} & 1 - \frac{\omega_p^2}{2\omega(\omega + \omega_b)} & 0 \\ 0 & 0 & 1 - \frac{\omega_p^2}{\omega^2} \end{pmatrix} \qquad (45a)$$

To order λ^2, the warm terms are given by Eqs. (44a - d) for $k_\parallel = 0$. Thus

$$(\varepsilon_{11})_{warm} = -\frac{\mu}{2}\frac{\omega_p^2}{\omega^2}\left[F_{5/2} - \lambda F_{7/2} + \frac{5}{8}\lambda^2 F_{9/2}\right] \tag{45b}$$

$$(\varepsilon_{33})_{warm} = -\frac{\mu}{2}\frac{\omega_p^2}{\omega^2}\left[F_{7/2} - \lambda F_{9/2} + \frac{5}{8}\lambda^2 F_{11/2}\right] \tag{45c}$$

$$(-i\varepsilon_{21})_{warm} = (i\varepsilon_{12})_{warm} = -\frac{\mu}{2}\left[F_{5/2} - 2\lambda F_{7/2} + \frac{15}{8}\lambda^2 F_{9/2}\right] \tag{45d}$$

$$(\varepsilon_{22})_{warm} = -\frac{\mu}{2}\left[F_{5/2} - 3\lambda F_{7/2} + \frac{37}{8}\lambda^2 F_{9/2}\right] \tag{45e}$$

If we wish to include $k_{\parallel}$ to first order we can use Eq. (23c) with $n = 1$.

X. RELATION TO OTHER WORK

Trubnikov (1961), Drummond and Rosenbluth (1960, 1961), Beard (1959), Beard and Baker (1961, 1962) and Bekefi et al (1961) have all considered cyclotron radiation from a hot plasma. Their basis is either the individual particle approach with perhaps some account for the distribution function or otherwise the full relativistic approach (Eq. 1) without applying the expansion in terms of Bessel functions. The values for the dielectric matrix elements are integrated either using a computer or applying a saddle point method as first indicated by Trubnikov. They also provide results as $k_{\parallel}$ varies away from zero. However one basic assumption of these workers is that $k^2c^2/\omega^2 = 1$ and $\omega >> \omega_p$ which simplifies the analysis exceedingly. Essentially, they consider only the electromagnetic extraordinary and ordinary waves near the light line rather than investigating wave dispersion for the whole range of k values with

$\lambda \lesssim 1$ as we do in Part 2. The saddle point method is useful when v_t/c is not too small and cyclotron harmonic lines can overlap. In the very slightly relativistic limit when the lines are distinct, the Bessel function expansion is more appropriate.

Demidov and Frank-Kamenetskii (1964) have treated less rigorously the same problem as Dnestrovskii et al (1964). Their results disagree and it seems that Demidov's final function, equivalent to our F function, is in error. On the other hand, the works of Rukhadze and Silin (1962) and Gershman (1961) conform in principle with our and Dnestrovskii et al's results.

Many authors have treated the line shape and absorption effects near cyclotron harmonics using nonrelativistic theory. (See for example, Silin and Rukhadze (1961 pp. 144-7), Gershman (1960).) If $k_\parallel$ is sufficiently large that Eq. (9) is satisfied, these analyses are valid and the concept of "cyclotron absorption" is meaningful. Our development here and in Part 2 covers the range of lower $k_\parallel$ values, after the transition from "cyclotron absorption" to "relativistic absorption" has occurred.

We complete this report having shown that the relativistic analysis is necessary for $\frac{\omega - n\omega_b}{\omega} > \frac{k_\parallel^2 c^2}{\omega^2}$ and especially in the region $(\omega - n\omega_b)/\omega \lesssim v_t^2/c^2$ and $k_\parallel \lesssim v_t\omega/c^2$. The transition to the nonrelativistic case has been clearly illustrated. The necessary dielectric tensor elements have been derived with which we can investigate the dispersion of waves near cyclotron harmonics.

REFERENCES

Beard, D.B. - Phys. Fluids 2, 379 (1959).

Beard, D.B. and J.C. Baker - Phys. Fluids 4, 611 (1961); 5, 1113 (1962).

Bekefi, G, J.L. Hirshfield and S.C. Brown - Phys. Rev. 122, 1037 (1961).

Demidov, V.P. and D.A. Frank-Kamenetskii, Sov. Phys. - Tech. Phys. 8, 686 (1964).

Dnestrovskii, Yu. N., D.P. Kostomarov, and N.V. Skrydlov - Sov. Phys.-Tech. Phys. 8, 691 (1964).

Drummond, W.E. and M.N. Rosenbluth - Phys. Fluids 3, 45 (1960); 3, 491 (1960); 6, 276 (1961).

Fried, B.D. and S.D. Conte - "The Plasma Dispersion Function", Academic Press, N.Y. (1961).

Gershman, B.N. - Sov. Phys. JETP 11, 657 (1960).

Gershman, B.N. - Sov. Phys. Doklady 6, 314 (1961).

Landau, L.D. and E.M. Lifshitz - "Electromagnetics of Continuous Media", Addison-Wesley Pub. Co.,Reading, Mass. (1960).

Magnus, W. and F. Oberhettinger, "Formulas and Theorems for the Special Functions of Mathematical Physics", Chelsea Pub. Co., N.Y. (1949).

Rukhadze, A.A. and V.P. Silin - Sov. Phys.-Tech. Phys. 7, 307 (1962).

Shkarofsky, I.P. - "The Dispersion of Waves in Cyclotron Harmonic Resonance Regions with Application to the Alouette", Part 2 of this report.

Silin, V.P. and A.A. Rukhadze - "Electromagnetic Properties of Plasma and Plasma-like Media", Glavatomizdat, Moscow (1961) (in Russian).

Stix, T.H. - "The Theory of Plasma Waves", McGraw-Hill Book Co., N.Y. (1962).

Trubnikov, B.A., Collection - "Plasma Physics and the Problem of Controlled Thermonuclear Reactions", Editor - M.A. Leontovich, Pergamon Press, N.Y. (1959), Vol. III, p. 122.

Trubnikov, B.A. - Phys. Fluids 4, 195 (1961).

CAPTIONS FOR FIGURES

Fig. 1: Graphs of the real and imaginary parts of $F_{n+3/2}(\mu\delta)$ for n = 1,2,3 versus $\mu\delta = \frac{c^2}{v_t^2}\left(\frac{\omega - n\omega_b}{\omega}\right)$ when ω is real. The dashed curves, $(\mu\delta)^{-1}$, are the asymptotic limits for large $\mu\delta$ and represent the nonrelativistic functions replacing F.

Fig. 2a: Position of $i\sqrt{z}$ in the complex z plane initially, for the positive F track when $\omega \geq n\omega_b$.

2b: Position of $i\sqrt{z}$ for the continued positive F track.

2c: Position of $i\sqrt{z}$ initially, for the negative F track.

2d: Position of $i\sqrt{z}$ for the continued negative F track.

Fig. 3a: The two tracks of real F in the complex z plane. The positive F track runs from $\omega = -0$ through $\omega = n\omega_b$ and then turns to the lower sheet. The negative F track runs from $\omega = 0$ on the lower sheet. Both tend towards the singularity of the F function.

3b: The same tracks in the complex $i\sqrt{z}$ plane.

Fig. 4a: Schematic plot of the values of F versus real part of ω for complex ω and real F. The rectangular cut indicates the region where the analysis is valid.

Fig. 4b: Expanded view of region where analysis is valid.

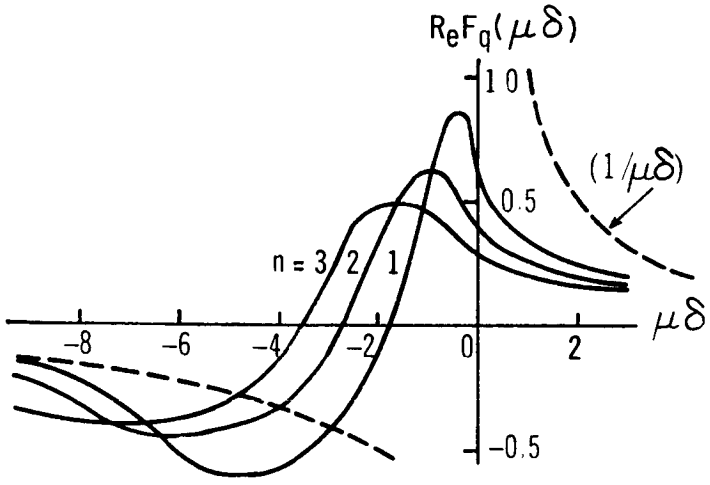

FIGURE 1(a)

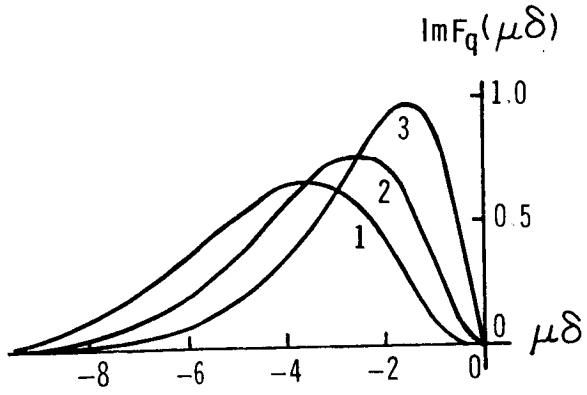

FIGURE 1(b)

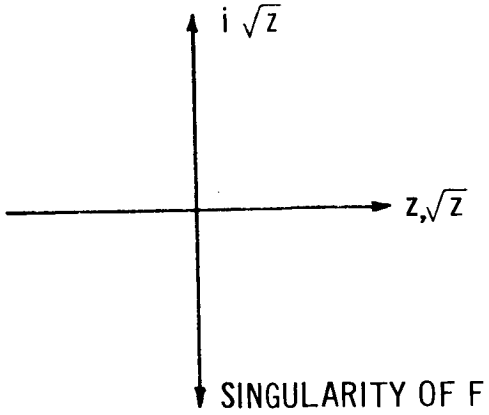

FIGURE 2(a)

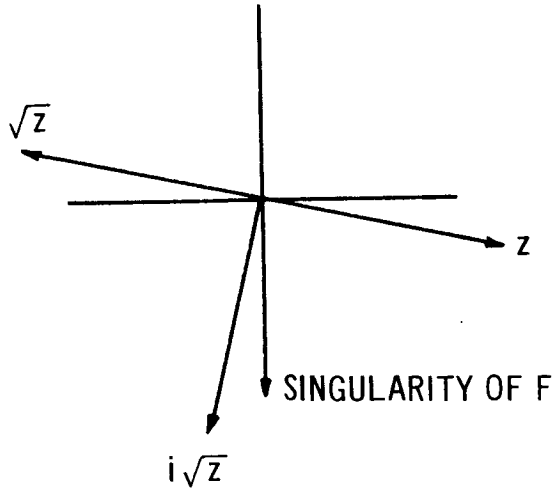

FIGURE 2(b)

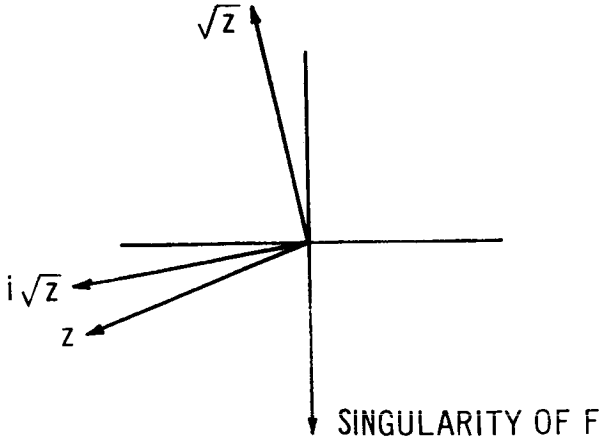

FIGURE 2(c)

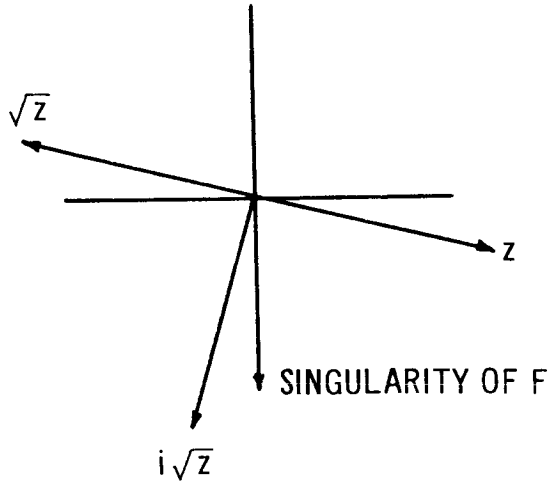

FIGURE 2(d)

THE DISPERSION OF WAVES IN CYCLOTRON HARMONIC RESONANCE REGIONS WITH APPLICATION TO THE ALOUETTE

I.P. Shkarofsky

RCA Victor Co. Ltd.
Research Laboratories
Montreal, Canada

- ABSTRACT -

The dispersion of waves near electron cyclotron harmonics is investigated including to first order, wave numbers parallel to the magnetic field. The proper relativistic form for the dielectric tensor elements is applied. Distinct different behaviours result depending on whether the wave number or frequency is taken to be complex. In the former case, the waves near the Appleton-Hartree values are localized and a gap exists between them and the plasma wave. In the latter case, no gap exists except as one tends to zero wave number where the dispersion curve indicates a rapid rise in frequency above the harmonic. Matching points of satellite velocity to the wave group velocity are found for the extraordinary and ordinary waves. The relativistic formulation is compared with the nonrelativistic one and the differences are noted.

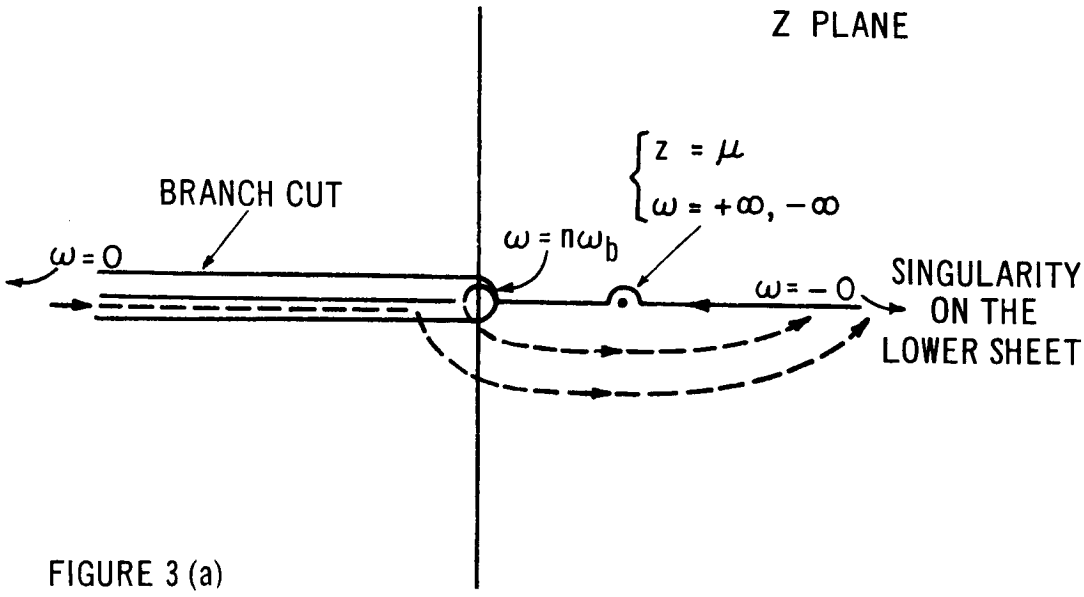

FIGURE 3 (a)

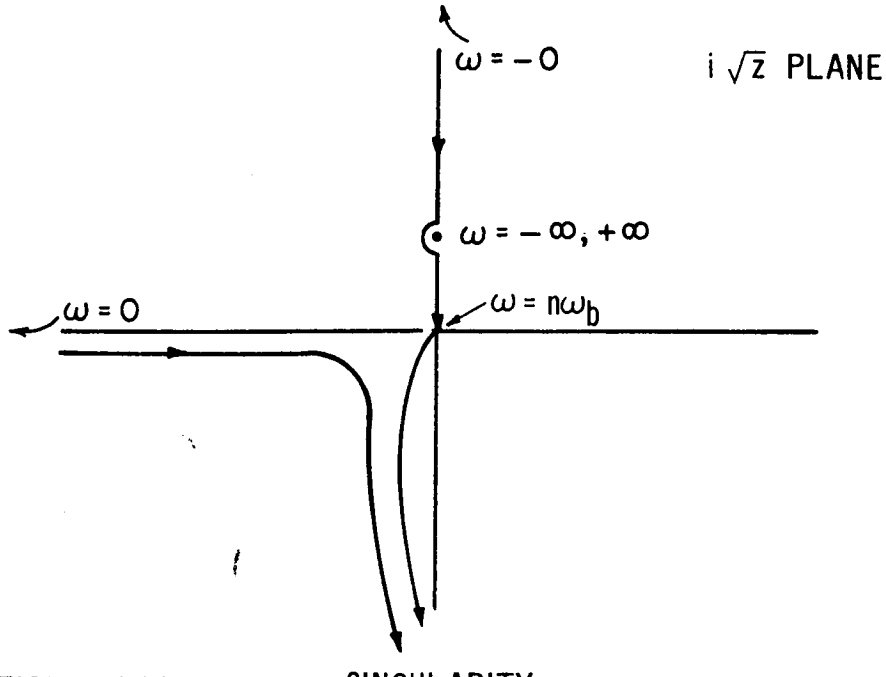

FIGURE 3 (b)

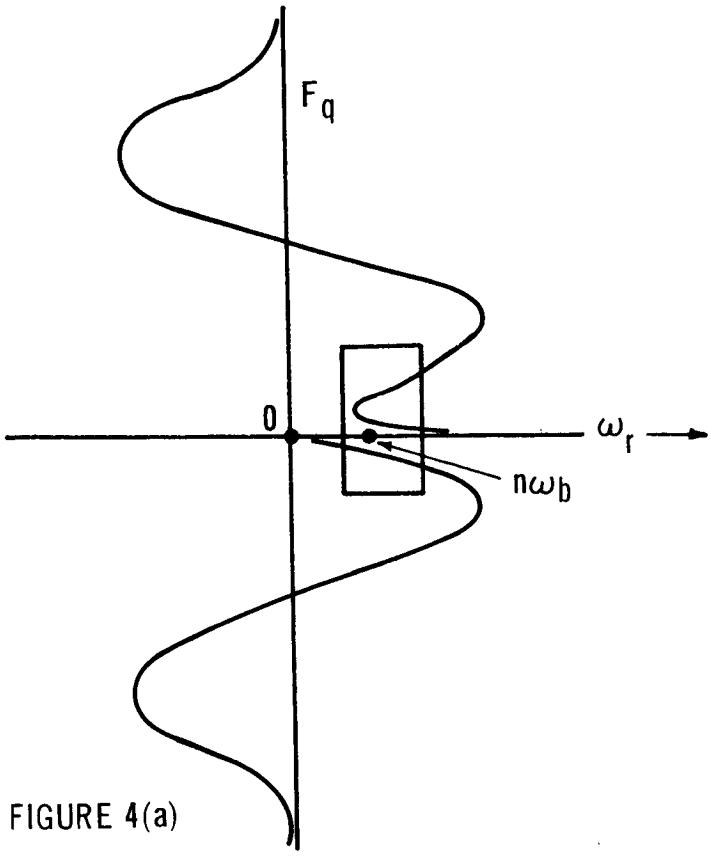

FIGURE 4(a)

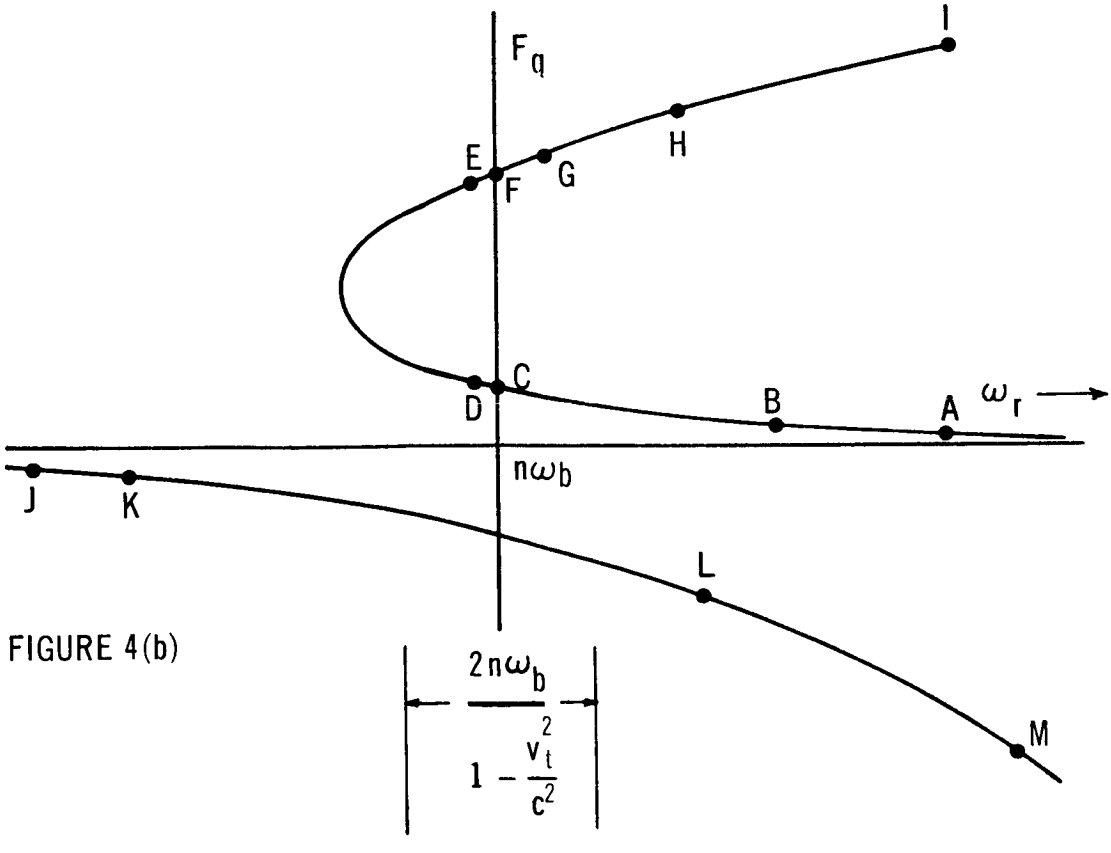

FIGURE 4(b)

I. INTRODUCTION

In this report we investigate the dispersion of plasma waves near cyclotron harmonics applying relativistic analysis and comparing the results with those found using nonrelativistic analysis. Whereas the latter predicts for $k_{\parallel} = 0$ three waves (i.e. three values of real ω for a given real $k_{\perp}$) near each cyclotron harmonic, the relativistic analysis requires either complex k or complex ω with totally different dispersion curves very near $n\omega_b$ for the two cases. For complex $k_{\perp}$ and real ω, it will be shown that we still get the extraordinary, plasma and ordinary waves but with gaps in the $k_{\perp}$ spectrum, that is regions where one cannot obtain a real ω for a given complex $k_{\perp}$. These gaps effectively separate the Appleton-Hartree and electrostatic plasma waves. On the other hand, for complex ω and real $k_{\perp}$, we can cover the complete $k_{\perp}$ spectrum except for a very tiny region near $k_{\perp} = 0$. Furthermore, there are now only two waves (the ordinary and a combined extraordinary-plasma wave) instead of three. These results are in essence the original contributions in this report on the subject of dispersion of cyclotron harmonics.

Dnestrovskii and Kostomarov (1961, 1962) have computed for $k_{\parallel} = 0$ the dispersion curves from the nonrelativistic analysis. In this report we give analytical results for values of $k_{\perp} < v_t/\omega_b$ and show how the three waves are derived. For the electrostatic modes, we investigate more fully larger values of $k_{\perp}$ and determine the points where the group velocity is a maximum and where it is zero. Plots are given of group velocity versus $k_{\perp}$.

In order to apply the above results to Alouette cyclotron harmonic data (Lockwood, 1963), we have to include the motion of the satellite. If the transmitter were stationary, the longest lasting response is derived from "stationary waves", i.e. those with zero group velocity. Since the satellite is moving, however, the longest response comes from waves moving at the satellite velocity. We shall prove that such a match can be accomplished both parallel and perpendicular to magnetic field lines. We need exceedingly small values of $k_{\parallel}$. The value of $k_{\perp}$ can be either of the order of the free space wave number or an order of magnitude less than the free space wave number. The Doppler shift in frequency is always very small. Furthermore, the small value of $k_{\parallel}$ necessitates a relativistic approach (see Part 1). Other possibly matching points as well as zero group velocity points will also be pointed out for both the relativistic and nonrelativistic analyses. In particular, it will be shown that it is very difficult to match for harmonics greater than the fourth, velocities perpendicular to magnetic field lines using the electrostatic modes.

II. THE DISPERSION EQUATION FOR $\lambda < 1$ AND $k_{\parallel}^2 c^4/v_t^2\omega^2 < 1$

(a) Basic Relations

We shall derive the dispersion relation for very small $k_{\parallel}$ and moderately small $k_{\perp}$ given by

$$\lambda \equiv k_{\perp}^2 v_t^2/\omega_b^2 < 1 \quad \text{and} \quad k_{\parallel}^2 c^4/v_t^2\omega^2 < 1 \tag{1a,b}$$

where $k_{\perp}$, $k_{\parallel}$ are wave number perpendicular and parallel to magnetic field lines, $\omega_b = |eB/m|$, $v_t^2 = \kappa T/m$, and e, m, B, c, ω, κ and T have their usual significance. The analysis will use the relativistic dielectric tensor elements expanded to first order in λ and $k_{\parallel}^2$. We shall point out in Secs. III and V the corresponding nonrelativistic results and the substitutions required to obtain them.

The dispersion relation for waves in a plasma is

$$\left| -\frac{k^2c^2}{\omega^2}\delta_{\alpha\beta} + \frac{c^2}{\omega^2}k_\alpha k_\beta + \varepsilon_{\alpha\beta} \right| = 0 \qquad (2a)$$

We write $\varepsilon_{\alpha\beta} = (\varepsilon_{\alpha\beta})_{cold} + (\varepsilon_{\alpha\beta})_{warm}$, which are respectively the cold Appleton-Hartree dielectric tensor elements and the "warm" elements associated with a particular cyclotron harmonic. Thus

$$\left| -\frac{k^2c^2}{\omega^2}\delta_{\alpha\beta} + \frac{c^2}{\omega^2}k_\alpha k_\beta + (\varepsilon_{\alpha\beta})_{cold} + (\varepsilon_{\alpha\beta})_{warm} \right| = 0 \qquad (2b)$$

We now insert the dielectric tensor elements given by Eqs. (23b) and (23e) of Part 1 of this collection. The determinent D to be evaluated is with $k_\perp$ along the x axis and $k_\parallel$ and B along the z axis:

$$0 = D = \begin{vmatrix} K_\perp - k_\parallel^2\frac{c^2}{\omega^2} - k_\perp^{2(n-1)}\frac{c^2}{\omega^2}P(\rho+\beta k_\parallel^2) & i\left[K_x + k_\perp^{2(n-1)}\frac{c^2}{\omega^2}P(\rho+\beta k_\parallel^2)\right] & k_\perp k_\parallel\frac{c^2}{\omega^2}\left(1-Qk_\perp^{2(n-1)}\frac{c^2}{\omega^2}\eta\right) \\ -i\left[K_x + k_\perp^{2(n-1)}\frac{c^2}{\omega^2}P(\rho+\beta k_\parallel^2)\right] & K_\perp - \frac{k^2c^2}{\omega^2} - k_\perp^{2(n-1)}\frac{c^2}{\omega^2}P(\rho+\beta k_\parallel^2) & -ik_\perp k_\parallel\frac{c^4}{\omega^4}Qk_\perp^{2(n-1)}\eta \\ k_\perp k_\parallel\frac{c^2}{\omega^2}\left(1-Qk_\perp^{2(n-1)}\frac{c^2}{\omega^2}\eta\right) & ik_\perp k_\parallel\frac{c^4}{\omega^4}Qk_\perp^{2(n-1)}\eta & K_\parallel - \frac{k_\perp^2c^2}{\omega^2} - k_\perp^{2n}\frac{c^2}{\omega^2}P'(\rho'+\beta' k_\parallel^2) \end{vmatrix} \qquad (3)$$

where $K_\perp = 1 - \frac{\omega_p^2}{(\omega^2-\omega_b^2)}$; $K_\parallel = 1 - \frac{\omega_p^2}{\omega^2}$; $K_x = \frac{\omega}{\omega_b}\left(K_\parallel - K_\perp\right) = \frac{\omega_p^2\omega_b}{\omega(\omega^2-\omega_b^2)}$ (4a,b,c)

$$P = \frac{\omega_p^2}{v_t^2}\left(\frac{v_t}{\omega_b}\right)^{2(n-1)}\frac{n^2}{n!2^n}\ ;\quad Q = \frac{\omega_p^2\omega}{n\omega_b v_t^2}\left(\frac{v_t}{\omega_b}\right)^{2(n-1)}\frac{n^2}{n!2^n}\ ;\quad P' = \frac{\omega_p^2}{v_t^2}\left(\frac{v_t}{\omega_b}\right)^{2n}\frac{1}{n!2^n} \qquad (4d,e,f)$$

$$\rho = F_{n+3/2}(\mu\delta)\ ;\quad \beta = \frac{c^4}{2v_t^2\omega^2}\left(F_{n+1/2} - 2F_{n+3/2} + F_{n+5/2}\right)\ ;\quad \eta = F_{n+3/2} - F_{n+5/2} \qquad (4g,h,i)$$

$$\rho' = F_{n+5/2}\ ;\quad \beta' = \frac{3c^4}{2v_t^2\omega^2}\left(F_{n+3/2} - 2F_{n+5/2} + F_{n+7/2}\right)\ ;\quad \mu = \frac{c^2}{v_t^2}\ ;\quad \delta = \frac{\omega - n\omega_b}{\omega} \qquad (4j,k,l,m)$$

Also $\omega_p = \sqrt{n_e e^2/\varepsilon_0 m}$ is the plasma frequency, $k^2 = k_\perp^2 + k_\parallel^2$, n_e is electron density and n is the order of the cyclotron harmonic ($n \neq 1$). The function F_q is defined by

$$F_q(z) \equiv -i\int_0^\infty \frac{e^{izt}dt}{(1-it)^q}\ , \qquad (4n)$$

and was investigated at length in Part 1.

(b) The Extraordinary and Plasma Modes

Let us restrict ourselves at present to the extraordinary and plasma waves; later we consider the ordinary wave. Since the ordinary wave is associated with the 33 element of the determinant, for the other waves the warm part of this element is of higher order in λ and can be neglected. That is we approximate the 33 element by $(K_\parallel - k_\perp^2 c^2/\omega^2)$. Now let us expand the determinant by using the subdeterminants of the 33, 32 and 31 elements and dividing the result by the 33 element. We obtain after some grouping

$$0 = D =$$

$$\left(K_\perp + \frac{k_\parallel^2 c^2}{\omega^2} - \frac{k_\perp^2 c^2}{2\omega^2}\right)\left\{K_\perp - K_x - \frac{k_\parallel^2 c^2}{\omega^2} - \frac{k_\perp^2 c^2}{2\omega^2} - 2k_\perp^{2(n-1)}\frac{c^2}{\omega^2}P(\rho+\beta k_\parallel^2)\right.$$

$$\left. + 2k_\perp^2 k_\parallel^2 \frac{c^6}{\omega^6}\frac{Q\eta k_\perp^{2(n-1)}}{\left[K_\parallel - \frac{k_\perp^2 c^2}{\omega^2}\right]} - 2k_\perp^2 k_\parallel^2 \frac{c^8}{\omega^8}\frac{\left(Q\eta k_\perp^{2(n-1)}\right)^2}{\left[K_\parallel - k_\perp^2\frac{c^2}{\omega^2}\right]}\right\}$$

$$- \frac{k_\perp^4 c^4}{4\omega^4} - \frac{k_\perp^2 k_\parallel^2 c^4}{\omega^4\left[K_\parallel - \frac{k_\perp^2 c^2}{\omega^2}\right]}\left\{K_\perp - \frac{k_\perp^2 c^2}{\omega^2} - \frac{k_\parallel^2 c^2}{\omega^2} - k_\perp^{2(n-1)}\frac{c^2}{\omega^2}P(\rho+\beta k_\parallel^2) + Q\eta k_\perp^{2(n-1)}k_\perp^2\frac{c^4}{\omega^4}\right\} \tag{5a}$$

The above form is useful only for small k. A somewhat different grouping yields the following dispersion equation, useful for larger k values.

$$D = \left(K_\perp + K_x - \frac{k_\parallel^2 c^2}{\omega^2}\right)\left(K_\perp - K_x - \frac{k_\parallel^2 c^2}{\omega^2}\right)$$

$$- \frac{k_\perp^2 c^2}{\omega^2}\left[K_\perp + 2k_\perp^{2(n-2)}P(\rho+\beta k_\parallel^2)\left(K_\perp + K_x - \frac{k_\parallel^2 c^2}{\omega^2}\right) - \frac{k_\parallel^2 c^2}{\omega^2}\left(1 - \frac{K_\perp - \frac{k^2 c^2}{\omega^2}}{K_\parallel - \frac{k_\perp^2 c^2}{\omega^2}}\right)\right]$$

$$+ \left(\frac{k_\perp^2 c^2}{\omega^2}\right)^2\left[k_\perp^{2(n-2)}P(\rho+\beta k_\parallel^2) + \frac{2k_\parallel^2 c^2}{\omega^2}\frac{Q\eta k_\perp^{2(n-2)}}{\left[K_\parallel - \frac{k_\perp^2 c^2}{\omega^2}\right]}\left(K_\perp + K_x - \frac{k^2 c^2}{\omega^2}\right)\right.$$

$$\left. + \frac{k_\parallel^2 c^2}{\omega^2}\frac{P(\rho+\beta k_\parallel^2)k_\perp^{2(n-2)}}{\left[K_\parallel - \frac{k_\perp^2 c^2}{\omega^2}\right]}\right]$$

$$+ \left(\frac{k_\perp^2 c^2}{\omega^2}\right)^3 \frac{k_\parallel^2 c^2}{\omega^2}\frac{\left(Q\eta k_\perp^{2(n-2)}\right)^2}{\left[K_\parallel - \frac{k_\perp^2 c^2}{\omega^2}\right]}\left[\frac{k_\perp^2 c^2}{\omega^2} - 2\left(K_\perp + K_x - \frac{k_\parallel^2 c^2}{\omega^2}\right)\right] = 0 \tag{5b}$$

An order of magnitude comparison of the terms involving Q with the product term $P\beta k_{\parallel}^2$ shows that all the Q terms are negligible for the ranges of $k_{\parallel}$ and $k_{\perp}$ of interest. In particular, the Q term within the x^3 bracket (where $x \equiv k_{\perp}^2 c^2/\omega^2$) is negligible with respect to the $P\beta k_{\parallel}^2$ within the x bracket. Furthermore both the second and third terms are negligible compared to the first within the x^2 bracket. Thus Eq. (5b) simplifies to

$$\left(K_l - \frac{k_{\parallel}^2 c^2}{\omega^2}\right)\left(K_r - \frac{k_{\parallel}^2 c^2}{\omega^2}\right)$$

$$- x\left[K_{\perp} - \frac{k_{\parallel}^2 c^2}{\omega^2}\left(1 - \frac{K_{\perp} - \frac{k^2 c^2}{\omega^2}}{K_{\parallel} - \frac{k_{\perp}^2 c^2}{\omega^2}}\right) + 2\left(K_l - \frac{k_{\parallel}^2 c^2}{\omega^2}\right) P k_{\perp}^{2(n-2)} (\rho + \beta k_{\parallel}^2)\right]$$

$$+ x^2\left[P k_{\perp}^{2(n-2)} (\rho + \beta k_{\parallel}^2)\right] = 0 \qquad (6)$$

where $K_l = K_{\perp} + K_x = 1 - \dfrac{\omega_p^2}{\omega(\omega + \omega_b)}$; $K_r = K_{\perp} - K_x = 1 - \dfrac{\omega_p^2}{\omega(\omega - \omega_b)}$ (7a,b)

$$K_{\perp} = (K_l + K_r)/2 = 1 - \frac{\omega_p^2}{(\omega^2 - \omega_b^2)} \quad \text{and} \quad x = \frac{k_{\perp}^2 c^2}{\omega^2} \qquad (7c,d)$$

The quadratic equation (6) in x can be solved when $P k_{\perp}^{2(n-2)} (\rho + \beta k_{\parallel}^2) \ll 1$. The smaller x solution is

$$x = \left(K_l - \frac{k_{\parallel}^2 c^2}{\omega^2}\right)\left(K_r - \frac{k_{\parallel}^2 c^2}{\omega^2}\right) \Big/ \left[K_{\perp} - \frac{k_{\parallel}^2 c^2}{\omega^2}\left(1 - \frac{K_{\perp} - \frac{k^2 c^2}{\omega^2}}{K_{\parallel} - \frac{k_{\perp}^2 c^2}{\omega^2}}\right)\right] \qquad (8a)$$

which is the extraordinary electromagnetic mode. The larger x solution is

$$x = \left[K_\perp - \frac{k_n^2 c^2}{\omega^2}\left(1 - \frac{K_\perp - \frac{k^2 c^2}{\omega^2}}{K_n - \frac{k_\perp^2 c^2}{\omega^2}}\right)\right] \Big/ \left[k_\perp^{2(n-2)} P(\rho + \beta k_n^2)\right] \tag{8b}$$

which is the mode for large wave numbers. If we consider real ω and complex $k_\perp$ or x, then ρ lies within bounds of order one in magnitude (see Part 1). Since $Pk_\perp^{2(n-2)}$ is always less than one for $\lambda \lesssim 1$, we see that the above condition on $Pk_\perp^{2(n-2)}$ $\rho << 1$ is satisfied. As a result the solution of Eq. (6) can never deviate much from the cold em mode or large wave number mode. One cannot propagate a wave for $k_\perp$ values between these two modes.

The situation for real $k_\perp$ or x and complex ω is different. As shown in Part 1, the F function or ρ can be continued into the lower half plane and can attain huge values. In fact the product $Pk_\perp^{2(n-2)}\rho$ can easily become of order one. Under these conditions one can obtain solutions of Eq. (6) for any value of x.

In particular let us look at the solution for $x < 1$. Then either Eq. (6) or (5a) yields

$$D = \left(K_\perp - \frac{x}{2} - \frac{k_n^2 c^2}{\omega^2}\right)\left\{K_r - \frac{k_n^2 c^2}{\omega^2} - \frac{x}{2} - 2k_\perp^{2(n-1)} \frac{c^2}{\omega^2} P(\rho + \beta k_n^2)\right\}$$

$$- \frac{k_\perp^4 c^4}{4\omega^4} - \frac{k_\perp^2 k_n^2 c^4}{\omega^4\left[K_n - \frac{k_\perp^2 c^2}{\omega^2}\right]}\left[K_\perp - \frac{k^2 c^2}{\omega^2}\right] = 0 \tag{9a}$$

In particular for $x \ll 1$ and $k_\parallel^2 c^2/\omega^2 \ll 1$, we have

$$D = \left(K_1 - \frac{x}{2} - \frac{k_\parallel^2 c^2}{\omega^2}\right)\left\{K_r - 2k_\perp^{2(n-1)}\frac{c^2}{\omega^2}P(\rho+\beta k_\parallel^2) - \frac{k_\parallel^2 c^2}{\omega^2} - \frac{x}{2}\right\} = 0 \qquad (9b)$$

This is the simple form the determinant attains as $k \to 0$. Since the first factor is non-zero, the dispersion relation is approximately

$$K_r - 2k_\perp^{2(n-1)}\frac{c^2}{\omega^2}P(\rho+\beta k_\parallel^2) = 0 \qquad (9c)$$

In the analysis above, we took $k_\perp$ along the x axis. To evaluate the Green's function we have to obtain the ratio of the subdeterminants to the determinant including the ϕ angle associated with a general $k_\perp$ in the x-y plane. (In the evaluation of the determinant itself, the k_x^2 and k_y^2 wave numbers combine to give $k_\perp^2$ independant of ϕ, which accounts for the reason why we were able to restrict the $k_\perp$ direction.) For the situation $\lambda < 1$ that we have considered above, the modifications are very simple. Essentially all $\sin\phi$ or $\cos\phi$ terms which appear in the warm terms are either multiplied by higher power of λ or by the Q term which is neglected in any case. Thus we only have to consider ϕ terms in the $k_\alpha k_\beta$ part of Eq. (2b). With this modification, the 11 subdeterminant — after dividing by the 33 element as we did for Eq. (5a) — is

$$R_{11} = K_\perp - \frac{k_\parallel^2 c^2}{\omega^2} - \frac{k_\perp^2 c^2}{\omega^2}\cos^2\phi - k_\perp^{2(n-1)}\frac{c^2}{\omega^2}P(\rho+\beta k_\parallel^2) - \frac{k_\perp^2 k_\parallel^2 c^4 \sin^2\phi}{\omega^4\left[K_\parallel - \frac{k_\perp^2 c^2}{\omega^2}\right]} \qquad (10a)$$

where $k_x = k_\perp \cos\phi$ and $k_y = k_\perp \sin\phi$. The last term is negligible compared to the $P\beta k_\parallel^2$ term. Similarly the 12 subdeterminant is

$$R_{12} = i\left[K_x + k_\perp^{2(n-1)} \frac{c^2}{\omega^2} P(\rho+\beta k_\parallel^2)\right] - \frac{k_\perp^2 c^2}{\omega^2} \sin\phi \cos\phi + \frac{k_\perp^2 k_\parallel^2 c^4 \sin\phi \cos\phi}{\omega^4 \left[K_\parallel - \frac{k_\perp^2 c^2}{\omega^2}\right]} \tag{10b}$$

The subdeterminants R_{11} and R_{12} are the relevant Green's function parameters for excitation by a source of current flow in the xy plane.

Let us average the ratio $R_{\alpha\beta}/D$ over ϕ, assuming that the only ϕ dependence is that shown in $R_{\alpha\beta}$ (and neglecting any ϕ dependence associated with satellite motion). Using the relations:

$$\int_0^{2\pi} d\phi\ e^{iz\sin\phi} \begin{pmatrix} 1 \\ \cos^2\phi \\ \sin^2\phi \\ \cos\phi\ \sin\phi \end{pmatrix} = \begin{pmatrix} 2\pi J_0(z) \\ J_0(z) + J_2(z) \\ J_0(z) - J_2(z) \\ 0 \end{pmatrix} \tag{11}$$

where J is a Beseel function, we find for $\overline{R_{ij}/D} = \int e^{-k_\perp r\cos\phi} R_{ij}/D\, d\phi$

$$\overline{R_{11}} = \left[K_\perp - \frac{k_\parallel^2 c^2}{\omega^2} - \frac{k_\perp^2 c^2}{2\omega^2} - k_\perp^{2(n-1)} \frac{c^2}{\omega^2} P(\rho + \beta k_\parallel^2)\right] J_0(k_\perp r) - \frac{k_\perp^2 c^2}{2\omega^2} J_2(k_\perp r) \tag{12a}$$

and

$$\overline{R_{12}} = i\left[K_x + k_\perp^{2(n-1)} \frac{c^2}{\omega^2} P(\rho+\beta k_\parallel^2)\right] J_0(k_\perp r) \tag{12b}$$

where r is the distance of the detector or receiver from the transmitter.

For satellites detecting their own transmitted signals, r is the distance travelled by the satellite, $r = Vt$ where V is its velocity and t is the time after transmission. For the case $k_\perp r = k_\perp Vt \ll 1$ or for times $t \ll (k_\perp V)^{-1}$, we can neglect $J_2(k_\perp r)$ and approximate $J_0(k_\perp r)$ by one. Usually this condition is satisfied for $x = k_\perp^2 c^2/\omega^2 \lesssim 1$. Note that in this situation we also have

$$\overline{R_{11} + iR_{12}} = K_r - \frac{k_\parallel^2 c^2}{\omega^2} - \frac{x}{2} - 2k_\perp^{2(n-1)}\frac{c^2}{\omega^2}P(\rho+\beta k_\parallel^2) \qquad (13a)$$

and

$$\overline{R_{11} - iR_{12}} = K_l - \frac{k_\parallel^2 c^2}{\omega^2} - \frac{x}{2} \qquad (13b)$$

Using Eq. (9b) we find that for $x \ll 1$,

$$\overline{R_{11} + iR_{12}/D} = \left[K_l - \frac{x}{2} - \frac{k_\parallel^2 c^2}{\omega^2}\right]^{-1} \qquad (14a)$$

which has no warm term in it and hence is of no interest for cyclotron harmonics. We also find

$$\overline{R_{12} - iR_{12}/D} \approx \left[K_r - 2k_\perp^{2(n-1)}\frac{c^2}{\omega^2}P(\rho+\beta_\parallel^2)\right]^{-1} \qquad (14b)$$

which has interesting cyclotron harmonic parameters. (Compare Eqs. (14b) and (9c).) The above two equations also indicate that as $x \to 0$ or $k \to 0$, the cyclotron harmonic wave becomes circularly polarized since only the $R_{11} - iR_{12}$ part has to be considered. This part is also most important if a circular wave in the xy plane is excited by the source current.

(c) The Ordinary Wave

Besides the extraordinary–plasma wave mode, there is another wave associated with the 33 element of Eq. (3), namely the ordinary wave. To obtain the dispersion relation for this ordinary wave including first order $k_\parallel$ terms, we expand D and divide this time by X, where X denotes the following combination of elements [(11)(22) - (12)(21)], viz

$$X = \left[K_\perp - \frac{k_\parallel^2 c^2}{\omega^2} - \frac{k_\perp^2 c^2}{2\omega^2}\right]\left[K_\perp - \frac{k_\parallel^2 c^2}{\omega^2} - \frac{k_\perp^2 c^2}{2\omega^2} - 2k_\perp^{2(n-1)} \frac{c^2}{\omega^2} P(\rho+\beta k_\parallel^2)\right] - \frac{k_\perp^4 c^4}{4\omega^4} \tag{15a}$$

To obtain any noticeable deviation from the "cold ordinary wave" $K_\parallel - k_\perp^2 c^2/\omega^2 = 0$, we require $k_\perp^{2n} c^2 P'\rho'/\omega^2$ to be of order one. In this case we note that the $k_\perp^{2(n-1)} \frac{c^2}{\omega^2} P\rho$ terms are much greater than one by order λ^{-1}, so that in X, we can neglect K_r, k^2c^2/ω^2, etc. with respect to the warm term.

$$X \approx -2k_\perp^{2(n-1)}\frac{c^2}{\omega^2}P(\rho+\beta k_\parallel^2)\left[K_\perp - \frac{k_\parallel^2 c^2}{\omega^2} - \frac{k_\perp^2 c^2}{2\omega^2}\right] \approx -2k_\perp^{2(n-1)}\frac{c^2}{\omega^2}P\rho\left[K_\perp - \frac{k_\parallel^2 c^2}{\omega^2} - \frac{k_\perp^2 c^2}{2\omega^2}\right] \tag{15b}$$

Similarly in evaluating D, we keep only products of warm terms, viz PQ, Q^2 and PQ^2. The PQ^2 and PQ terms cancel. The determinant thus becomes the following, after division by X and then inserting Eq. (15b).

$$D = K_{11} - \frac{k_\perp^2 c^2}{\omega^2} - k_\perp^{2n}\frac{c^2}{\omega^2}P'(\rho'+\beta' k_\parallel^2) - \frac{2}{X}\left[Q\eta\frac{c^4}{\omega^4}k_\perp k_\parallel k_\perp^{2(n-1)}\right]^2\left(K_\perp - \frac{k_\parallel^2 c^2}{\omega^2} - \frac{k_\perp^2 c^2}{2\omega^2}\right)$$

$$= K_{11} - \frac{k_\perp^2 c^2}{\omega^2} - k_\perp^{2n}\frac{c^2}{\omega^2}P'\rho' - k_\perp^{2n}k_\parallel^2\frac{c^2}{\omega^2}\left[P'\beta' - \frac{Q^2\eta^2 c^4}{P\rho\,\omega^4}\right] \tag{16a}$$

Now from Eqs. (4f,g,i,k) we have

$$P'\beta' - \frac{Q^2\eta^2c^4}{P\rho\omega^4} = \frac{\omega_p^2}{v_t^2}\left(\frac{v_t}{\omega_b}\right)^{2n}\frac{1}{n!2^n}\frac{c^4}{2v_t^2\omega^2}\left\{3F_{n+\frac{1}{2}} - 6F_{n+3/2} + 3F_{n+5/2} - \frac{2(F_{n+3/2}-F_{n+5/2})^2}{F_{n+3/2}}\right\}$$

$$= \frac{\omega_p^2}{v_t^2}\left(\frac{v_t}{\omega_b}\right)^{2n}\frac{1}{n!2^n}\frac{c^4}{2v_t^2\omega^2}\left\{7F_{n+5/2} - 8F_{n+3/2} + 3F_{n+1/2} - 2F^2{}_{n+5/2}/F_{n+3/2}\right\}$$

$$\equiv P'\beta''$$

where $$\beta'' = \frac{c^4}{2v_t^2\omega^2}\left\{7F_{n+5/2} - 8F_{n+3/2} + 3F_{n+1/2} - 2F^2{}_{n+5/2}\Big/F_{n+3/2}\right\} \qquad (16b)$$

The dispersion eq. for the ordinary wave is thus

$$D = K_n - \frac{k_\perp^2c^2}{\omega^2} - k_\perp 2n\frac{c^2}{\omega^2}P'(\rho' + \beta''k_n^2) \qquad (16c)$$

The subdeterminant of the 33 element, R_{33}, after division by X and approximating as in Eq. (15b) is simply unity, (even including ϕ terms in $k_\alpha k_\beta$). Hence

$$\frac{R_{33}}{D} = \left[K_n - \frac{k_\perp^2c^2}{\omega^2} - k_\perp 2n\frac{c^2}{\omega^2}P'(\rho'+\beta''k_n^2)\right]^{-1} \text{ and } \overline{\frac{R_{33}}{D}} = \frac{R_{33}}{D}J_0(k_\perp r) \approx \frac{R_{33}}{D} \qquad (16d)$$

if $k_\perp r << 1$. This ratio is relevant for the Green's function if excitation is caused by a current source in the z-direction.

III. THE DISPERSION EQUATION FOR $k_{\parallel} = 0$ AND $\lambda < 1$

In this section, by restricting ourselves to $k_{\parallel} = 0$, we can investigate more fully the higher powers of λ neglected previously. Using the proper relativistic approach, we find the additional terms negligible except when $2K_1 = x$. If, however, we incorrectly insert the nonrelativistic limits into the relations in the region where they are not applicable viz. where $\mu\delta < 1$, a new wave results. This wave has appeared in calculations of cyclotron harmonics upon ad hoc application of nonrelativistic analysis (e.g. Dnestrovskii and Kostomarov 1962 — see Sec. V for a full discussion).

For $k_{\parallel} = 0$, the dispersion equation (2a) for the extraordinary and plasma waves reduces to

$$\varepsilon_{11}(\varepsilon_{22} - x) - \varepsilon_{12}\varepsilon_{21} = 0 \quad \text{with } x = k^2c^2/\omega^2,\ k = k_{\perp} \tag{17a}$$

Inserting the cold elements given in Eq. (23b) and the warm elements given in Eq. (44) of Part 1, we find

$$K_1K_r - xK_{\perp} - 2xK_1k^{2(n-2)}P\left[F_{n+3/2} - \frac{\lambda}{n}F_{n+5/2}(1+n) + \frac{\lambda^2}{n}F_{n+7/2}\left(\frac{n+2}{4(n+1)} + 1 + \frac{n}{2}\right)\right]$$

$$- k^{2(n-2)}Px\lambda^2K_{\perp}\frac{(2+n)}{n^2(n+1)}F_{n+7/2} + x^2k^{2(n-2)}P\left[F_{n+3/2} - \lambda F_{n+5/2} + \lambda^2 F_{n+7/2}\left(\frac{1}{4(n+1)} + \frac{1}{2}\right)\right]$$

$$+ k^{4(n-2)}\frac{P^2x^2\lambda^2}{n^2}\left[F_{n+3/2}F_{n+7/2}\left(\frac{n+2}{n+1}\right) - F^2_{n+5/2}\right] = 0 \tag{17b}$$

where K_1, K_r, $K_{\perp}$, P are defined in Eqs. (4) and (7) and where $\lambda = k^2v_t^2/\omega_b^2$.

If higher powers in λ are neglected in (17b), we simply obtain

$$K_l K_r - xK_\perp - 2xK_l k^{2(n-2)}{}_P F_{n+3/2} + x^2 k^{2(n-2)}{}_P F_{n+3/2} = 0 \qquad (18a)$$

or

$$\left(k^{2(n-2)}{}_P\, F_{n+3/2}\right)^{-1} = \frac{(2K_l - x)x}{K_l K_r - K_\perp x} \quad \text{or} \quad \left[\frac{\omega_b{}^2 2^n n!}{\omega_p^2 \lambda^{n-2} n^2}\right] \frac{1}{F_{n+3/2}} = \frac{(2K_l - x)x}{K_l K_r - K_\perp x} \qquad (18b)$$

Since $k^{2(n-2)}{}_P$ is extremely small, $F_{n+3/2}$ has to be large for x to deviate away from the electromagnetic mode ($K_l K_r \approx K_\perp x$) or the electrostatic mode ($x >> 1$). For large F all x values are possible except when $x \to 2K_l$ for which we might seem to require $F \to \infty$. This however is not necessary since we then include the higher powers of λ given in Eq. (17b). In fact, when $x \approx 2K_l$, Eq. (17b) gives the following equation that the F's have to satisfy.

$$1 = 4\lambda k^{2(n-2)}{}_P\, F_{n+5/2}\left\{1 + k^{2(n-2)}\, \frac{\lambda P}{n}\left[\frac{F_{n+3/2}\, F_{n+7/2}}{F_{n+5/2}}\left(\frac{n+2}{n+1}\right) - F_{n+5/2}\right]\right\} \qquad (19)$$

Thus a higher order of magnitude of F is required, $(\lambda k^{2(n-2)}{}_P)^{-1}$ instead of $(k^{2(n-2)}{}_P)^{-1}$. Equation (17) also shows that the only case we need these higher λ values for $\lambda < 1$ is near $x \approx 2K_l$.

We also note that for $n \geq 2$

$$K_{\binom{l}{r}} = 1 - \frac{\omega_p{}^2}{\omega(\omega \pm \omega_b)} \quad ; \quad K_\perp = 1 - \frac{\omega_p{}^2}{\omega^2 - \omega_p{}^2} \qquad (20a)$$

whereas for $n = 1$, we use Eq. (45a) of Part 1 to find equivalently that

$$K_\perp = K_x + 1 = 1 - \frac{\omega_p^2}{2\omega(\omega+\omega_b)}$$

so that

$$K_l = 1 - \frac{\omega_p^2}{\omega(\omega+\omega_b)}\ ,\quad K_r = 1\ ,\quad K_\perp = \frac{K_l + 1}{2} \tag{20b}$$

and Eq. (18b) becomes $\frac{\omega^2}{\omega_p^2}\frac{v_t^2}{c^2}\frac{1}{F_{5/2}} = \frac{2K_l - x}{2K_l - (K_l+1)x}$ (20c)

Real ω, Complex k Curves

We can now plot ω-k dispersion curves based on the above analysis. First we consider the case of real ω, complex F_q and hence complex k. Then we investigate the case of greater concern to us, namely real F_q, real k and complex ω.

When ω is real, the complex function F_q is plotted in Fig. 1 of Part 1. We note that both the real and imaginary parts of F_q lie within bounds of order one. As a result $k^{2(n-2)}{}_P\, F_q$ is an extremely small number for $n > 2$. Noting that $K_\perp = (K_l + K_r)/2$, we can readily solve the quadratic equation (18a) to yield under these conditions:

$$x = \frac{K_l K_r}{K_\perp}\left(1 - k^{2(n-2)}{}_P\, F_{n+3/2}\,\frac{K_l^2}{K_\perp^2}\right) \tag{21a}$$

and $$x = \frac{K_\perp}{k^{2(n-2)}{}_P\, F_{n+3/2}} + 2K_l - \frac{K_l K_r}{K_\perp} \approx \frac{K_\perp}{k^{2(n-2)}{}_P\, F_{n+3/2}} \tag{21b}$$

The first solution in Eq. (21a) only exists if $K_l K_r/K_\perp$ is positive and then it represents the Appleton-Hartree equation (extraordinary mode)

$k^2c^2/\omega^2 = x = K_1K_r/K_\perp$ with a small correction term (for $n > 2$).

For $n = 2$, the correction is noticeable. (The $n = 1$ case is investigated separately later.) The slope $\partial\omega/\partial k$ at $\omega = n\omega_b$ is altered negligibly by the warm terms for $n > 3$. To see this, let us evaluate $\partial k/\partial\omega = (\partial\omega/\partial k)^{-1}$. Note that F is real for $\omega \geq n\omega_b$ and at $\omega = \omega_b$, using Eq. (31a) of Part 1, we have

$$F_{n+3/2} = \frac{1}{n+1/2} \; ; \quad \frac{dF_{n+3/2}(\mu\delta)}{d(\mu\delta)} = F_{n+3/2} - F_{n+1/2} = -\frac{1}{(n^2-1/4)} \tag{22a,b}$$

and

$$\frac{d^2F_{n+3/2}}{d(\mu\delta)^2} = \frac{2}{(n^2-1/4)(n-3/2)} \; ; \quad \frac{\partial(\mu\delta)}{\partial\omega} = \frac{\mu n\omega_b}{\omega^2} \tag{22c,d}$$

From Eq. (21a), one finds that $(\partial k/\partial\omega)/(k/\omega)$ involves terms of order c_1, a constant, and a terms of order $(v_t^2/c^2)^{n-3}c_1$. This latter term comes from the derivative of $F_{n+3/2}$. One sees that for $n = 3$, $\partial\omega/\partial k(\omega/k) \approx c_1$ with the warm terms contributing about the same as the cold terms, whereas for $n > 3$, $\partial\omega/\partial k/(\omega/k) \approx c_1$ again but the warm terms give negligible correction. For $n = 2$, the warm term is larger by c^2/v_t^2 and therefore the dominant term. In fact for $n = 2$

$$\left.\frac{(\partial\omega/\partial k)}{\omega/k}\right|_{\omega=\omega_b} = 15\left(\frac{K_\perp v_t\omega_b}{K_1 c\,\omega_p}\right)^2 \tag{22e}$$

Hence the slope is very minute at this point, changing greatly as ω recedes from $n\omega_b$. One also notes from (21a) that for $\omega \geq n\omega_b$, $x < K_1K_r/K_\perp$ since $F > 0$ whereas for $\omega \ll n\omega_b$, F is more or less real and negative so that

$x > K_1 K_r / K_\perp$ (see Fig. 1 of Part 1). Hence the dispersion curve has a "wiggle" around $n\omega_b$. This wiggle is large only for n = 2 and negligible for $n \geq 3$. See Figs. 1a and 1b where this behaviour is illustrated. The dashed part indicates the region where k is complex.

For n = 1 we use Eq. (20c) and note that since $F_{5/2}$ is of order one, x is localized around $2K_1$. In fact

$$x \simeq 2K_1 + \frac{2\omega^2}{\omega_p^2} K_1^2 \frac{v_t^2}{c^2 F_{5/2}} \tag{23}$$

The warm term provides a negligible correction (see Fig. 1c). This solution exists only if $K_1 > 0$.

We now investigate the other branch of the dispersion curve associated with the solution in Eq. (21b). This solution occurs for large values of x when $n > 2$ but even for n = 2, it is separated completely from the em waves. When n = 1, Eq. (20c) shows that no extra solutions exist for $x \gg 1$ so that this effect or mode does not exist. Equation (21b) can be written in any one of the following ways (using Eq. (4d) for P).

$$k^{2(n-1)} = \frac{v_t^2}{c^2}\left(\frac{\omega_b^2}{v_t^2}\right)^{n-1}\left(\frac{\omega}{n\omega_b}\right)^2\left[\frac{\omega_b^2}{\omega_p^2} - \frac{\omega_b^2}{\omega^2 - \omega_b^2}\right]\frac{2^n n!}{F_{n+3/2}} \tag{24a}$$

$$k^2 = \left(\frac{v_t}{c}\right)^{\frac{2}{n-1}} \frac{\omega_b^2}{v_t^2}\left\{\left(\frac{\omega_b^2}{\omega_p^2} - \frac{\omega_b^2}{\omega^2 - \omega_b^2}\right)\frac{2^n n!\omega^2}{F_{n+3/2}(n\omega_b)^2}\right\}^{\frac{1}{(n-1)}} \tag{24b}$$

$$\frac{k^2 c^2}{\omega^2} = \left(\frac{c^2}{v_t^2}\right)^{\frac{n-2}{n-1}} \frac{\omega_b^2}{\omega^2}\left\{\left(\frac{\omega_b^2}{\omega_p^2} - \frac{\omega_b^2}{\omega^2 - \omega_b^2}\right)\frac{2^n n!\,\omega^2}{F_{n+3/2}(n\omega_b)^2}\right\}^{\frac{1}{(n-1)}} \tag{24c}$$

We thus see that $k^2 \propto F^{-1/(n-1)}$. Using the plot of complex F versus $\mu\delta$ in Fig. 1 of Part 1, we present here in Fig. 2a, a polar plot of F_{real} versus F_{imag}, in Fig. 2b, F_r^{-1} versus F_i^{-1} and in Fig. 2c, $F^{-1/(n-1)}$. The latter can be used to give the variation of k_r^2 versus $\mu\delta$ when $K_\perp > 0$ or $\omega_b^2/\omega_p^2 > \omega_b^2/(\omega^2 - \omega_b^2)$. See Fig. 3a. In the opposite situation when $K_\perp < 0$ or $\omega_b^2/\omega_p^2 < \omega_b^2/(\omega^2 - \omega_b^2)$, we present in Fig. 2d, 2e, 2f plots involving (-F) similar to Figs 2a - 2c. The dispersion curve is shown in Fig. 3b.

The dashed portions of the curve are the regions where k is quite complex. Figs. 3a and 3b show a minimum k or λ value below which the dispersion relation cannot be satisfied. This minimum value is much larger than the k values associated with the extraordinary em mode.

In Figs. 4a to 4d, we show together the em and es modes for the 4 possible situations, namely

(i) $K_\parallel > 0$, $K_r > 0$, $K_\perp > 0$ (ii) $K_\parallel < 0$, $K_r < 0$, $K_\perp < 0$

(iii) $K_\parallel > 0$, $K_r < 0$, $K_\perp > 0$ (iv) $K_\parallel > 0$, $K_r < 0$, $K_\perp < 0$.

Let us now evaluate the group velocity of the es mode when $K_\perp > 0$ at the point $\omega = n\omega_b$. Write k equal to $F^{-1/[2(n-1)]}$ times a factor which is more or less constant with respect to ω. That is, we assume that the crucial variation in ω is due to F. Using Eqs. (22a-d), we find using $\partial k/\partial\omega = 1/(\partial\omega/\partial k)$

$$\left.\frac{\partial\omega/\partial k}{\omega/k}\right|_{\omega = n\omega_b} = 2(n-1)(n-\tfrac{1}{2})\,\frac{v_t^2}{c^2} \qquad (25a)$$

Also since $\partial^2 k/\partial\omega^2 = -\partial^2\omega/\partial k^2/(\partial\omega/\partial k)^3$, we can evaluate the next derivative to obtain

$$\left.\frac{\partial^2\omega/\partial k^2}{\omega/k^2}\right|_{\omega = n\omega_b} = \frac{4(n-1)(n-\frac{1}{2})^3}{(n-\frac{3}{2})}\frac{v_t^2}{c^2} \tag{25b}$$

These relations indicate that the slope and curvature of the es mode are very small. The slope only becomes large in the immediate vicinity of the turn around point where k is quite complex.

We also note that the nonrelativistic limit for F is

$$F = \omega\, v_t^2/[c^2(\omega - n\omega_b)] = 2\omega^2\, v_t^2/[c^2\,(\omega^2 - n^2\omega_b^2)] \tag{26a}$$

The latter expression includes $-\omega$ values as well. Equation (26a) applies outside of the relativistic range at both ends of the em solution, but only when $K_\perp > 0$ and $\omega > n\omega_b$ for the es-solution. In the latter case, one can write using Eq. (24a)

$$\frac{\omega^2 - n^2\omega_b^2}{2\omega^2} = \left(\frac{v_t k}{\omega_b}\right)^{2(n-1)}\left(\frac{n\omega_b}{\omega}\right)^2 \frac{1}{2^n n!}\left[\frac{\omega_b^2}{\omega_p^2} - \frac{\omega_b^2}{\omega^2-\omega_b^2}\right]^{-1} \tag{26b}$$

which is the usual relation quoted for the Bernstein (1958) es mode when $\lambda << 1$. Essentially Eq. (26b) is equivalent to $\varepsilon_{11} = 0$. If we wish to include higher values of λ, we substitute $e^{-\lambda}I_n(\lambda)$ for $\lambda^n/2^n n!$ (see Eq. 20 of Part 1) where $\lambda = (k v_t/\omega_b)^2$. Equation (26b) becomes

$$\omega^2 - n^2\omega_b^2 = 2\omega_p^2 n^2 I_n(\lambda)e^{-\lambda}\Big/\left(1 - \frac{\omega_p^2}{\omega^2-\omega_b^2}\right)\lambda \tag{26c}$$

Besides the extraordinary wave, of great importance is the ordinary wave. When $k_{\parallel} = 0$, its dispersion relation is simply

$$\varepsilon_{33} = 0 \quad \text{or} \quad \frac{\omega_b^2}{\omega_p^2} \frac{2^n n!}{\lambda^{n-1} F_{n+5/2}} = \frac{x}{\left(1 - \frac{\omega_p^2}{\omega^2}\right) - x} \tag{27a}$$

where $\lambda = k^2 v_t^2/\omega_b^2$ and $x = k^2c^2/\omega^2$. Because of the bound character of F for real ω, a solution exists only when $\omega^2 \geq \omega_p^2$, i.e. when the denomenator on the right-hand side is near zero. When $n > 1$ (including $n = 2$), one can readily show (see Fig. 4e) that a wiggle occurs in the dispersion curve similar to that for the extraordinary wave and that the deviation of k from the $x = 1 - \omega_p^2/\omega^2$ curve is very small.

When $n = 1$, the wiggle is quite large. Neglecting higher order λ terms (viz $\lambda F_{9/2} \ll 1$), Eq. (27a) is valid for $n = 1$ also and reduces to

$$x = \left[1 - \frac{\omega_p^2}{\omega^2}\right] \Big/ \left[1 + \frac{\omega_p^2}{2\omega_b^2} F_{7/2}\right] \tag{27b}$$

In particular at $\omega = \omega_b$, $F_{7/2} = 2/5$ and

$$x = \left[1 - \omega_p^2/\omega_b^2\right] \Big/ \left[1 + \omega_p^2/5\omega_b^2\right] \tag{27c}$$

Equation (27c) has been derived by Dnestrovskii et al (1964) and Gershman (1961). If we keep higher order λ terms, we find using Eq. (44b) of Part 1 and Eq. (20b) that

$$x^2\left[\frac{\omega_p^2\omega^2}{\omega_b^4\mu} F_{9/2}\right] - x\left[1 + \frac{\omega_p^2}{2\omega_b^2} F_{7/2}\right] + \left(1 - \frac{\omega_p^2}{\omega^2}\right) = 0 \tag{27d}$$

Real k, Complex ω Dispersion Curves

In contrast to the real ω situation, a slightly complex frequency permits dispersion for all k values except a tiny region near $k = 0$. The reason for this is that F becomes very large for complex ω (see Fig. 4b of Part 1) and the k variation in Eqs. (18b), (24c) and (27a) is unlimited. The dispersion in the regions where the nonrelativistic analysis is valid is identical to the real ω case. As pointed out previously these regions occur when $|\mu\delta| >> 1$ at both ends of the em solution and when $\omega > n\omega_b$ and $K_\perp > 0$ for the es solution.

Let us consider 4 possible situations for the dispersion curves illustrated in Figs. 5a to 5d.

For the high-frequency case in Fig. 5a, $K_\parallel$, K_r and $K_\perp$ are positive and $K_\parallel > K_r$ or $n\omega_b > \omega_R > \omega_T > \omega_L$ where ω_R, ω_L and ω_T are the ω values for which $K_r = 0$, $K_\parallel = 0$ and $K_\perp = 0$ respectively:

$$\omega_L = -\frac{\omega_b}{2} + \left(\frac{\omega_b^2}{4} + \omega_p^2\right)^{\frac{1}{2}}; \quad \omega_R = \frac{\omega_b}{2} + \left(\frac{\omega_b^2}{4} + \omega_p^2\right)^{\frac{1}{2}}; \quad \omega_T = \left(\omega_p^2 + \omega_b^2\right)^{\frac{1}{2}}$$

The solution for the combined extraordinary-plasma wave is that given in (18b) with the correction in (19) when $x \approx 2K_\parallel$. We also require the plot of F versus ω_{real} given in Fig. 4b of Part 1. We can follow the Bernstein es mode from large to small λ up to $\omega = n\omega_b$ using real ω, real k and the real positive branch of F. As k further decreases, we continue using Eq. (24c) along this positive branch, passing through a minimum $\omega_r < n\omega_b$ value when $\partial k/\partial\omega_r = \infty$ or $\partial F/\partial\omega_r = \infty$ in Fig. 4b of Part 1. Then the curve passes again through $\omega_r = n\omega_b$ (see Eq. (39i) of Part 1). The frequency rises steadily above $n\omega_b$ as k decreases and $x \to 2K_\parallel$ since F

appears to be infinite at this point according to Eq. (18b). However Eq. (19) limits the maximum values that F and ω attain. Essentially around $x = 2K_1$, coupling occurs between the $F > 0$ and $F < 0$ branches which accounts for the awkward behaviour. For values of $x < 2K_1$, we therefore shift to the $F < 0$ track and the dispersion curve connects with the em wave when $\omega << n\omega_b$. On the opposite side of the Appleton-Hartree solution, we again use the $F > 0$ track. We follow the same behaviour as for the es mode, with ω decreasing slightly below $n\omega_b$ and rising again. The most remarkable result is that near $k = 0$, F becomes larger and larger resulting in ω increasing more and more above $n\omega_b$ rather than tending to $n\omega_b$. As ω increases above $n\omega_b$ by an appreciable fraction of $n\omega_b$, over analysis which restricts ω to be near $n\omega_b$, fails. A full investigation of what actually happens then, is beyond the scope of this work and is actually not necessary for further analysis.

The low-frequency case, shown in Fig. 5b, is for $K_1 < 0$, $K_r < 0$ $K_\perp < 0$ and $|K_r| > |K_1|$ or $n\omega_b < \omega_L < \omega_T < \omega_R$. Equation (18b) becomes

$$-\left(\frac{\omega_b{}^2 2^n n!}{\omega_p{}^2 \lambda^{n-2} n^2}\right) \frac{1}{F_{n+3/2}} = \frac{(2|K_1| + x)\, x}{|K_1 K_r| + |K_\perp|\, x}$$

For large k values, we must choose the $F < 0$ track and, since no Appleton-Hartree solution exists, we follow this track for all lower k values as shown in Fig. 5b.

The high-intermediate-frequency sit uation in Fig. 5c is for $K_1 > 0$, $K_r < 0$, $K_\perp > 0$ with $K_1 > |K_r|$ or $\omega_L < \omega_T < n\omega_b < \omega_R$. In this case, (18b) is

$$-\left(\frac{\omega_b^2 2^n n!}{\omega_p^2 \lambda^{n-2} n^2}\right)\frac{1}{F_{n+3/2}} = \frac{(2K_1 - x)x}{|K_1 K_r| + K_\perp x}$$

For large k, we must use the $F > 0$ track which can be followed for lower k values up to $x \approx 2K_1$. At $x = 2K_1$, we apply the correction in Eq. (19). For $x < 2K_1$, we change to the $F < 0$ track and continue for all lower k values.

When $K_1 > 0$, $K_r < 0$, $K_\perp < 0$ with $|K_r| > K_1$, or $\omega_L < n\omega_b < \omega_T < \omega_R$, (the low-intermediate-frequency situation) the Appleton-Hartree solution $x = K_1 K_r / K_\perp$ occurs at a higher x value than $x = 2K_1$. This case is illustrated in Fig. 5d, and for it Eq. (18b) becomes

$$-\left(\frac{\omega_b^2 2^n n!}{\omega_p^2 \lambda^{n-2} n^2}\right)\frac{1}{F_{n+3/2}} = \frac{(2K_1 - x)x}{|K_1 K_r| - |K_\perp| x}$$

For large k values we require the $F < 0$ track which connects to the Appleton-Hartree solution as shown in Fig. 5d. Between $x = K_1 K_r / K_\perp$ and $x = 2K_1$, we use the $F > 0$ track and for $x < 2K_1$ we use the $F < 0$ track.

In all four cases, the large-k portions of the curve make a smooth transition to the appropriate well known electrostatic cyclotron harmonic mode (sometimes called a Bernstein mode).

The above formulation applies to $n = 2$ as well except that the excursion from the Appleton-Hartree solution occurs for larger values of $\omega - n\omega_b$ and it connects up sooner with the es mode.

For n = 1, ω_b has a negligible effect. Equation (20c) shows that for a large excursion from the Appleton-Hartree solution, $F_{5/2}$ must become exceedingly small (rather than large as for n > 1). Since F cannot go to zero before going to ∞ (see Fig. 4a of Part 1), the dispersion curve for complex ω is about the same as for real ω (see Fig. 1c) and only exists if $K_1 > 0$.

Figures 6a and 6b show corresponding curves for the ordinary wave when $\omega \gtrless \omega_p$ respectively. Equation (27a) (valid for n = 1 also) shows that if $\omega > \omega_p$, one needs $F < 0$ for large x values, $x > (1 - \omega_p^2/\omega^2)$, and $F > 0$ for $x < (1 - \omega_p^2/\omega^2)$. If $\omega < \omega_p$, one can follow the $F < 0$ track for all k values. Compare Figs. 6a and 6b with 4e.

At this stage, it is informative to look at ω versus k plots including several harmonics on each plot for ratios of ω_p^2/ω_b^2 ranging from one to 12. The ratio of ω_p/ω_b is plotted in Fig. 7 (for the equatorial region, daytime and sunspot minimum) versus ionospheric altitudes of 500 - 30,000 kms using the data in Table I. We note that ω_p/ω_b varies between one and ten. This ratio is also equal to r_b/l_D, the electron Larmor radius to Debye length. In the polar regions, ω_p/ω_b may be smaller (as low as $\frac{1}{2}$) than for the equatorial regions. In Fig. 8 to 15, the dispersion curves are shown schematically for the ordinary wave or for the combined extraordinary-plasma waves. These plots are obtained by making use of our previous results in Figs. 5 and 6.

Of interest is to note in Figs. 8 to 15 or 5 and 6, the points where $\partial\omega/\partial k$ can match the satellite velocity. Such points exist on either side of the $x = K_1 K_r/K_\perp$ or $x = K_\parallel$ dispersion curves provided these electromagnetic waves can propagate. Another point for matching which always seems to occur (except for $\omega = \omega_b$ with the

TABLE I

ht in km	n in cm^{-3}	ω_p in Mc	B in Gauss	ω_b in Mc	ω_p/ω_b
450	10^6	56.5	.262	4.62	12.2
610	4×10^5	35.8	.244	4.30	8.34
730	2×10^5	25.2	.232	4.07	6.2
840	10^5	17.9	.222	3.90	4.6
1,000	4×10^4	11.3	.208	3.65	3.1
1,200	1.9×10^4	7.8	.190	3.35	2.3
1,400	1.17×10^4	6.1	.176	3.09	1.97
1,600	7.85×10^3	5.0	.162	2.85	1.75
1,800	5.8×10^3	4.3	.148	2.60	1.65
2,000	4.3×10^3	3.7	.136	2.40	1.54
2,500	2.6×10^3	2.88	.1125	1.98	1.45
3,000	2.19×10^3	2.64	.0965	1.70	1.55
4,000	1.68×10^3	2.28	.0738	1.30	1.74
5,000	1.27×10^3	1.98	.0563	0.99	2.0
7,000	8.10×10^2	1.58	.0335	0.59	2.68
10,000	4.60×10^2	1.19	.0188	0.33	3.62
15,000	2.12×10^2	0.81	.00846	0.149	5.44
20,000	1.08×10^2	0.577	.00448	0.079	7.3
30,000	3.70×10	0.338	.00173	0.0304	11.2
40,000	1.75×10	0.232	.00084	0.0148	15.7
50,000	1.0×10	0.176	.000466	0.0082	21.5

extraordinary wave) is near k = 0 where the dispersion curve rises above $n\omega_b$. In the next section, we turn to this problem of matching satellite to group velocity. In fact, we associate the long duration cyclotron harmonic signals with waves travelling at the satellite velocity. Such points occur both for the extraordinary and ordinary waves.

IV. MATCHING SATELLITE VELOCITY TO GROUP VELOCITY

(a) Matching $k_{\parallel}$

All the above dispersion relations are in a stationary frame of reference. Since the satellite is moving, the actual ω and k values within the plasma are shifted from that of a stationary transmitter. The shifted values (ω', k') can be obtained by a Lorentz transformation with the result (see for example Silin and Rukhadze, 1961, p. 174):

$$\omega' = (\omega - \underset{\sim}{k} \cdot \underset{\sim}{V}) \Big/ \sqrt{1 - V^2/c^2} \tag{28a}$$

$$\underset{\sim}{k}' = \underset{\sim}{k} + \frac{\underset{\sim}{V}}{V^2\sqrt{1 - V^2/c^2}} \left[\underset{\sim}{k} \cdot \underset{\sim}{V}(1 - \sqrt{1 - V^2/c^2}) - \omega V^2/c^2 \right] \tag{28b}$$

where primes refer to a moving frame of reference and where $\underset{\sim}{V}$ is the satellite velocity vector and V its magnitude. For c >> V

$$\underset{\sim}{k}' \approx \underset{\sim}{k} - \frac{\underset{\sim}{V}}{c^2}\left(\omega - \frac{\underset{\sim}{k} \cdot \underset{\sim}{V}}{2}\right) \quad \text{and} \quad \omega' = \omega - \underset{\sim}{k} \cdot \underset{\sim}{V} \tag{28c,d}$$

Hence
$$\underset{\sim}{k} = \underset{\sim}{k}' + \underset{\sim}{V}(\omega' + \underset{\sim}{k}' \cdot \underset{\sim}{V}/2)/c^2 \tag{28e}$$

Let us first attempt to match satellite velocity to group velocity in the direction parallel to magnetic field. An examination of Eq. (5a) reveals that the most rapid variations of ω and $k_{\parallel}$

arise from the $\rho + \beta k_{\parallel}^2$ term (or $\rho' + \beta'' k_{\parallel}^2$ for the ordinary wave). Differentiating this and setting $\partial\omega/\partial k_{\parallel} = V_{\parallel}$, one gets to first order $V_{\parallel}\partial\rho/\partial\omega + 2\beta k_{\parallel} = 0$ or

$$k_{\parallel} = -\frac{\mu V_{\parallel}}{2\omega}\frac{\rho'}{\beta} = -\frac{\omega V_{\parallel}}{c^2}\frac{F'_{n+3/2}}{F''_{n+5/2}} \tag{29a}$$

since $\rho = F_{n+3/2}$ and $F_{n+5/2} - 2F_{n+3/2} + F_{n+1/2} = F''_{n+5/2}$ for the extraordinary wave. (A prime denotes a derivative with respect to $\mu\delta$.) Similarly for the ordinary wave we find from Eq. (16c)

$$k_{\parallel} = -\frac{\omega V_{\parallel}}{c^2}\frac{F'_{n+5/2}}{\left[7F_{n+5/2} - 8F_{n+3/2} + 3F_{n+1/2} - 2F^2_{n+5/2}/F_{n+3/2}\right]}$$

$$= -\frac{\omega V_{\parallel}}{c^2}\frac{F'_{n+5/2}\,F_{n+3/2}}{\left[3F''_{n+5/2}\,F_{n+3/2} - 2\left(F'_{n+5/2}\right)^2\right]} \tag{29b}$$

Inserting the value of $k_{\parallel}$ (Eq. 29a) into $\beta k_{\parallel}^2$ yields

$$\beta k_{\parallel}^2 = (V_{\parallel}^2/2v_t^2)\frac{\left(F'_{n+3/2}\right)^2}{F''_{n+5/2}} \tag{30}$$

which is very small compared to $\rho = F_{n+3/2}$ since $V_{\parallel}/v_t \sim 1/16$. This substantiates our use in Sec. 2 of first order $k_{\parallel}^2$ terms and treating $\beta k_{\parallel}^2$ as a small correction to ρ.

In order to provide a more convincing argument valid for a wider range of $k_{\parallel}$ values, we apply the generalization of $\rho + \beta k_{\parallel}^2$, namely the function, $\mathcal{F}_q\left(\frac{n\omega_b}{\omega}, \frac{k_{\parallel}c}{\omega}\right)$, discussed in Part 1. The most rapid variation of the dispersion relationship with $k_{\parallel}$ occurs in the $\mathcal{F}_q$ function. We therefore solve for the value of $k'_{\parallel}$ such that $\partial\mathcal{F}_q/\partial k'_{\parallel} = 0$. We have in the transformed

frame of reference using Eq. (7) of Part 1

$$\mathcal{J}_q\left(\frac{n\omega_b}{\omega}\,,\ \frac{k_{\parallel}c}{\omega}\right) = -i\int_0^{\infty} dt\left[(1-it)^2 + \left(k'_{\parallel} + \frac{V_{\parallel}}{c^2}\left(\omega' + \frac{\underset{\sim}{k'}\cdot\underset{\sim}{V}}{2}\right)\right)^2 \frac{t^2c^2}{(\omega' + \underset{\sim}{k'}\cdot\underset{\sim}{V})^2}\right]^{-q/2} \times$$

$$\exp\left\{\mu - \mu\left[(1-it)^2 + \left(k'_{\parallel} + \frac{V_{\parallel}}{c^2}\left(\omega' + \frac{\underset{\sim}{k'}\cdot\underset{\sim}{V}}{2}\right)\right)^2 \frac{t^2c^2}{(\omega' + \underset{\sim}{k'}\cdot\underset{\sim}{V})^2}\right]^{\frac{1}{2}} - \frac{\mu i n t \omega_b}{\omega' + \underset{\sim}{k'}\cdot\underset{\sim}{V}}\right\}$$

Differentiating with respect to $k'_{\parallel}$ and neglecting $V_{\parallel}^2/c^2$ with respect to one

$$\frac{\partial \mathcal{J}}{\partial k'_{\parallel}} = iq\int \frac{dt \exp\{\cdots\}}{[\cdots]^{\frac{q}{2}+1}}\left[k'_{\parallel} + \frac{V_{\parallel}}{c^2}\left(\omega' + \frac{\underset{\sim}{k'}\cdot\underset{\sim}{V}}{2}\right)\right]\frac{(\omega' + k'_{\perp}V_{\perp})t^2c^2}{(\omega' + \underset{\sim}{k'}\cdot\underset{\sim}{V})^3}$$

$$+ n\omega_b\mu\int \frac{dt \exp\{\cdots\}}{[\cdots]^{\frac{q}{2}}}\left[\frac{V_{\parallel}t}{(\omega' + \underset{\sim}{k'}\cdot\underset{\sim}{V})^2}\right]$$

$$+ i\mu\int \frac{dt \exp\{\cdots\}}{[\cdots]^{\frac{q}{2}+\frac{1}{2}}}\left[k'_{\parallel} + \frac{V_{\parallel}}{c^2}\left(\omega' + \frac{\underset{\sim}{k'}\cdot\underset{\sim}{V}}{2}\right)\right]\frac{(\omega' + k'_{\perp}V_{\perp})t^2c^2}{(\omega' + \underset{\sim}{k'}\cdot\underset{\sim}{V})^3}$$

$$= \frac{V_{\parallel}n\omega_b\mu}{\omega(\omega' + \underset{\sim}{k'}\cdot\underset{\sim}{V})}\frac{\partial \mathcal{J}_q}{\partial\mu\delta} + \left[k'_{\parallel} + \frac{V_{\parallel}}{c^2}\left(\omega' + \frac{\underset{\sim}{k'}\cdot\underset{\sim}{V}}{2}\right)\right]\frac{(\omega' + k'_{\perp}V_{\perp})c^2}{(\omega' + \underset{\sim}{k'}\cdot\underset{\sim}{V})\omega^2}\left[\mu\frac{\partial^2 \mathcal{J}_{q+1}}{\partial(\mu\delta)^2} + q\frac{\partial^2 \mathcal{J}_{q+2}}{\partial(\mu\delta)^2}\right]$$

where $(\mu\delta) = \dfrac{c^2}{v_t^2}\dfrac{(\omega - n\omega_b)}{\omega}$ and $\partial(\mu\delta) = -\dfrac{\mu}{\omega}\partial(n\omega_b)$, $\mu = \dfrac{c^2}{v_t^2}$.

Equating the above to zero yields

$$-k'_{\parallel} = \frac{V_{\parallel}}{c^2}\left(\omega' + \frac{k'_{\perp}V_{\perp}}{2}\right) + \frac{V_{\parallel}n\omega_b\omega}{(\omega' + k'_{\perp}V_{\perp})c^2}\ \frac{\partial \mathcal{J}_q/\partial(\mu\delta)}{\left[\partial^2 \mathcal{J}_{q+1}/\partial(\mu\delta)^2 + \left(\frac{q}{\mu}\right)\partial^2 \mathcal{J}_{q+2}/\partial(\mu\delta)^2\right]}$$

From Eq. (28e) we obtain the same result as Eq. (29a), viz.

$$k_{\parallel} \approx -\left(\frac{\omega V_{\parallel}}{c^2}\right) \frac{\partial \mathcal{F}_q/\partial(\mu\delta)}{\partial^2 \mathcal{F}_{q+1}/\partial(\mu\delta)^2} \tag{31}$$

since $\omega' > k_{\perp}' V_{\perp}$. Since for many cases of interest, the ratio of $\mathcal{F}$'s is less than one, $-k_{\parallel}$ is somewhat less than $\omega V_{\parallel}/c^2$. [Some care is however needed in the region where $\partial \mathcal{F}_q/\partial(\mu\delta) = \infty$].

(b) Attempt to Match $k_{\perp}$ for the Electrostatic Wave

The next task is to match satellite and group velocities perpendicular to the magnetic field direction. Since the $k_{\parallel}$ term is very small (see Eq. 30) we assume in the following discussion that $k_{\parallel} = 0$.

First we show that for $n > 4$, it requires unrealistically small values of $V_{\perp}$ to obtain a match using the Bernstein electrostatic mode in the region where $k = k_{\perp}$ and ω are real. From Eq. (26c) the Bernstein mode is given by

$$\omega^2 - n^2\omega_b^2 = \frac{2\omega_p^2 n^2 I_n}{\lambda} e^{-\lambda} \Big/ \left(1 - \frac{\omega_p^2}{\omega^2 - \omega_b^2}\right) \tag{32}$$

where $k = \sqrt{\lambda}\omega_b/v_t$, and we assume that $\omega^2 > (\omega_b^2 + \omega_p^2)$.

Parenthetically, we note the point for which the group velocity is zero, $\partial\omega/\partial k = 0$, namely

$$\frac{\partial}{\partial\lambda}(I_n e^{-\lambda}/\lambda) = 0 \quad \text{or} \quad \lambda\left(1 - \frac{I_{n+1}}{I_n}\right) = n - 1 \tag{33a}$$

This relation is more appropriate to use than the tangent method pointed out by Stix (1962, p. 229) involving the maximum value of $(I_n e^{-\lambda})$.

(The tangent method of Stix turns out to be very insensitive for obtaining the value of λ.) Equation (33a) can be solved by a trial and error method using tabulated values of the I_n Bessel function. The results are given in Table 2, where for n = 2 to 5 the value of λ is given and also the value of $(nI_n/\lambda)e^{-\lambda}$ which is required for obtaining $\omega - n\omega_b$ from Eq. (32). These results are compared with the following good empirical relations for λ and $\omega - n\omega_b$, viz.

$$\lambda \approx 0.342n^2 \qquad \text{and} \qquad \omega - n\omega_b \approx \frac{0.45}{n^2}\frac{\omega_p^2}{\omega_b}\left(1 - \frac{\omega_p^2}{\omega^2 - \omega_b^2}\right)^{-1} \qquad (33b,c)$$

We are however more interested in matching $\partial\omega/\partial k$ to $V_\perp$ than equating it to zero. Letting $\partial\omega/\partial k = V_\perp$, Eq. (32) yields

$$\frac{V_\perp}{v_t}\left(\frac{\omega_b}{\omega_p}\right)^2\left(1 - \frac{\omega_p^2}{\omega^2 - \omega_b^2}\right)\frac{\omega}{n\omega_b} = \frac{2nI_n e^{-\lambda}}{\lambda^{3/2}}\left[-\lambda\left(1 - \frac{I_{n+1}}{I_n}\right) + n - 1\right] \qquad (34a)$$

Since $V_\perp/v_t$ can be as high as 1/16 and ω_p^2/ω_b^2 varies between 1/4 and 100 (see discussion after Table 1), we note that the maximum value of the left-hand-side is 4/16 = 0.25. However we show below (in Table 3) that the right-hand-side never attains such high values for any n. One may argue that the satellite seldom moves perpendicular to the magnetic field. But even assuming $V_\perp/V \approx 1/10$, we require the right hand side to attain a value of 0.025. This is possibly for $n \leq 4$ only and not for larger n, as follows from Table 3.

The above discussion indicates the importance of the maximum value of $\partial\omega/\partial k$. Differentiating again Eq. (34a) and equating the result to zero yields

$$\frac{I_n}{I_{n+1}} = \frac{\lambda(4\lambda + 5)}{4\lambda^2 + \lambda(3 - 4n) + 2n^2 - 5n + 3} \qquad (34b)$$

Equations (34a,b) are difficult to solve analytically in the region where $\lambda \sim n$, so that we resort to plotting the right-hand-side of Eq. (34a) for various n. In Figs. 17a to 17d, we present plots for n = 2 to 5. We pick out the points of the maximum slope and tabulate these in Table 3.

Table 3 corroborates our assertion on the difficulty of matching $V_\perp$ to $\partial\omega/\partial k$ for $n > 4$. The reason for this is that the dispersion relation for the es mode varies over a very large range of k for a slight change in ω. Tables 2 and 3 also show that for the lower harmonics, a match also requires a measurable shift of $\omega - n\omega_b$, which is not observed on the Alouette. The Alouette frequency sensitivity is at least one part in 200.

TABLE 2

The Values for Zero Group Velocity
for the Bernstein Mode

n	λ(exact)	Eq. (33b)	$(\omega-n\omega_b)\frac{\omega_b}{\omega_p^2}\left(1-\frac{\omega_p^2}{\omega^2-\omega_b^2}\right)$(exact)	Eq. (33c)
2	1.26	1.37	0.1025	0.1125
3	3.05	3.08	0.0479	0.050
4	5.50	5.47	0.0278	0.0281
5	8.55	8.55	0.0179	0.018

TABLE 3

The Exact Values for Maximum Group Velocity
for the Bernstein Mode

n	λ	$\left(\frac{\partial\omega}{\partial k}\right)_{max}\left(\frac{\omega_b^2}{v_t^2\omega_p^2}\right)\left(1-\frac{\omega_p^2}{\omega^2-\omega_b^2}\right)$(see Eq. 34a)	$(\omega-n\omega_b)\frac{\omega_b}{\omega_p^2}\left(1-\frac{\omega_p^2}{\omega^2-\omega_b^2}\right)$
2	0.2	0.1475	0.041
3	1	0.055	0.0245
4	2	0.0269	0.0137
5	3	0.0151	0.00757

The case of real ω and complex $k = k_r + ik_i$ may seemingly hold hope of obtaining a match near the turn-around point in Figs. 3 or 4. However, near these points, k_r and k_i are of the same order, so that the wave is attenuated as the exponent of $-k_i r \approx -k_r r \approx -k_r Vt \approx -0.1\,\omega Vt/v_t$, since we estimate k_r to be about $0.1\ \omega/v_t$ near the turn-around point. This gives much stronger attenuation than observed since taking $V/v_t = 1/16$, one finds a e-folding time of $\omega t \approx 160$ rather than 10^4 as recorded by the Alouette. Another point against the es mode is that one would sometimes expect a measurable Doppler shift of $k_r V_\perp \approx 0.1\omega V_\perp/v_t \approx \omega V_\perp/160\,V$ which is not observed. A large k_r is also associated with a small region (a characteristic length of $1/k_r$) of excitation less than the antenna size, which would require consideration of sheath effects. Our analysis is inadequate for considering sheath effects. Furthermore, as discussed in Part 1, the detection of a signal after the transmitter is shut requires consideration of complex ω rather than real ω. Essentially, we are dealing with an initial value problem in time. For very slightly complex ω, the above turn-around point or matching point does not occur (see Figs. 5). In conclusion, we must relinquish attempts which are consistent with observed effects for a match using the Bernstein mode, at least for $n > 4$.

(c) Matching $k_\perp$ for the Extraordinary Wave

Let us now attempt to obtain a match for lower k values near or less than the Appleton-Hartree wave numbers. We start with our fundamental Eq. (18b) for the extraordinary wave:

$$\frac{1}{Pk^{2(n-2)}_F} = \frac{(2K_1 - x)x}{K_1 K_r - K_\perp x} \tag{35}$$

where $x = \frac{k^2c^2}{\omega^2}$, $K_{(l/r)} = 1 - \frac{\omega_p^2}{\omega \pm \omega_b}$, $K_\perp = 1 - \frac{\omega_p^2}{\omega^2 - \omega_b^2}$, $P = \frac{\omega_p^2}{\omega_b^2}\left(\frac{v_t}{\omega_b}\right)^{2(n-2)} \frac{n^2}{2^n n!}$

Since ω is complex, we differentiate with respect to ω_r and equate $\partial\omega_r/\partial k = V_\perp$. Note however that $\omega_i \ll\ll \omega_r$ (see Part 1, Sec. VII) so that we let $\partial\omega/\partial\omega_r \approx 1$. We also neglect throughout the derivative $\partial\omega_i/\partial\omega_r$ since this is of order ω_i/ω_r and hence negligible. We denote the F derivative for convenience as

$$F' = \frac{\partial F}{\partial(\mu\delta)}\frac{\partial\omega}{\partial\omega_r} \approx \frac{\partial F}{\partial(\mu\delta)} \quad \text{so that} \quad \frac{\partial F}{\partial\omega_r} = F'\frac{\partial\mu\delta}{\partial\omega} = \frac{F'\mu n\omega_b}{\omega^2}$$

The derivative of F with respect to ω_r is taken along the track of real F. The parameters which have to be differentiated are k, F, K_l, K_r, $K_\perp$ and x. The result is

$$-\left(\frac{F'\mu}{Pk^{2(n-2)}F^2}\right)\left(\frac{kV_\perp n\omega_b}{\omega^2}\right) - \frac{2(n-2)}{Pk^{2(n-2)}F} = \frac{2x(\omega - kV_\perp)}{(K_lK_r - K_\perp x)\omega}\left[-x + (2K_l - x) + \frac{(2K_l - x)K_\perp x}{K_lK_r - K_\perp x}\right]$$

$$+\frac{kV_\perp \omega_p^2 2x}{K_lK_r - K_\perp x}\left[\frac{-2\omega + \omega_b}{\omega^2(\omega+\omega_b)^2} - \frac{(2K_l - x)2\omega}{(K_lK_r - K_\perp x)(\omega^2 - \omega_b^2)^2} + \frac{\omega_p^2(2\omega^2 - \omega_b^2)(2K_l - x)}{(K_lK_r - K_\perp x)\omega^3(\omega^2 - \omega_b^2)^2} + \frac{(2K_l - x)x\omega}{(K_lK_r - K_\perp x)(\omega^2 - \omega_b^2)^2}\right] \tag{36a}$$

Since $\omega >> kV_\perp$, the $kV_\perp$ terms on the right hand side are negligible. Essentially this means that we neglect the derivatives of K_l, K_r, $K_\perp$ and x with respect to ω. We can substitute Eq. (35) into the last term on the left hand side of (36a) and combine this with the remaining first term on the right hand side to yield

$$(n-1)2K_1 - nx + \frac{(2K_1 - x)K_\perp x}{K_1K_r - K_\perp x} = -\left(\frac{K_1K_r - K_\perp x}{2x}\right)\left(\frac{F'\mu}{Pk^{2(n-2)}F^2}\frac{kV_\perp}{\omega}\right) \qquad (36b)$$

$$= -\left(\frac{2K_1 - x}{2}\right)\left(\frac{F'\mu}{F}\frac{kV_\perp}{\omega}\right) = -\left(\frac{x(2K_1 - x)^2}{2(K_1K_r - K_\perp x)}\right)\left(Pk^{2(n-2)}F\mu\frac{kV_\perp}{\omega}\right) \qquad (36c,d)$$

where Eq. (36c) or (36d) is obtaining by substituting into (36b) values for F or F^2 respectively from (35).

There seems to be three regions where one can satisfy the above equations, namely near

(i) the Appleton-Hartree solution, $x \approx K_1K_r/K_\perp$

(ii) near $x \approx 2K_1$ and

(iii) for $x \ll 1$.

Let us consider these separately.

Case (i) - When $x \approx K_1K_r/K_\perp > 0$ we find from Eqs. (35) and (36c)

$$x - \frac{K_1K_r}{K_\perp} \approx -\frac{K_1{}^3K_r}{K_\perp{}^3}k^{2(n-2)}PF = \frac{2K_1K_r}{K_\perp}\frac{F\omega}{F'\mu kV_\perp} \qquad (37a)$$

where $K_\perp = (K_1 + K_r)/2$. Also from Eq. (36d), we note that

$$2\left(\frac{K_\perp}{K_1}\right)^2 = -Pk^{2(n-2)}\mu\frac{F'kV_\perp}{\omega} \qquad (37b)$$

which shows that $(V_\perp kF'/\omega) < 0$. Hence from Eq. (37a), we can have $x \gtrless K_1K_r/K_\perp$ depending on whether $F \lesseqgtr 0$. This is consistent with the signs of F used in Figs. 5 near the electromagnetic solution. Since

$\pm k = \omega\sqrt{x}/c$, Eq. (37a) gives a very small deviation of x from $K_l K_r/K_\perp$, of the order of $v_t^2/cV_\perp$.

$$\left| x - \frac{K_l K_r}{K_\perp} \right| = 2\sqrt{\frac{K_l K_r}{K_\perp}} \frac{F}{F'} \frac{v_t^2}{cV_\perp} \tag{37c}$$

Equation (37b) cannot be satisfied for n = 1 since the right-hand-side is much larger than the left-hand-side. This is again consistent with the results in Sec. 3. For n = 2, Eqs. (37a-c) can be satisfied for values of F of order one. In fact for $x < K_l K_r/K_\perp$, we can use the region where $F > 0$ and both ω and k are real. As is shown in Eq. (22e) the slope $\partial\omega/\partial k$ is of order v_t^2/c^2 at $\omega = n\omega_b$ and increases to about c as ω tends towards the Appleton-Hartree solution. At some intermediate point, the slope must equal $V_\perp$. Thus a match is readily obtained for n = 2 and $\omega > n\omega_b$ on the $F > 0$ branch in contrast to $n > 2$ where it occurs on the $F > 0$ branch for $\omega < n\omega_b$. In all cases the difference $(\omega - n\omega_b)/\omega$ is relativistically small.

Note that these matching points are present only when there exists an Appleton-Hartree solution, i.e. when $K_l K_r/K_\perp > 0$. However, resonances are observed on the Alouette apparently unaffected by the extraordinary wave cut off, $K_r = 0$. (See Alouette data in Fejer and Calvert (1964), and in Calvert and Goe (1963)). Apparently, the cyclotron harmonics exist whether or not the extraordinary wave can propagate. This seems to indicate the additional importance of other matching points, namely case (iii) below and the ordinary wave. Also the value of x from Eq. (37c) yields a wavelength nearly equal to the free space wavelength which is also of the order of the antenna size. The analysis may have to include

both finite antenna size and possibly sheaths around the satellite. We do not propose to do this. The above remarks also apply to case (ii) which we proceed to discuss. Cases (i) and (ii) are of interest nonetheless for situations with very small antennas in a uniform medium.

In conclusion, the matching points in cases (i) and (ii) may be very important. Since two exist for either case differing relativistically in ω and by about $v_t^2/cV_\perp$ in x, beating between these resonances or between resonances of various modes may perhaps produce the modulation effect actually observed for the second harmonic resonance in S-48 (see Calvert et al, 1964).

Case (ii) - When $x \approx 2K_1 > 0$, we can also get, from Eqs. (35) and (36), two matching points depending on whether $x \gtrless 2K_1$ and $F \gtrless 0$ respectively. To see this, we expand around $x \approx 2K_1$, we find that $(F'kV_\perp/\omega) < 0$ from Eq. (36b), and from Eq. (36c) we obtain

$$x - 2K_1 = -4\frac{K_1}{\mu}\frac{F}{F'}\frac{\omega}{kV_\perp} \quad \text{or} \quad |x - 2K_1| = 2\sqrt{2K_1}\,\frac{F}{F'}\frac{v_t^2}{cV_\perp} \tag{38}$$

Besides the remarks discussed under (i), we note another. Our basic Eq. (35) is not valid very close to $x \approx 2K_1$ since in this region the $F > 0$ and $F < 0$ branches couple (see Sec. 3) and in fact we should use the more exact relation, Eq. (17b). (Note that Eq. (19) gives the correction at $x = 2K_1$.) A more complete analysis is necessary to see if the matching points around $x = 2K_1$ actually exist or not.

Case (iii) - We now consider the matching point for $x << 1$. This point is a direct consequence of the relativistic analysis which shows (see Figs. 5a to d) that ω rises rapidly above $n\omega_b$ as $k_\perp$ tends to zero. Because of the rapid rise, the slope $\partial\omega/\partial k_\perp$ becomes large enough to effect a match with $V_\perp$. For $x << 1$, Eqs. (35) and (36) reduce to

$$k_\perp = \pm \frac{2(n-1)v_t^2}{c^2 V_\perp} \omega \frac{F}{F'} \quad \text{and} \quad Pk_\perp^{2(n-2)} \frac{F^3}{(F')^2} = \frac{K_r}{8(n-1)^2}\left(\frac{V_\perp c}{v_t^2}\right)^2 \qquad (39a,b)$$

Since in this region F is large and of exponential form, F' is more or less of the same order as F so that the order of magnitude of $k_\perp$ is

$$k_\perp \approx \pm \frac{2(n-1)v_t^2}{c^2 V_\perp} \omega \qquad (39c)$$

We also note that when $K_r > 0$, $F' \approx F > 0$ and vice versa, which is in agreement with Figs. 5a to d. Again for $n = 1$, we obtain no matching point. Equation (39c) gives the value of $k_\perp$. Comparing this with Eq. (29a) for $k_\parallel$ (neglecting the ratio of F-factor) shows that

$$\frac{k_\perp}{k_\parallel} = 2(n-1)\frac{v_t^2}{V_\perp V_\parallel} \qquad (39d)$$

which is a large number greater than 500. This is consistent with the fact that the group velocity vector can acquire a substantial component perpendicular to the magnetic field only when $k_\perp >> k_\parallel \to 0$. Otherwise it points nearly directly along the magnetic field direction.

Equation (39b) can generally be satisfied for values of $\mu\delta$ between 3 and 40. This gives a value for $\delta \equiv (\omega - n\omega_b)/\omega < 40\ v_t^2/c^2 \approx 10^{-5}$ which is negligible. Thus the resonance occurs practically at $n\omega_b$ as far as any measurements are concerned.

Equation (39c) indicates that the characteristic length L of excitation perpendicular to the magnetic field is larger than the antenna length but smaller than ambient ionospheric inhomogeneity. Taking $\omega = 2\pi \times 10^6 \text{sec}^{-1}$, $V_\perp = 0.3\ V = 3 \times 10^3 \text{m/s}$, $v_t = 1.6 \times 10^5 \text{m/s}$ and $n = 5$ we find

$$L_\perp = 1/|k_\perp| = 210 \text{ meters}$$

This length is between the Alouette antenna length ~ 47 m and the thickness ~ 1500 m of ionospheric sheets of ionization (see Muldrew, 1963). As a result we can proceed with our analysis without considering the minor effects of finite antenna length, sheaths around the satellite and inhomogeneities in the ionospheric medium. From Eq. (39d), the characteristic length parallel to magnetic field with $V_n = 0.96\ V$ is

$$L_n \sim \frac{1}{|k_n|} \sim 1.5 \times 10^6 \text{m}$$

This length, although large, is still less than an earth radius $= 6.4 \times 10^6$m. The second harmonic as observed by Calvert et al (1964) on S-48 occurs over a latitude range of 6° or $\frac{1}{10}$ radian so that the magnetic field is uniform for distances of the order of 6.4×10^5 m. Nonuniformities will produce some effect on the signal amplitude. This suggests to look for possible

correlations of variations in signal strength with nonuniformities along rather than perpendicular to magnetic field lines.

The Doppler shifts associated with $k_\perp$ and $k_\parallel$ are negligible. Using Eq. (39c), the Doppler shift,

$$|k_\perp V_\perp/\omega| \sim 2(n-1)v_t^2/c^2 \tag{39e}$$

is relativistically small. That due to $k_\parallel$ is even less.

Since ω is complex, the exponentially time decaying part $\exp(-\omega_i t)$ has to be examined. On the sheet where F is real and very large, we have $\omega_i < 0$ so that $\exp(-i\omega t)$ does give a decaying part. However since our effects are restricted to the region where $\delta \ll 1$, we know from Part 1, Eq. (40d), that $\omega_i/\omega_r \approx n\pi/\mu$. The exponential term is thus of order $\exp(-\omega_r t v_t^2/n\pi c^2)$. For the times of interest, $\omega_r t \approx 10^4$, the argument of the exponential term is very small, so that this time decay is negligible and of no concern. The actual time decay will be shown in Part 3 to arise from the other time-amplitude factors multiplying this exponential. On the same basis, we can neglect collisional damping since even taking $\nu = 10\ \text{sec}^{-1}$ for the collision frequency, $\nu t \ll 1$ for the times of interest.

The above matching point is independent of whether or not an electromagnetic wave can propagate and thus always occurs for $n > 1$, except for one case mentioned below. When $K_r = 0$ (see Eq. 39b), we still get a matching point by including the next order term in x. From Eqs. (35) and (36a), we see that for $x \ll 1$, $K_r = 0$ and $K_\perp = (K_l + K_r)/2 = K_l/2$, we have

$$Pk_\perp^{2(n-2)}F = -1/4 \quad \text{and} \quad \frac{F'}{F}\frac{c^2}{v_t^2}\frac{kV_\perp}{\omega} + 2(n-2) = \frac{x}{K_1} \qquad (40a,b)$$

$$\text{If } n \neq 2 \qquad k = -2(n-2)\frac{v_t^2}{c^2 V_\perp}\omega\frac{F}{F'} \qquad (40c)$$

so that the $k_\perp$ matching point is not changed much. The value of F required to satisfy (40a) is somewhat less than for (39b) so that ω is very slightly nearer to $n\omega_b$. When $K_1 = 0$ and $n = 2$, no matching point seems possible for $x \ll 1$. Recall also that no match exists for $n = 1$. We note that in Alouette data (see Fejer and Calvert, 1964) resonances are observed for the first harmonic and for the second even when it passes through $K_1 = 0$. Below we show that with the ordinary wave we can obtain matching points even for the above two situations.

(d) Matching $k_\perp$ for the Ordinary Wave

A similar analysis can be performed using the ordinary wave dispersion relation given in Eq. (27a).

$$\frac{1}{P'k_\perp^{2(n-1)}F_{n+5/2}} = \frac{x}{K_n - x} \quad \text{where} \quad P' = \frac{\omega_p^2}{\omega_b^2}\left(\frac{v_t}{\omega_b}\right)^{2(n-1)}\frac{1}{2^n n!}\,; \quad K_n = 1 - \frac{\omega_p^2}{\omega^2} \qquad (41)$$

Equating $\partial\omega/\partial k_\perp = V_\perp$ and letting $\omega >> k_\perp V_\perp$ we find

$$n(K_n - x) + x = -\frac{(K_n - x)^2}{2x}\frac{F'}{F^2}\frac{\mu}{Pk_\perp^{2(n-1)}}\frac{k_\perp V_\perp}{\omega} = -k_\perp(K_n - x)\frac{F'\mu V_\perp}{2F\omega} \qquad (42a)$$

where F refers here to $F_{n+5/2}$ with argument $\mu\delta$ and $F' \equiv \frac{\partial F}{\partial \mu\delta}\frac{\partial \mu\delta}{\partial \omega_r} \approx \frac{\partial F}{\partial \mu\delta}$.

As $x \to 0$, we obtain a matching point when

$$k_\perp = -2n \frac{v_t^2}{c^2} \frac{\omega}{V_\perp} \frac{F}{F'}, \quad \text{and} \quad P' k_\perp^{2(n-1)} \frac{F^3}{(F')^2} = \frac{K_\parallel}{4n^2} \left(\frac{V_\perp c}{v_t^2} \right)^2 \qquad (42b,c)$$

(Compare with Eqs. 39a,b.)

This time we can include the fundamental ($n = 1$) cyclotron frequency (see also Figs. 6a,6b). Besides this advantage, the previous favorable remarks in Sec. IV apply as well to this matching point. These are the relatively minor dependence on antenna size and on ionospheric inhomogeneity, the negligible difference $(\omega - n\omega_b)/\omega$, the negligible imaginary part of ω, the negligible Doppler shift and the independence of whether or not an electromagnetic wave can propagate. When $K_\parallel = 0$, Eq. (42a) yields

$$k = -2(n-1) \frac{v_t^2}{c^2} \frac{\omega}{V_\perp} \frac{F}{F'} \quad \text{and} \quad P k_\perp^{2(n-1)} F = -1 \qquad (42d,e)$$

so that we again obtain a matching point provided $n \neq 1$. This time, experimental data (see Fejer and Valvert 1964) on the Alouette actually indicates a drop of signal for $n = 1$ as $K_\parallel \to 0$ or $\omega \to \omega_p$.

Similarly we can get matching points on both sides of $x \approx K_\parallel$:

$$x - K_\parallel = \pm 2K_\parallel \frac{F}{F'} \frac{\omega}{\mu k_\perp V_\perp} \quad \text{or} \quad |x - K_\parallel| = 2\sqrt{K_\parallel} \frac{F}{F'} \frac{v_t^2}{c V_\perp} \qquad (42f)$$

In particular for $n = 1$ and $x \lesssim K_\parallel$, there is a matching point for real k, ω and $F_{7/2}$ (see Figs. 6a and 4e).

The advantages of these matching points are the negligible difference $(\omega - n\omega_b)/\omega$, the negligible imaginary part of ω, the negligible Doppler shift, that it may be easier to excite a wavelength of the order of the free space wavelength and that the n = 1 case can be included.

In the next section, we give the nonrelativistic approach, the results obtained and a comparison with the more proper approach given above. We point out the inadequacies and errors introduced by not using relativistic analysis.

V. NONRELATIVISTIC ANALYSIS

If we apply the nonrelativistic formulation we get a completely different picture. The nonrelativistic formulation is incorrect for $(\omega - n\omega_b)/\omega < v_t^2/c^2$ and the analytic continuation in terms of the Z "plasma dispersion function" is always incorrect for $(\omega - n\omega_b)\omega < (k_\parallel c/\omega)^2$ and in particular for $k_\parallel \approx 0$ (see Sec. VI of Part 1). Let us nonetheless use the following nonrelativistic limit of the F function to see what results are obtained. (For simplicity, we perform the analysis only when $k_\parallel = 0$).

$$F_q \to (\mu\delta)^{-1} = \frac{v_t^2}{c^2} \frac{\omega}{\omega - n\omega_b} \tag{43a}$$

Strictly, Eq. (43a) is only valid for $|\mu\delta| > 1$ and Im $\omega > 0$ (see Part 1). If we wish to include $-\omega$ values as well in the same formulation, we use instead of (43a)

$$F_q \to \frac{v_t^2}{c^2}\,\omega\left(\frac{1}{\omega - n\omega_b} + \frac{1}{\omega + n\omega_b}\right) = \frac{2v_t^2}{c^2}\,\frac{\omega^2}{\omega^2 - n^2\omega_b^2} \tag{43b}$$

In Eq. (17b) we again neglect higher order λ terms except for the last product $(k^{4(n-2)})$-term. The equation for $\omega^2 - n^2\omega_b^2$ becomes

$$(\omega^2 - n^2\omega_b^2)^2(K_1K_r - xK_\perp) - (\omega^2 - n^2\omega_b^2)(2K_1 - x)2\omega_p^2\,\frac{\lambda^{n-1}n^2}{2^n n!} + \frac{4\omega_p^4\lambda^{2n}n^2}{(n+1)2^{2n}(n!)^2} = 0 \tag{44a}$$

where we used the expression for P in Eq. (4d). Solving Eq. (44a) for $\omega^2 - n^2\omega_b^2$ yields with

$$K_1 = 1 - \frac{\omega_p^2}{\omega(\omega+\omega_b)}\,, \quad K_r = 1 - \frac{\omega_p^2}{\omega(\omega - \omega_b)} \quad \text{and} \quad K_\perp = 1 - \frac{\omega_p^2}{(\omega^2 - \omega_b^2)}$$

$$\omega^2 - n\omega_b^2 \approx \frac{4\omega_p^2 n^2\lambda^{n-1}}{K_r n!2^n}\left[1 - \frac{k^2c^2}{2\omega^2K_1}\right]\Big/\left[1 - \frac{k^2c^2}{\omega^2}\,\frac{K_\perp}{K_1K_r}\right] \tag{44b}$$

and

$$\omega^2 - n^2\omega_b^2 \approx \frac{\omega_p^2\lambda^{n+1}}{K_1(n+1)n!2^n}\Big/\left[1 - \frac{k^2c^2}{2\omega^2K_1}\right] \tag{44c}$$

These two solutions are decoupled provided k^2c^2/ω^2 is not near $2K_1$.

We note that Eq. (44b) is the nonrelativistic equivalent of Eq. (18b) as is evident upon substituting Eqs. (43b) and (4d). In addition however we have succeeded in deriving a new wave given by (44c), which is not present in the more accurate relativistic formulation. Since for this wave $\omega^2 - n^2\omega_b^2 \sim \lambda^{n+1}$, the $\omega - k$ dispersion curve is very much localized

around $\omega \approx n\omega_b$ and never deviates appreciably from $n\omega_b$ except near coupling points between it and the other waves. This is the localized third wave which appears in the calculation of Dnestrovskii and Kostomarov (1962) using nonrelativistic analysis. We note however from Eqs. (44b,c) that $\omega^2 - n^2\omega_b^2 < v_t^2/c^2$ for

$$\left(\frac{k^2c^2}{\omega^2}\right) < \left(\frac{c^2}{v_t^2}\right)^{\frac{n-2}{n-1}} \quad \left(\text{since } \lambda \sim \frac{k^2c^2}{\omega^2}\,\frac{\omega^2}{\omega_b^2}\left(\frac{v_t^2}{c^2}\right)\right)$$

so that the basis of derivation from nonrelativistic analysis is incorrect. Furthermore we know from Part 1 that for F to be large we require its analytic continuation with $\mathrm{Im}\,\omega < 0$, and then its form differs from the large values derived from (43b) as $\omega \to n\omega_b$. (In fact, as already pointed out, Eqs. (43a,b) are valid only for $\mathrm{Im}\,\omega > 0$.) Actually as F becomes large, ω increases above $n\omega_b$ (see Fig. 5) rather than approaches $n\omega_b$.

Before we leave the nonrelativistic analysis, we point out the features of the dispersion curves based on this analysis and actually draw schematic curves for various situations. These curves will be compared with those including relativistic effects.

As $k \to 0$, the nonrelativistic dispersion equations (44b,c) yield

$$\omega^2 - n^2\omega_b^2 = \frac{4\omega_p^2 n^2 \lambda^{n-1}}{n!2^n} \Big/ \left[1 - \frac{\omega_p^2}{\omega(\omega-\omega_b)}\right] \quad \text{and} \quad \omega^2 - n^2\omega_b^2 = \frac{\omega_p^2 \lambda^{n+1}}{(n+1)n!2^n} \Big/ \left[1 - \frac{\omega_p^2}{\omega(\omega+\omega_b)}\right]$$

(45a,b)

When $k^2c^2/\omega^2 >> 1$, the equations yield the Bernstein longitudinal wave

$$\omega^2 - n^2\omega_b^2 = \frac{2\omega_p^2 n^2 \lambda^{n-1}}{n!2^n} \Big/ \left[1 - \frac{\omega_p^2}{(\omega^2 - \omega_b^2)}\right] \tag{46a}$$

plus the additional wave $-\omega^2 + n^2\omega_b^2 = \dfrac{2\omega_p^2\omega^2\lambda^{n+1}}{(n+1)n!2^n k^2c^2}$ (46b)

We next locate the points of zero group velocity. Obviously Eqs. (46a,b) predict such points at $k = 0$ or $\lambda = 0$ and $\omega = n\omega_b$. Other points exist near the electromagnetic solutions. Differentiating Eq. (44b) and equating $\partial\omega/\partial k = 0$ yields for $x_o = k_o^2c^2/\omega^2$

$$x_o^2 - \frac{x_o 2K_l}{K_l + K_r}\left(2K_r + K_l\frac{(n-2)}{n-1}\right) + \frac{4K_l^2K_r}{K_l + K_r} = 0 \tag{47}$$

where $K_\perp = (K_l + K_r)/2$ and $\omega \approx n\omega_b$. Let ω_R, ω_L and ω_T be ω values for which $K_r = 0$, $K_l = 0$ and $K_\perp = 0$ respectively. Also let $x_1 = K_lK_r/K_\perp$ and $x_2 = 2K_l$. Then there are four cases:

(i) $K_l > 0$, $K_r > 0$ and $K_l > K_r$ $(n\omega_b > \omega_R > \omega_T > \omega_L)$. There may be two zero group velocity points between x_1 and x_2 ($x_2 > x_1$ here) provided $(n^2 - 8n + 8) > \dfrac{\omega_p^2(n-8)}{\omega_b^2(n-1)}$ and $\dfrac{\omega_p^2}{\omega_b^2} < n(n-1)$. This occurs infrequently.

(ii) $K_l < 0$, $K_r < 0$ and $|K_r| > |K_l|$. $(n\omega_b < \omega_L < \omega_T < \omega_R)$. There are no zero group velocity points.

(iii) $K_l > 0$, $K_r < 0$ with $K_l > |K_r|$. $(\omega_R > n\omega_b > \omega_T > \omega_L)$. There is one zero group velocity point for $x < x_2$.

(iv) $K_l > 0$, $K_r < 0$ and $|K_r| > K_\perp$. $(\omega_L < n\omega_b < \omega_T < \omega_R)$. There are two zero group velocity points, one for $x < x_2$ and one for $x > x_1$ with $x_1 > x_2$ here.

Differentiating Eq. (44c) and equating $\partial\omega/\partial k = 0$ gives one zero group velocity point for $x > x_2$ and $\omega > \omega_L$. The values of ω for all these zero group velocity points are relativistically close to $n\omega_b$, so that the above results are questionable. Furthermore the $k = 0$, $\omega = n\omega_b$ point does not exist relativistically, since for large F, the ω curve rises above $n\omega_b$ and one never actually gets a $k = 0$ value.

Near $x = 2K_l$ or $x_2 = 1$, the $n-1$ and $n+1$ waves (viz $\omega^2 - n^2\omega_b{}^2 \propto \lambda^{n-1}, \lambda^{n+1}$) couple. Also the n-1 wave comples to the em wave near $x_1 = 1$. For the four cases discussed above, the dispersion curves including the wave coupling are drawn schematically in Figs. 18a to 18d up to values of x slightly beyond x_1 and x_2. The solid curves represent the n-1 or n+1 waves and the checked parts refer to coupling regions. Circles indicate the possible zero group velocity points. In order to match group velocity to satellite velocity we require $d\omega/dk = V_\perp$ where $V_\perp$ is the satellite velocity. Usually $d\omega/dk$ is much less than $V_\perp$. A match can only be found on either side of x_1 and only when an electromagnetic solution exists, as in cases (a) and (d). These points are indicated by x. Thus in the nonrelativistic approach, satellite motion eliminates any "pinch" (or matching) points near $k = 0$. Near the "light line", a match can be accomplished only if an em wave exists at frequency $n\omega_b$. Relativistic analysis however indicates that match can also be accomplished near $k = 0$ (See Sec. IVc, d.) The above illustrates the major differences in Figs.18 as compared to the relativistic equivalents in Figs.5.

The nonrelativistic approach agrees with the relativistic analysis for Eq. (46a) in the region $(\omega - n\omega_b)/\omega > v_t^2/c^2$. (Compare Eqs. (46a) and (24).) The form of this Bernstein es mode and matching points to satellite velocity have been discussed in Sec. 4b and the analysis given there is essentially nonrelativistic. As it should, the nonrelativistic theory also provides the correct variation of the Appleton-Hartree waves outside of the $|\mu\delta| < 1$ region, which is according to (44a)

$$x - \frac{K_l K_r}{K_\perp} = - \frac{1}{(\omega^2 - n^2\omega_b^2)} \left(\frac{K_l}{K_\perp}\right)^2 \frac{2\omega_p^2 \lambda^{n-1} n^2}{2^n n!} \tag{48}$$

(Compare this with Eq. (18b) with (43b) inserted in it.)

We can similarly investigate the nonrelativistic version of the ordinary wave dispersion when $\lambda << 1$. Substituting Eq. (43b) into (27a) gives

$$K_\parallel - x - \frac{2\omega_p^2}{\omega^2 - n^2\omega_b^2} \frac{\lambda^n}{n!2^n} = 0 \quad \text{where } K_\parallel = 1 - \frac{\omega_p^2}{\omega^2}$$

or

$$\omega^2 - n^2\omega_b^2 = \frac{2\omega_p^2}{n!2^n} \frac{\lambda^n}{(K_\parallel - x)}$$

For $K_\parallel > 0$ or $\omega > \omega_p$, a plot of ω versus k is given in Figs. 18e. One point of zero group velocity occurs at $\omega = k = 0$ and another at

$$x = nK_\parallel/(n-1)$$

and $\partial\omega/\partial k$ can be equated to $V_\perp$ on either side of $x = K_\parallel$. The case of

$K_{\parallel} < 0$ is indicated in Fig. 18f. A monotonic decreasing variation in ω with respect to k results for $\lambda << 1$ with $\partial\omega/\partial k = 0$ only at $\omega = k = 0$. There is no possibility of matching satellite to group velocity in this case when $\lambda << 1$.

In Figs. 19 to 27, schematic dispersion curves are drawn for propagation at 90° and various ω_p/ω_b ratios, showing several harmonic cyclotron frequencies together. These curves show the behaviour for large λ values as well and include the three cases actually computed by Dnestrovskii et al (1961, 1962) both for the ordinary and extraordinary waves. The relativistic versions have been given in Figs. 8 to 16. Many features of these curves differ. These differences and their interpretation have been discussed above. In a nutshell, this report shows that nonrelativistic dispersion theory in the vicinity of cyclotron resonances is incorrect for very small $k_{\parallel}$. We have also pointed out the significance of dispersion effects near $k \to 0$, where the curves rapidly rise above $\omega = n\omega_b$, as well as dispersion effects in regions where electromagnetic modes can propagate.

REFERENCES

Bernstein, I.B. - Phys. Rev. 109, 10 (1958).

Calvert, W. and G.B. Goe - J. Geophys. Res. 68, 6113 (1963).

Calvert, W., R.W. Knecht, T.E. VanZandt - Science 146, 391-395, (Oct. 16 1964).

Dnestrovskii, Yu.N. and D.P. Kostomarov - Sov. Phys. JETP 13, 986(1961); 14, 1089 (1962).

Dnestrovskii, Yu.N., D.P. Kostomarov and N.V. Skrydlov - Sov. Phys. Tech. Phys. 8, 691 (1964).

Fejer, J.A. and W. Calvert - J. Geophys. Res. 69, 5049 (1964).

Gershman, B.N. - Sov. Phys. - Doklady 6, 314 (1961).

Lockwood, G.E.K. - Can. J. Phys. 41, 190 (1963).

Muldrew, D.B. - J. Geophys. Res. 68, 5355 (1963).

Shkarofsky, I.P. - "The Dielectric Tensor Near Cyclotron Harmonics", Part 1 of this Report.

Shkarofsky, I.P. and T.W. Johnston - "Time Decay for Cyclotron Harmonics", Part 3 of this Report

Silin, V.P. and A.A. Rukhadze - "Electromagnetic Properties of Plasma and Plasma-like Media", Glavatomizdat, Moscow (1961) (In Russian).

Stix, T.H. - "The Theory of Plasma Waves", McGraw Hill Book Co., N.Y. (1962).

CAPTIONS FOR FIGURES

Fig. 1. The dispersion curve for the extraordinary electromagnetic wave near cyclotron harmonics, $n\omega_b$, for real ω and $n > 2$ (Fig. 1a), $n = 2$ (Fig. 1b) and $n = 1$ (Fig. 1c). The dashed part of the curve is the region where k is complex.

Fig. 2. A polar plot of the complex function F (Fig. 2a), F^{-1} (Fig. 2b), $F^{-(n-1)^{-1}}$ (Fig. 2c) which are required when $\omega^2 > \omega_T^2$ and of $-F$ (Fig. 2d), $-F^{-1}$ (Fig. 2e) and $(-F)^{-(n-1)^{-1}}$ (Fig. 2f) required when $\omega^2 < \omega_T^2 \equiv \omega_b^2 + \omega_p^2$. Subscripts r and i refer to real and imaginary parts. The numbers $0, \pm\infty$ are values of $\mu\delta$, the argument of F, marked off on the polar plot.

Fig. 3. The dispersion curves for the plasma wave for real ω, complex k, near the cyclotron harmonics when $\omega^2 > \omega_T^2$ (Fig. 3a) and $\omega^2 < \omega_T^2$ (Fig. 3b). The dashed parts indicate regions where k is very complex.

Fig. 4. Schematic dispersion curves for the extraordinary and plasma waves for real ω and complex k. (Dashed parts indicate very complex k values.)

(4a) $n\omega_b > \omega_R > \omega_T > \omega_L$ or $K_\parallel > 0$, $K_r > 0$, $K_\perp > 0$.

(4b) $\omega_R > \omega_T > \omega_L > n\omega_b$ or $K_\parallel < 0$, $K_r < 0$, $K_\perp < 0$.

(4c) $\omega_R > n\omega_b > \omega_T > \omega_L$ or $K_\parallel > 0$, $K_r < 0$, $K_\perp > 0$.

(4d) $\omega_R > \omega_T > n\omega_b > \omega_L$ or $K_\parallel > 0$, $K_r < 0$, $K_\perp < 0$.

where $\omega_{(R)}^{(L)} = \mp \frac{\omega_b}{2} + \sqrt{\frac{\omega_b^2}{4} + \omega_p^2}$ or $X = 1 \pm Y$ or $K_{(r)}^{(\parallel)} = 0$

$$\omega_T = \sqrt{\omega_p^2 + \omega_b^2} \quad \text{or} \quad X = 1 - Y^2 \quad \text{or} \quad K_\perp = 0$$

$$X = \frac{\omega_p^2}{\omega^2}\ ,\quad Y = \frac{\omega_b}{\omega}\ ,\quad K_{(\frac{l}{r})} = 1 - \frac{\omega_b^2}{\omega(\omega \pm \omega_b)}\ ,\quad K_\perp = 1 - \frac{\omega_p^2}{\omega^2 - \omega_b^2}$$

(4e) Dispersion curve for the ordinary wave when ω is real, $\omega > \omega_p$ and k complex. No solution is possible when $\omega < \omega_p$. When n = 1, the wiggle is substantial but for n > 1 it is negligible. Here $K_\parallel = 1 - \frac{\omega_p^2}{\omega^2}$.

Fig. 5. Dispersion curves for the coupled extraordinary and plasma waves, for complex ω and real wave numbers near or less than the electromagnetic values. The 4 cases correspond to those in Figs. 4a-d. The dashed parts indicate the coupling regions between F > 0 and F < 0 branches.

Fig. 6. Dispersion curve for the ordinary wave when ω is complex and k is real. Also $\omega > \omega_p$ (Fig. 6a) or $\omega < \omega_p$ (Fig. 6b).

Fig. 7. Ratio of plasma to cyclotron frequency (or Larmor radius to Debye length) versus altitude with an assumed model of electron density and magnetic field at the equator for daytime and sunspot minimum.

Fig. 8. Schematic complex ω - real k dispersion curves including several harmonics for the coupled extraordinary and plasma waves when $2\omega_b^2 > \omega_p^2$.

Fig. 9. Complex ω - real k dispersion curves for the ordinary wave when $\omega_b > \omega_p$.

Fig. 10. Complex ω - real k dispersion curves for the coupled waves when $3\omega_b^2 > \omega_p^2 > 2\omega_b^2$.

Fig. 11. Complex ω - real k dispersion curves for the ordinary wave when $2\omega_b > \omega_p > \omega_b$.

Fig. 12. Complex ω - real k dispersion curves for the coupled waves when $6\omega_b^2 > \omega_p^2 > 3\omega_b^2$.

Fig. 13. Complex ω - real k dispersion curves for the ordinary wave when $3\omega_b > \omega_p > 2\omega_b$.

Fig. 14. Complex ω - real k dispersion curves for the coupled waves when $8\omega_b^2 > \omega_p^2 > 6\omega_b^2$.

Fig. 15. Complex ω - real k dispersion curves for the coupled waves when $12\omega_b^2 > \omega_p^2 > 8\omega_b^2$.

Fig. 16. Complex ω - real k dispersion curves for the ordinary wave when $4\omega_b > \omega_p > 3\omega_b$.

Fig. 17. Plot of the normalized group velocity versus $\lambda = k_\perp^2 v_t^2/\omega_b^2$ for the Bernstein electrostatic mode for n = 2 (Figs. 17a), n = 3 (Fig. 17b), n = 4 (Fig. 17c) and n = 5 (Fig. 17d).

Fig. 18a - d. Nonrelativistic version of the dispersion curves for the coupled extraordinary and plasma waves. The four cases (Figs. 18a to 18d) correspond to a to d in Figs. 4 or 5. The checked portions on the curves indicate coupling regions between the waves, circles indicate zero group velocity points and crosses indicate points where the group velocity can be matched to satellite velocity. The waves varying as $\omega - n\omega_b \propto \lambda^{n-1}$ or λ^{n-1} are designated respectively n-1 and n+1. The values $x_{1,2}$ are $x_1 = K_1 K_r/K_\perp$ and $x_2 = 2K_1$.

18e,f. Nonrelativistic version of the dispersion curves for the ordinary wave when $\omega > \omega_p$ (Fig. 18e) and $\omega < \omega_p$ (Fig. 18f).

Fig. 19. Nonrelativistic version of the schematic dispersion curves including several harmonics for the coupled extraordinary and plasma waves when $2\omega_b^2 > \omega_p^2$.

Fig. 20. Nonrelativistic dispersion curves for the ordinary wave when $\omega_b > \omega_p$.

Fig. 21. Nonrelativistic dispersion curves for the coupled waves when $3\omega_b^2 > \omega_p^2 > 2\omega_b^2$.

Fig. 22. Nonrelativistic dispersion curves for the ordinary wave when $2\omega_b > \omega_p > \omega_b$.

Fig. 23. Nonrelativistic dispersion curves for the coupled waves when $6\omega_b^2 > \omega_p^2 > 3\omega_b^2$.

Fig. 24. Nonrelativistic dispersion curves for the ordinary wave when $3\omega_b > \omega_p > 2\omega_b$.

Fig. 25. Nonrelativistic dispersion curves for the coupled waves when $8\omega_b^2 > \omega_p^2 > 6\omega_b^2$.

Fig. 26. Nonrelativistic dispersion curves for the coupled waves when $12\omega_b^2 > \omega_p^2 > 8\omega_b^2$.

Fig. 27. Nonrelativistic dispersion curves for the ordinary wave in $4\omega_b > \omega_p > 3\omega_b$.

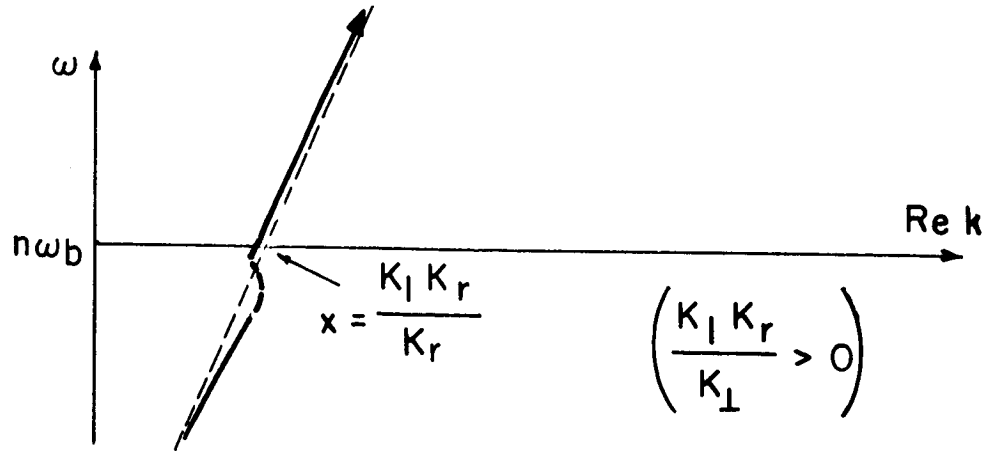

FIGURE 1(a)

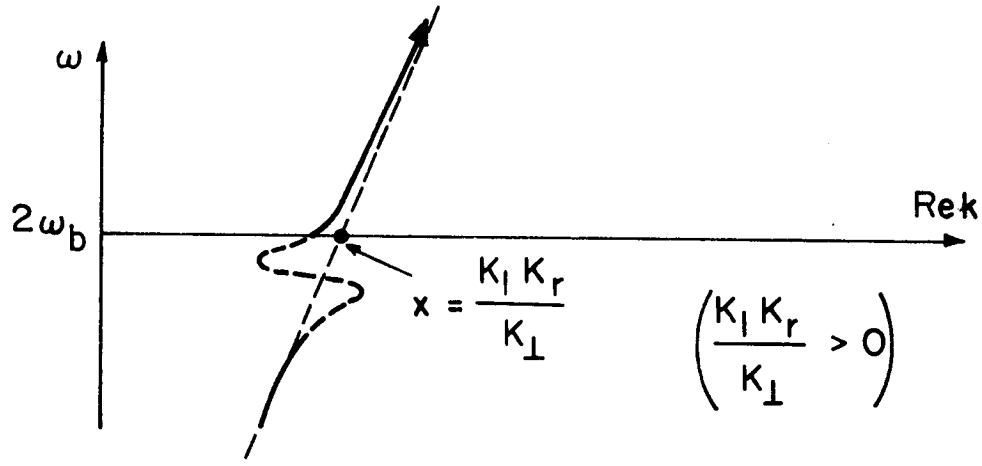

FIGURE 1(b)

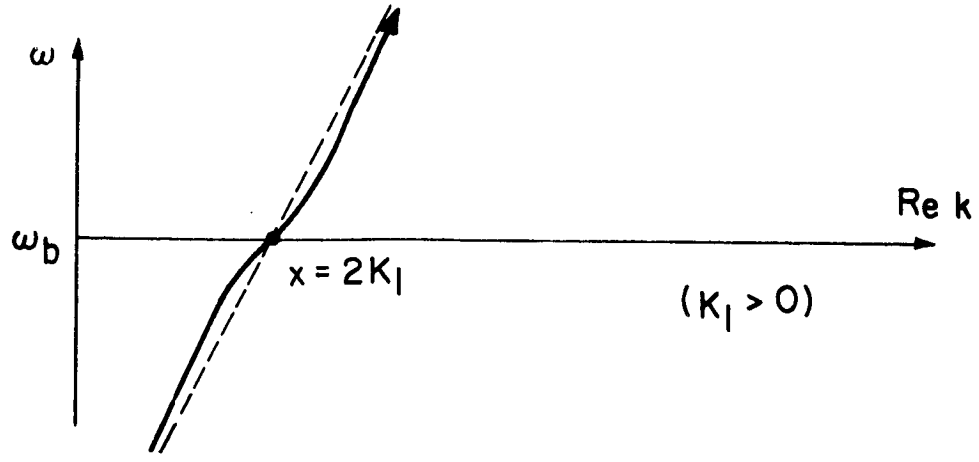

FIGURE 1(c)

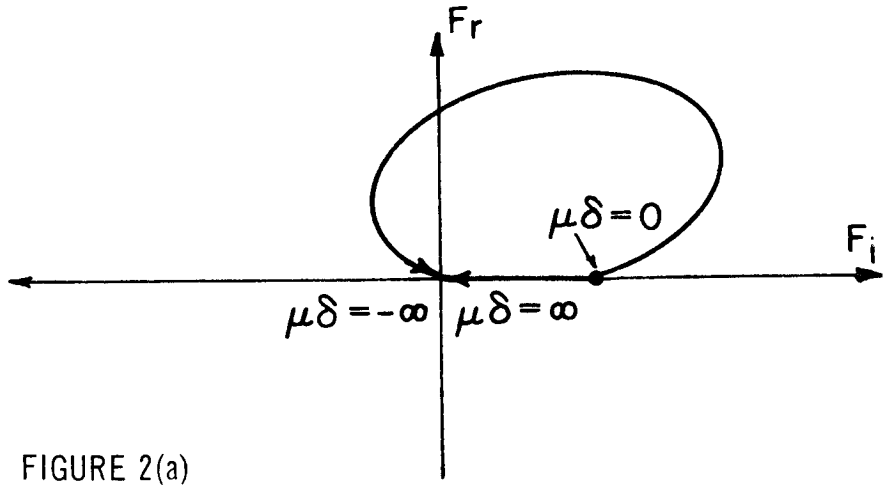

FIGURE 2(a)

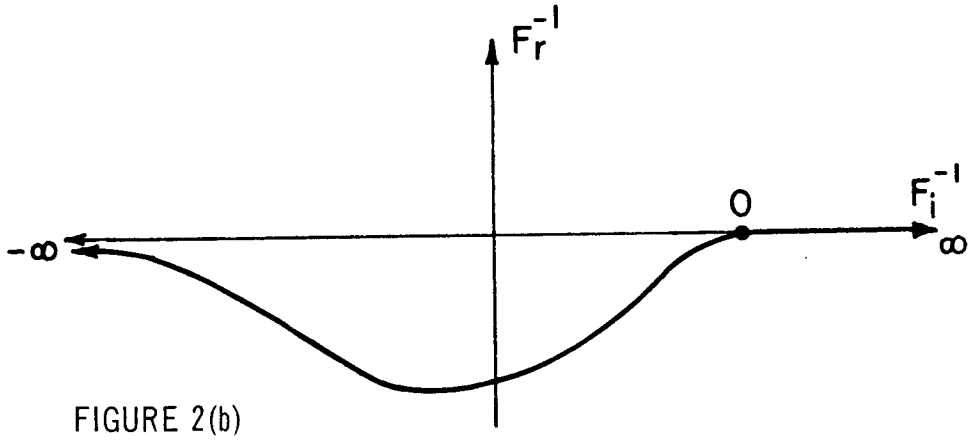

FIGURE 2(b)

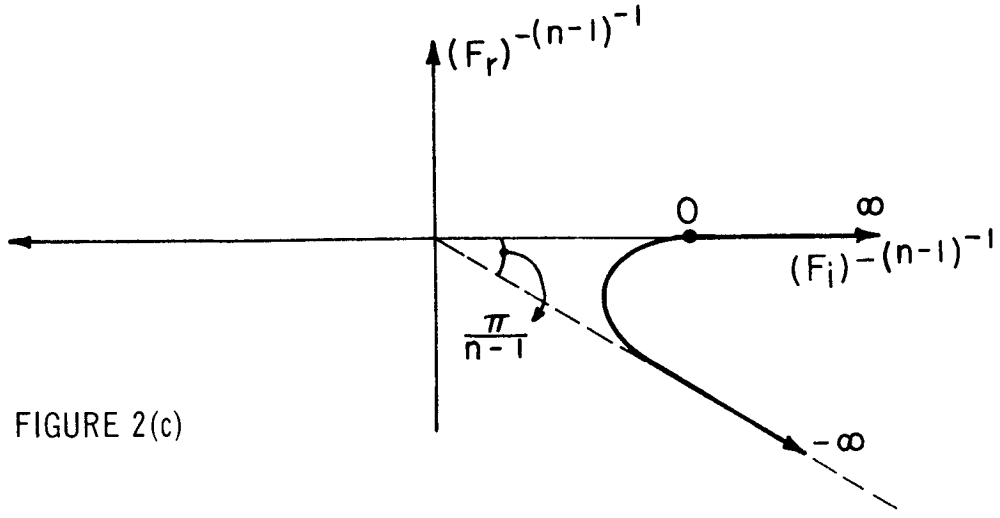

FIGURE 2(c)

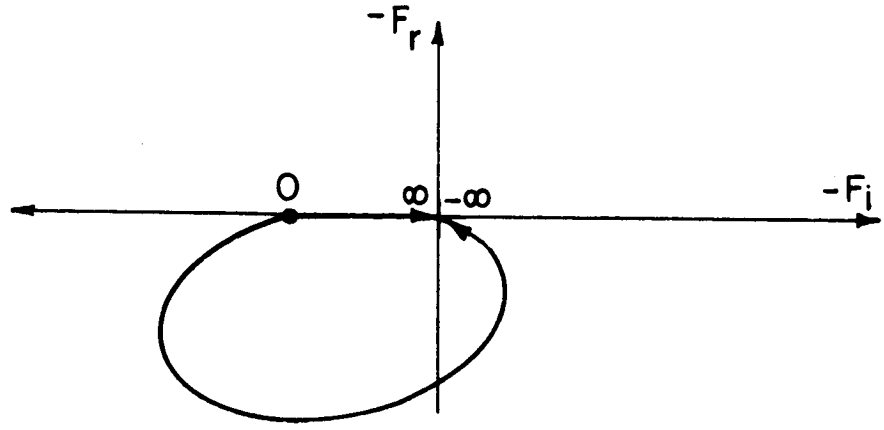

FIGURE 2(d)

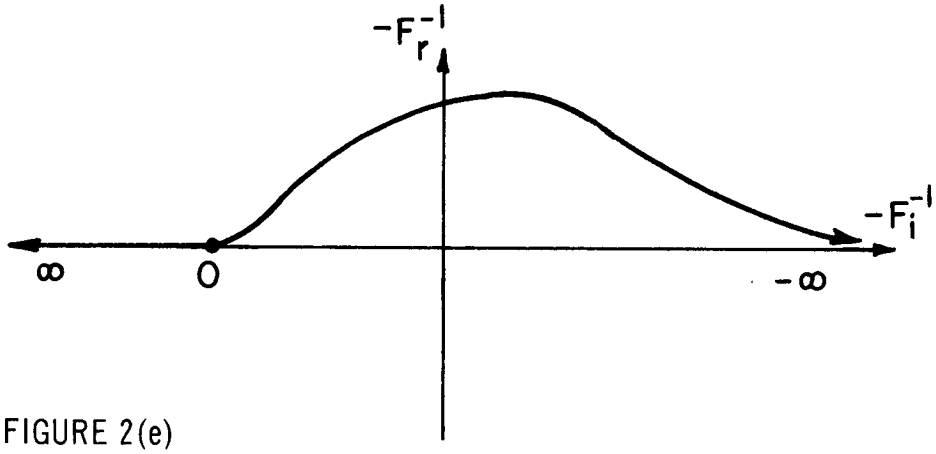

FIGURE 2(e)

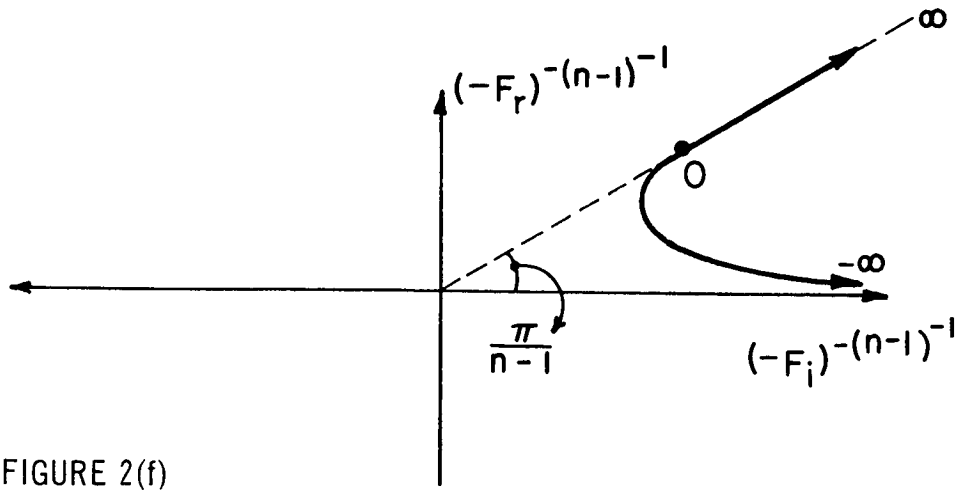

FIGURE 2(f)

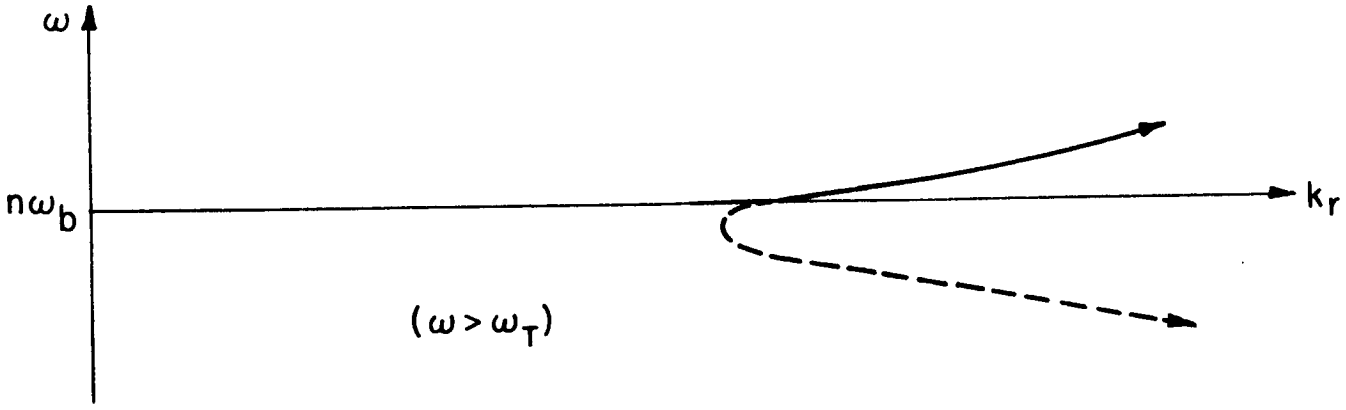

FIGURE 3(a)

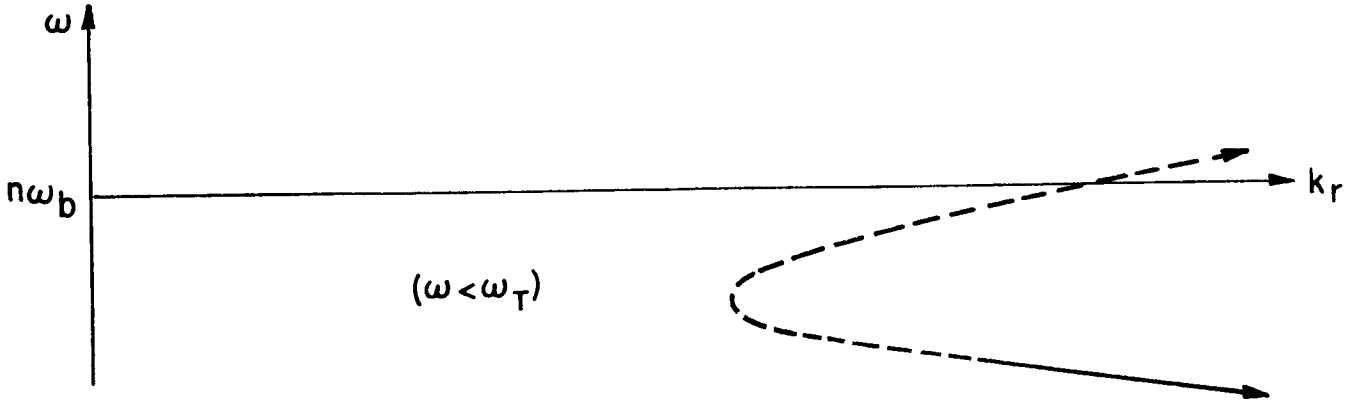

FIGURE 3(b)

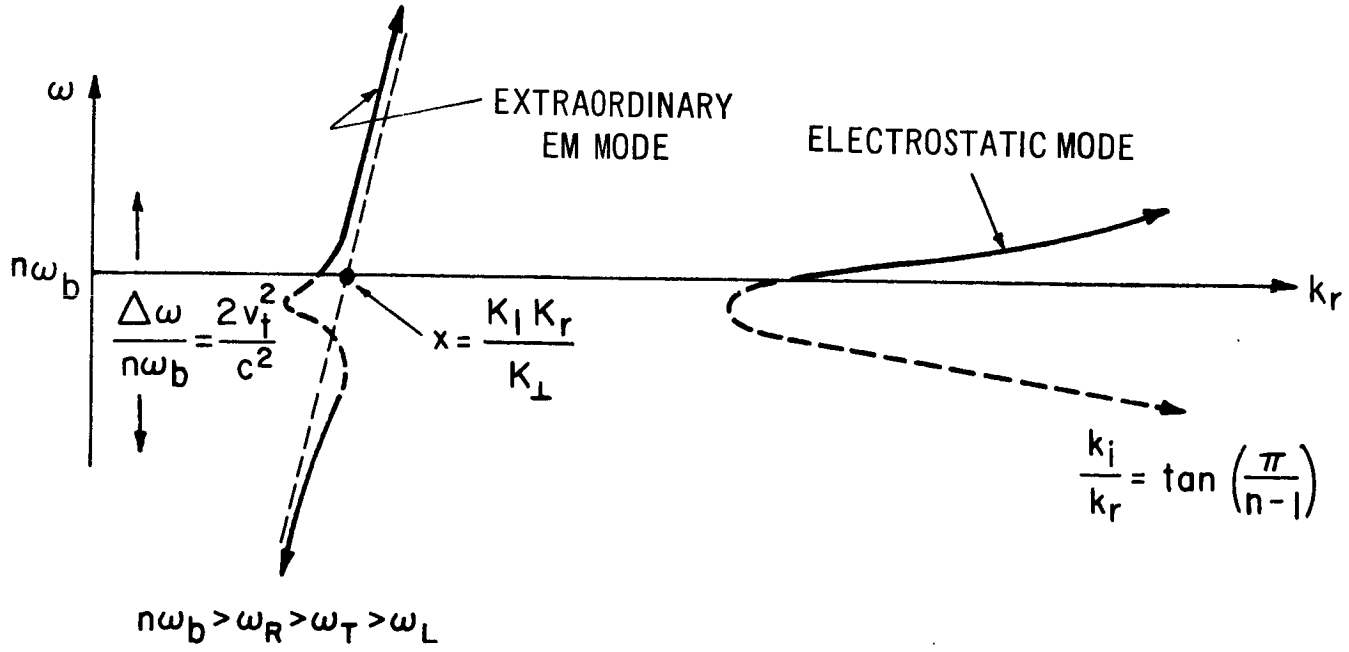

$n\omega_b > \omega_R > \omega_T > \omega_L$

FIGURE 4(a)

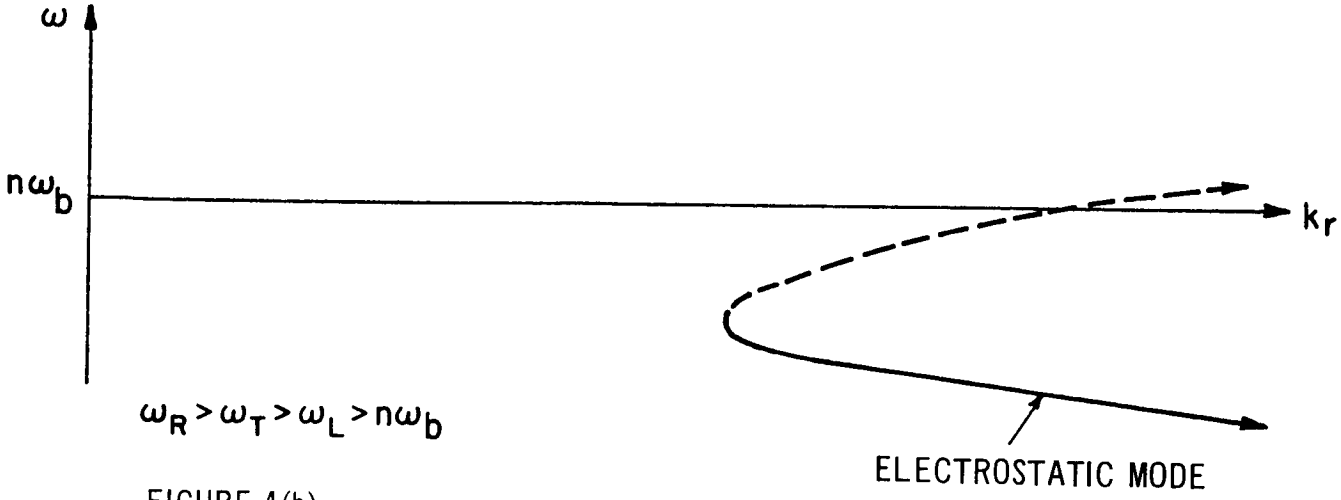

$\omega_R > \omega_T > \omega_L > n\omega_b$

FIGURE 4(b)

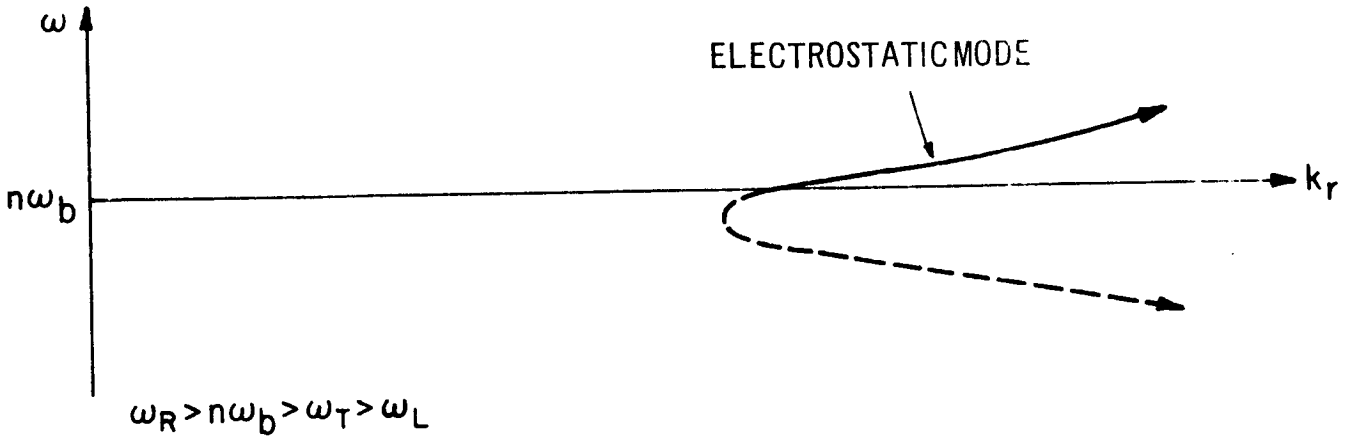

FIGURE 4(c)

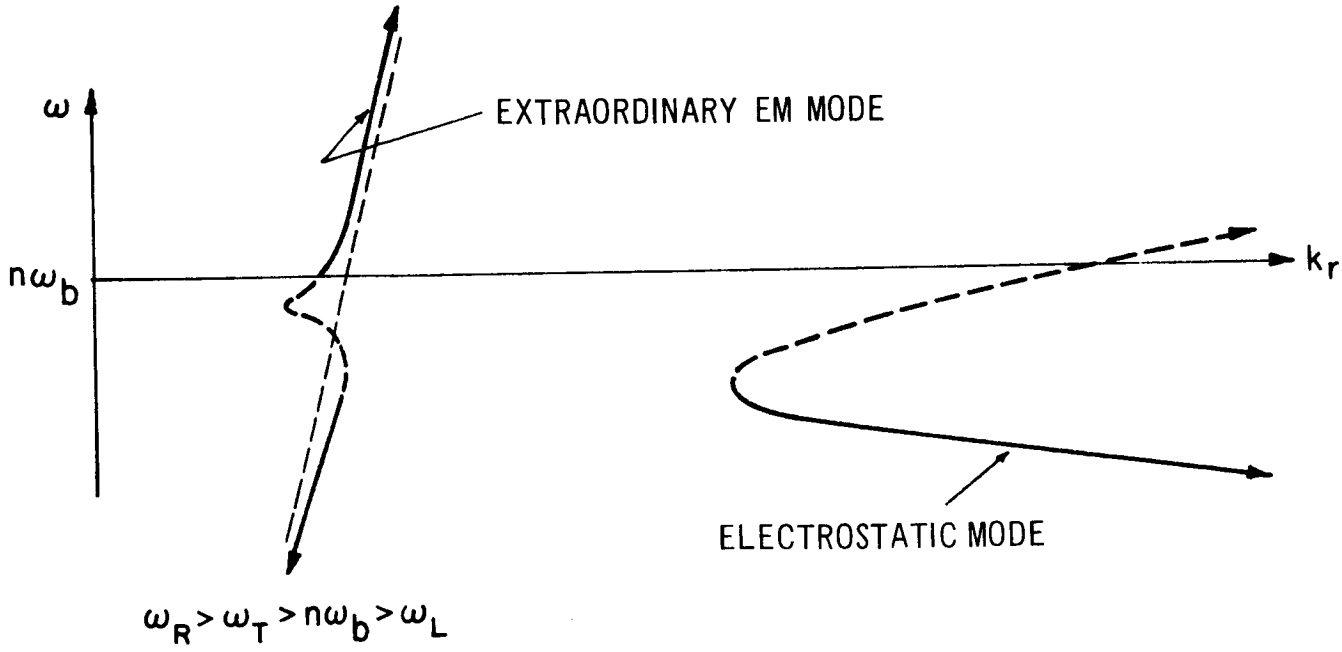

FIGURE 4(d)

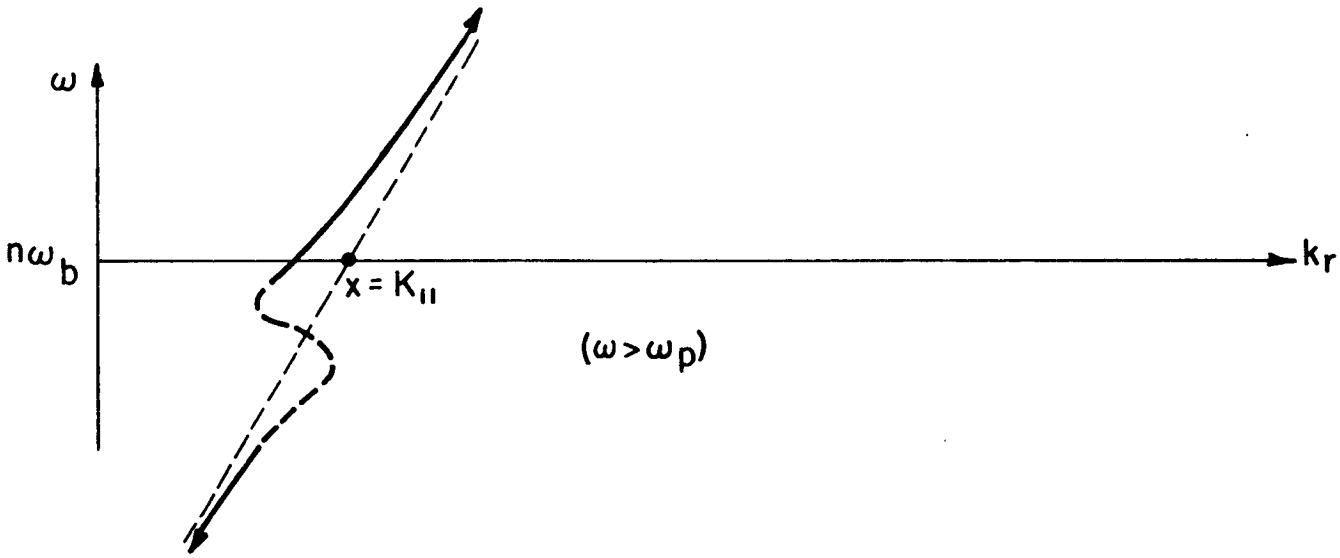

FIGURE 4(e)

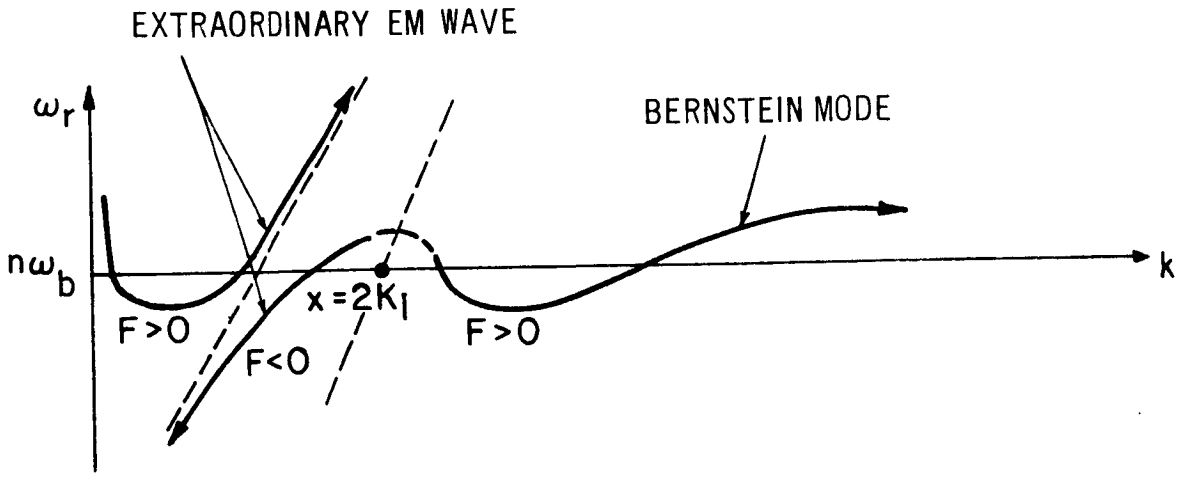

FIGURE 5(a) $n\omega_b > \omega_R > \omega_T > \omega_L$

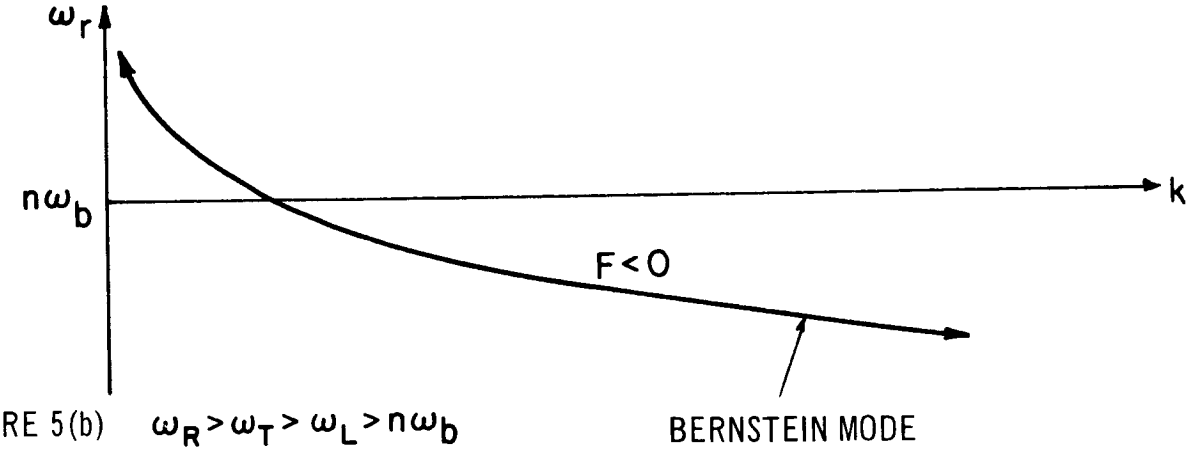

FIGURE 5(b) $\omega_R > \omega_T > \omega_L > n\omega_b$

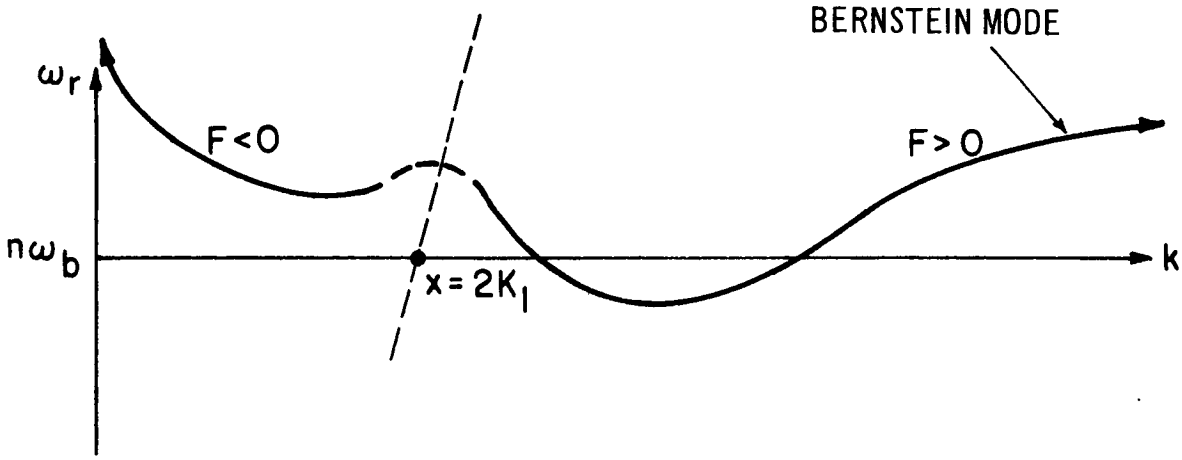

FIGURE 5(c) $\omega_R > n\omega_b > \omega_T > \omega_L$

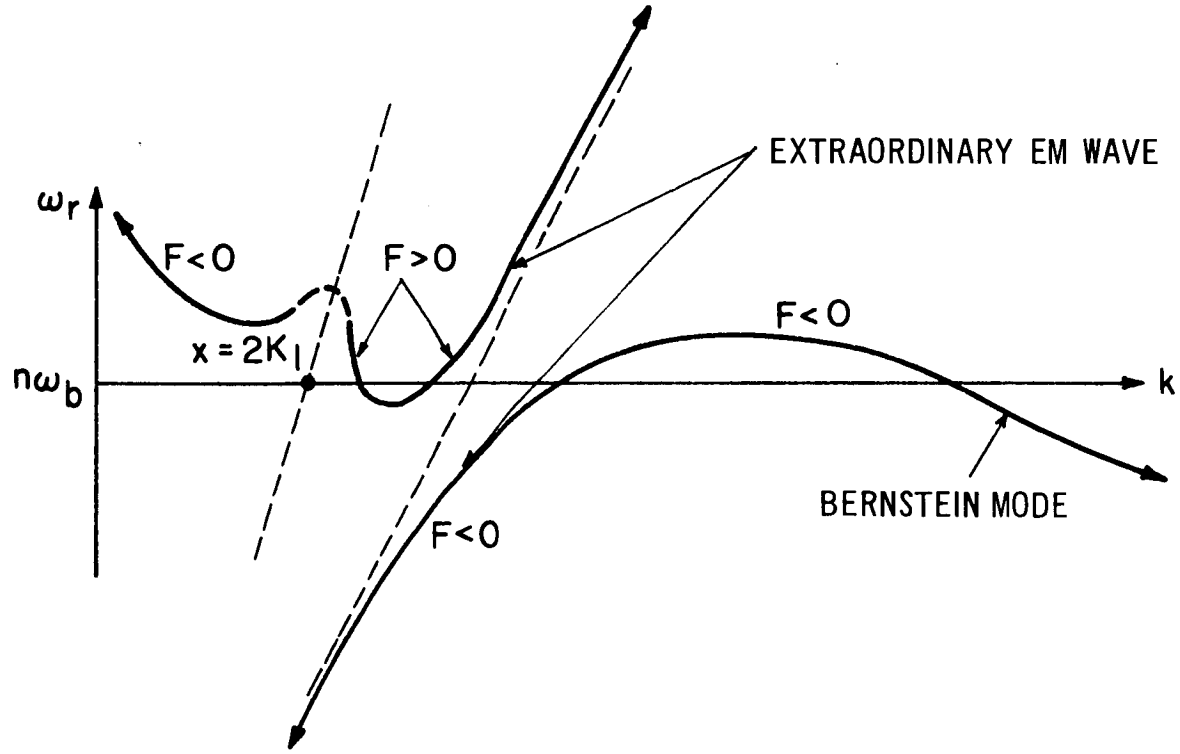

FIGURE 5(d) $\omega_R > \omega_T > n\omega_b > \omega_L$

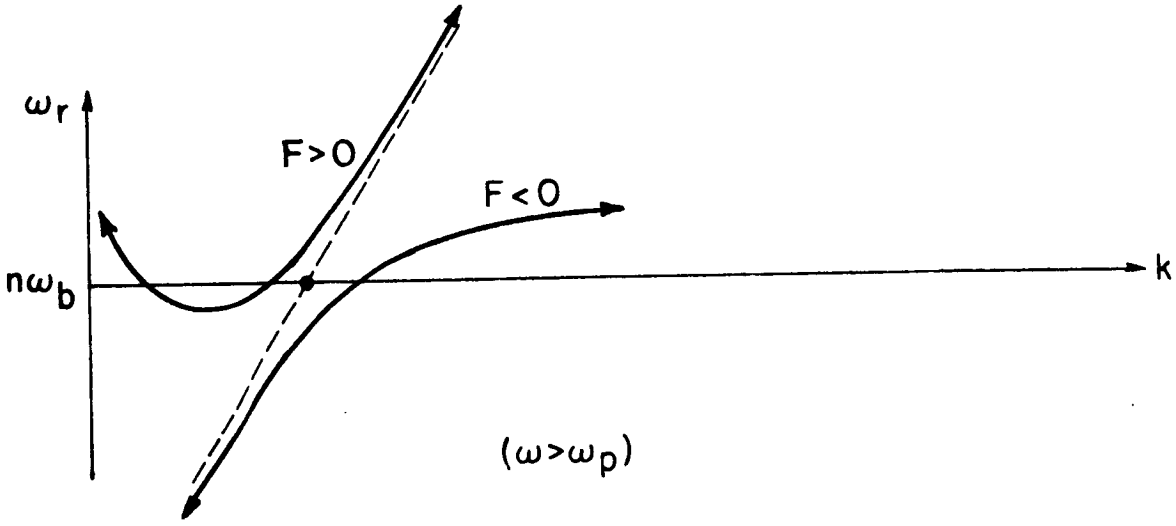

FIGURE 6(a)

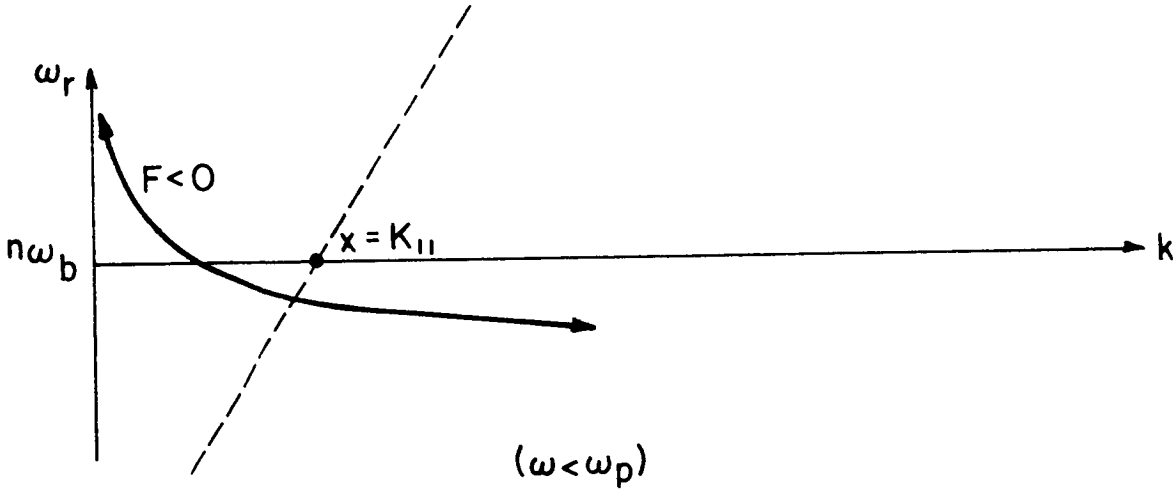

FIGURE 6(b)

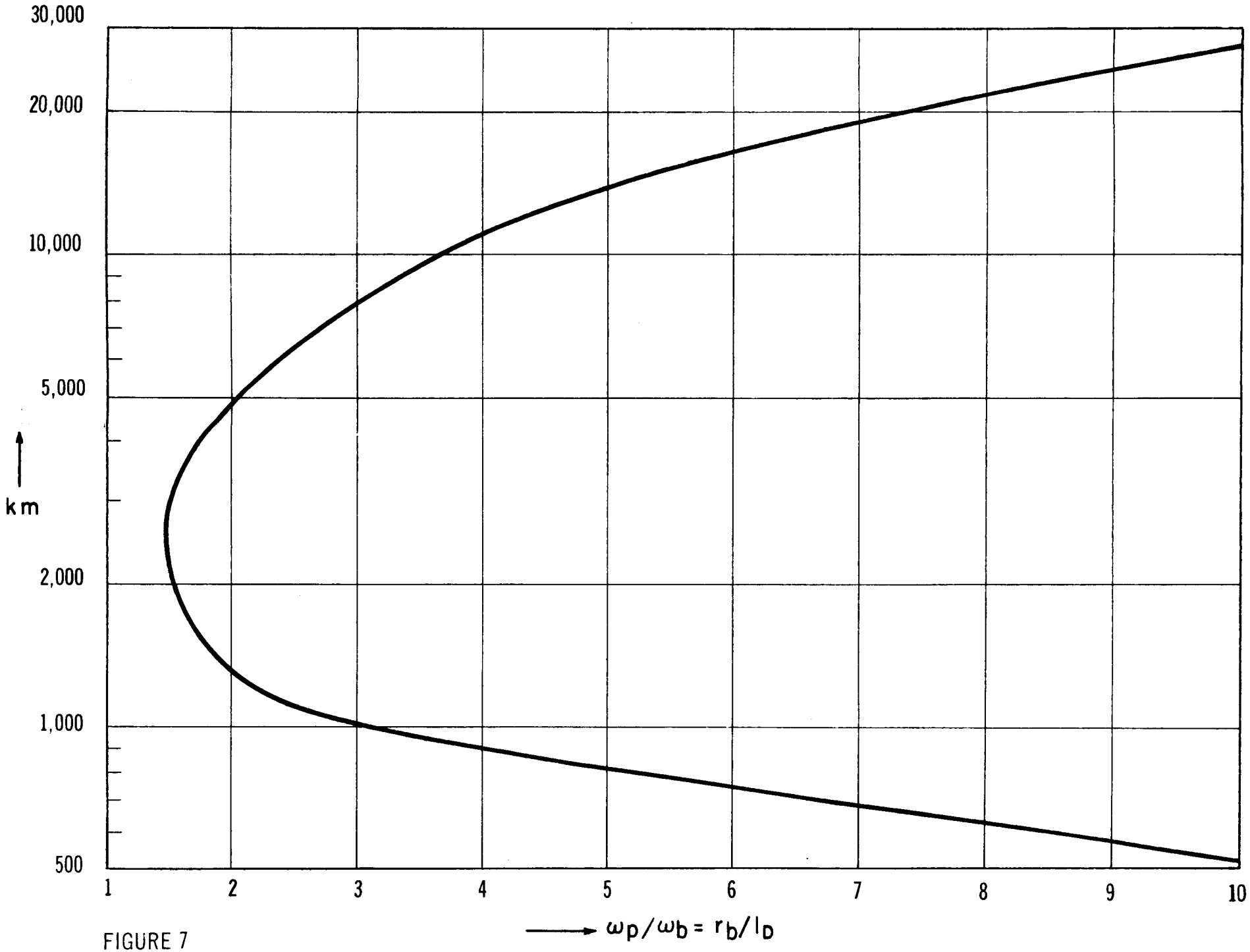
30,000
20,000
10,000
5,000
2,000
1,000
500
km
1
2
3
4
5
6
7
8
9
10
ωp/ωb = rb/lD

FIGURE 7

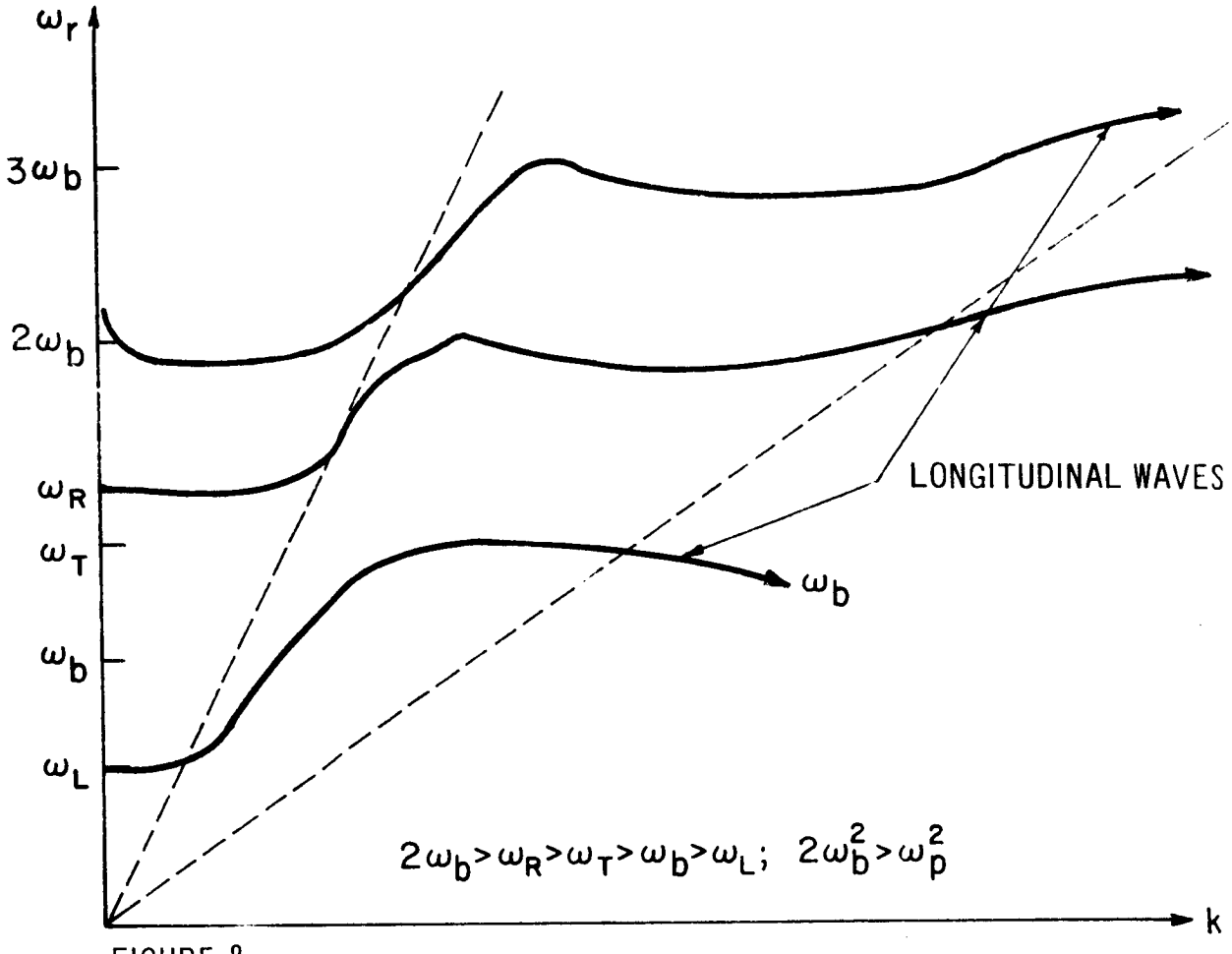

FIGURE 8

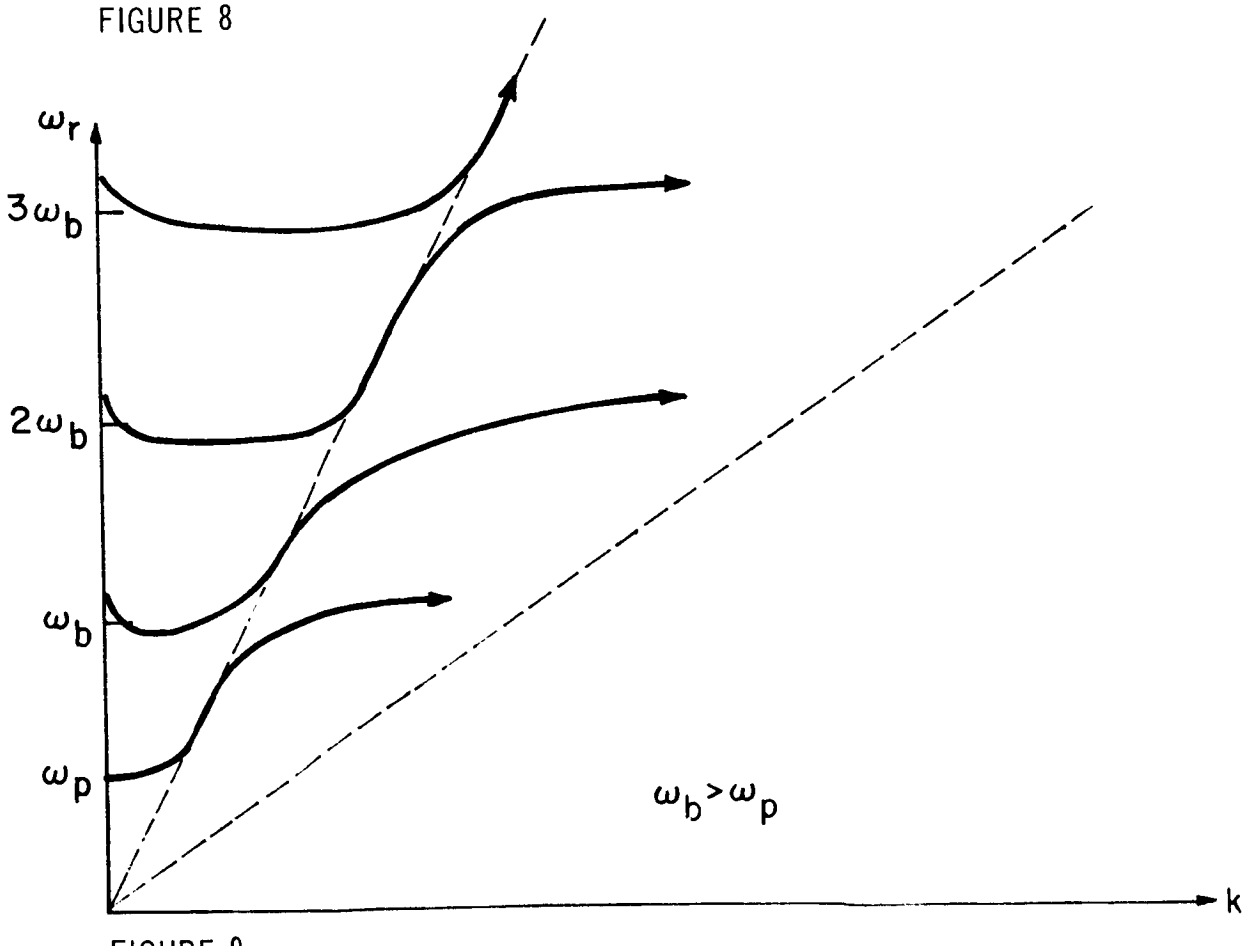

FIGURE 9

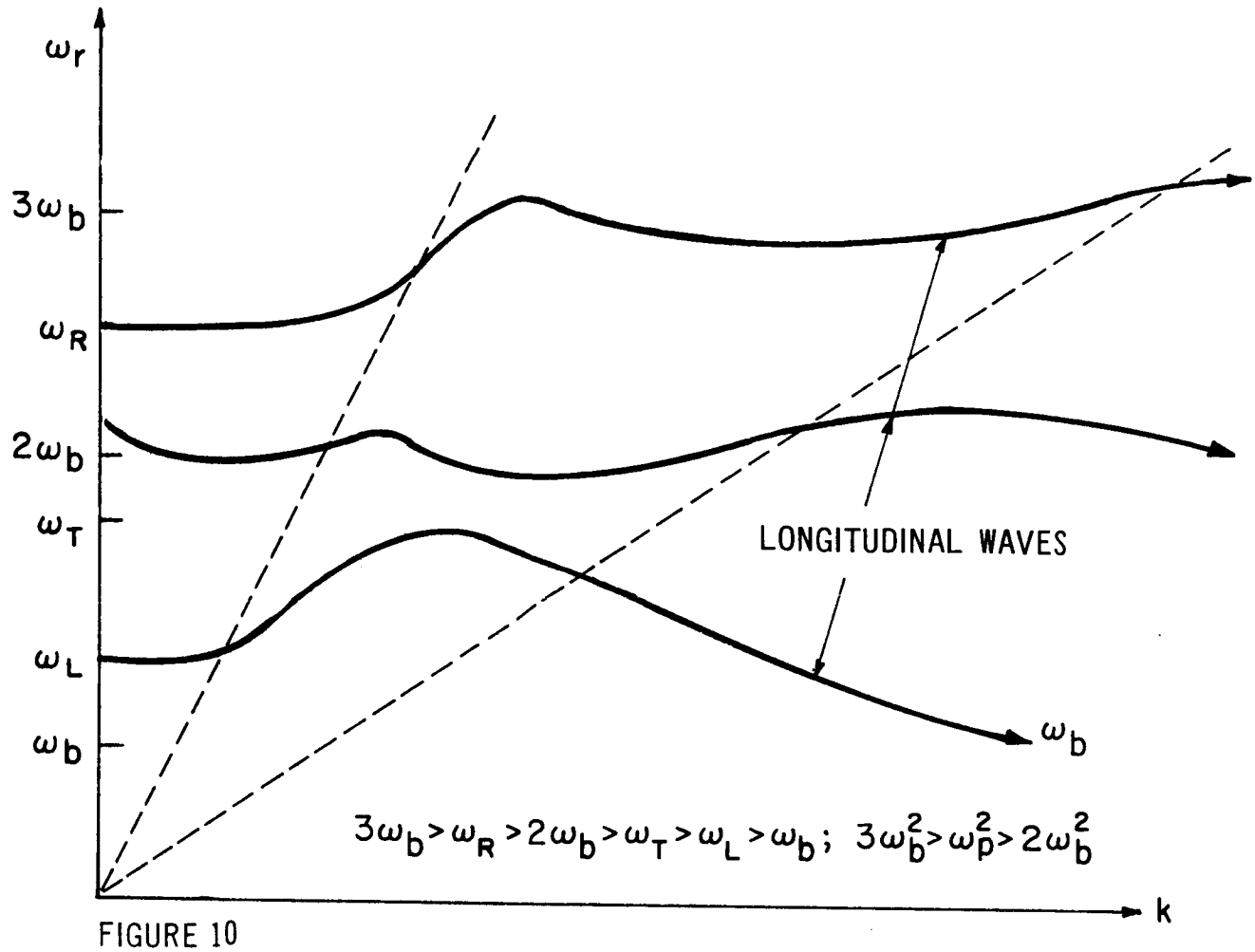

FIGURE 10

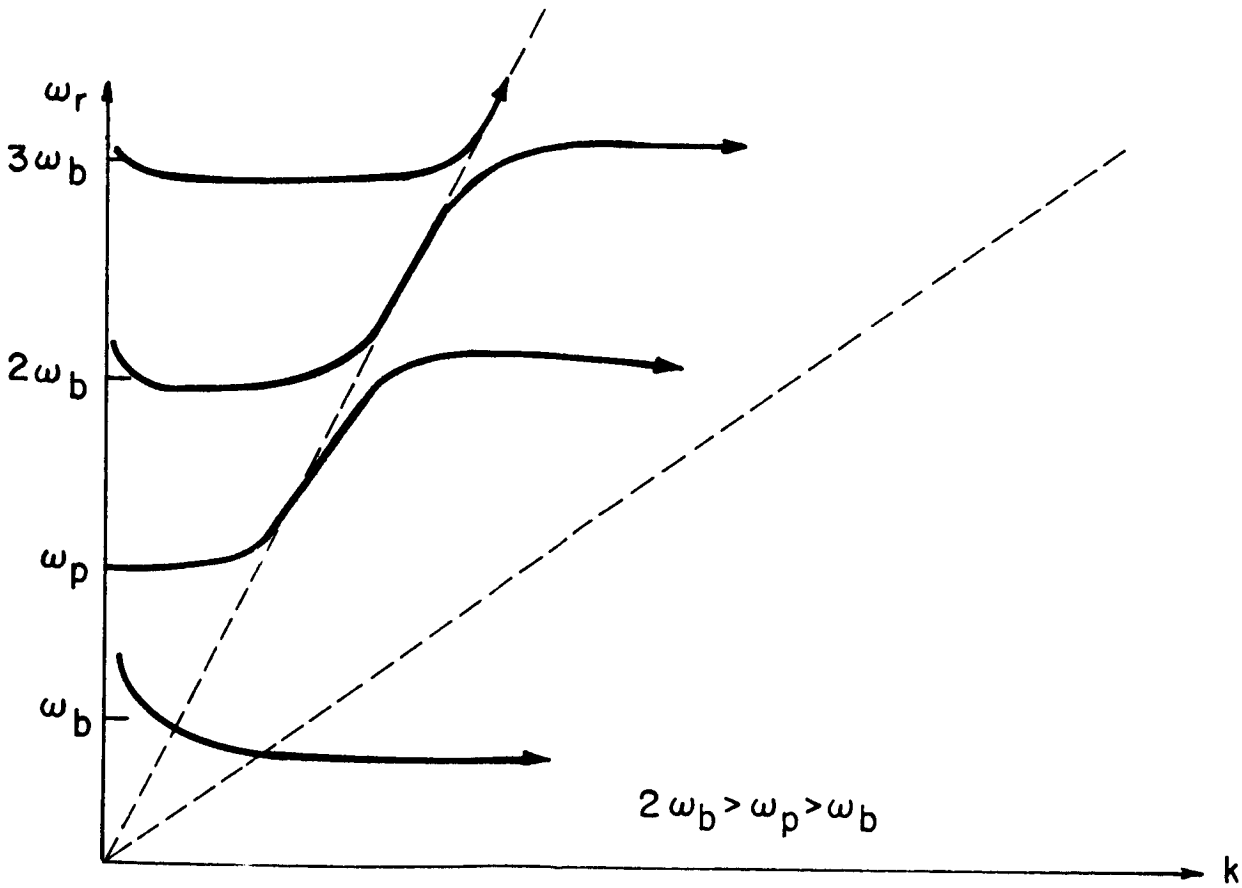

FIGURE 11

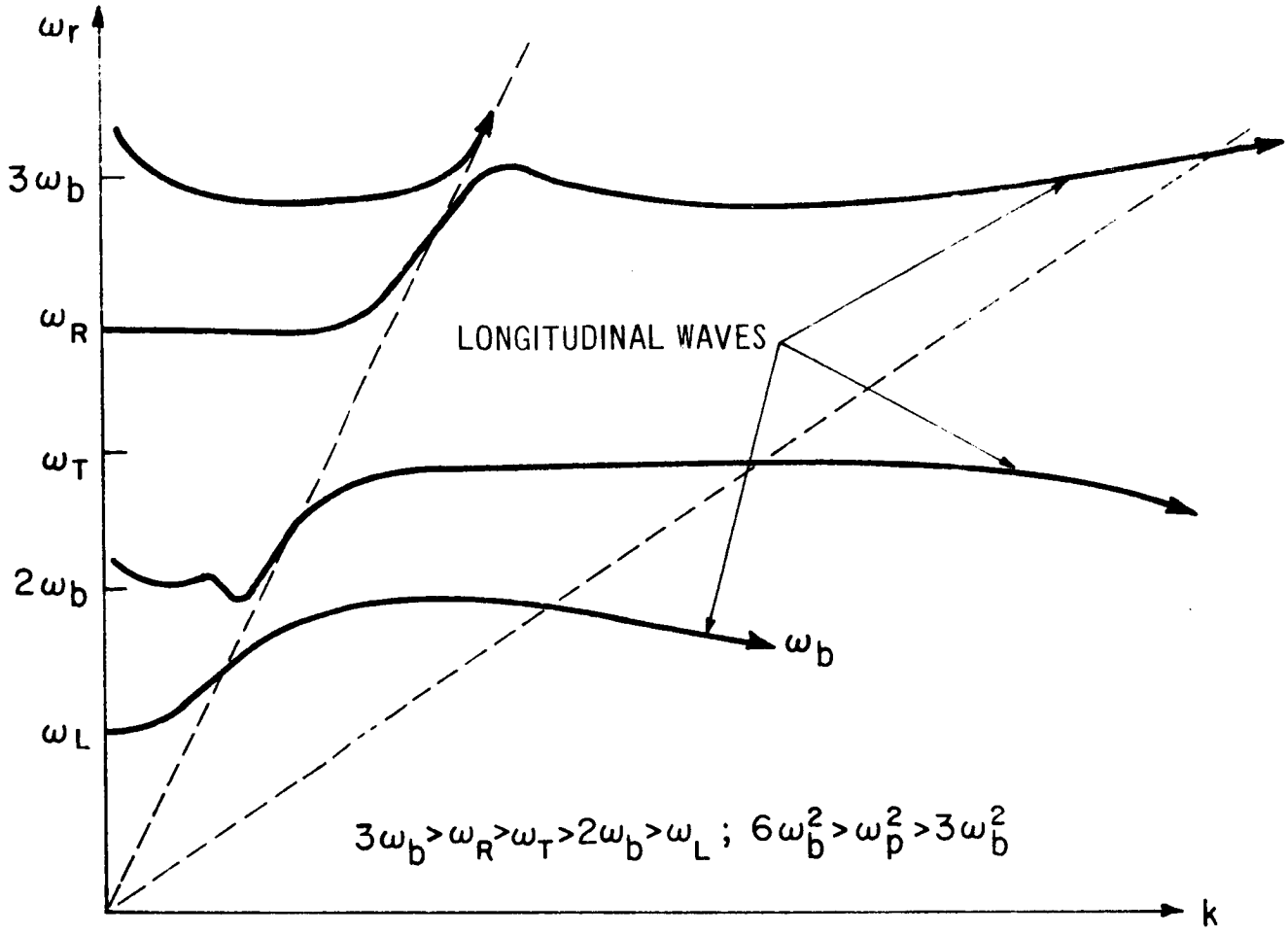

FIGURE 12

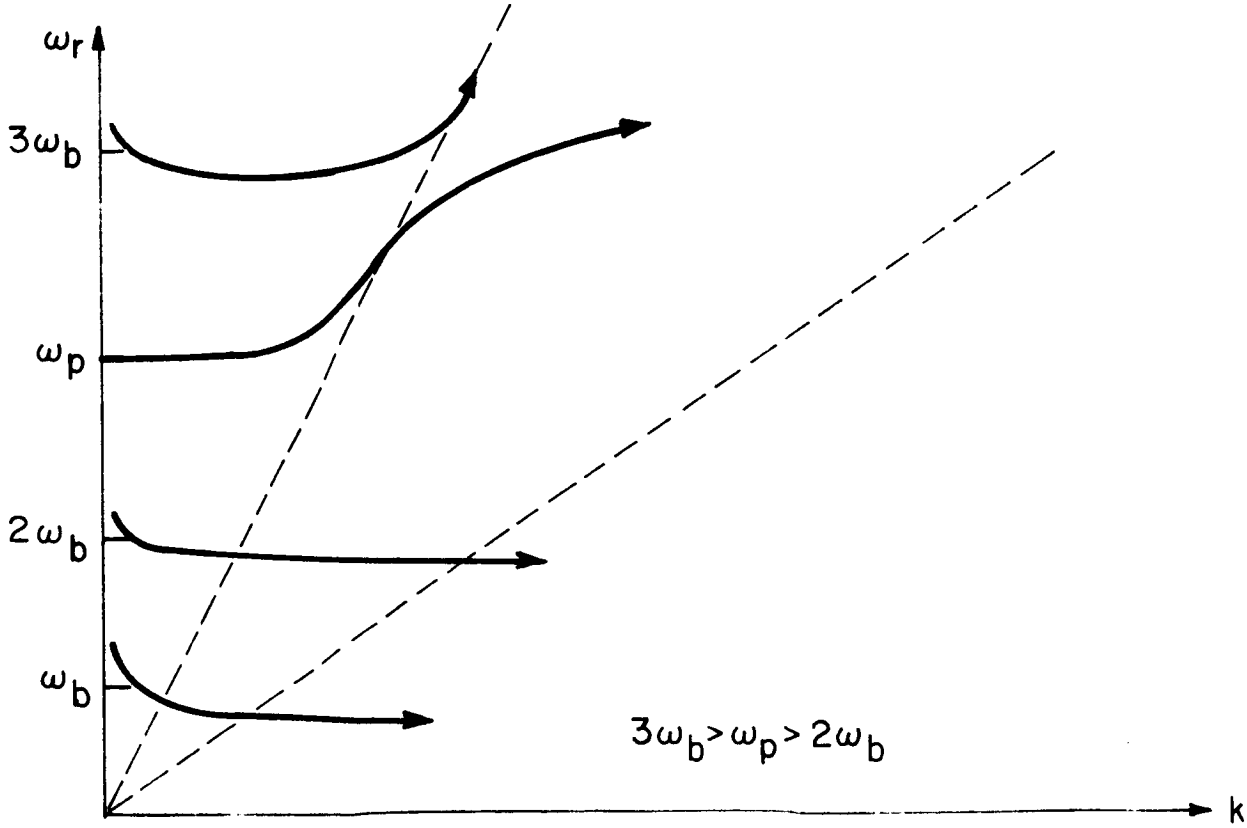

FIGURE 13

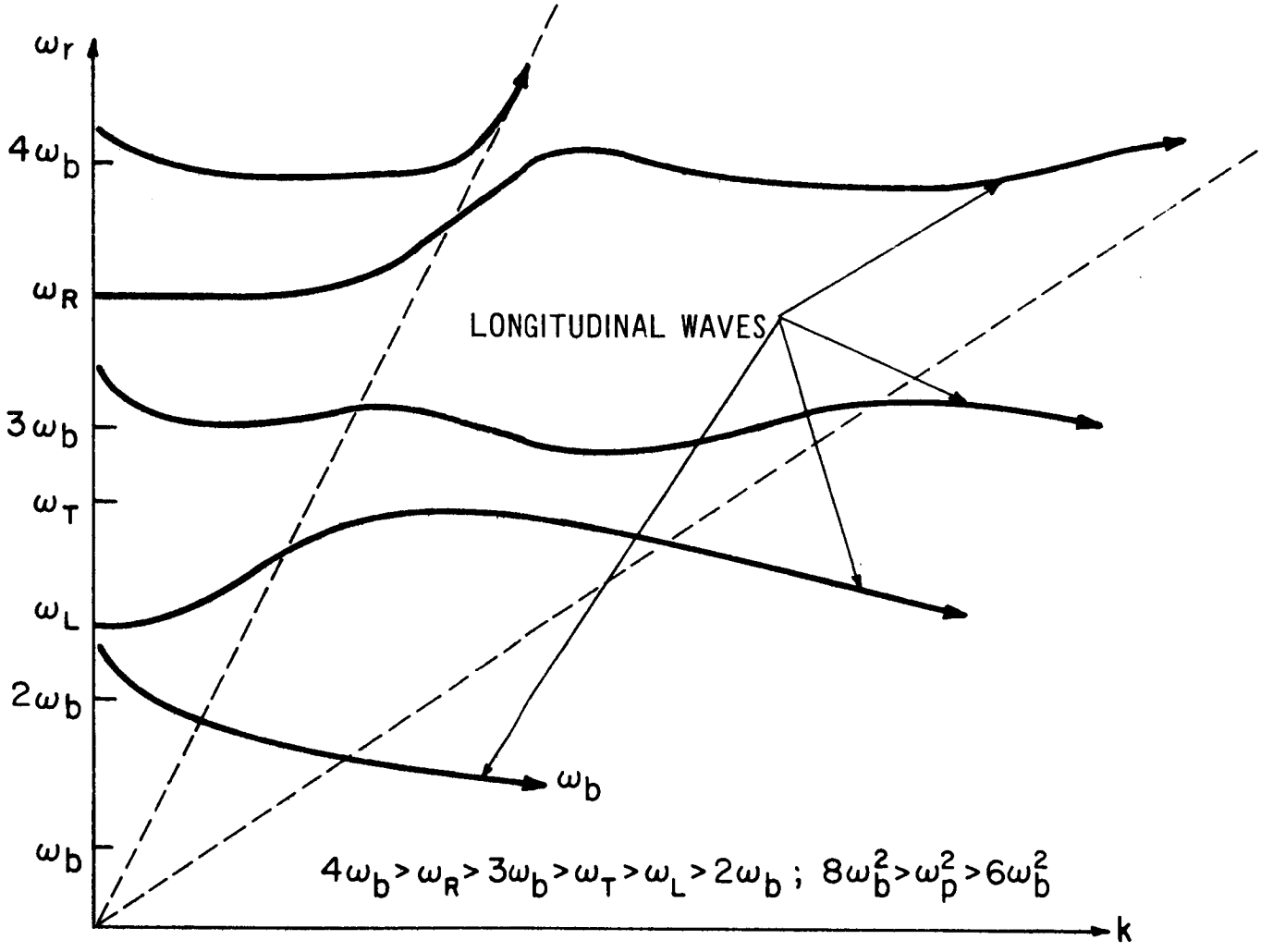
ω_r
$4\omega_b$
ω_R
$3\omega_b$
ω_T
ω_L
$2\omega_b$
ω_b
ω_b
LONGITUDINAL WAVES
$4\omega_b > \omega_R > 3\omega_b > \omega_T > \omega_L > 2\omega_b$; $8\omega_b^2 > \omega_p^2 > 6\omega_b^2$
k

FIGURE 14

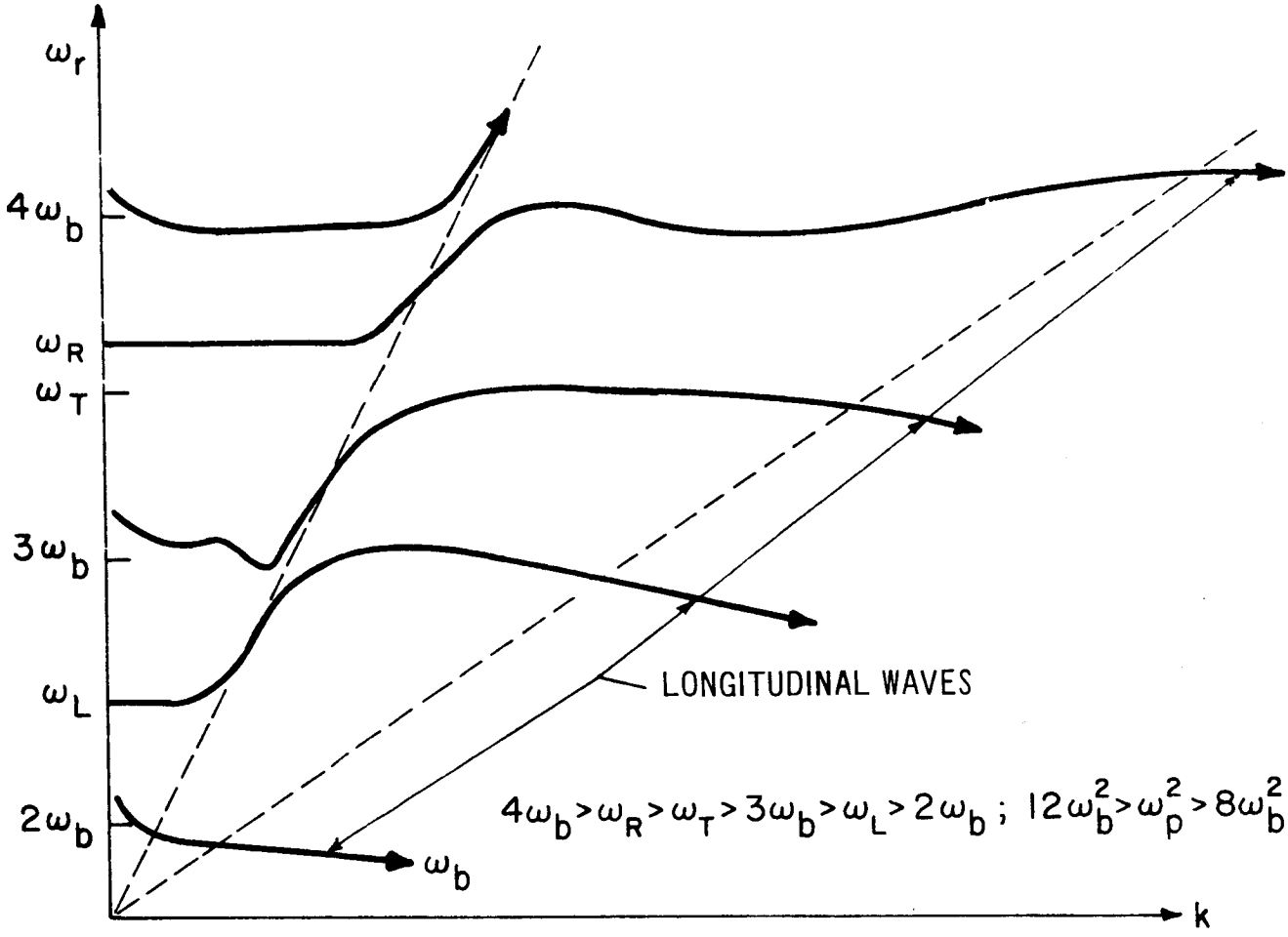

FIGURE 15

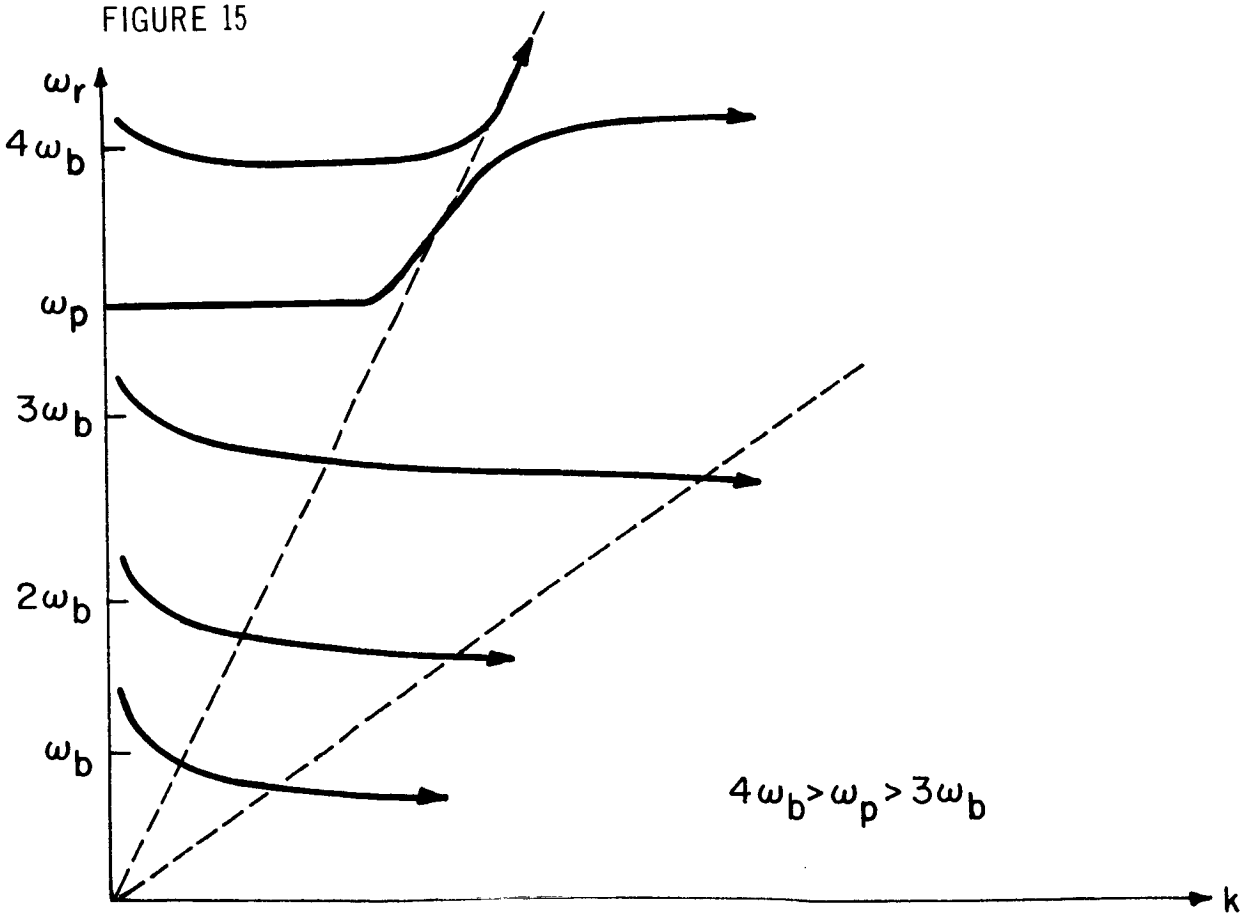

FIGURE 16

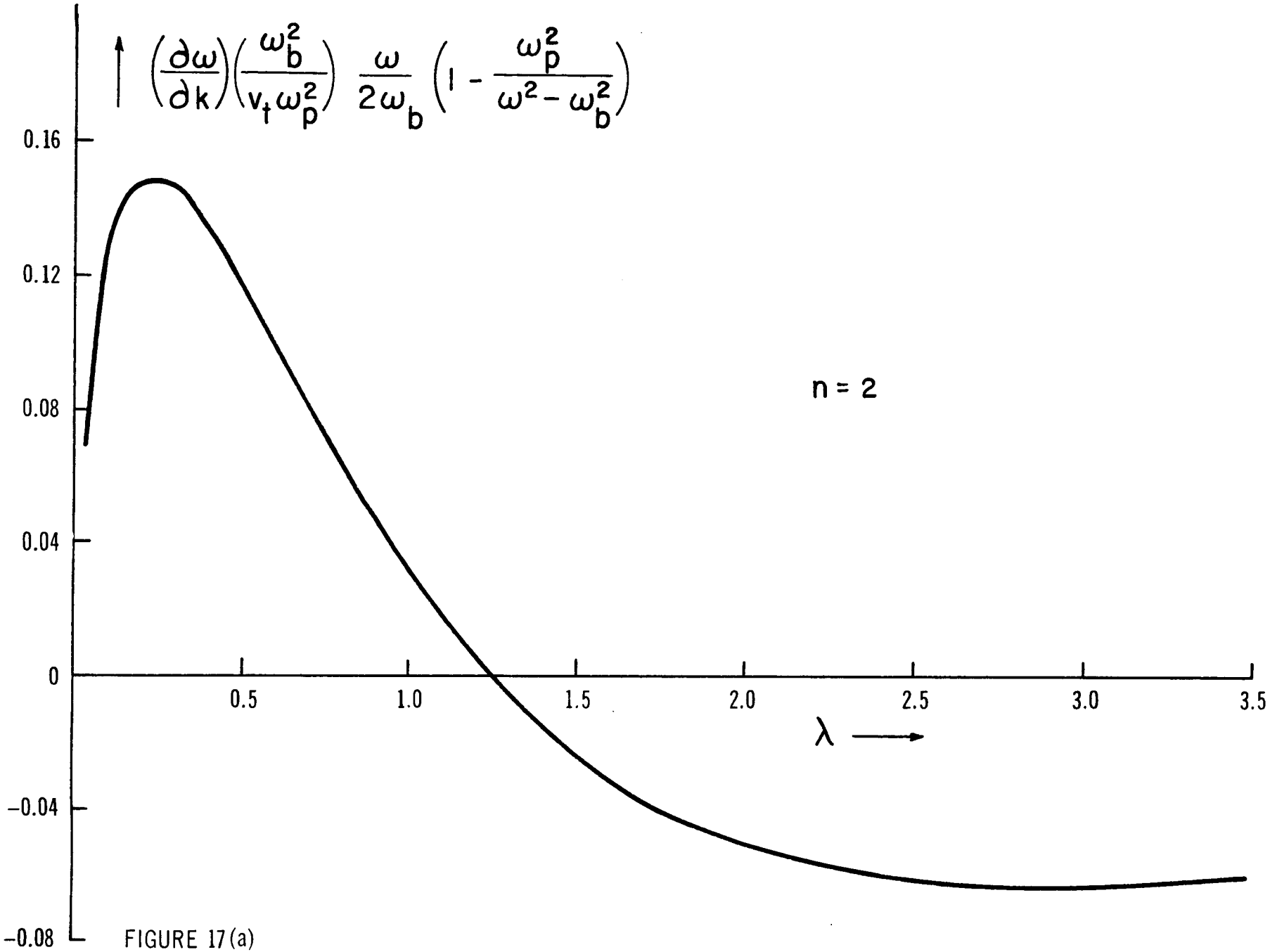
$\left(\frac{\partial\omega}{\partial k}\right)\left(\frac{\omega_b^2}{v_t\omega_p^2}\right)\frac{\omega}{2\omega_b}\left(1-\frac{\omega_p^2}{\omega^2-\omega_b^2}\right)$
0.16
0.12
0.08
0.04
0
−0.04
−0.08
0.5
1.0
1.5
2.0
2.5
3.0
3.5
λ
n = 2

FIGURE 17(a)

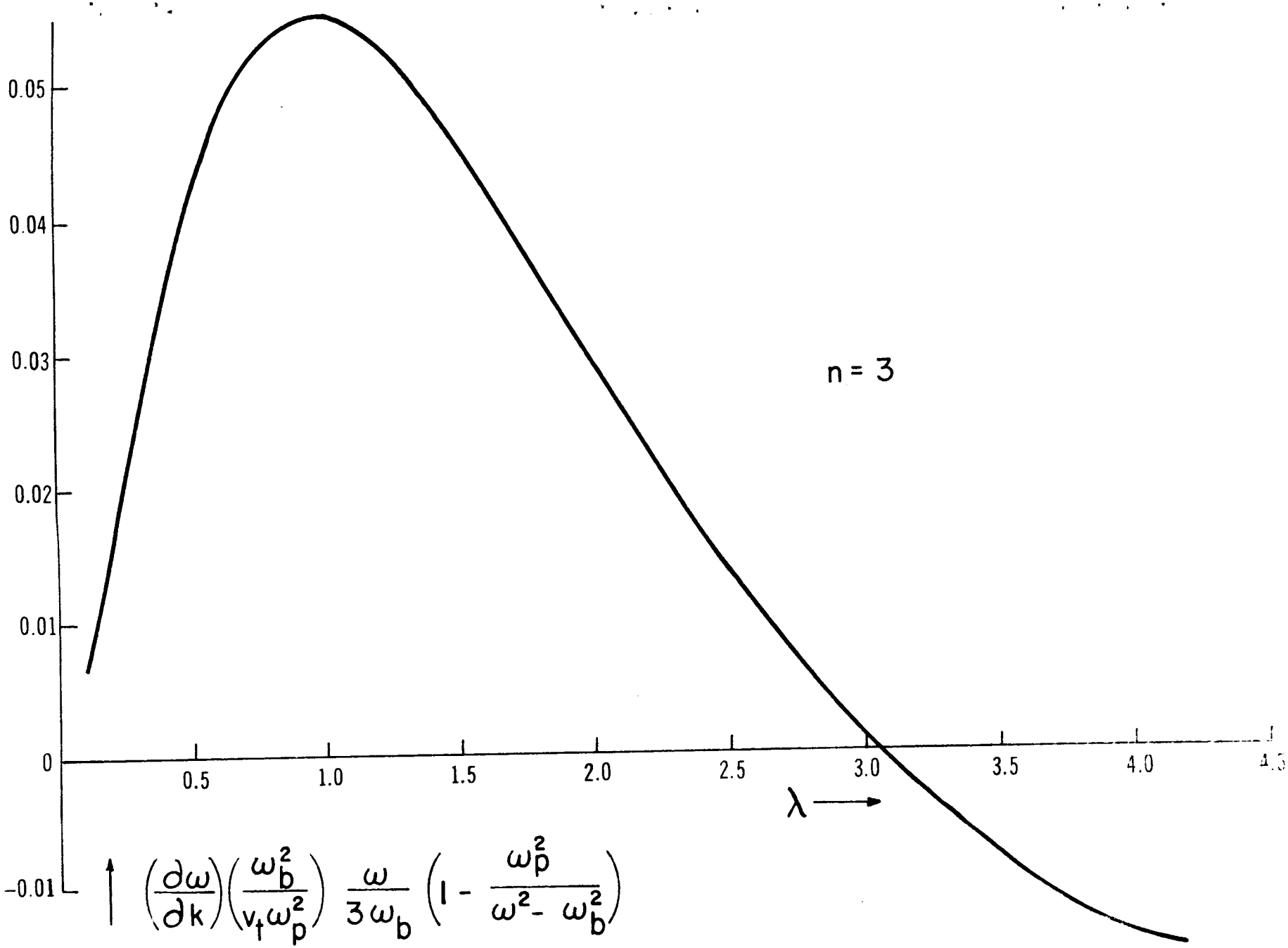
0.05
0.04
0.03
0.02
0.01
0
-0.01
0.5
1.0
1.5
2.0
2.5
3.0
3.5
4.0
λ
n = 3
$\left(\frac{\partial\omega}{\partial k}\right)\left(\frac{\omega_b^2}{v_t\omega_p^2}\right)\frac{\omega}{3\omega_b}\left(1-\frac{\omega_p^2}{\omega^2-\omega_b^2}\right)$

FIGURE 17(b)

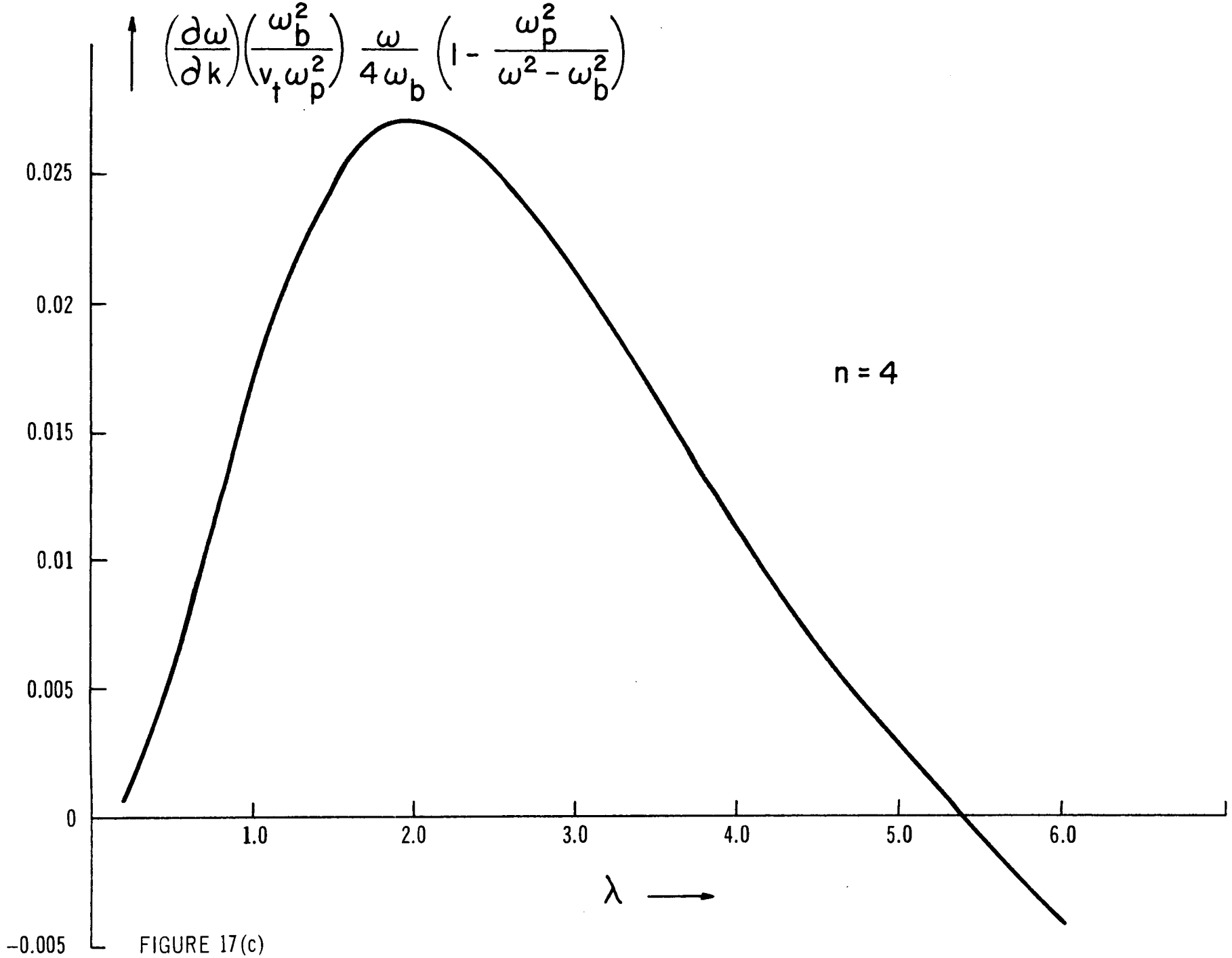
$\left(\frac{\partial\omega}{\partial k}\right)\left(\frac{\omega_b^2}{v_t\omega_p^2}\right)\frac{\omega}{4\omega_b}\left(1-\frac{\omega_p^2}{\omega^2-\omega_b^2}\right)$
0.025
0.02
0.015
0.01
0.005
0
-0.005
1.0
2.0
3.0
4.0
5.0
6.0
λ
n = 4

FIGURE 17(c)

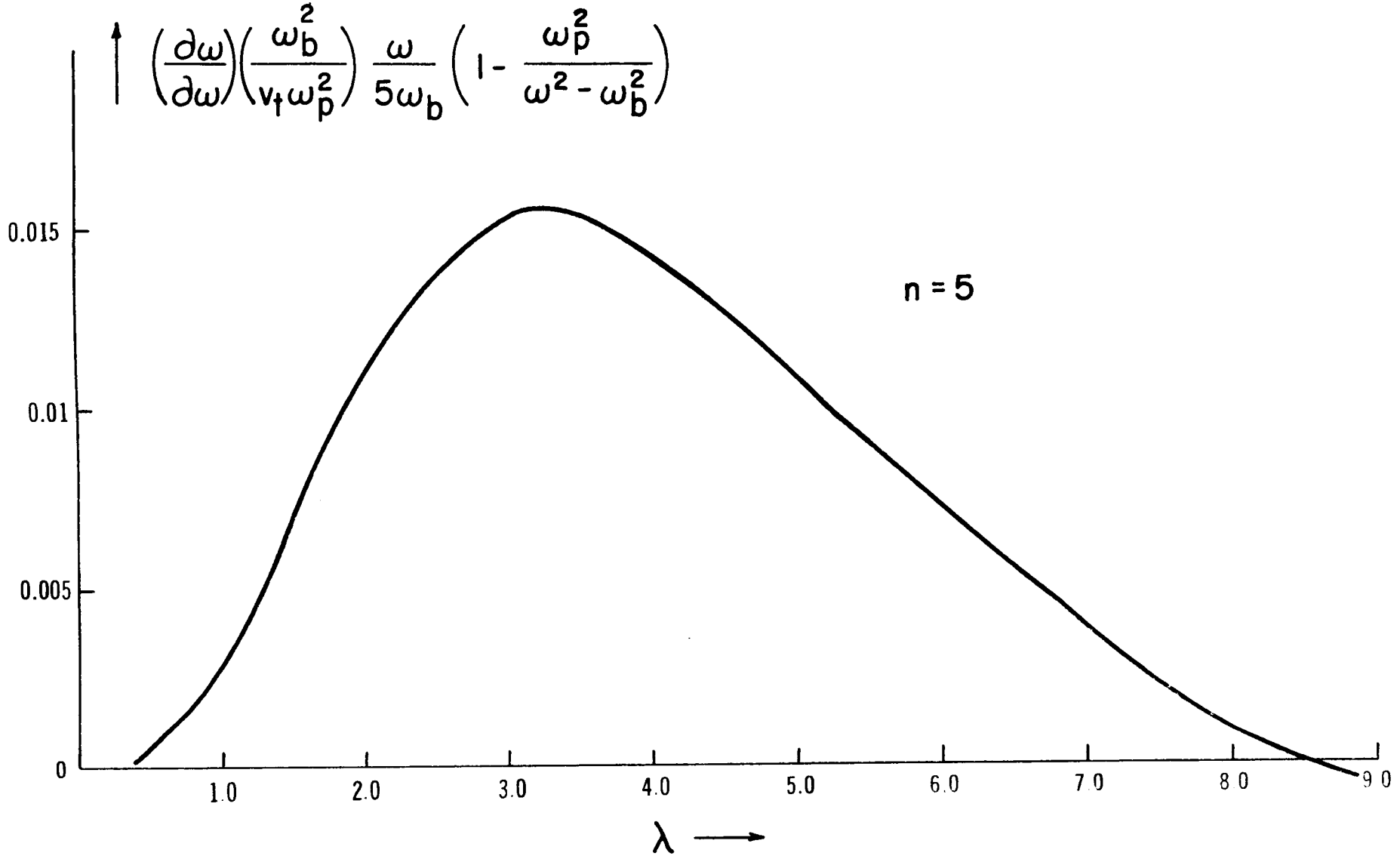
$\left(\frac{\partial\omega}{\partial\omega}\right)\left(\frac{\omega_b^2}{v_t\omega_p^2}\right)\frac{\omega}{5\omega_b}\left(1-\frac{\omega_p^2}{\omega^2-\omega_b^2}\right)$
0.015
0.01
0.005
0
n = 5
1.0
2.0
3.0
4.0
5.0
6.0
7.0
8.0
9.0
λ

FIGURE 17(d)

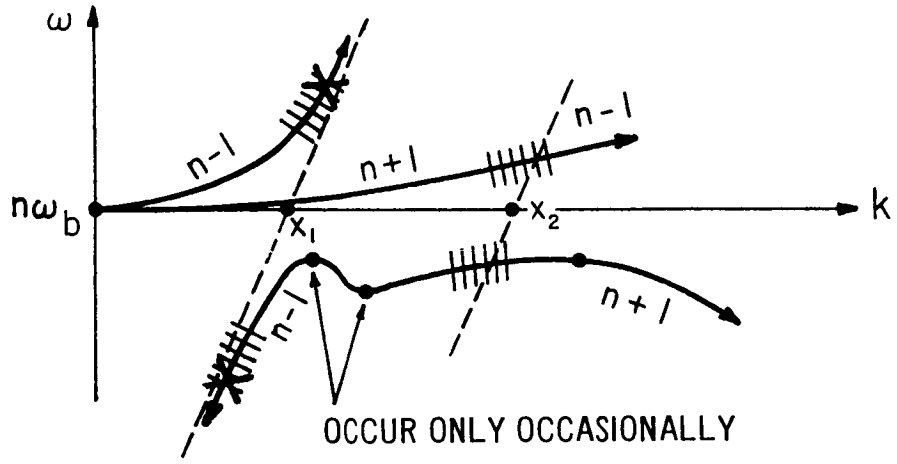

FIGURE 18(a) $n\omega_b > \omega_R > \omega_T > \omega_L$

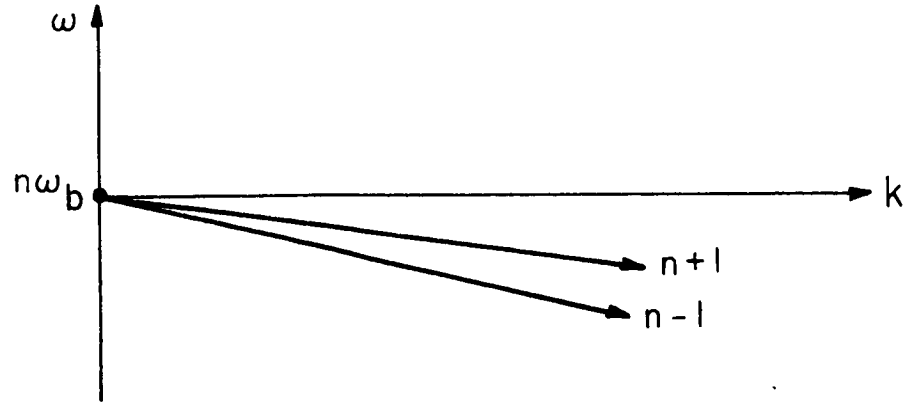

FIGURE 18(b) $\omega_R > \omega_T > \omega_L > n\omega_b$

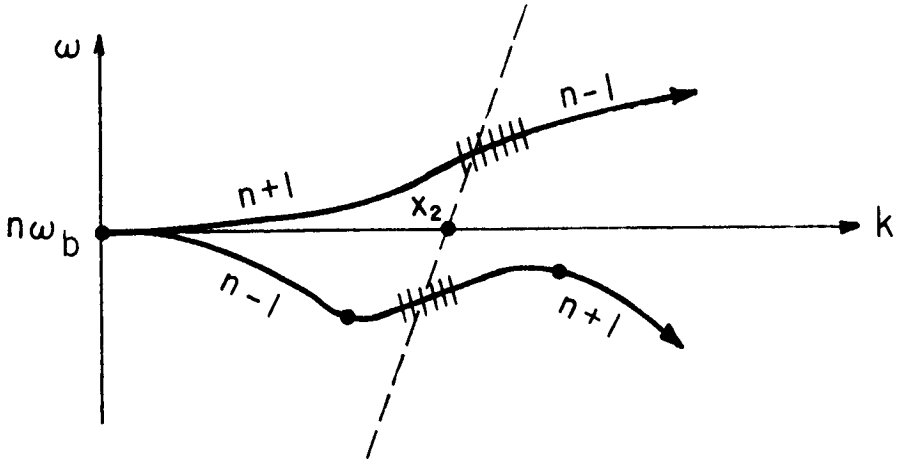

FIGURE 18(c) $\omega_R > n\omega_b > \omega_T > \omega_L$

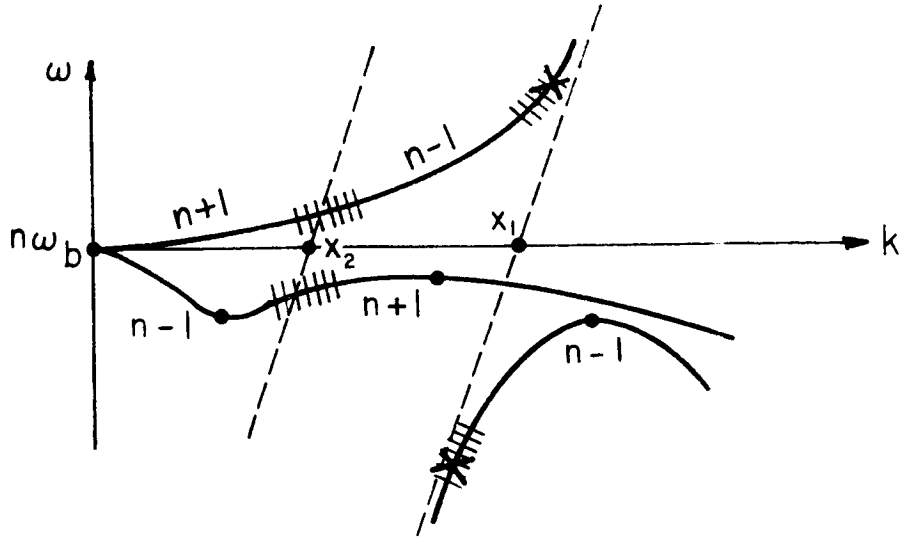

FIGURE 18(d) $\omega_R > \omega_T > n\omega_b > \omega_L$

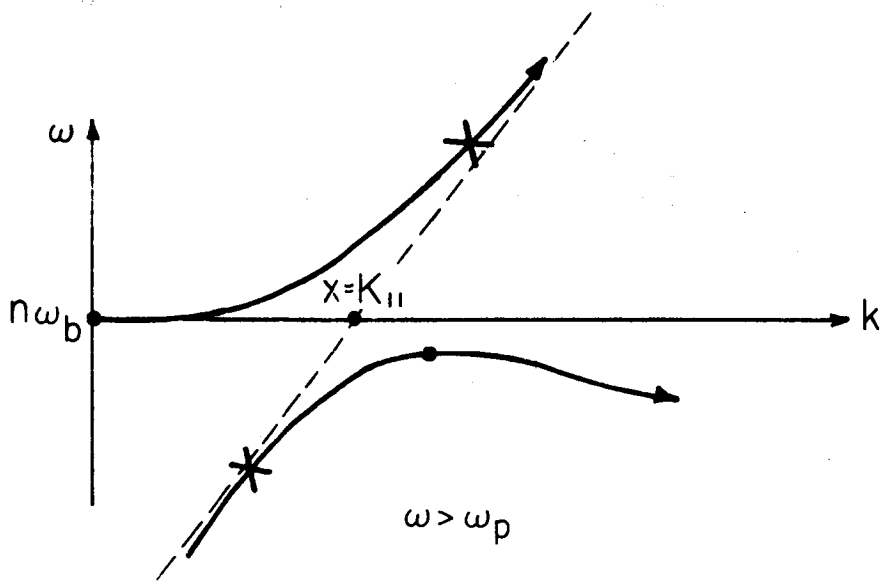

FIGURE 18(e)

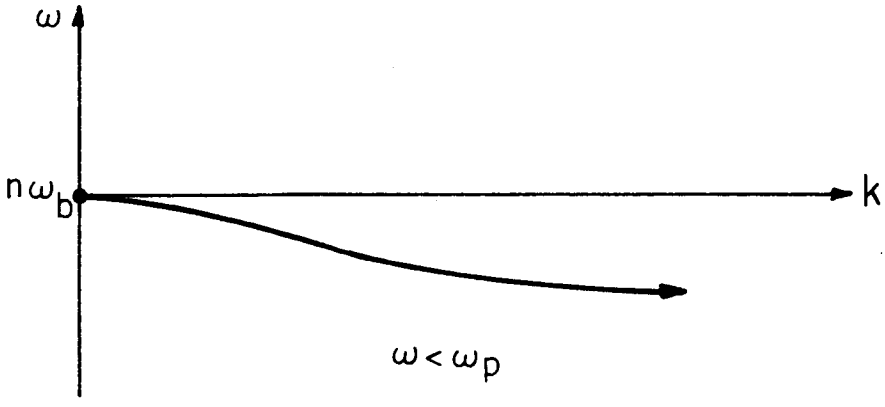

FIGURE 18(f)

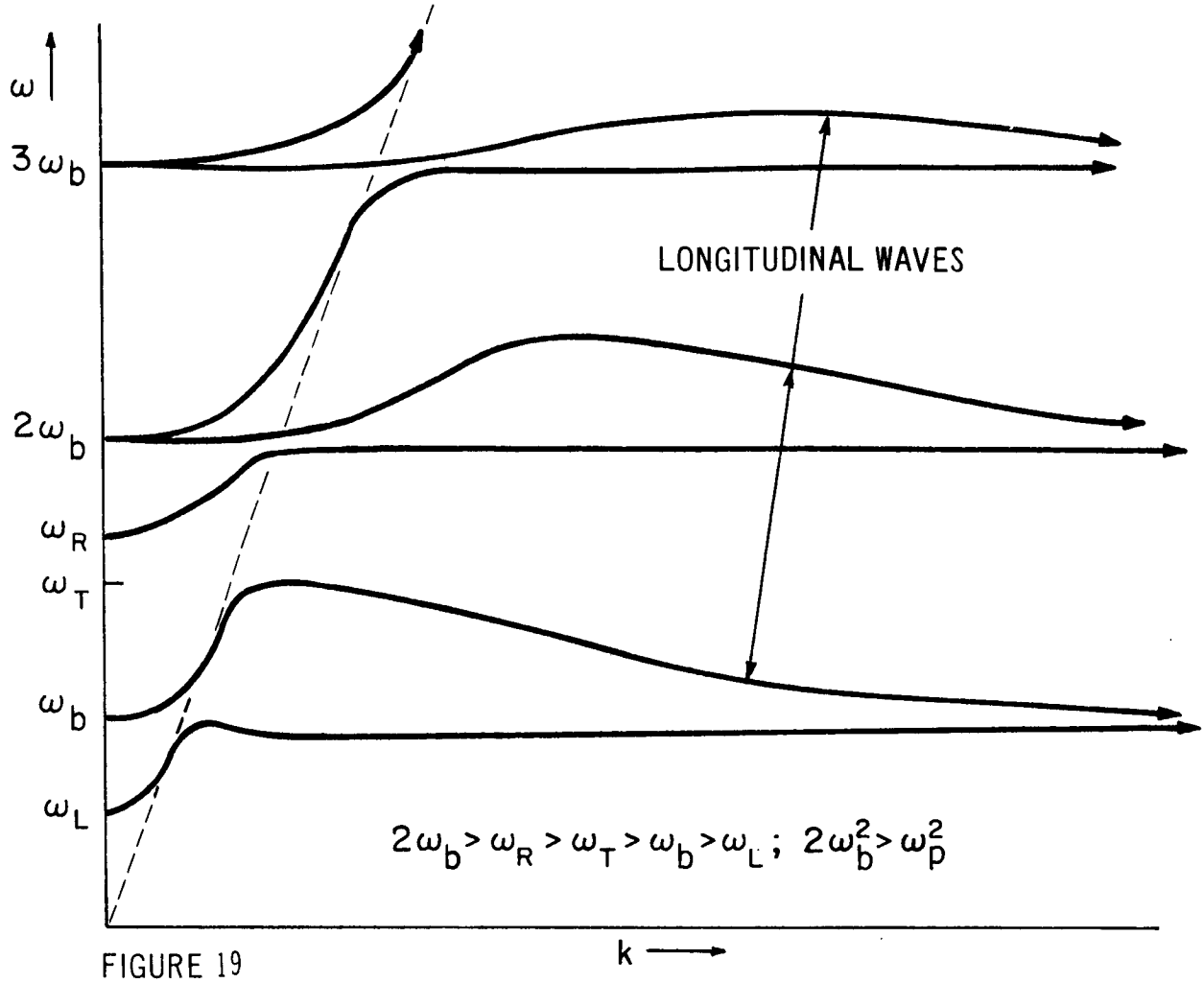

FIGURE 19

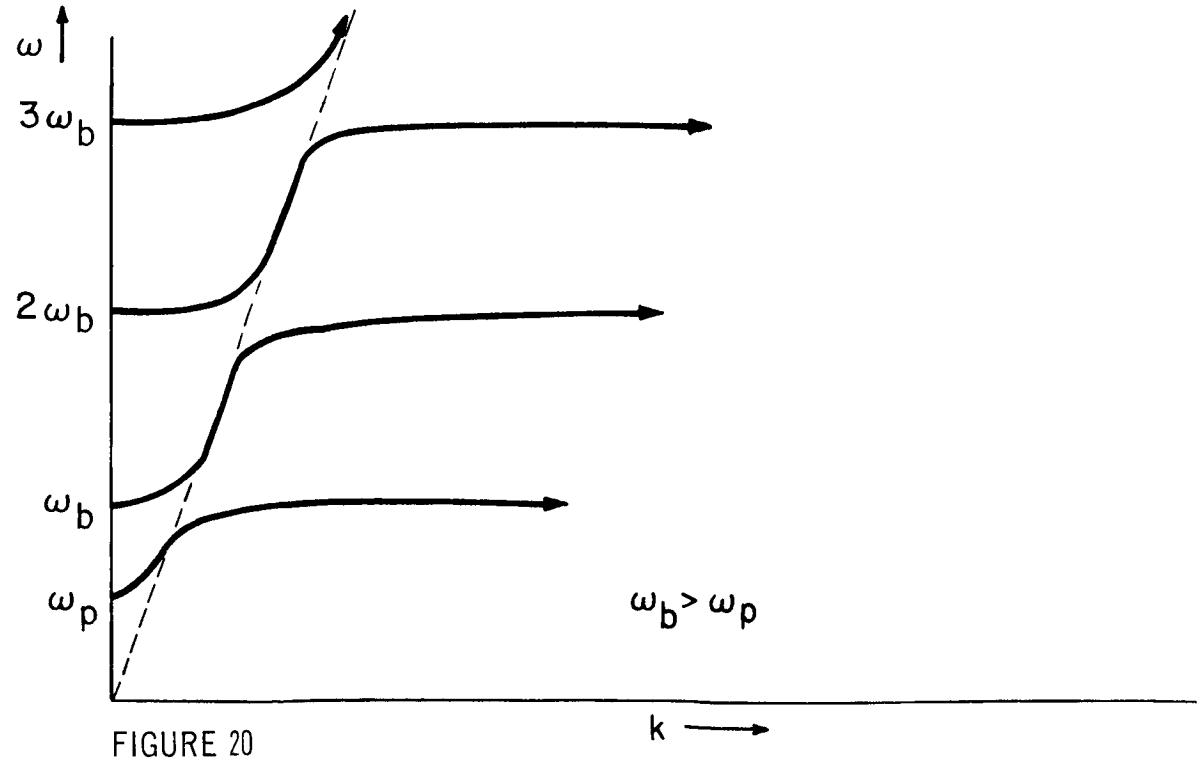

FIGURE 20

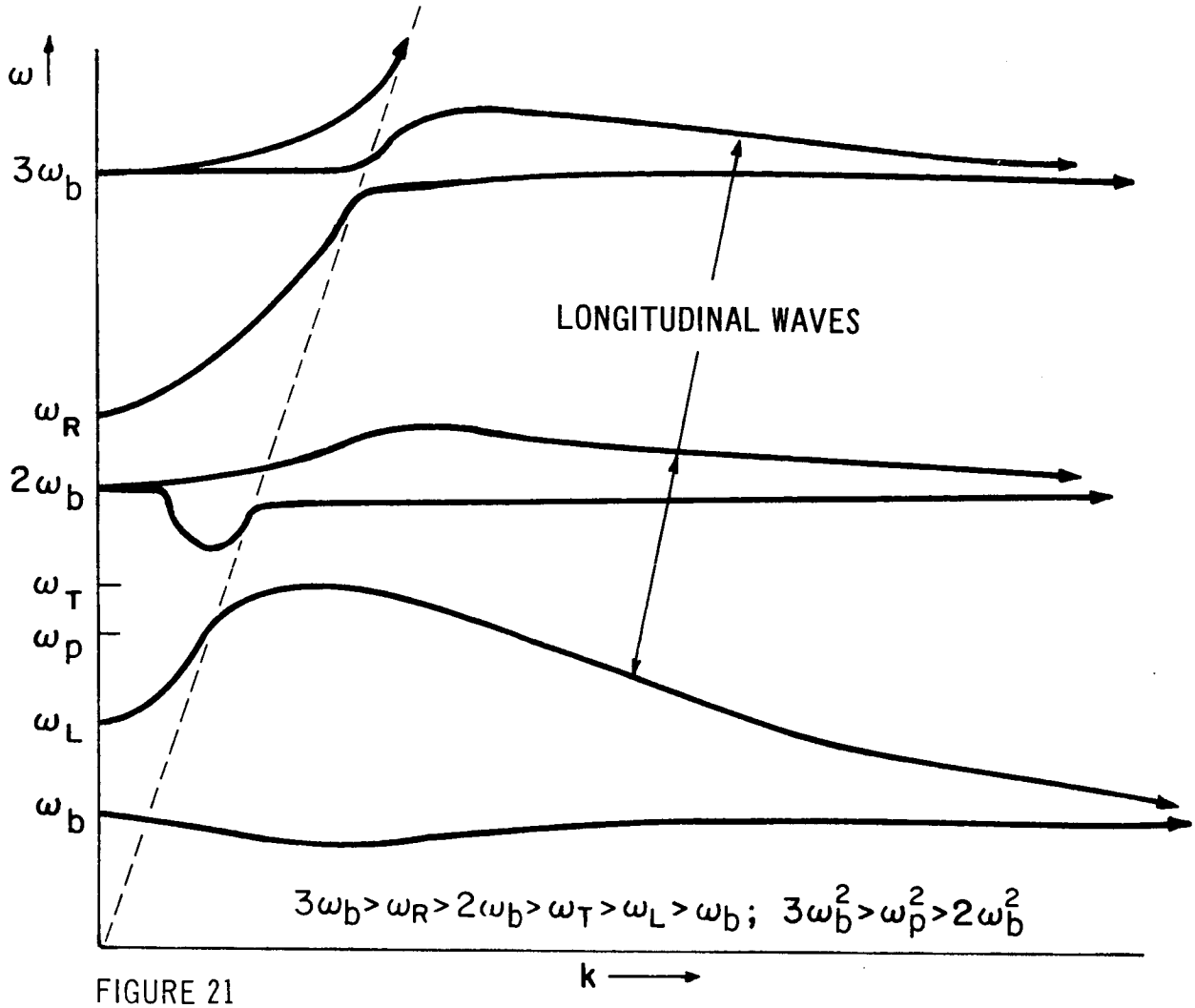

FIGURE 21

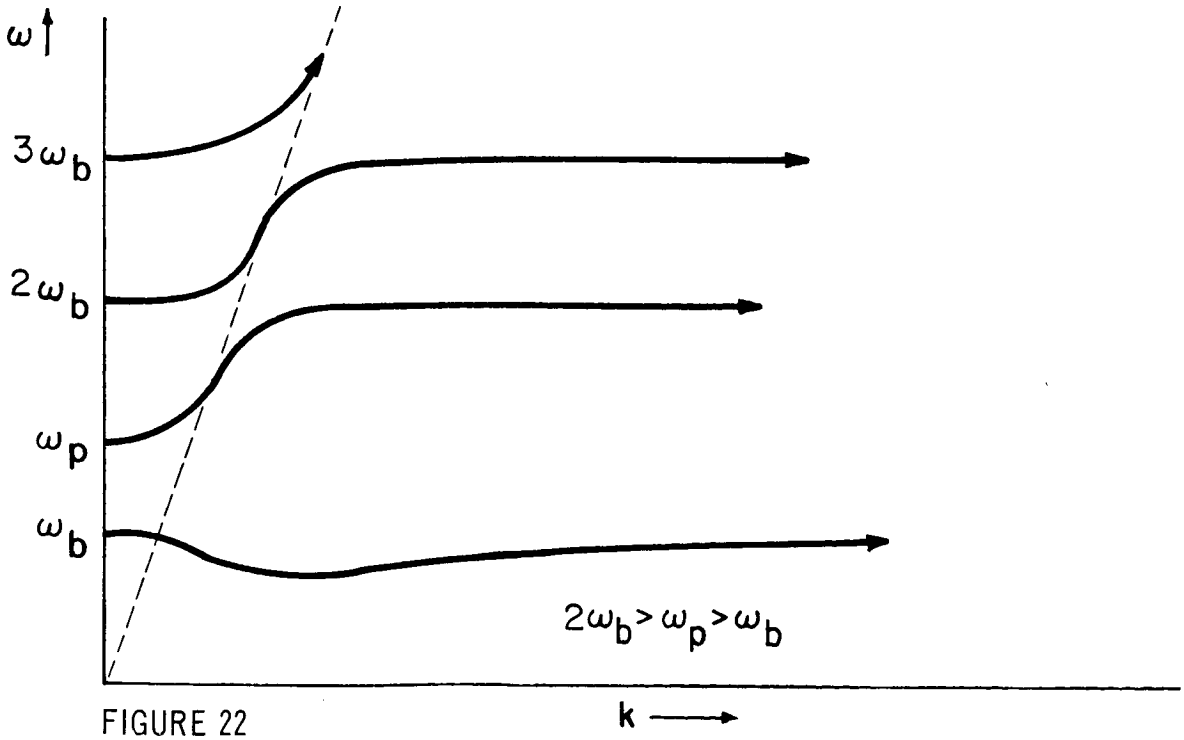

FIGURE 22

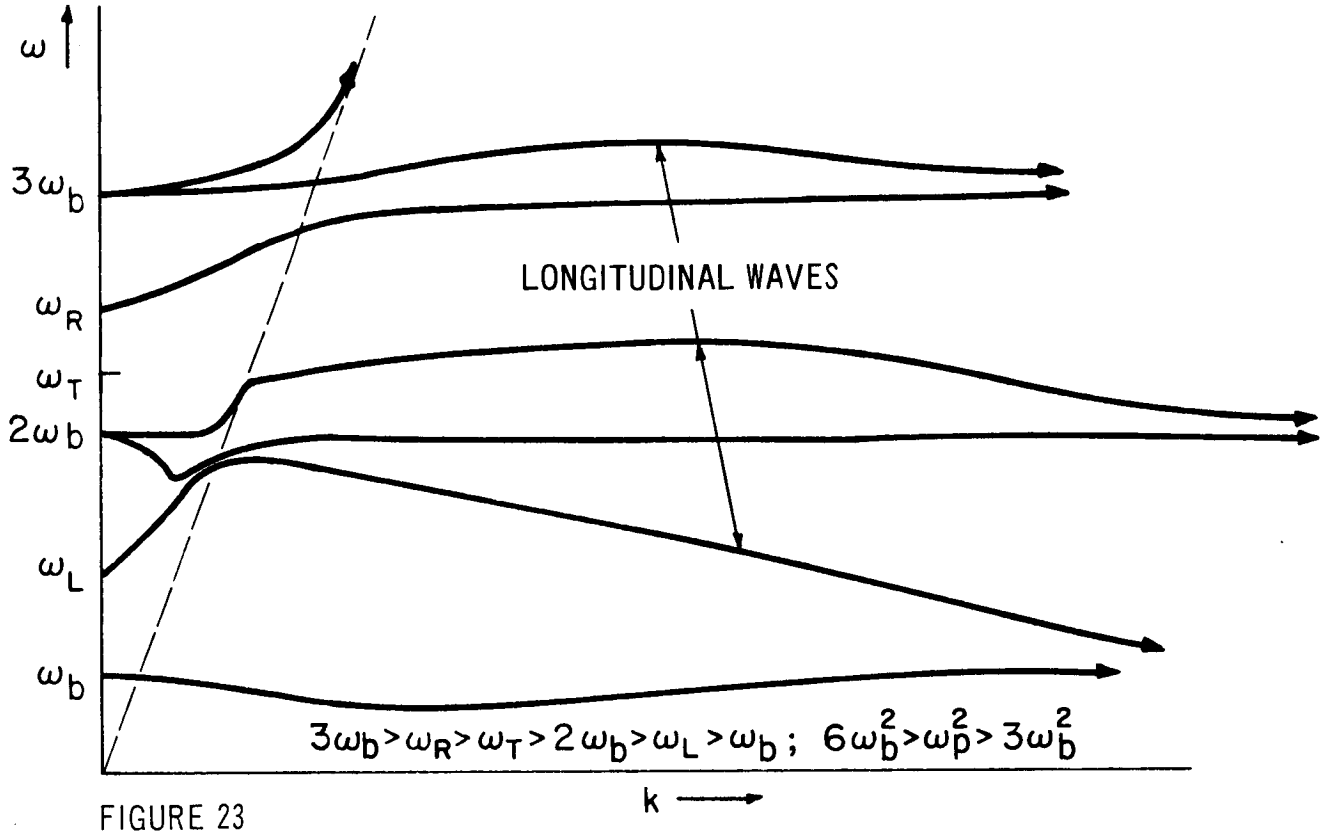

FIGURE 23

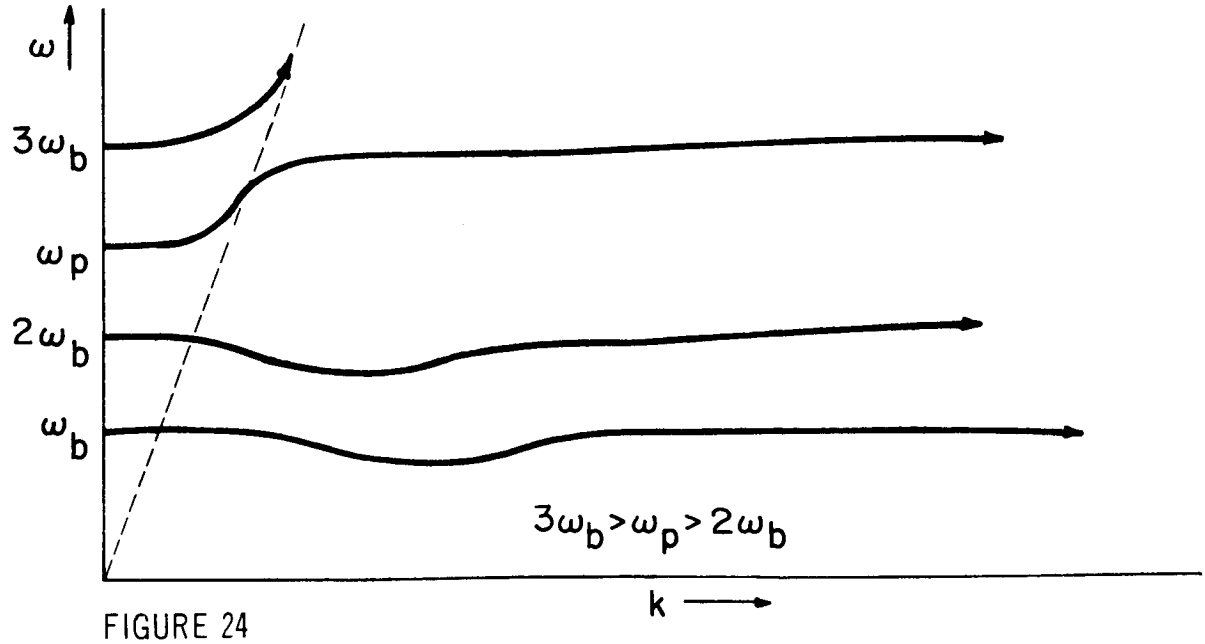

FIGURE 24

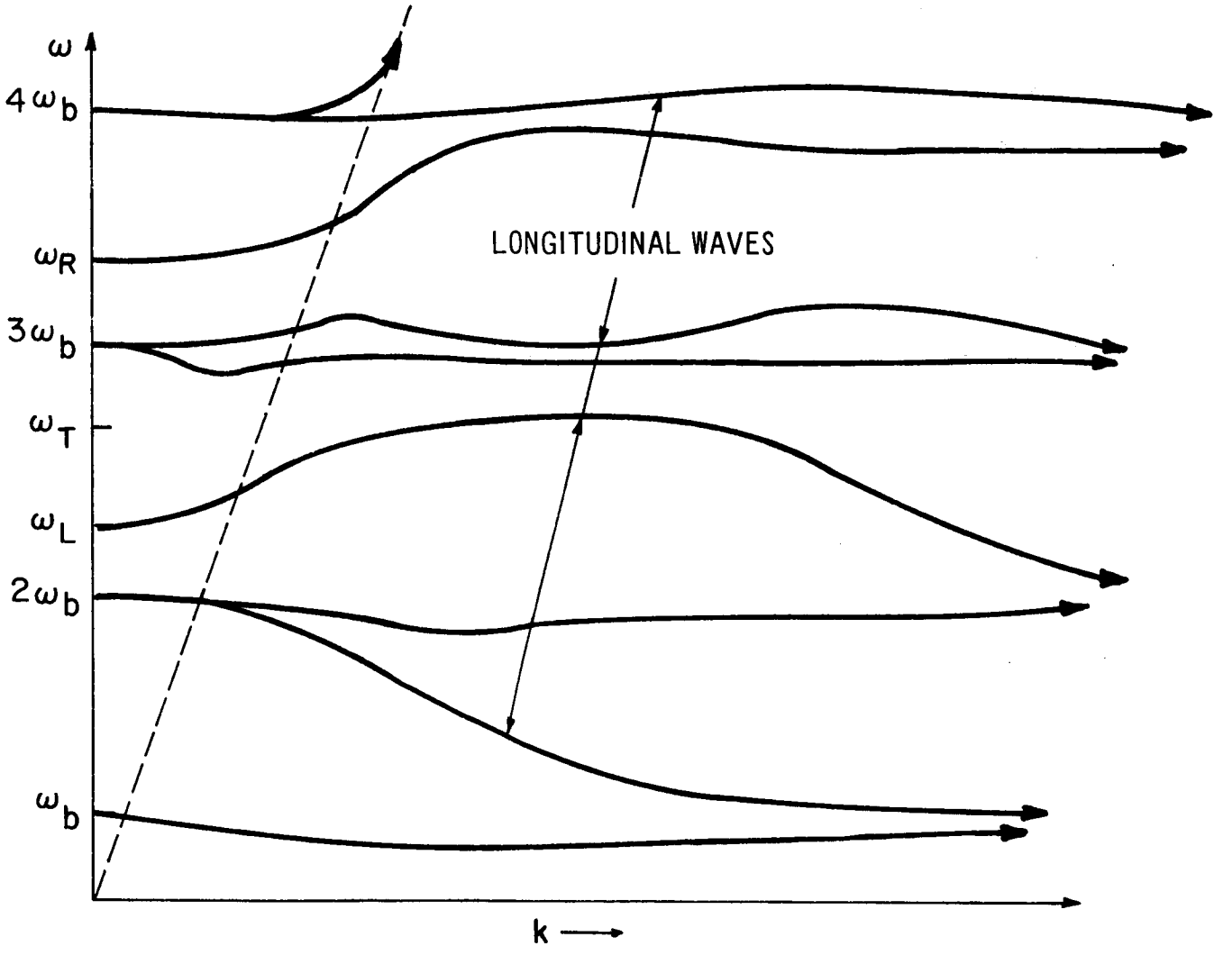

$$4\omega_b > \omega_R > 3\omega_b > \omega_T > \omega_L > 2\omega_b \; ; \; 8\omega_b^2 > \omega_p^2 > 6\omega_b^2$$

FIGURE 25

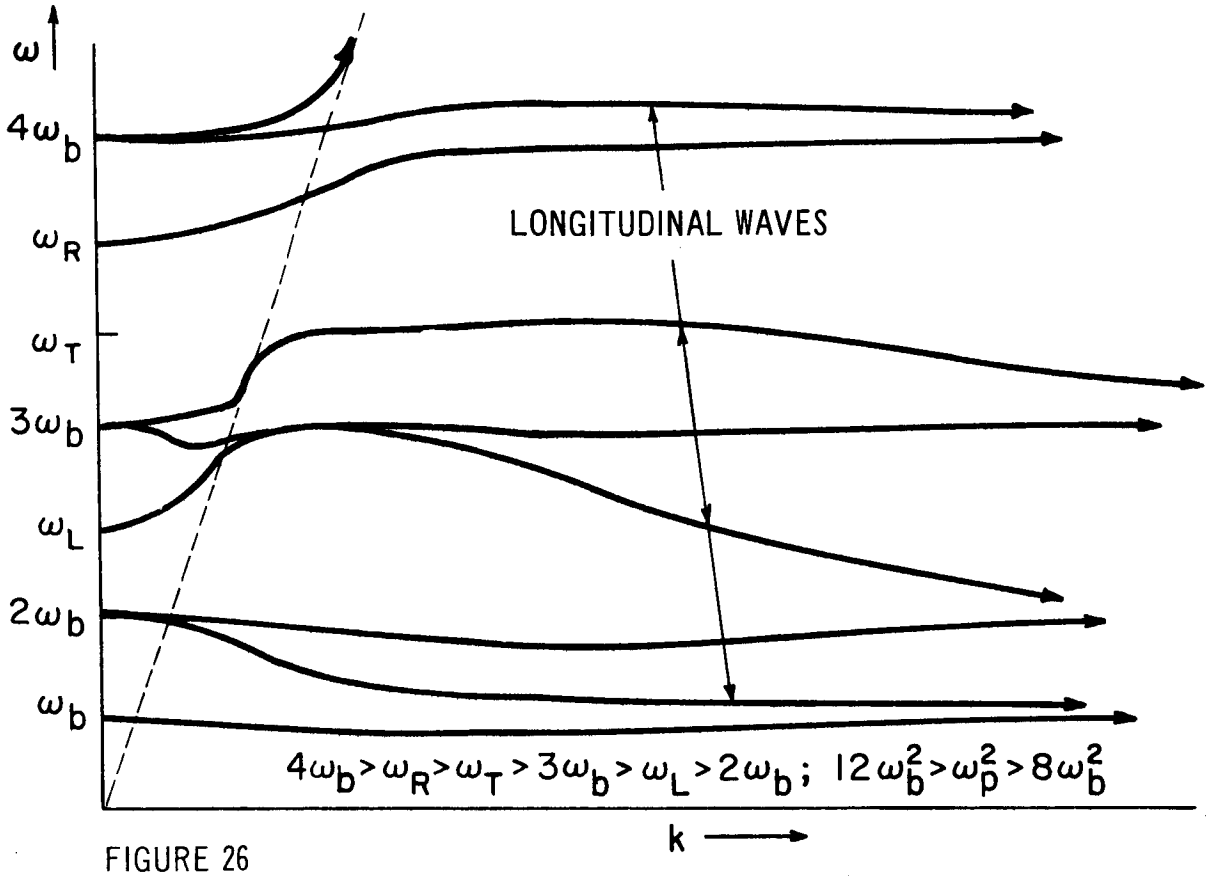

FIGURE 26

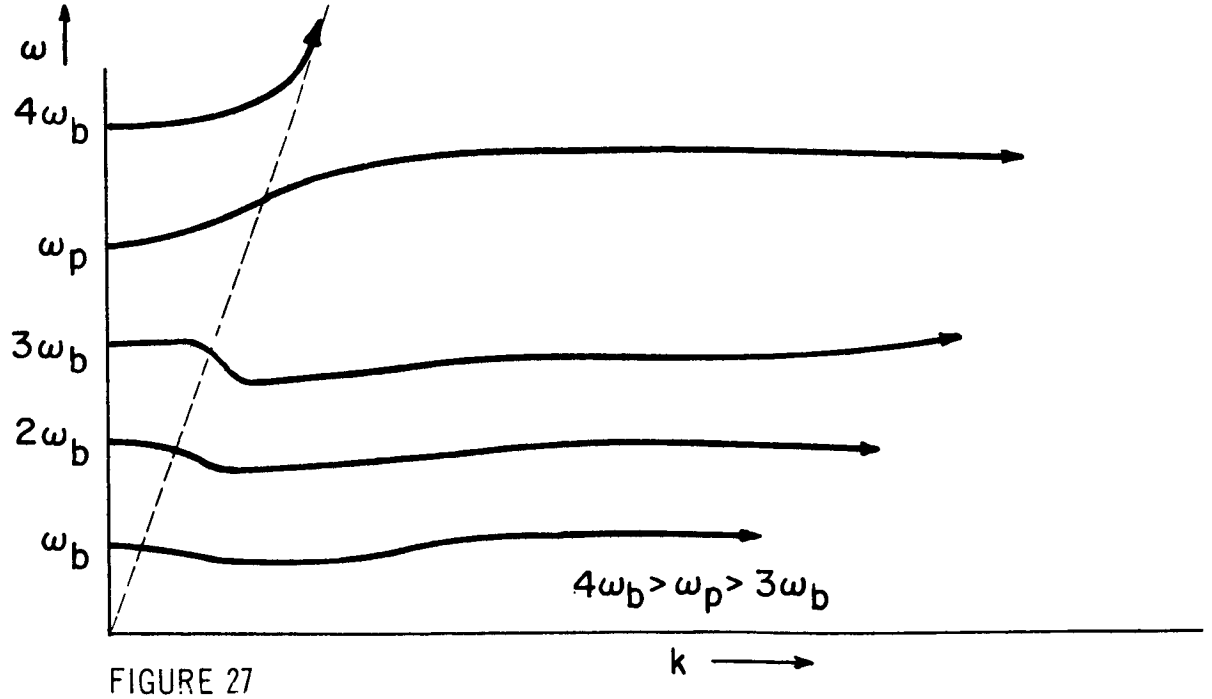

FIGURE 27

TIME DECAY FOR CYCLOTRON HARMONICS

I.P. Shkarofsky
T.W. Johnston

RCA Victor Co. Ltd.
Research Laboratories
Montreal, Canada

- ABSTRACT -

The calculation is discussed of the time behaviour associated with the frequency singularities resulting from pinches in wave number integration. The pinches occur when an integration contour in wave number space is pinched between poles.

This technique is then applied, for the Alouette situation, to the singular case for very small wave number when the satellite and group velocity are equal.

The relevant Alouette signal is found to be indistinguishable from galactic noise in a time of order 20 μsec, well before the Alouette receiver is turned on. The cyclotron resonance must be found elsewhere, probably in the coupling resonances or in the Bernstein modes.

I. INTRODUCTION

In this section we discuss the calculation of the asymptotic time behaviour of the cyclotron harmonic signal. As indicated in the Basic Theory section in the General Introduction, the singular time behaviour will be obtained by considering the behaviour of so-called complex plane "pinches". By a complex pinch we mean the pinching of an integration contour between two converging singularities which coalesce at some critical value. The pinch analysis will give the Laplace transform which proves to have a singularity other than a simple pole: e.g. a branch point or a logarithmic singularity. We must then invert the Laplace transform to obtain the time behaviour.

We first consider the general method of pinch points, following the treatment given by Briggs (1964), and then the detailed calculation for the pinch in the ordinary and extraordinary cyclotron harmonic waves which occurs for small $\underset{\sim}{k}$ ($\underset{\sim}{k}$ << Appleton-Hartree value for $\underset{\sim}{k}$).

II. SINGULAR TIME BEHAVIOUR FROM PINCHES IN THE COMPLEX k-PLANE

The solution to many perturbation problems for a uniform medium is very often obtained by using Fourier transforms ($\underset{\sim}{k}$) in space and Laplace transforms (ω) in time, i.e. a plane wave transform.

The characteristic dispersion of the medium usually emerges in the form of an expression, say $D(\underset{\sim}{k},\omega)$, in the denominator of the transform whose zeroes give poles in the complex $\underset{\sim}{k}$ or ω plane (which ever one is first inverted).

Depending on the method of excitation the result is a set of waves (normal modes) with frequency $\omega(\underset{\sim}{k})$ or wave number $\underset{\sim}{k}(\omega)$ determined both from the excitation and from setting $D(\underset{\sim}{k},\omega)$ equal to zero.

The group velocity (the velocity of a wave packet with some spread in ω or $\underset{\sim}{k}$) is usually given by $\partial\omega/\partial\underset{\sim}{k}$. This is the standard result.

Further information requires more advanced technique. For instance, although only simple theory is needed to discover the dispersion and group velocity relations, it requires ingenuity to discover how the wave packet will decay, as it will in a dispersive medium.

It is evident that, to an observer moving at some arbitrary uniform velocity, the amplitude of the wave packet travelling at that group velocity will seem to change very slowly and only because the packet itself is spreading due to dispersion.

This is held to be the situation for the Alouette resonances, so the calculation of the decay with time of the wave packets which travel with the Alouette is the heart of the problem. The preceding two parts have been devoted to obtaining the appropriate dispersion equations etc. Now we must use these quantities to give the time behaviour. The first step is to transform the system into a wave packet frame of reference in which the wave packet stands still, so that in the new system $\partial\omega/\partial\underset{\sim}{k}$ is zero.

This proves to be essentially similar to the general problem of absolute instabilities in uniform systems (Briggs (1964)). The mathematics was applied originally to quantum mechanics and was applied to the Alouette collective resonances by Nuttall (1965). Dougherty and Manoghan (1964) also use this technique, but only investigate the location of singularities.

The characteristic feature is the coalescing of two (or more) $\underset{\sim}{k}$-solutions to the dispersion equation at some value $\underset{\sim}{k}_o$ for a frequency ω_o, to give a double (or higher) root with $\partial D/\underset{\sim}{k} = 0$ (or all $\partial^{n-1}D/\partial k^{n-1} = 0$ for n-fold degeneracy). If the $\underset{\sim}{k}$ solutions at some frequency ω_o come together from opposite sides of the line integrals in the complex $\underset{\sim}{k}$-planes used to invert the Fourier space transforms, the integration contour is described as being pinched between the $\underset{\sim}{k}$-poles of the characteristic function. The Laplace transform then proves to have a singularity at ω_o giving singular time behaviour. A simple example should make this clear.

Example

This simple one-dimensional example is the one given by Briggs (1964) (also Bers and Briggs (1963)). With $\partial D/\partial k = 0$, from expansion around ω_o, k_o, we have for a first order approximation to D.)

$$D(\omega,k) \approx \frac{\partial D}{\partial \omega}(\omega - \omega_o) + (k - k_o)^2 \tfrac{1}{2}\frac{\partial^2 D}{\partial k^2} . \qquad (1)$$

Note

$$D = 0 \text{ gives } k_{1,2} = k_o \pm \left[(\omega - \omega_o) \frac{\partial D}{\partial \omega} \left(\tfrac{1}{2} \frac{\partial D}{\partial k^2} \right)^{-1} \right]^{\frac{1}{2}} \qquad (2)$$

Also $\quad \frac{\partial D}{\partial k} = 0$ and $D = 0$ mean $\frac{\partial \omega}{\partial k}\frac{\partial D}{\partial \omega} = 0$ so if $\frac{\partial D}{\partial \omega} \neq 0$, $\frac{\partial \omega}{\partial k} = 0$

For the Laplace transform inversion (done last) which gives the time behaviour, the inversion line integral in the complex ω-plane is on the same side of all singularities of the transform (in our case above since we use $\int dt \exp(i\omega t) \ldots$ for our transform).

In the vicinity of ω_o, as ω runs along a line parallel to the real axis and slightly above ω_o, the two poles in the k-plane will move as shown in Fig. 1 for real positive $(\partial D/\partial\omega)(\frac{1}{2}\partial^2 D/\partial k^2)^{-1}$. (For a real negative coefficient the same tracks are traversed in the opposite direction.)

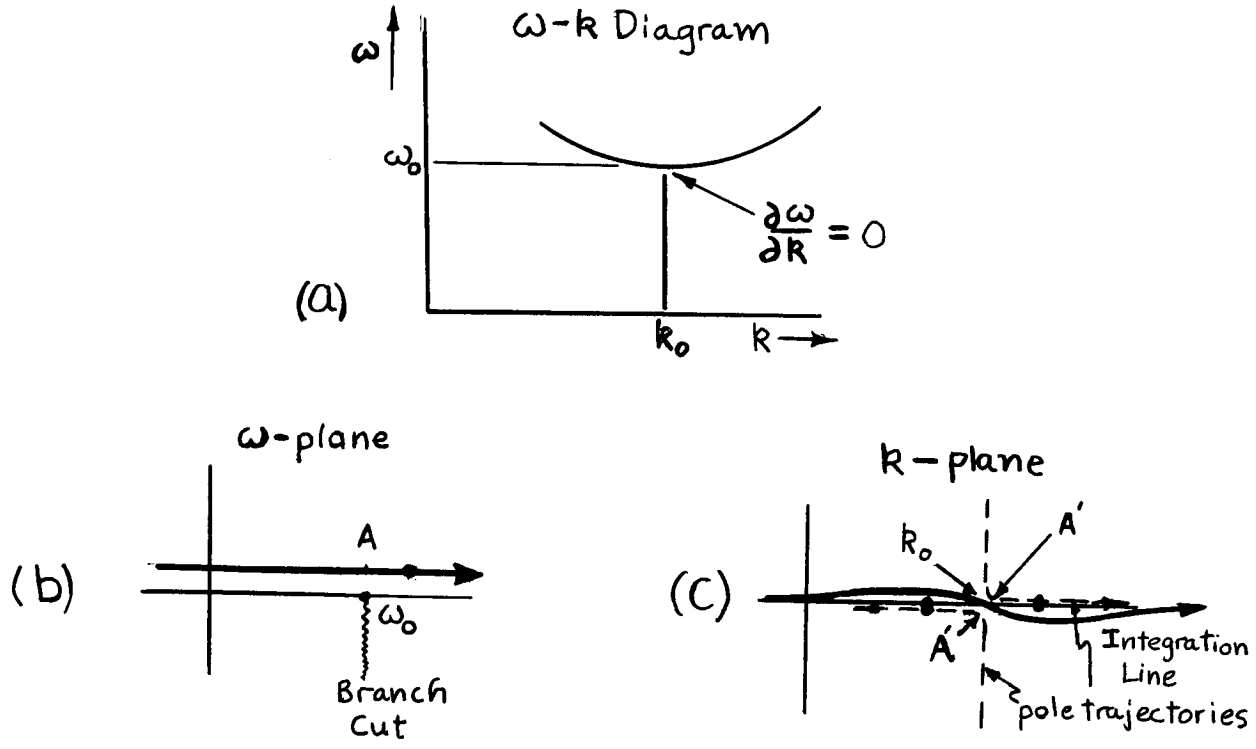

Fig. 1. Anatomy of a pinch. Shown in (a) ω vs k, (b) ω, (c) k planes.

The Fourier transform line integrals go between these poles for cases of interest. Far from ω_o one or the other residue (depending on which half plane Re ik x < 0), say k_1, gives a result for the Laplace transform $L(\omega,x)$

$$L(\omega,x) = k\,\frac{g(k_1)\exp(ikx)}{\left(\frac{\partial}{\partial k}D\right)_{k=k_1}} \tag{3}$$

In general this will be a function of $[\omega - \omega_1(k_1)]$ form and will give a simple result. Near ω_0 the appropriate value of D is $(k-k_0)^2\partial^2D/\partial k^2$ and with the $k-k_0$ value from $D = 0$, we have

$$L(\omega,x) = \frac{g(k_0)\exp(ik_0x)}{\left[2\,\frac{\partial D}{\partial\omega}\,\frac{\partial^2 D}{\partial k^2}\right]^{\frac{1}{2}}_{\omega_0 k_0}(\omega-\omega_0)^{\frac{1}{2}}} \tag{4}$$

There is a branch pole of $L(\omega,x)$ at ω_0. Notice that if $\partial D/\partial\omega \neq 0$ as is true for cases of interest then $\partial^2D/\partial k^2$ is equal to $\frac{\partial}{\partial k}\left(\frac{\partial\omega}{\partial k}\frac{\partial D}{\partial\omega}\right) = (\partial D/\partial\omega)(\partial^2\omega/\partial k^2)$ since $\frac{\partial\omega_0}{\partial k_0} = 0$ and we have

$$L(\omega,x) = \frac{g(k_0)\exp(ik_0x)}{\left(\frac{\partial D}{\partial\omega}\left[2\,\frac{\partial^2\omega}{\partial k^2}\right]^{\frac{1}{2}}\right)_{\omega_0 k_0}}\,\frac{1}{(\omega-\omega_0)^{\frac{1}{2}}} \tag{5}$$

The quantity $(\partial^2\omega/\partial k^2)$ is essentially the curvature of the ω vs k locus for $D = 0$ and so the flatter the curve the larger the signal.

By a standard formula or by appealing to the integral definition of the gamma function $\Gamma(\nu)$ $(\nu > 0)$ for $(\omega - \omega_0)^{-\nu}$ it is easily seen that

$$F(t,x) = \frac{g(k_0)}{\sqrt{\pi}}\,\frac{\exp\left(-i(\omega_0 t - k_0 x)\right)}{\left(\frac{\partial D}{\partial\omega}\left(2\,\frac{\partial^2\omega}{\partial k^2}\right)^{\frac{1}{2}}\right)_{k_0\omega_0} t^{\frac{1}{2}}} \tag{6}$$

[In three dimensions the singular ω result would have been $(\omega - \omega_0)^{\frac{1}{2}}$ and the asymptotic time behaviour would have a $t^{-3/2}$ decay. This one-and three-dimensional time decay is the same as for the behaviour at the origin of the diffusion solution to an initial δ-function and indicates the connection between wave packet decay and diffusion.]

Discussion

This example has the essential features of the analysis: the location and understanding of the behaviour of the k-plane poles and recognition of the pinch situation, the calculation of the Laplace transform by the space Fourier transform inversion to find the spatial variation and, finally, the inversion of the Laplace transform to obtain the time behaviour. The result is valid for many simple cases of interest. The extra point which could have been (but was not) explicitly included was the transformation of the dispersion equation to the moving frame in which $\partial\omega/\partial k$ was zero.

In the Alouette case the moving frame is the Alouette and the velocity that of the satellite itself. The Green's function and dispersion equation formulation is far more complicated than in the example but in essence all we try to do is to locate parts of the plasma dispersion characteristic where the group velocity equals the Alouette velocity, and then find the resultant time behaviour at the Alouette.

In complex situations there are many other considerations and the reader had best refer to the literature cited at the end of Part 3. The object here was simply to convey the basic idea of the pinch method.

N O T E

[Note added on the pinch calculation (III, IV, V)].

The motive for concentrating the pinch region discussed in the ensuing sections was the fact that the Fejer-Calvert data (Fig. 4 (Part 4)) in general showed no marked cut-off at ω_R or ω_p.

A pronounced minimum in duration was observed very near ω_p for the $3\omega_b$ resonance, but a data point beyond this indicated that the resonance had, so to speak, recovered. The $2\omega_b$ result showed a slight but definite decrease for ω_p above $2\omega_b$, but the complexity and multiplicity of the $2\omega_b$ dispersion means that it is difficult to make an unambiguous interpretation of this result.

On the basis, then, of the $3\omega_b$ "recovery point" it seemed that coupling between cyclotron harmonic waves and Appleton-Hartree waves was not the answer. Hence we concentrated on the small $k_\perp$ or near-cut-off pinch.

The calculation of field strength (V) performed after the mathematical analysis gave results in reasonable agreement with theory, so the other pinches were not examined closely.

The minimum detectable field criterion (E min) was taken from Sturrock's (1965, Sec. VIII) analysis with only a numerical check on the numbers given. In the final stages of proof-reading the report, however, it was discovered that Sturrock had misinterpreted a loosely-stated receiver specification given by Thomas and Sader (1963, p 3). The receiver minimum signal detection, including antenna, mismatch was given as "19 db" (20 db actually quoted by the Alouette workers) "above KTB".

Sturrock used the plasma temperature ($\sim 10^{3\,0}$K) for T. In fact the number should be nearer the galactic noise temperature which is $\sim 10^{7\,0}$K (Hartz, 1964). The error in power is 10^4 and in field 10^2.

The agreement previously obtained was spurious, the small $k_\perp$ resonance should be masked by galactic noise in about 10^{-2} of the previous time or about 20 μsec. The receiver, turned on 100 μsec after the transmitter is off, will never see this signal.

Hence it is evident that the small $k_\perp$ pinch discussed at length here cannot be responsible for the Alouette cyclotron harmonic resonances.

It is absolutely necessary that the Appleton-Hartree coupling and the Bernstein mode effects be investigated further using the techniques already developed, but applied to the weak small-$k_\perp$ resonance.

The small-$k_\perp$ analysis is nonetheless presented to show how the field strength value was reached, and how the general method is applied.

III. PINCHES AND CYCLOTRON HARMONIC TIME BEHAVIOUR

Now the pinch method will be applied to the problem of the Alouette type using the dispersion equations of Part 2.

Recapitulating briefly, the pinch in the satellite frame of reference must occur close to the cyclotron harmonic and come from matching the wave group velocity to the satellite velocity. The resonances occur even below ω_R and ω_p and so cannot be then due to coupling between cyclotron modes and Appleton-Hartree waves. Nor can they be due to waves with large $k_\perp$ since velocity matching is not possibly at high harmonics and the Doppler shift would be quite noticeable. The pinches of interest are therefore those for small $k_\perp$ (but $k_\perp >> k_\parallel$) for both the ordinary ($E \parallel B$) and extraordinary ($E \perp B$) dispersion equations discussed in Part 2. These are a feature of the relativistic theory.

Since the analysis for both waves is essentially the same we give the extraordinary wave first and merely indicate the differences for the ordinary wave.

IV. EXTRAORDINARY WAVE DISPERSION EQUATION

From the plasma dispersion equations (Part 2, Eq. 14b) we have the following approximate dispersion equation for small k, providing $k_\perp^2 c^2/\omega^2$ proves to be much less then $K_r = 1 - \omega_p^2(\omega(\omega-\omega_b))^{-1}$ i.e. for frequencies other than ω_R:

$$D_r = 1 - \frac{\omega_p^2}{\omega(\omega-\omega_b)}$$

$$- 2k_\perp^{2(n-1)} \frac{\omega_p^2}{\omega^2} \left(\frac{v_t}{\omega_b}\right)^{2(n-1)} \frac{n^2}{2^n n!} \frac{c^2}{v_t^2} \left\{ F_{n+3/2} + \frac{c^4}{2v_t^2\omega^2} \left(k_\parallel + \frac{\omega V_\parallel}{c^2}\right)^2 \left[F_{n+5/2} - 2F_{n+3/2} + F_{n+1/2} \right] \right\}$$

(8)

In nonrelativistic plasma theory (valid for $(\omega - n\omega_b)\omega^{-1}c^2/v_t^2 >> 1$) the curly bracket term is

$$\frac{v_t^2}{c^2}\frac{\omega}{\omega - n\omega_b + \underset{\sim}{k}\cdot\underset{\sim}{V}}\left[1 + \left(k_\parallel + \frac{\omega V_\mu}{c^2}\right)\frac{v_t^2}{(\omega - n\omega_b + \underset{\sim}{k}\cdot\underset{\sim}{V})^2}\right]$$

In contrast to preceding sections we will be working in the satellite frame of reference so it is convenient to take the frequency and $\underset{\sim}{k}$ as measured by the satellite and to call this ω and the rest frame frequency be ω' and k: we have $\omega' = \omega$ (plasma) $= \omega + k\cdot V$; $k_\perp' = k_\perp$ $k_\parallel' = k_\parallel$(plasma) $= k_\parallel + \frac{\omega V_\mu}{c^2}$. The argument of the F functions is really $\mu(1 - (n\omega_b/\omega'))$ or $\mu(1 - n\omega_b(\omega + \underset{\sim}{k}\cdot\underset{\sim}{V})^{-1})$, however $k_\parallel$ proves to be very much smaller than $k_\perp$ and its effects are explicitly contained in the $(k_\parallel + \omega V_1/c^2)$ term. The azimuthal k dependence frame $\underset{\sim}{k}\cdot\underset{\sim}{V}$ can only be expected to add a numerical factor which we ignore and take the argument of F functions as

$$\mu\delta = \mu\left(1 - \frac{n\omega_b}{\omega'}\right) \approx \mu\left(1 - \frac{n\omega_b}{\omega - k_\perp V_\perp}\right)$$

For small k the $\underset{\sim}{R}^{-1}$ function can be factored for a nearly circularly polarized wave, leaving only the D_r term in the denominator.

Excitation

For simplicity in this complicated problem we take the exciting antenna to be an infinitesimal current dipole with a predetermined current, unaffected by the plasma response (i.e. an infinite impedance source). The spatial Fourier transform of the current $\underset{\sim}{I}L\delta(\underset{\sim}{r})$ is $\underset{\sim}{I}L$ with

I the same in k-space as ordinary space ($\underset{\sim}{IL}$ has the dimensions of current × length not current × density) and is the current dipole moment. Beyond multiplication by the appropriate direction cosines in $\underset{\sim}{R}_2^{-1} \cdot \underset{\sim}{i}_k$, further source influence on the result is nil. This, of course, is why the infinitesimal dipole was chosen. It would be desirable in future work to use a more realistic source to gauge antenna size effects.

Fourier Inversion - $k_\parallel$

The first step is to invert the spatial Fourier transform which depends on $R(k,\omega)$ alone because of the infinitesimal dipole assumption. We need not consider the time behaviour yet, so we will be able to put in an arbitrary excitation function transform $P(\omega)$ later. For the low value of $\underset{\sim}{k}$ of interest we can write for the relevant behaviour upon integration over azimuthal angle:

$$\frac{1}{(2\pi)^3}\int d^3k \, \frac{e^{i\underset{\sim}{k}\cdot\underset{\sim}{r}}}{D_r(k,\omega)} \approx \frac{1}{(2\pi)^2}\int_0^\infty k_\perp dk_\perp \int_{-\infty}^{\infty} \frac{dk_\parallel}{D_r(k,\omega)} \tag{10}$$

We have gone into cylindrical coordinates $(k_\perp,\phi,k_\parallel)$ in k-space and as discussed above, ignored any complicated angle variation. The $\exp(i\,\underset{\sim}{k}\cdot\underset{\sim}{r})$ has also been dropped because k is so small, but it should be borne in mind when behaviour or convergence away from singular regions is considered.

We change the $k_\parallel'$ variable back to $k_\parallel' = k_\parallel + \omega V_\parallel/c^2$ in order to eliminate $k_\parallel$ terms and get an obvious pinch in $k_\parallel'$ at zero. (This introduces a factor $\exp[-i\omega(V_\parallel r_\parallel/c^2)]$ which is negligible and is ignored.) With this new variable D_r can be rewritten as

$$D_r = \left\{ \left[1 - \frac{\omega_p^2}{\omega(\omega-\omega_b)} - 2k_\perp^{2(n-1)} \frac{\omega_p^2 c^2}{\omega^2 v_t^2} \left(\frac{v_t}{\omega_t}\right)^{2(n-1)} \frac{n^2}{2^n n!} \left[F + k'^2_{\parallel} \frac{c^4}{v_t^2 \omega^2} \frac{F''_{q+1}}{2} \right] \right] \right.$$

$$\left. \equiv (A - k'^2_{\parallel} B) \right. \tag{11}$$

where the F functions are understood to be of order $q = n + \frac{3}{2}$ and F_{q+1} is of order $n + 1 + \frac{3}{2}$. Also $F''_{q+1} \equiv F_{q+1} - 2F_q + F_{q-1}$ since $F'_q = F_q - F_{q-1}$. The integral over $dk_\parallel$ can now be done readily as follows:

$$\int_{-\infty}^{\infty} \frac{dk'_\parallel}{A - k'^2_\parallel B} = \frac{1}{B} \int_{-\infty}^{\infty} \frac{dk'_\parallel}{2\sqrt{A/B}} \left[\frac{1}{\sqrt{A/B} - k'_\parallel} + \frac{1}{\sqrt{A/B} + k'_\parallel} \right] \tag{12}$$

By deforming the contour on the side where $\mathrm{Im}\, \underset{\sim}{k} \cdot \underset{\sim}{r} < 0$ and remembering that we really have $\exp(-i\, \underset{\sim}{k} \cdot \underset{\sim}{r})$, the result is evidently

$$\int_{-\infty}^{\infty} \frac{dk'_\parallel}{A - k'^2_\parallel B} = \frac{1}{2\sqrt{AB}}\, 2\pi i = \frac{\pi i}{\sqrt{AB}} \tag{13}$$

Fourier Inversion - $k_\perp$

It now remains to integrate over $k_\perp$ i.e.

$$\frac{1}{(2\pi)^3} \int \frac{d^3k}{D_r}\, e^{i\, k \cdot r} \approx \frac{i}{4\pi} \int_0^{\infty} \frac{k_\perp dk_\perp}{\sqrt{AB}} \tag{14}$$

Now B has a factor $k_\perp^{2(n-1)}$ which is conveniently factored out leaving:

$$M = \sqrt{B}\, k_\perp^{-(n-1)} = \frac{c^3 \omega_p}{v_t^2 \omega^2} \left(\frac{v_t}{\omega_b}\right)^{n-1} \left(\frac{n^2}{2^n n!}\right)^{\frac{1}{2}} \left(F''_{q+1}\right)^{\frac{1}{2}} \tag{15}$$

Our $k_\perp$ integral now becomes

$$\frac{1}{(2\pi)^3} \int \frac{d^3k e^{i\underset{\sim}{k}\cdot\underset{\sim}{r}}}{D_r} = \frac{i}{4\pi M} \int_0^\infty \frac{dk_\perp}{k_\perp^{n-2} A^{\frac{1}{2}}} \tag{16}$$

The pinch occurs when two solutions of A = 0 coalesce and pinch the integration line. As discussed earlier the pinch condition is then the simultaneous solution of A = 0 and $\partial A/\partial k_\perp = 0$. Recall that A is given explicitly by the following, which defines a convenient quantity H:

$$A = K_r - 2k_\perp^{2(n-1)}\, F \frac{\omega_p^2}{n^2 \omega_b^2} \frac{c^2}{v_t^2} \left(\frac{v_t}{\omega_b}\right)^{2(n-1)} \frac{n^2}{2^n n!} \tag{17a}$$

$$A \equiv K_r - H \tag{17b}$$

Note that we can write M in terms of H as

$$M = \frac{c^2}{\omega v_t} \left(F''_{q+1}\right)^{\frac{1}{2}} \left(\frac{H}{2F k_\perp^{2(n-1)}}\right)^{\frac{1}{2}} = \frac{c^2}{\omega v_t} \frac{1}{k_\perp^{(n-1)}} H^{\frac{1}{2}} \left(\frac{F''_{q+1}}{2F}\right)^{\frac{1}{2}} \tag{18}$$

Hence setting A equal to zero gives

$$K_r = 1 - \frac{\omega_p^2}{\omega(\omega - \omega_b)} = H \tag{19}$$

For $\omega, k_\perp$ values satisfying the dispersion equation H can be replaced in the relation for M by K_r.

The condition that $\partial A/\partial k_\perp$ be zero for the pinch is as follows (remembering $\delta' = 1 - \frac{n\omega_b}{\omega'}$, $\omega' = \omega - k_\perp V_\perp$)

$$0 = \frac{\partial A}{\partial k_\perp} = - H \left(\frac{2(n-1)}{k_\perp} + \frac{F'}{F} \frac{c^2}{v_t^2} \frac{\partial \delta'}{\partial k_\perp} \right) = -H \left(\frac{2(n-1)}{k_\perp} - \frac{F'}{F} \frac{c^2}{v_t^2} \frac{V_\perp n\omega_b}{(\omega + k_\perp V_\perp)^2} \right)$$

$$\approx - H \left(\frac{2(n-1)}{k_\perp} + \frac{F'}{F} \frac{c^2}{v_t^2} \frac{V_\perp}{n\omega_b} \right)$$

with $H \neq 0$ (i.e. $K_r \neq 0$ in simultaneous solution with $H = K_r$)

$$- k_\perp = 2(n-1) \frac{v_t^2}{c^2} \frac{F}{F'} \frac{n\omega_b}{V_\perp} \tag{20}$$

The minus sign reminds us that the phase and wave group velocities were opposite in the plasma frame, i.e. the wave was a backward wave. The simultaneous solution of these equations is ω_o, k_o, say. Except in the argument of the F functions ω_o can be taken to be $n\omega_b$ where convenient while

$$k_o = - 2(n-1) \frac{v_t^2}{c^2} \frac{n\omega_b}{V_\perp} \frac{F}{F'} \tag{21}$$

For a typical Alouette combination of parameters $\mu = 10^6$, $V_\perp/v_t \approx 10^{-2}$ we have k_o of order 10^{-1} of $n\omega_b/c$, the free space wavelength.

The next step is the expansion of A in the neighbourhood of ω_o and k_o as described previously (Eq. (1)) i.e.

$$A(\omega,\underset{\sim}{k}) \approx (\omega - \omega_o)\left.\frac{\partial A}{\partial \omega}\right|_{\omega_o,k_o} + \frac{(k_\perp - k_o)^2}{2}\left.\frac{\partial^2 A}{\partial k_\perp^2}\right|_{\omega_o,k_o}$$

The $k_\perp$ derivative is as follows:

$$\frac{\partial^2 A}{\partial k_\perp^2} = -\frac{\partial H}{\partial k_\perp}\left(\frac{2(n-1)}{k_\perp} + \frac{F'\mu V_\perp}{F\omega}\right) - H\left[-\frac{2(n-1)}{k_\perp^2} + \left(\frac{\mu V_\perp}{\omega}\right)^2\left(\frac{F''}{F} - \left(\frac{F'}{F}\right)^2\right)\right]$$

(We revert to using $\mu = c^2/v_t^2$ for brevity.)

The first term is zero and F'/F can be expressed in terms of $k_\perp$ from the $\partial H/\partial k_\perp = 0$ condition, Eq. (20), so we have with $H(\omega_o,k_o) = K_r$

$$\left.\frac{\partial^2 A}{\partial k_\perp^2}\right|_{k_o,\omega_o} = +2K_r\left((n-1)\frac{(2n-1)}{k_o^2} - \left(\frac{\mu V_\perp}{\omega}\right)^2\frac{F''}{2F}\right)$$

The ω derivative is simple; neglecting the $\partial K_r/\partial\omega$ term we obtain

$$\left.\frac{\partial A}{\partial \omega}\right|_{\omega_o,k_o} = -H\frac{F'}{F}\frac{\mu}{\omega_o} = +H\frac{2(n-1)}{k_o V_\perp} = +K_r\frac{2(n-1)}{k_o V_\perp}$$

Thus we have

$$A(\omega,k) \approx K_r\left\{+2\frac{(\omega-\omega_o)}{k_oV_\perp}(n-1) + (k_\perp-k_o)^2\left[\frac{(n-1)(2n-1)}{k_o^2} - \left(\frac{\mu V_\perp}{\omega}\right)^2\frac{F''}{2F}\right]\right\} \tag{22}$$

The argument of F and of F' is $\mu\delta'$, with $\omega' = \omega_o + k_oV_\perp$, so the only $k_\perp$ variation left is that explicitly in $(k_\perp - k_o)^2$.

Again choosing a few convenient abbreviations

$$k_\perp - k_o \equiv k_o\varepsilon\,; \quad + 2(n-1)\frac{(\omega-\omega_o)}{k_oV_\perp} = f\,; \tag{23a,b}$$

$$g \equiv (n-1)(2n-1) - \left(\frac{\mu k_oV_\perp}{\omega}\right)^2\frac{F''}{2F} = (n-1)\left[(2n-1) - 2(n-1)\frac{FF''}{F'^2}\right] \tag{23c}$$

The singular part of the integral is using Eqs.(16), (22) and (23)

$$\frac{1}{(2\pi)^3}\int\frac{d^3k}{D_r}e^{ik\cdot r} = \frac{i}{4\pi M}\frac{k_o^2}{k_o^{n-1}K_r^{\frac{1}{2}}}\int_{-1}^{\infty}\frac{d\varepsilon}{(f+g\varepsilon^2)^{\frac{1}{2}}} \tag{24}$$

Now only the singular part of the integral is of interest around t = 0 and so the singular part of the integral is as follows, with the value of $M(\omega_o,k_o)$ expressed using Eq. (18) in terms of $H(\omega_o,k_o)$ i.e. of $K_r(n\omega_b)$,

$$\frac{1}{(2\pi)^3}\int\frac{d^3k}{D_r}e^{ik\cdot r} = \frac{i}{4\pi}\frac{n\omega_b v_t k_o^2}{c^2K_r}\left(\frac{2F}{gF''q+1}\right)^{\frac{1}{2}}\int_{-\delta}^{\delta}\frac{d\varepsilon}{(fg^{-1}+\varepsilon^2)^{\frac{1}{2}}} \tag{25}$$

The integral is elementary and is 2 $\sinh^{-1}[\delta g^{\frac{1}{2}} f^{-\frac{1}{2}}]$ or 2 $\cosh^{-1}[\,]$ for gf^{-1} greater or less than zero. In fact the case of interest is when f is small, i.e. in the vicinity of ω_o, so we can use the logarithmic approximation for $\sinh^{-1}$ or $\cosh^{-1}$ of large argument viz:

$$\sinh^{-1}(x) \approx \ln x \approx \cosh^{-1} x \qquad (|\ln x| >> 1)$$

Thus we have for the singular part of the Fourier inversion

$$\frac{1}{(2\pi)^3} \int \frac{d^3k}{D_r} e^{ik\cdot r} \approx - \frac{i\, n\omega_b v_t k_o^2}{4\pi c^2 K_r} \left(\frac{2F}{gF''_{q+1}} \right)^{\frac{1}{2}} \ln\left(\frac{\omega - \omega_o}{\omega_o} \right) \qquad (26)$$

Where we have kept only the interesting terms in the logarithm.

This is very close to Nuttall's (1965) Eq. 21. We now need to investigate the inversion of the Laplace transform to obtain the asymptotic time behaviour.

Laplace Inversion

We cannot expand the logarithm about its singularity directly. There is a method, more or less equivalent to integration by parts, due to Nuttall (1964) which will give the result, but a simpler way is to note the following inverse Laplace transform formula

$$E_i(-i\omega_o t) = - \frac{1}{2\pi} \int_{ic-\infty}^{ic+\infty} \frac{d\omega}{i\omega} e^{-i\omega t} \ln\left(\frac{\omega - \omega_o}{\omega_o} \right) \qquad (27)$$

where E_i is the exponential integral and $c > 0$ is the usual constant in Laplace inversion.

For $\omega_o t >> 1$

$$E_i(-i\omega_o t) \to i\pi - \frac{e^{-i\omega_o t}}{i\omega_o t} \tag{28}$$

The non-singular $i\pi$ factor can be dropped. Multiplication by ω-terms analytic at ω_o merely means replacing ω by ω_o in those terms since we are interested only in ω_o effects. All this can also be explicitly shown by using Nuttall's (1964) method using the full equation for the pulse form.

If the time behaviour of the current source is given by some function whose Laplace transform $P(\omega)$ with dimensions is not singular at ω_o, then one simply has $P(\omega_o)$.

Time Behaviour

With all this, then, we have the result that the cyclotron harmonic resonance (electric field at right angles to the magnetic field) at late times at the moving satellite due to an initial infinitesimal current dipole at right angles to the magnetic field with perpendicular dipole moment $IL_\perp$ is

$$E_r(t) = \frac{IL_\perp}{\varepsilon_o}\frac{1}{2\pi}\int_{ic-\infty}^{ic+\infty} d\omega i\omega P(\omega) e^{-i\omega t}\left[\frac{1}{(2\pi)^3}\int \frac{d^3k e^{i\underset{\sim}{k}\cdot\underset{\sim}{r}}}{\omega^2 D_r}\right]$$

$$= \frac{IL_\perp}{2\pi\varepsilon_o}\frac{n\omega_b v_t k_o^2}{c^2 K_r}\left(\frac{2F}{gF''_{q+1}}\right)^{\frac{1}{2}}\frac{1}{4\pi}\int_{ic-\infty}^{ic+\infty} e^{-i\Omega t}\frac{\omega}{\omega^2} P(\omega)\ln\left(\frac{\omega-\omega_o}{\omega_o}\right) d\omega$$

$$\approx \frac{IL_\perp}{4\pi\varepsilon_o}\frac{n\omega_b}{c^2}\frac{v_t k_o^2}{K_r}\left(\frac{2F}{gF''_{q+1}}\right)^{\frac{1}{2}} P(n\omega_b)\frac{e^{-in\omega_b t}}{n\omega_b t} \tag{29}$$

Putting in the value of k_o^2 from Eq. (21)

$$E_r(t) \approx \frac{IL_\perp}{4\pi\varepsilon_o}\,(2(n-1))^2\left(\frac{2F}{2F''_{q+1}}\right)^{\frac{1}{2}}\left(\frac{F}{F'}\right)\frac{v_t^{\,5}(n\omega_b)^3}{c^6 V_\perp^{\,2} K_r}\,P(n\omega_b)\,\frac{e^{-in\omega_b t}}{n\omega_b t} \tag{30}$$

This is the same time behaviour as obtained by Nuttall (1965) for the perpendicular plasma resonance, as one might expect since the same logarithmic singularity was obtained.

For the finite length (τ) pulse train at frequency Ω of the Alouette

$$P(n\omega_b) = \frac{e^{i(n\omega_b-\Omega)\tau}-1}{i(n\omega_b-\Omega)} = \tau\left[\frac{e^{i(n\omega_b-\Omega)\tau}-1}{i(n\omega_b-\Omega)\tau}\right] \tag{31}$$

The results are valid for $|(t-\tau)(n\omega_b-\Omega)| \gg 1$.

We do not have values for F_q, F'_q, F''_q or F''_{q+1} but we can say that the ratio of F to its derivatives is not too extreme because of the exponential behaviour for large arguments (see Part 1, Eqs. 38e, 40e). On the other hand F''_{q+1} is roughly $\mu[F' - (n\omega_b/\omega')]/q$ greater than F_q but the exact dependence must wait for an actual calculation. It must also be borne in mind that the term in g may be small if the two factors in it are nearly equal. This variation with n may be most important. Failing detailed calculation it is premature to make any statement about the trends in signal strength for different harmonics. So much for the extrordinary wave time behaviour.

V. ORDINARY WAVE

The ordinary wave behaviour is the same in all the essentials. The chief differences are as follows (see Part 2, Eq. (16)).

(a) Now $K_{\parallel}$ replaced K_r and the wave is polarized along B.

(b) The explicit power of $(k_\perp v_t/\omega_b)$ is 2n rather than 2(n-1) and the numerical coefficient is $(n!2^n)^{-1}$ instead of $2n^2(n!2^n)^{-1}$. Thus n factors which come from the power of $k_\perp$ are to be converted to n + 1.

(c) Now $F_{n+3/2}$ is replaced by $F_{n+5/2}$.

(d) Finally, $F_{q+1}{}'' = F''_{n+5/2} = F_{n+5/2} - F_{n+3/2} + F_{n+1/2}$ is replaced by

$$F_{+1} = (-2F^2_{n+5/2}\ F^{-1}_{n+3/2} + 7F_{n+5/2} - 8F_{n+3/2} + 3F_{n+1/2})$$

The actual dispersion equation (compare Eqs. 8 and 11) is as follows:

$$D_{\parallel} = K_{\parallel} - k_\perp{}^{2n} \frac{c^2}{v_t{}^2} \frac{\omega_p{}^2}{\omega^2} \left(\frac{v_t}{\omega_b}\right)^{2n} \frac{1}{n!2^n}$$

$$\times\left[F_{n+5/2} + \frac{c^4}{2v_t{}^2\omega^2}\left(k_{\parallel} + \frac{\omega V_{\parallel}}{c^2}\right)^2\left(-2F^2_{n+5/2}\ F^{-1}_{n+3/2} + 7F_{n+5/2} - 8F_{n+3/2} + 3F_{n+1/2}\right)\right] \tag{32}$$

$$K_{\parallel} = 1 - \frac{\omega_p{}^2}{\omega^2}$$

The same steps as used for the extraordinary solution will give

$$\frac{1}{(2\pi)^3}\int \frac{d^3k}{D_n} e^{-ik\cdot r} \approx -\frac{i}{4\pi} \frac{n\omega_b v_t k_o{}^2}{c^2 K_{\parallel}} \left(\frac{2F}{gF_{+1}}\right)^{\frac{1}{2}} \ln\left(\frac{\omega - \omega_o}{\omega_o}\right) \tag{33}$$

Here $$k_o = -2n\frac{v_t^2}{c^2}\frac{F}{F'}\frac{n\omega_b}{V_\perp}\ ,\ g \equiv n\left[(2n+1) - \frac{2nFF''}{(F')^2}\right] \qquad (34a,b)$$

with $F = F_{n+5/2}$ and ω_o very nearly $n\omega_b$.

Putting in the value of k_o gives

$$\frac{1}{(2\pi)^3}\int \frac{d^3k}{D_n} e^{-ik\cdot r} \approx -\frac{i4n^2}{4\pi}\frac{v_t^5(n\omega_b)^3}{c^6 V_\perp^2 K_n}\cdot\left(\frac{2F}{gF+1}\right)^{\frac{1}{2}}\left(\frac{F}{F'}\right)^2 \ln\left(\frac{\omega-\omega_o}{\omega_o}\right) \qquad (35)$$

The result for E is then

$$E_n(t) \approx \frac{IL_n}{4\pi\varepsilon_o} 4n^2\left(\frac{2F}{gF+1}\right)^{\frac{1}{2}}\left(\frac{F}{F'}\right)^2 \frac{v_t^5(n\omega_b)^3}{c^6 V_\perp^2 K_n} P(n\omega_b)\frac{e^{-in\omega_b t}}{n\omega_b t} \qquad (36)$$

This result looks virtually the same as for $E_r(t)$ and is distinguishable by the appearance of K_n instead of K_r and in the F and g functions. Since, as mentioned above in connection with $E_r(t)$, explicit knowledge of the F values is required for a detailed analysis we cannot make quantitative statements about the comparative strength of the signal, either from harmonic to harmonic or between E_r and E_n.

Comparison Between Perpendicular and Parallel Resonance

There are two points of distinction between the perpendicular and parallel resonances:

(a) Orientation: The antenna (at least for the infinitesimal dipole) is oriented in the same direction as the electric field i.e. parallel to B for the parallel resonances and perpendicular to B for the

perpendicular resonance.

(b) Cut-off Frequency Effect: Although the dispersion equation approximations are invalid when K_r or $K_{\shortparallel}$ goes to zero at ω_R or ω_p, nonetheless it is evident that some change will take place there. Evidently the parallel small-k cyclotron harmonic resonance will be affected near ω_p and the perpendicular resonance near ω_R.

This theory does not indicate that either resonance is any stronger than the other.

Applying these criteria to the Alouette it seems that there are three points in favour of parallel resonance being the one observed (Lockwood (1965)).

(a) Cyclotron spikes are apparently unaffected at ω_R (Fejer and Calvert (1964) Figs. 4d, 4e, also Part 4).

(b) Cyclotron spikes are apparently strongly affected at ω_p (Fejer and Calvert (1964), Fig. 4e, also Part 4).

It is possible that the reason for this may lie in the finite size of the antenna. Since for both waves we need a very small $k_{\shortparallel}$ it is likely that having the finite length antenna oriented along the magnetic field is most favourable for a small $k_{\shortparallel}$ and so the antenna is more effective for excitation when oriented along the magnetic field.

Signal Strength

Although we do not know the exact values of F and related quantities in the final results we can estimate the field expected and, using the receiver parameters, the length of time over which the signal can be detected. The result is in quite reasonable agreement with the Alouette observations. The method of estimation is similar to that

employed by Sturrock (1965), except we work in MKS units.

The Receiver Sensitivity is given as 20 db above noise i.e. 10^2 above KTB, which for the Alouette at 10^7 ^oK and 2×10^4 cps bandwidth is a power sensitivity of 2.76×10^{-10} watts. This result is 10^4 greater than that of Sturrock (1965) who used the ionosphere temperature ($\sim 10^3$ ^oK) instead of the galactic noise temperature, which at 2 Mc is about 10^4 ^oK Hartz (1964).

With a matched load of 400 ohms (matching is not likely but the value is a reasonable rough estimate) the antenna voltage at the terminals is $(2.76 \times 10^{-10} \times 400)^{\frac{1}{2}}$ or 3.32×10^{-4} volts. In the absence of the antenna the minimum detectable field, which is very roughly the minimum voltage divided by the antenna length (47 meters), gives a field sensitivity

$$E_{min} = 3.32 \times 10^{-4}/47 = 7 \times 10^{-6} \text{ volts/meter}$$

The transmitter dipole moment (IL) is obtained using the output of 100 watts into 400 ohms to give 0.5 amps current. The dipole moment is then 23 amp-meters.

The scale factor for the pulse train is τ i.e.

$$P(\omega) = \tau \frac{e^{i(\omega - \Omega)\tau} - 1}{i(\omega - \Omega)\tau} \sim \tau$$

For the Alouette τ is 10^{-4} seconds.

Representative values for the satellite velocity are 10^4 meters/sec and for the electrons 1.6×10^5 meters/sec (at 2000°K). For an 80° orbit the satellite velocity component ($V_\perp$) perpendicular to the field lines is one fifth or more of the satellite velocity, say 3×10^3 meters/sec.

The number of cycles for which the signal might be detectable from the formulas for either resonance field, neglecting the F functions etc., is

$$\left(\frac{n\omega_b t}{2\pi}\right) \approx \frac{1}{2\pi} \frac{4\Pi L}{4\pi\varepsilon_0} \frac{(n\omega_b)^3}{E_{min}} \frac{v_t^5}{c^6 V_\perp^2} P(n\omega_b) \qquad (37)$$

Taking 2 Mc as a representative frequency for resonance and inserting the values given above we obtain

No. of 2Mc cycles = 46

Ringing time $46 \times (2 \times 10^6)^{-1} = 2.3 \times 10^{-5}$ sec = 23 μsec

A ringing time of 2-6 milliseconds is usual in Alouette records and thus evidently the estimate gives a value at least a factor of 100 too low. In fact, since the Alouette receiver does not turn on until 100 μsec after the transmitter, the signal calculated here would be swamped by galactic noise long before the Alouette could detect it.

Hence the Alouette cyclotron harmonic resonances must be explained by the coupling resonances and in some cases perhaps by the backward electrostatic or "Bernstein" modes.

A very crude estimate of the coupling resonances indicates they are stronger than those considered here by a rough factor $(cV_\perp/v_t^2)^3$.

REFERENCES

Nuttall, J. - Phys. Fluids 8 286 (1965), J. Geophys. Res. 70 1119 (1965)
Deals with collective Alouette resonances
using the pinch method but ignores satellite motion.

Briggs, R.J. - Electron Stream Interaction with Plasmas, MIT Press, Cambridge, Mass. Res. Mono. 29, 1964. Chapters 1 and 2 are excellent discussions of pinches and related topics. See also

Bers, A, R.J. Briggs - MIT Electronics Labs., Quarterly Progress Report 71, October 1963, pp. 122-131.

Dougherty, J.P., J.J. Monoghan (1964) unpublished report Dept. Appl. Math. Theor. Phys, Univ. Cambridge.

The following references on pinches are drawn from the work on quantum dispersion theory rather than plasma physics.

Cutkosky, R.E. (1960) - J. Math. Phys. 1, 429 (1960) (remarks after Eq.5)

Eden, R.J. (1952) - Proc. Roy. Soc. A210, 388 (1952) (Sec. 3)

Polkinghorne, J.C., G.R. Screaton (1960) - Nuovo Cim. 15, 289, 925 (1960) (pp. 290 - 298 in particular).

The topics are also discussed by Eden (Sec. 3) and by Polkinghorne (Sec. 2) in

Eden, R.J., J.C. Polkinghorne, G. Kallen, J.J. Sakuvai - Lectures in Theoretical Physics, Brandeis Summer Institute (1961) W.A. Benjamin, New York (1962).

Alouette Publications

Fejer, J.A., W. Calvert (1964) - J. Geophys. Res. 69, 5049 (1964).

Hartz, T.R. (1964) - Nature 203, 173 (1964).

Lockwood, G.E.K. (1965) - Can. J. Phys. 43, 291 (1965).

Nuttall, J. (1965) - Phys. Fluids 8, 286 (1965), J. Geophys. Res. 70 1119 (1965)

Sturrock, P.A. (1965) - Phys. Fluids 8, 88 (1965).

Thomas, J.O., A.Y. Sader (1963) - Stanford University Stanford Electronics Laboratory Report SEL-64-007 (unpublished).

ALOUETTE CYCLOTRON HARMONICS OBSERVATIONS AND RESULTS

T.W. Johnston

- ABSTRACT -

The Alouette results are summarized and discussed. A non-mathematical exposition is given of the course of mathematical analysis pursued and the results obtained. The numerical result obtained for the particular case of small wave number gave a signal which was one hundred times too small, so concentration of future work on coupling resonance is urged.

In view of the apparent importance of parallel resonance the physical basis of this mechanism is explained.

Recommendations for future work complete the exposition.

1. SUMMARY OF OBSERVATIONS

Enough of the Alouette results have been made public (by Lockwood (1963, 1965), Warren (1963), Calvert and Goe (1963) and Calvert and Fejer (1964)) that some useful conclusions can be drawn from them. As well as giving references to the literature it seems worthwhile to summarize the features of the results and show typical records to give the reader some feeling for the general results, the data and the form in which it is available.

Sounding Satellite Operation

The Alouette satellite operation circuitry and construction has been described in detail by Franklin et al (1963) and by Molozzi (1963).

The transmitter in the satellite sends out a train of waves which lasts for 100 μsec. at a given frequency. After a 100 μsec. dead time the signal is picked up through one of two perpendicular dipole antennas (a 46 m (tip-to-tip) dipole for frequencies less than 4.5 Mc/s, a 23 m antenna above) by a receiver which is turned on for 14.6 milliseconds. The cycling time is 15 milliseconds. The frequency of both transmitter and receiver are steadily increased at a rate of 1 Mc/sec/sec. Thus in one cycle the frequency changes by about 15 kcs and it takes about 11 seconds for a scan from .5 to 11.5 Mc. Since the satellite travels at about 10^4 m/sec it moves about 150 meters in a sounding cycle and 110 km for a frequency sweep.

Part of a typical ionogram is shown in Fig. 1 with the second and third harmonic resonances indicated. The actual receiver records are given in the montage of Fig. 2. Fig. 3 shows a full ionogram.

Many such ionograms have been examined but little work has been done on the detailed line records.

Analysis of Results

There are four papers and one available as an abstract which contain analyses of results. Three also contain some theory as well: that aspect is discussed in the critique given in the Appendix. Here the emphasis is on the data analysis.

In the first paper Lockwood (1963) identified the cyclotron harmonics in the Alouette ionograms. In a later paper Lockwood (1965) examined the orientation data from the Alouette magnetometer and come to the conclusion that, for the high-frequency cyclotron harmonics at any rate, the resonance depends on antenna orientation and is favoured when the antenna element is parallel to the magnetic field. The orientation had been shown to be important by Johnston and Nuttall (1964) (their Fig. 2, and related discussion).

Hagg (1963) has compared the magnetic field results with those deduced from the spherical harmonic coefficients for the field near the earth's surface. In general it is usually possible to pick one scan line which gives a stronger resonance than its neighbours (see Fig. 2), giving a frequency accuracy of 15 kc, which is .15% at 10 Mc. Hagg comes to the conclusion that the agreement between the spherical harmonic result and the value from the assumption that the resonance occurs exactly at the cyclotron harmonic is as good as the expansion accuracy (1%) Unpublished work (private communication) indicates that within this error limit the trend of results indicates that the cyclotron harmonic resonance occurs slightly below the cyclotron harmonic frequency. These are vital

points, since the moving satellite can be expected to see a Doppler-shifted resonance. The fact that the Doppler shift is small immediately sets an upper limit on the wave number of the cyclotron wave of interest. Positive or negative shifts should indicate whether a backward or forward wave is involved.

In addition to these publications there are two papers on cyclotron harmonics and electron concentration-dependent plasma resonances. In the first, written by Calvert and Goe (1963), the identification of the plasma resonances and cut-offs (zero-range traces) was adroitly checked by choosing two easily identifiable phenomena to calculate ω_p and ω_b and check the frequency values of the others. The correspondence was excellent, thus establishing the proper identification and correcting an earlier error by Lockwood (1963) which led to a short-lived concept of "displaced" plasma resonances (Warren (1963)).

Calvert and Goe plotted the results of a series of ionograms taken in succession on a satellite pass and demonstrated how it then became relatively easy to distinguish true plasma effects and instrument defects. This way of abstracting results also made it very easy to follow a given resonance as the ratio of ω_p/ω_b charged along the satellite path and led to the idea of investigating the ionograms for which interesting frequency conditions held, e.g. $\omega_R \approx n\omega_b$. One now looked at related series of ionograms rather than isolated examples. (It was in just this way that Johnston and Nuttall (1964) later detected the "tuning out" of the cyclotron harmonic due to satellite spin.)

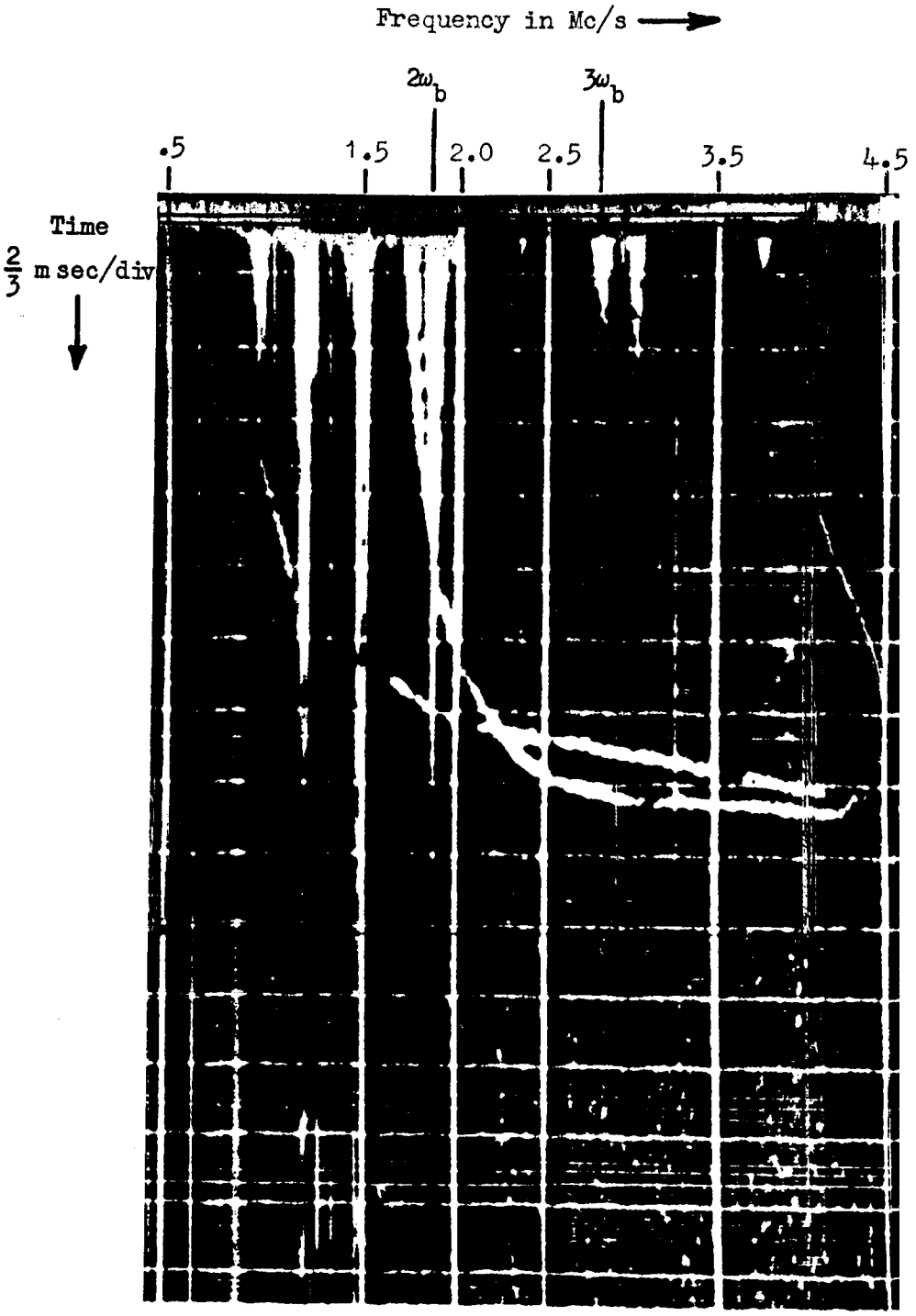

Fig. 1 Selected portion of an Alouette ionogram (.5Mc/s to 4.5Mc/s and 0 - 10m sec delay) from Ottawa, day 276 16:48:51 U.T.

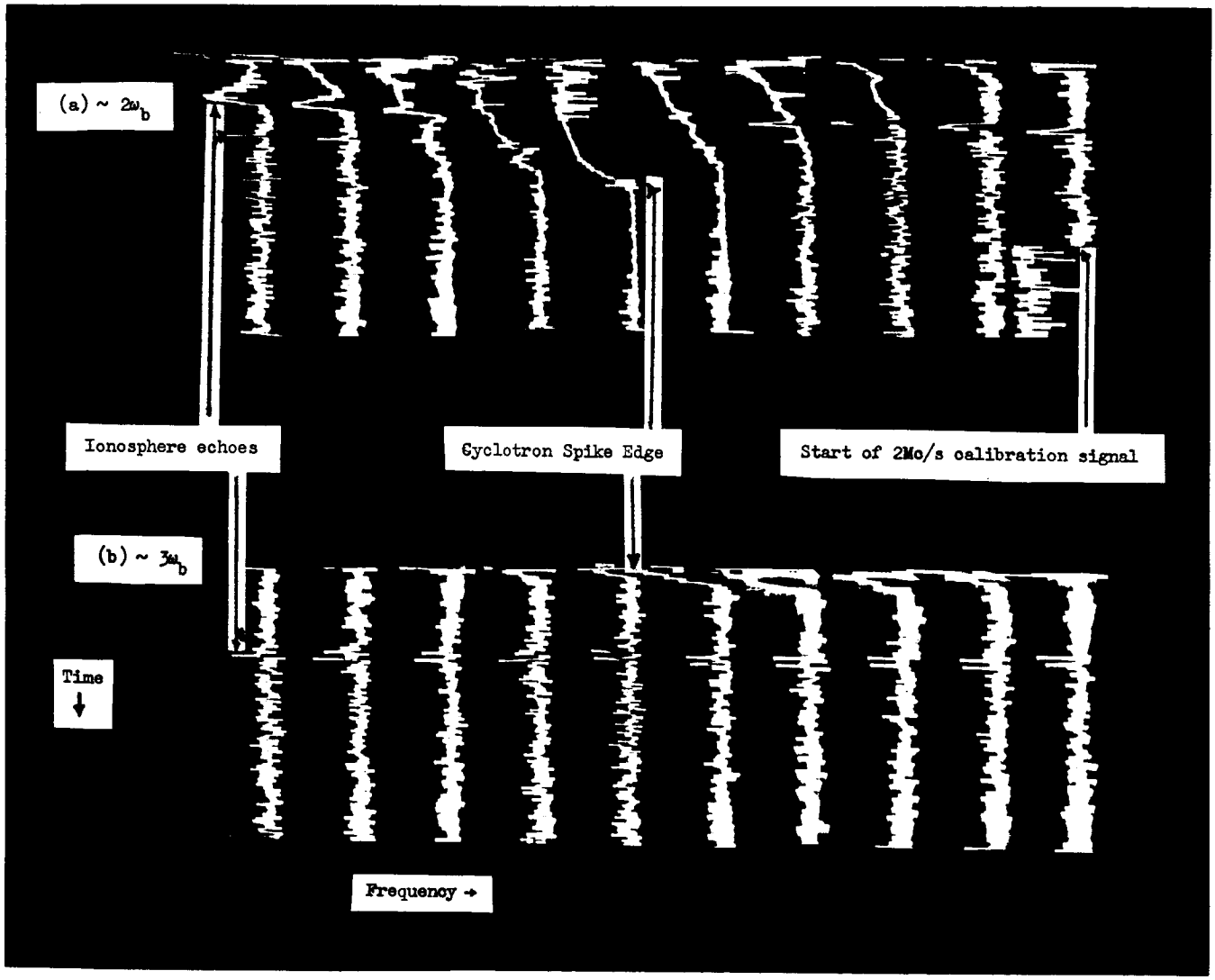

Fig. 2 Selected A (line) scans (67m sec long, ~ 15kc uniform shift/line) from Fig. 1, (a) across $2\omega_b$ and (b) across $3\omega_b$.

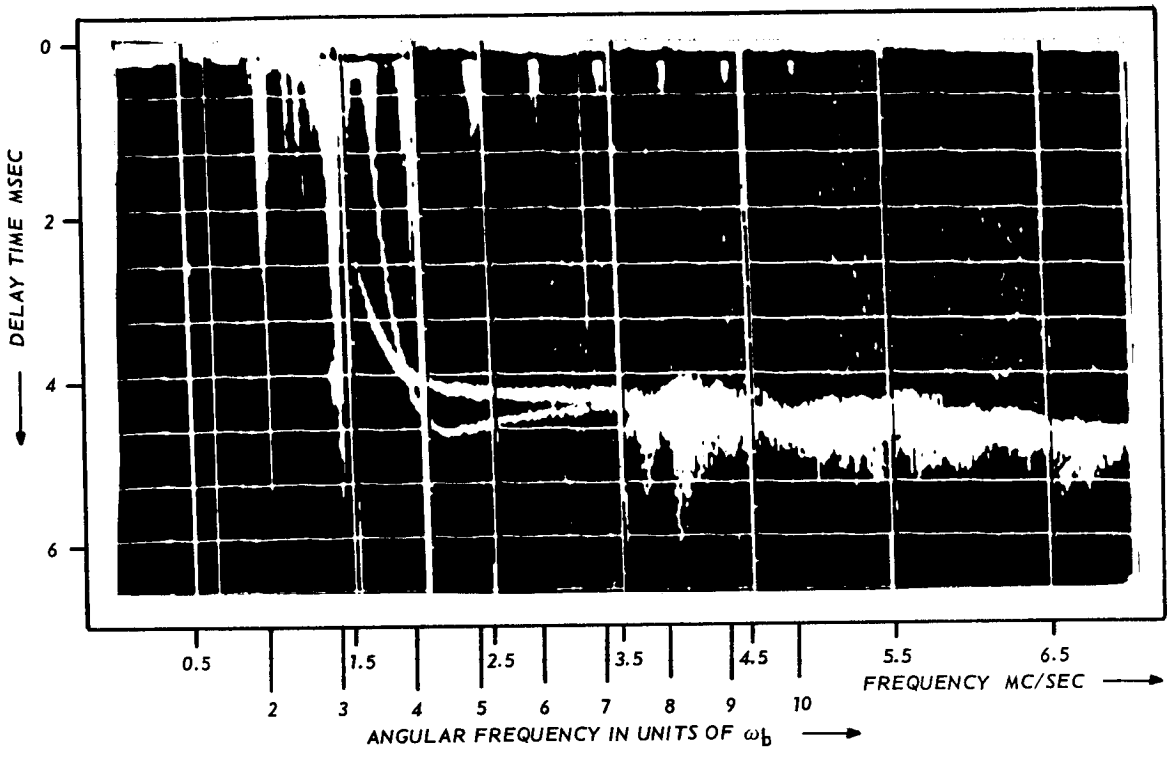

Figure 3: Alouette ionograms taken above Quito, Ecuador on October 7, 1962 at 13.46.58 U.T.

Following this concept Fejer and Calvert (1964) assembled the results of many ionograms and plotted the average (over one to three dozen results) duration in cycles of resonances as a function of ω_p/ω_b for the lowest four cyclotron harmonics. These results are reproduced in Fig. 4 with the theoretical curves of Fejer and Calvert removed to let the data stand alone. The values for $n\omega_b = \omega_R$ and $n\omega_b = \omega_p$ have been inserted where relevant.

Without any preconceived theory, what significant features can be discerned? The duration of resonance is typically 10^3 to 10^4

n = 4, Fig. 4(4). The fourth cyclotron harmonic is too high to show interesting effects since it is apparently always above ω_R.

n = 1, Fig. 4(1) - The fundamental is nearly always in the range .5 to 1 Mc (see Calvert and Goe) and hence is near the lower limit of the receiver response. The apparent drop as ω_b approaches ω_p should be viewed with suspicion unless corrected for receiver response.

n = 2, Fig. 4(2) - The second harmonic duration data shows no strong features but a tendency to decrease somewhat when $2\omega_b$ is less than ω_p. Perhaps there is an indication of an increase when $\omega_b \approx \omega_p$, but this, if genuine, is probably a non-linearity on ω_b just as the $2\omega_T$ resonance is associated with ω_T non-linearity.

n = 3, Fig. 4(3) - The third harmonic shows an interesting marked decrease in the vicinity of $3\omega_b = \omega_p$.

These would seem to be the major conclusions to be drawn from this data. These points and those obtained from Lockwood and Hagg (above) are the general features which should guide the theoretician in the choice amongst the many possibilities of cyclotron harmonic phenomena.

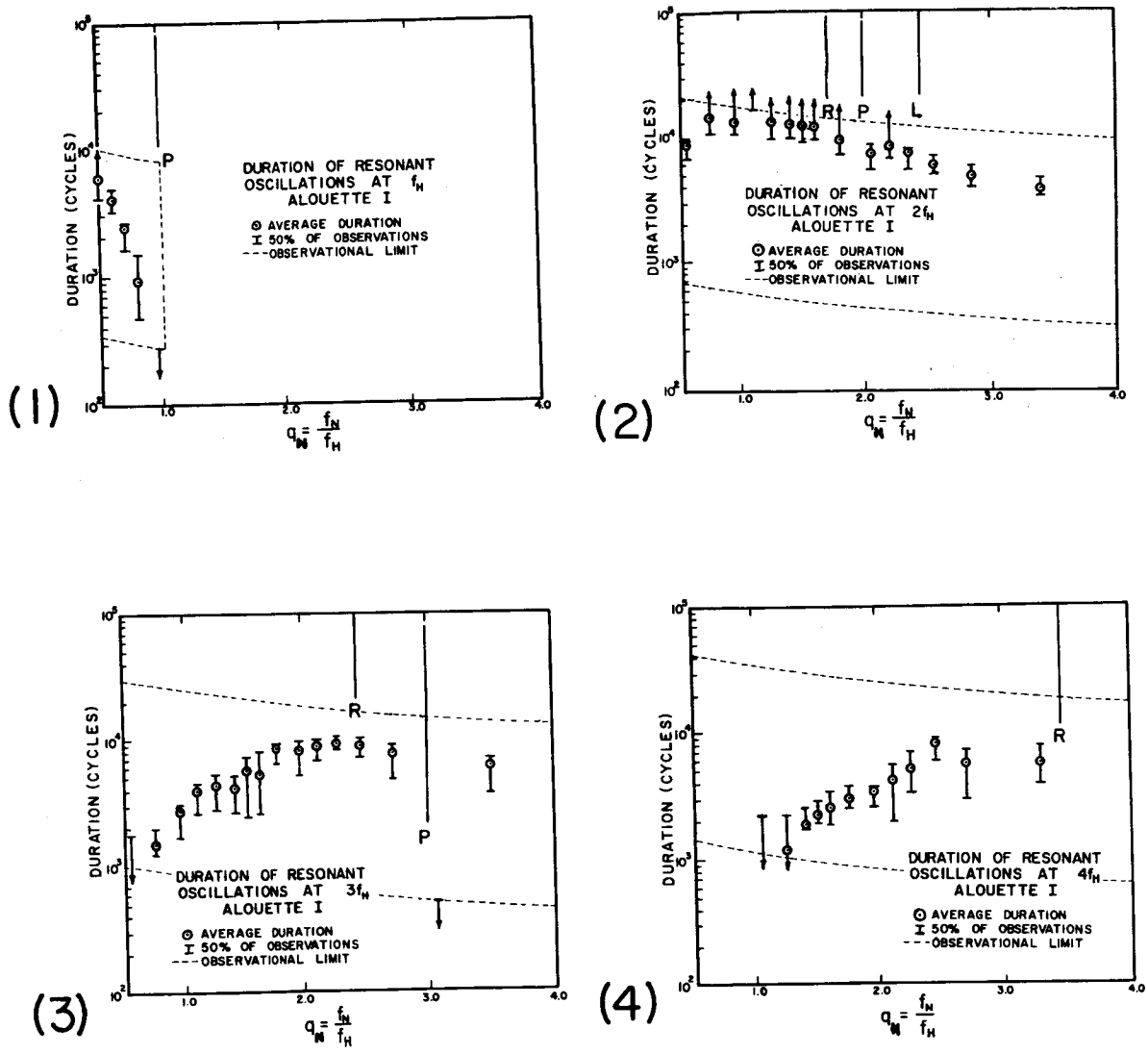

Fig. 4. These cyclotron harmonic observational results are from Fejer and Calvert (1964) Fig. 4. Their theoretical curves have been removed and relevant frequency conditions - $n\omega_b$ equals ω_R, ω_p, ω_L - have been indicated by R,P,L respectively. In their notation f_H and f_N are the cyclotron and plasma frequencies $\omega_b/2\pi$ and $\omega_p/2\pi$. According to Fejer and Calvert the data points represent the results of averaging one to three dozen observations.

There appears to be a strong ω_p effect in (1), (3) but not in (2), while for (4) the ω_b/ω_p ratio is never small enough for $4\omega_b$ to approach ω_p.

In order to verify some points from the theory, typical ionograms for $n\omega_b \approx \omega_R$ and $n\omega_b \approx \omega_p$ were felt to be worth investigation. The first condition could be met with ionograms already in our possession, made available to us by Dr. R. Barrington of the Canadian Defence Research Telecommunications Establishment near Ottawa. Ionograms for the second condition were not in our possession and were not available in time for this report although they should be in our hands in due course.

The $\omega_R \approx n\omega_b$ situation is exemplified in Fig. 5 for n = 3, n = 2, where 1.0 - 1.5 Mc sections of ionograms are shown and indicate that coincidence of ω_R and $n\omega_b$ has no noticeable effect - a particular case confirming what can be deduced from the Fejer-Calvert presentation.

Results from Data Analysis

Let us summarize these briefly.

(1) The cyclotron harmonic ringing lasts typically for 10^3 to 10^4 cycles (Fejer-Calvert).

(2) The maximum effect is obtained for a frequency which agrees with the earth based calculations to 1 %, the accuracy of the calculations (Hagg). The Doppler shift, if any, is evidently small.

(3) The only pronounced effect from the duration vs ω_p/ω_b data is a deep minimum for the $3\omega_b$ resonance when $3\omega_b = \omega_p$ (Fejer-Calvert Fig. 4, our Fig. 4(3)). There appears to be no effect at ω_R in any of the possible cases (n = 2, n = 3).

(4) The favoured orientation for cyclotron harmonic resonance is when the antenna is oriented along the magnetic field (Lockwood (1965)).

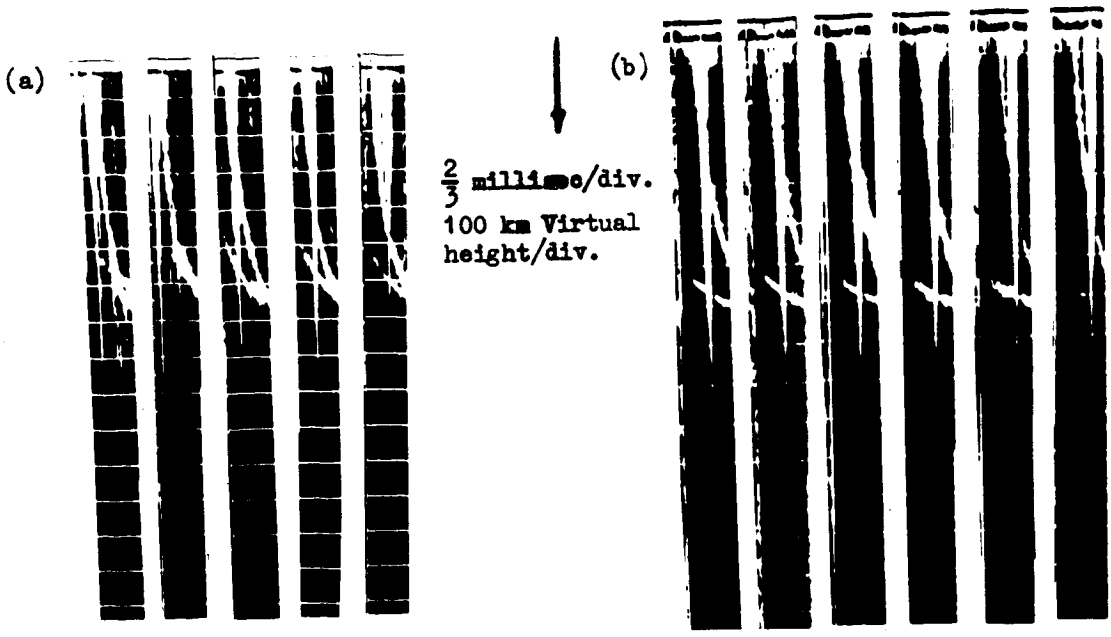

Fig. 5. Ionograms extracts (between 1 and 1.5 Mc) showing the lack of effect of $n\omega_b$ near to ω_R for (a) $3\omega_b$ (b) $2\omega_b$. The ionogram references for (a) and (b) are from left to right:

(a) October 7, 1962, Quito (Station 7) Day 280 U.T. 13 hours and 50:04, 50:41, 51:55, 52:32 (alternate ionograms)(46:58 was used by Johnston and Nuttall(1964)).

(b) October 2, 1962, Ottawa (Station 3) Day 275 U.T. 14 hours and 26:08, 26:26, 26:45, 27:03, 27:22, 27:59.

Ionograms courtesy Canadian Defence Research and Telecommunications Establishment, Ottawa.

II. THEORY WITHOUT MATHEMATICS

The mathematical analysis presented in parts 1,2 and 3 is forbidding in appearance and is not likely to be assimilated in one or two readings. It seems useful, therefore, to give an outline of the philosophy and ideas involved and the results obtained without going through the mathematical manipulations, without even giving the equations, only the formulas for the results.

The basic problem was to explain the Alouette results.

Basic Concept

At the time this work began we were closely connected with Nuttall's work on the parallel plasma frequency resonance (ω_p) and the perpendicular transverse frequency resonance (ω_T)(ω_Δ in Nuttall's notation) since published Nuttall (1965).

The basic concept (borrowed from fundamental particle dispersion theory) was that singular behaviour would result from the coalescing of two dispersion equation solutions in such a manner that a certain integral line was "pinched" between the associated poles (see Nuttall (1965) and references after Part 3).

This degeneracy condition can usually be linked to the concept of a wave whose group velocity in some appropriate frame of reference is zero.

In the Alouette case the logical frame of reference is that of the satellite. The concept is one of a plasma wave packet which is set up by the sounder pulse and which then travels with the satellite (group velocity = satellite velocity). This wave packet then slowly decays because of higher-order dispersion effects. When the wave

packet or (group) velocity is not equal to the satellite velocity the packet would move quickly away from the satellite and become undetectable.

The concept of zero group velocity (usually the satellite motion is ignored) has been employed by all the serious analysts of the problem. This group-velocity criterion gives the observed resonance frequencies except for $2\omega_T$ (a non-linear effect) and ω_R and ω_L which are singular but give no resonance in most cases.

The next point is the close agreement between the cyclotron harmonic resonances and the exact multiples of the gyro frequency. This satellite velocity is considerably smaller (1/16) than the electron thermal velocity but nonetheless the observations indicate that the perpendicular and parallel wave numbers must be less than 6 m^{-1} and 2 m^{-1} respectively, the wavelengths being greater than .16 m and .5 m. Thus our attention is focussed on small but non-zero wave numbers. The wave numbers cannot in any case be exactly zero because of satellite motion.

We are thus led to examine solutions for the plasma dispersion equation which are very near $n\omega_b$, which give group velocities equal to the satellite velocity and have small wave numbers compared with the thermal wave numbers $(n\omega_b/v_t)$. To obtain the dispersion equation the plasma dielectric coefficient must be known.

Dielectric Coefficient (Part 1)

The plasma dielectric coefficient to use is evidently the one derived from the Vlasov equation as indicated in the introduction since collisions are known to be utterly negligible in the cases of interest. At first (progress reports July - October, 1964) the

nonrelativistic equations were used and satellite motion was ignored. Later (progress reports November, December 1964) it was realized that the nonrelativistic equation was invalid very close to $n\omega_b$ and that relativistic analysis must be used.

Part 1 of this report was therefore devoted to the exposition of both the relativistic and nonrelativistic dielectric coefficients.

When not very near the cyclotron harmonics the differences are completely negligible for a plasma which has kinetic energy for less than the rest energy ($kT << mc^2$ $kT/mc^2 \sim 2.5 \times 10^{-7}$ for the Alouette).

The relativistic cyclotron harmonic terms for small $k_\perp$ contribute poles in nonrelativistic theory and branch points with large discontinuities at the average relativistic cyclotron harmonic, which is very slightly (50 kT/mc^2 %) below the rest-mass cyclotron harmonic frequency. The difference may appear to be small but gives dispersion equation results which differ in two important features from those of nonrelativistic dispersion theory.

Dispersion Equations (Part 2)

As indicated in the Introduction this report, the dispersion equation and other parts of the Laplace-transformed Green's function need to be calculated to obtain the electric field. Since the relativistic and nonrelativistic dielectric coefficients differ only very near the cyclotron harmonics it is only there that dispersion equations differ. The dispersion equation results have been obtained and discussed in Part 2. The relativistic and nonrelativistic results differ qualitatively in two important respects:

(1) A nonrelativistic feature which gave one wave very close to the cyclotron harmonic frequency proves to be spurious and vanishes in the relativistic analysis. A typical change ie shown in Fig. 6.

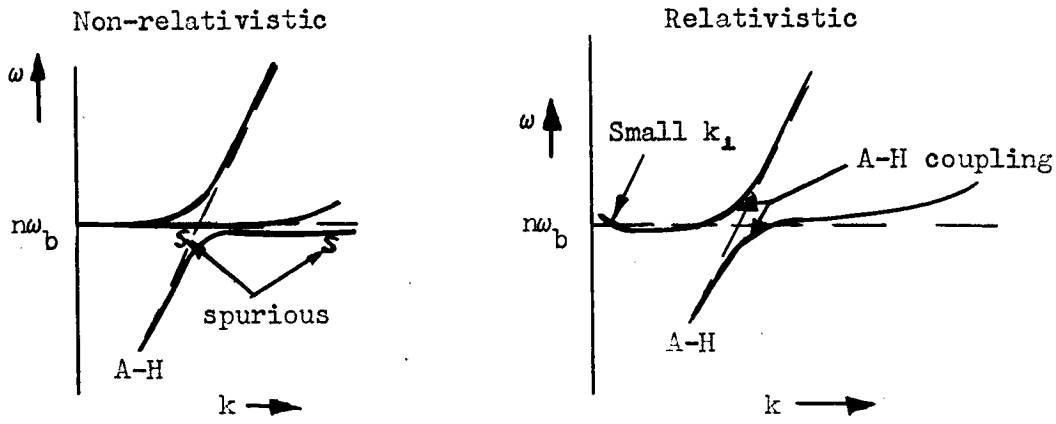

Fig. 6 - Disappearance of spurious wave (s).

(2) The relativistic dispersion solution for the cyclotron harmonic very near zero wave number increases in frequency while the nonrelativistic solution goes right to zero wave number (see Fig. 7)

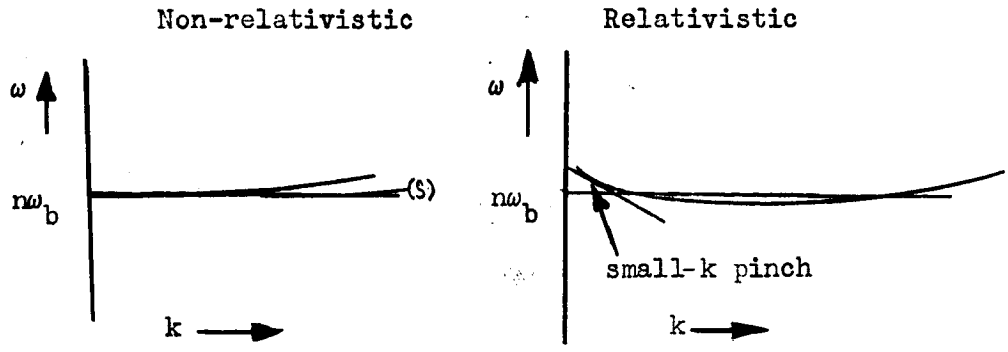

Fig. 7 - Change in behaviour for small wave numbers.

The first feature eliminates a spurious wave from consideration (the wave had already given peculiar results in the nonrelativistic analysis).

The second feature is interesting since it now becomes possible to match perpendicular group and satellite velocity for small wave number.

Selection of Dispersion Regions

As indicated earlier the small Doppler shift indicates a modest value of wave number. We wish to match the group and satellite velocities. One possibility is that indicated in Fig. 7. Another possibility is the region where the cyclotron harmonic solution couples to the Appleton-Hartree solution, as sketched in Fig. 8.

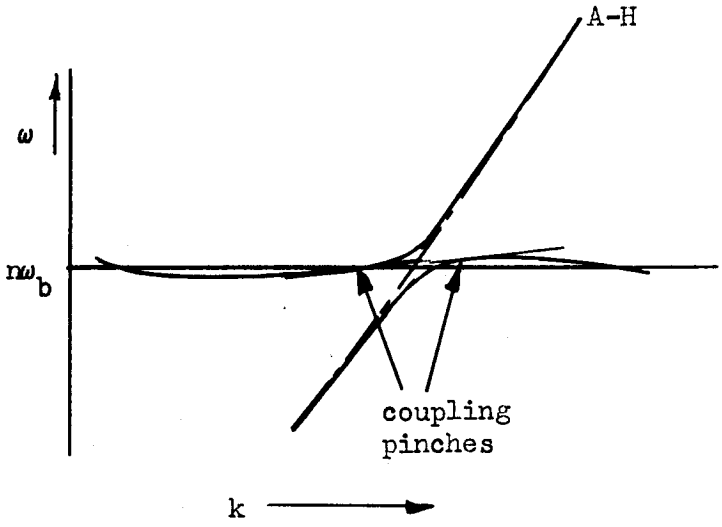

Fig. 8 - Appleton-Hartree and cyclotron harmonic coupling pinches.

There are two possibilities for each Appleton-Hartree solution, four in all. These would disappear with increasing ω_p/ω_b as $n\omega_b$ becomes less than the relevant cut-off frequency, ω_R, or ω_p. (Note that ω_L applies instead of ω_R if $n\omega_b$ is less than ω_T and greater than ω_L.)

The collected results of Fejer and Calvert (1964) show no such frequency cut-off, only a dip in the $3\omega_b$ case at ω_p. Hence it seemed that these cyclotron harmonic resonance and Appleton-Hartree wave coupling possibilities did not fit the observations and so they were not pursued further. Last-minute corrections on the numerical work showed that the small-k signal was undetectable and so, in spite of appearances, the coupled resonances must be considered as prime targets for analysis.

Time Behaviour and Numerical Result

Having decided to concentrate on the dispersion equation behaviour near zero wave number the calculation in Part 3 was essentially only mathematical technique. It involved the mathematical concept of k-poles pinching the integration line and expansion around the singular region.

The final result from Part 3 (Eq. 30 and Eq. 36) proves to be very much the same, at least superficially, for both the resonances both extraordinary (electron resonant circularly polarized) and ordinary (polarized parallel to the magnetic field).

After the correct galactic noise temperature was inserted at the eleventh hour, the field proved to be too small by a factor of 100 to fit the observations.

The mathematical technique must therefore be applied to the other pinch points in future work.

There is a possibility that the parallel resonance might be more effective when one considers the wave number required. This demands a very much lower value of parallel than perpendicular wave number, i.e. the most gentle variation along the magnetic field.

Examination of the infinitesimal dipole field shows that the most gradual variation occurs when one moves parallel to the dipole line. Hence one might expect the dipole parallel to the magnetic field to give the most excitation. Apparently this does not seem to emerge naturally from the analysis but appearances may be deceptive. Finite antenna size may be important here.

III. COMPARISON OF THEORY WITH EXPERIMENT

The observations seem to point in three different ways, two positive and one negative, to the ordinary or parallel cyclotron resonance rather than to the other. These points are as follows:

(1) According to Lockwood (1965) the favoured antenna orientation is that with the element along the magnetic field. This fits the orientation of the infinitesimal dipole model for ordinary resonance and is opposite to the orientation for extraordinary resonance.

(2) As shown in Fig. 4(3) the Fejer-Calvert data show an ω_p dip consistant with a $K_{\parallel}$ effect in the ordinary resonance formula. Ionograms should soon be forthcoming to check this point further.

(3) As shown in Fig. 4(2),(3),(5) there appears to be no ω_R effect at least for the second and third harmonics. This is confirmed and exemplified by the ionogram extracts of Fig. 5.

Parallel or Ordinary Cyclotron Harmonic Resonance

In view of our conclusions on the importance of parallel resonance, some remarks on the basic concept are in order. (The basic picture for perpendicular effect has already been described by Lockwood (1963) and Johnston and Nuttall (1964). The parallel effect basic concept has not been discussed, but it is equally easy to visualize.

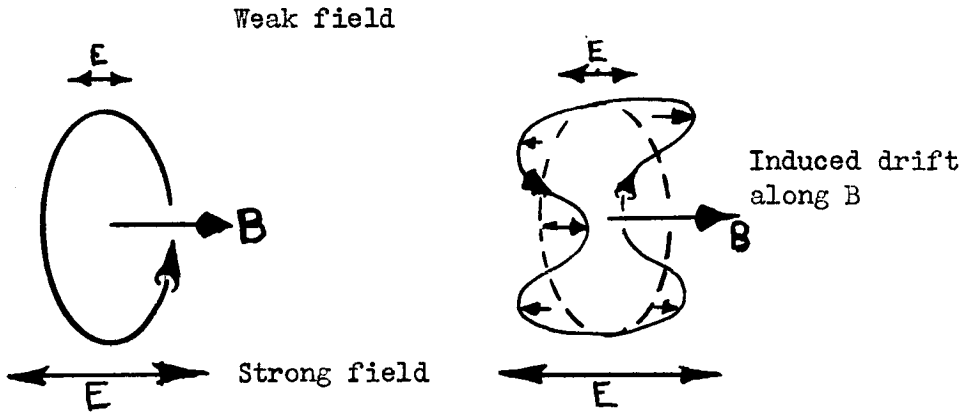

Figure 9. Parallel cyclotron harmonic excitation effect on electron ring systems orbiting around a common central magnetic field line.

We consider a ring of electrons of the same velocity magnitude circulating around a common magnetic field line and drifting along it. If the electric field parallel to the magnetic field varies in a direction across the magnetic field, the electrons in the ring will be given different rf velocities at different positions around the ring. If the radio frequency is a cyclotron harmonic, the effect of the non-uniformity will not average out in time and will be cumulative. The effect will be that our ring will begin to stretch along the magnetic field lines due to the acceleration. The effect will alternate around the ring, the number of cycles being equal to the frequency harmonic number ($\omega/\omega_b = n$). If the excitation is non-uniform (i.e. $\partial^2 E/\partial x^2$ is not zero) then there will be a net current at $n\omega_b$.

Before the analysis was well under way some qualitative reasoning had been carried out (given in the June progress report) on the question of perpendicular and parallel resonance. This is reproduced below as it is not without interest.

If we consider the case observed to be favourable to cyclotron harmonic ringing of parallel orientation (antenna parallel to the magnetic field), the excitation decays by flow of electrons along the magnetic field lines. The electrons travel at an average velocity of 2×10^5 meters/sec and so can travel the antenna length (~ 10 or 20 meters) in times of the order of 50 μsec or 100 μsec. Hence the excitation of both antenna elements should be well mixed by the time receiver observations are begun, one hundred microseconds after the exciting pulse ends. Hence we are forced to the conclusion that the in-phase or symmetric E_z excitation parallel to the magnetic field is much more likely to persist and the antiphase, antisymmetric E_r effects perpendicular to the magnetic field are likely to be rapidly mixed and cancelled. Only if E_r effects are initially far stronger than E_z are they likely to be observed in the late decay.

When the antenna is across the magnetic field then the even excitation comes from the E_z field, which is now perpendicular to the magnetic field, and from the component of E_r which is also perpendicular to the magnetic field, so that the excitation would be predominantly perpendicular. Since cyclotron harmonic effects are not observed when the antenna is across the magnetic field it seems that perpendicular excitation is not effective.

Let us look at the effectiveness of the excited decaying current and charge in inducing a signal on the antenna.

Parallel excitation gives a cylindrical current system with axis more or less along the antenna and current parallel to the cylinder axis. This is very effective in inducing current in the antenna.

By contrast, the radial current from the charge excitation due to the perpendicular electric field only induces antenna effects to the extent it is non-uniform.

Thus, from the consideration of antenna field parity, electron flow along magnetic field lines and the Alouette antenna orientation effect on cyclotron harmonic signals, we are led to the following conclusion. The dominant cyclotron harmonic mechanism due to non-uniform antenna field is due to the electric field component along the magnetic field lines. For the favourable parallel and near-parallel orientation this can be thought of as the induction electric field (E_z) of the antenna current rather than the electrostatic field of the antenna charge.

From this reasoning we feel that if it becomes necessary for reasons of time, computer cost, etc., to concentrate on one aspect, then the parallel excitation is the mechanism on which to concentrate."

IV. SUMMARY

The theory as developed in this report and the available observations point slightly but definitely to the excitation of an ordinary wave cyclotron harmonic where it couples to the ordinary Appleton Hartree wave as the basic cyclotron harmonic phenomenon in the Alouette records.

It is not theoretically well established that this mechanism is dominant. More work should be done to clear this point up, of the kind that showed the small-k pinch could be ignored.

V. FUTURE WORK

The problem and the results are not yet in as clear and as definite form as is desirable. Much analysis has been accomplished yet more should be done to clear up the situation further and give more definite results. Additional data analysis and theory are required. The main lines which suggest themselves are as follows:

Observations

More Alouette and S-48 data should be analyzed: the S-48 for modulation and orientation effects (but unfortunately cyclotron harmonic effects only occur if the fixed frequency coincides with a cyclotron harmonic) and the Alouette for the effects of variation of frequency and electron density, not to mention comparison between resonances of different harmonic number. Points to check are: details of critical frequency behaviour $n\omega_b \approx \omega_p$, ω_R, ω_T; the form of the time variation including AGC; orientation; and form of roll and any other modulation.

Theory

The coupled pinches of Fig. 8 should be investigated immediately and intensively to obtain $E(t)$ for them. The mechanism for the behaviour of the three lowest harmonics for high densities should be studied carefully particularly when they are comparable with ω_L, ω_p, ω_T or ω_R.

REFERENCES

Calvert, W., G.B. Goe (1963) - J. Geophys. Res. 68 6113 (1963).

Fejer, J.A., W. Calvert (1964) - J. Geophys. Res. 64 5049 (1964).

Franklin, C.A., R.J. Bibby, R.F. Sturrock, D.F. Page (1963) - Inst. Elect. Electron. Engrs. Convention Record 1963.

Hagg, E.L. (1963) - Congress of Can. Assoc. of Physicists, (June 1963) Paper 5.12, abstracted in Physics in Canada 19, No. 3 (Addenda).

Johnston, T.W., J. Nuttall (1964) - J. Geophys. Res. 69, 2305 (1964).

Lockwood, G.E.K. (1963) - Can. J. Phys. 41 190 (1963), (1965) Can. J. Phys. 43, 291 (1965).

Molozzi, A.R. - COSPAR Symp. Warsaw (June 4, 1963).

Warren, E.S. (1963) - Nature 197 636 (1963).

APPENDIX

CRITIQUE OF THE THEORETICAL WORK ON TOPSIDE SOUNDER RESONANCES

Theories of resonances can be called either identification theories when the observed resonant frequencies are correlated with characteristic calculated frequencies or behaviour theories if an attempt is made to calculate such features as damping, frequency widths and other effects. "Identification" is far easier than "behaviour!!

Identification

In the case of the Alouette resonances, one set were easily identified immediately as cyclotron harmonics by Lockwood (1963). Lockwood attempted to identify other plasma resonances but chose incorrectly and it was left to Calvert and Goe (1963) to identify the other plasma resonances as the plasma frequency ($\omega_p \sim X = 1$) the transverse plasma resonance ω_T (upper hybrid or Pythagoras frequency $\sqrt{\omega_p^2 + \omega_b}$, $\sim X = 1 - Y^2$) and often its second harmonic ($2\omega_T$).

Johnston (1964) and independently Wallis (1965) also noted that, from the Calvert and Goe results, the $2\omega_T$ resonance could only appear for $\omega_T < 2\omega_b$. This was confirmed by Calvert (1964) after further study of a large number of cases.

Behaviour

The various frequencies associated with the Alouette resonances appear as characteristic frequencies for the Vlasov plasma

dispersion equation and its two main simplifications viz. simple cold plasma electromagnetic (Appleton-Hartree) theory and warm (Vlasov) plasma simple electrostatic theory.

Cold Plasma Appleton-Hartree Theory

In cold plasmas $\frac{\underset{\sim}{k}\cdot}{\omega}\frac{\partial\omega}{\partial\underset{\sim}{k}}$ goes to zero and $k\to\infty$ (where the equations are not valid) for frequencies $\omega_{\theta\pm}$ which satisfy the following equation.

$$\omega^2_{\theta\pm} = \tfrac{1}{2}\left[\omega_T{}^2 \pm (\omega_T{}^4 - 4\omega_p{}^2\omega_b{}^2\cos^2\theta)^{\frac{1}{2}}\right]$$

However, as Sturrock (1961) pointed out in connection with radio bursts from the sun, $\partial\omega/\partial\underset{\sim}{k}$ itself only goes to zero for $\theta = 0$ and $\pi/2$ i.e. $\omega = \omega_p$ and $\omega = \omega_T$. The behaviour at ω_p is degenerate for all $k_\parallel$ ($k_\parallel = 0, \infty$ and $(\omega_p/c)(\omega_b/(\omega_p+\omega_b))^{\frac{1}{2}}$ in particular) and can only be disentangled with a warm plasma to remove the degeneracy.

Cyclotron harmonics do not appear.

Vlasov Plasma Electrostatic Theory

Using the Vlasov equation with the velocity of light set equal to infinity (i.e $\underset{\sim}{k} >> \omega/c$) one obtains the Vlasov electrostatic dispersion equation which gives $\omega_{\theta\pm}$ as $|k| \to 0$ (where the electrostatic approximation is generally invalid) for fixed θ. The cyclotron harmonic harmonic frequencies are the $k_\parallel = 0$, $k_\perp \to 0$, $k_\perp \to \infty$ limits of perpendicular cyclotron modes.

Vlasov Plasma Electromagnetic Theory

In this, the most general collisionless uniform plasma theory, ω_p behaviour is no longer degenerate because electron random motion is now considered. Satellite motion may well be important. The ω_T resonance is associated with a real ($\partial\omega/\partial\underset{\sim}{k} = 0$, for real $\underset{\sim}{k},\omega$) pinch for $\omega_T < 2\omega_b$ and with a complex pinch for $\omega_T > 2\omega_b$, for zero $k_\parallel$ finite $k_\perp$ of order $\omega_T/\sqrt{v_t c}$. The cyclotron harmonic behaviour is in evidence for $k_\perp = 0$, $k_\perp \to \infty$ and for finite $k_\perp$ where an Appleton-Hartree solution would exist.

Neither cold plasma electromagnetic theory nor Vlasov plasma electrostatic theory is valid at the ω_T resonance since the resonance occurs outside the limits of their validity ($k \ll \omega/v_t$, $k \gg \omega/c$ respectively). One must in general use the full Vlasov plasma theory with the electromagnetic theory to get useful results.

Very near $n\omega_b$ and particularly as $k \to 0$ the relativistic Vlasov equation must be used.

To date, besides the connected work of Nuttall, Johnston and Shkarofsky there are three other papers or reports which attempt to come to grips with the behaviour of the Alouette resonances.

Two of these have been published. These are the work of Fejer and Calvert (1964) and of Sturrock (1965). Both are alike in that they begin with the electrostatic nonrelativistic Vlasov plasma dispersion equation.

The third report has just come to hand. It is the work of Dougherty and Monaghan (1964) of Cambridge. The spirit of this last

work is the same as that of Nuttall, Shkarofsky and Johnston and they agree as far as they have gone. They reach the same conclusions as we do as to the form of the nonrelativistic dispersion equation and discuss likely pinches but have gone no further. We have no criticism of the work as it stands except to say that we agree with it as far as it goes but that it is a beginning only and that relativity is important very near $n\omega_b$.

Let us return to the Vlasov electrostatic analyses of Sturrock and of Fejer and Calvert. The focus of these is on $\underset{\sim}{k} \to 0$, i.e. on what might be called electrostatic cut-offs.

The first and most serious criticism is directed at the use of the electrostatic approximation ($\underset{\sim}{E} = -\underset{\sim}{\nabla}\phi$) near cut-offs.

In the electrostatic approximation the field is linearly polarized along $\underset{\sim}{k}$, and only the highest terms in k are kept in the dispersion equation, which becomes

$$\underset{\approx}{K} : \underset{\sim}{n}\underset{\sim}{n} = 0$$

where $\underset{\sim}{n} \equiv \underset{\sim}{k}c/\omega$ is the refractive index vector and $\underset{\approx}{K}$ is the relative dielectric tensor. This is a near-resonance condition ($n \to \infty$).

The near-cut-off condition is an expansion in n around the cut-off condition.

$$|\underset{\approx}{K}| = 0$$

In general (in contrast with the longitudinal polarizational parallel to $\underset{\sim}{k}$ in resonance) there are parallel cut-offs when the electric field

is linearly polarized along the magnetic field and there are perpendicular cut-offs when the electric field is circularly polarized in a plane perpendicular to the magnetic field.

In general the behaviour of the electrostatic solutions near n = 0 differs markedly from the nonrelativistic electromagnetic near-cut-off solutions (see Figs. 1 - 3 of Dnestrovskii and Kostomarov (1963)). Hence the electrostatic equations cannot be expected to produce correct results for small n. For sufficiently large n the electrostatic solution is adequate and has been successfully used by Crawford, Kino and Weiss (1964) in calculating the displaced cyclotron harmonic frequency.

Nuttall,(1965) in his work, took particular pains to treat ω_N and ω_T phenomena properly. We are pursuing the same course for the cyclotron harmonics.

The common serious criticism of these two analyses is that they rest on the electrostatic dispersion equation applied where it is invalid and gives incorrect results.

Apart from this fundamental objection (which might be removed if the correct dispersion equation were employed) there are other objections as well, but they are different for the two treatments.

Sturrock

The ω_R, ω_L electromagnetic effects are properly based on the cold electromagnetic equations and seem adequate although limited to an infinite-impedance infinitesimal dipole. (On the other hand Dougherty and Monaghan (1964) come to the conclusion that, although there is a dispersion singularity, the associated field is not singular so the spike is unlikely to be observed.)

The other results are incorrectly based on the electrostatic formulation.

Apart from the dispersion equation used there are still points to question in the procedure.

The plasma (ω_p) and transverse (ω_T) resonance frequencies do not emerge correctly, since the value for ω as $n \to 0$ for a given θ is $\omega_{\theta+}$ which is between $\omega_T = (\omega_p^2 + \omega_b^2)^{\frac{1}{2}}$ and the higher of ω_b or ω_p, viz:

$$\omega_{\theta+} = \left[\frac{\omega_T^2}{2}\left(\frac{\omega_T^4}{4} - \omega_p^2\omega_b^2\cos\theta\right)^{\frac{1}{2}}\right]^{\frac{1}{2}}$$

This is the function that should enter the θ integration. The results obtained may be justified as approximations but this requires some demonstration or discussion since the change in $\omega_{\theta+}$ with θ is not small. The ω_T result is for a <u>non-zero</u> k as shown by Nuttall. Nuttall's (1965) ω_p result for k = 0 gives a Green's function of $-i(\omega^2 - \omega_p^2)^{\frac{1}{2}}/4\sqrt{3}\, v_t c^2$ or an asymptotic time dependence $e^{i\omega_p t}/v_t c^2(\omega_p t)^{3/2}$ as compared with Sturrock's (1965) $e^{i\omega_p t}/v_t^3(\omega_p t)^{5/2}$. For, say 10^3 cycles This is a difference of 10^3 from Sturrock's result. In the Alouette case the pinch occurs for $\partial\omega/\partial\underset{\sim}{k} = \underset{\sim}{V}$ so the k = o region is probably not involved. A pair of electrostatic - Appleton-Hartree coupling pinches with $k_n \approx \omega_p/c\ (\omega_b/(\omega_p \mp \omega_b))^{\frac{1}{2}}$ are the probable points of interest.

The cyclotron harmonic results using the incorrect (i.e. electrostatic) equation near $k \to 0$ give serious divergences unlike the the electromagnetic solution.

Using the Green's function for ω_p at least the asymptotic excitation is locally uniform, which seems to rule out Sturrock's conjecture that satellite motion might be a major course of signal reduction.

In view of the foregoing little reliance can be placed on the conclusions. Nonetheless the overall method of attack is well founded. The asymptotic time behaviour is deduced from certain integrals (A.7 to A.13) which, strictly speaking, do not converge.. The results can be justified for asymptotic behaviour but this should be done explicitly to avoid misleading readers.

Fejer-Calvert

The same objection to their quasi-static analysis applies as mentioned in connection with Sturrock's work. Instead of the more-or-less direct Fourier Laplace transform approach, Fejer and Calvert attempt to employ the concept of group velocity. The concept of a group velocity is only well defined when the characteristic spread in wave number Δk is much less than the wave numberk. Then one can say that the size of the wave packet is of the order of $2\pi/(\Delta k)$. When the group velocity tends to zero, as it does for cases of interest, the spreading becomes more a phenomenon of phase mixing or destructive interference rather than of group velocity. When the group velocity goes to zero, one is warned to re-examine the situation (see Brillouin, particularly Chapter 5, Sec. 4). It might be quite useful to discuss the dispersion of a wave packet, but this would be irrelevant to this critique. (See Part 3.)

So long as the group velocity is not nearly zero then the Fejer-Calvert argument of their Page 5055 applies and the time of passage of the wave packet measured in $\underset{\sim}{\Delta k}$ direction in ω periods is

$$T_\omega = \frac{\omega}{\underset{\sim}{\Delta k} \cdot \frac{\partial \omega}{\partial \underset{\sim}{k}}}$$

But for $\underset{\sim}{\Delta k}$ we should use $\underset{\sim}{\Delta k} = \Delta\omega \frac{\partial \underset{\sim}{k}}{\partial \omega}$

so we obtain $T_\omega = \frac{\omega}{\Delta\omega}$ as one expects.

When this formula is invalid (i.e. when $\partial\omega/\partial\underset{\sim}{k}$ goes to zero) then so is the use of group velocity. One must use higher derivative, but the general t^{-p} amplitude behaviour, obtained by Sturrock, Nuttall and ourselves, means that a natural time scale is not likely to be found.

Apart from the objections given above, the τ and θ_m expressions given in their Appendix diverge for $k \to 0$ and there seems no way of setting a lower limit on k nor do they suggest one. Unless the ad hoc assumption, that θ_m is the same finite constant for each resonance, can be justified, the comparisons between harmonics or between measurements in different conditions is meaningless.

Let us also discuss the useful experimental data presented by Fejer and Calvert.

Their Figs. 4a and 4b suggest that the $\omega_p\omega_H$ characteristics cannot be unambiguously ascertained with the present Alouette's low-frequency limitation.

The ω_T observations in Fig. 4c show a striking change when $\omega_T \gtrless 2\omega_H$ (i.e. $\omega_p \gtrless \sqrt{3}\omega_H$). (See Nuttall (1965a), also private communication to Calvert by Johnston.) The quasi-static theory should also show this (F-J Eq. 26) but apparently not as treated by Fejer and Calvert.

The $2\omega_H$, $3\omega_H$ data do not (except perhaps slightly for $2\omega_H$) show any violent effect at $n\omega_H = \omega_T$ ($\omega_N = \sqrt{n^2 - 1}\,\omega_H$) but nor do they at $n\omega_H = \omega_\pm$ ($\omega_N = \sqrt{n-1}\,\omega_H$) as predicted by the equivalent zero-k stationary frame nonrelativistic electromagnetic theory. There is an apparent effect in the $3\omega_H$ data when $3\omega_H = \omega_p$.

Apart from the useful data and the general heuristic value of the dispersion equation contours of their Fig. 3, the Fejer-Calvert approach cannot be said to be satisfactory.

CONCLUSION

For these reasons given above the electrostatic analyses discussed here cannot be considered successful or adequate and the problem still awaits a proper treatment.

The Sturrock paper has the better theory (although a little shaky) but is incorrectly based on electrostatic dispersion. It would be vastly improved using the correct dispersion equation. The Fejer-Calvert theory is quite inadequate but the review and observation data is quite useful.

The Dougherty-Monaghan approach is essentially the same as ours, but they have gone no further than a preliminary investigation of theory and give no results for time behaviour.

Wallis (1965) has really done no more than comment on the Calvert-Goe data and draw attention to the work of Dnestrovskii and Kostomarov.

REFERENCES

Brillouin, L. (1960) - "Wave Propagation and Group Velocity", Academic Press, New York.

Calvert, W., G.B. Goe (1963), J. Geophys. Res 68 6113 (1963).

Calvert, W. (1964) - (June 29 Letter to J. Nuttall, unpublished).

Crawford, F.W., G.S. Kino, H.H. Weiss (1964) - Phys. Rev. Letters 13 229 (1964)

Dnestrovskii, Yu N., D.P. Kostomarov (1961) - Soviet Physics JEPT 13 986 (1961), Soviet Physics JETP 14 1089 (1963).

Dougherty, J.P., J.J. Monoghan (1964) - "Theory of Resonances observed in the Ionosphere by Sounders Above the Ionosphere", Dept. Appl. Math., Theor. Phys. Univ. Cambridge, England submitted to Proc. Roy. Soc.

Fejer, J.A., W. Calvert (1964) - J. Geophys. Res. 69 5049 (1964).

Johnston, T.W. (1964) - (quoted in a letter from J. Nuttall to J.A. Fejer, February 1964).

Lockwood, G.E.K. (1963) - Can. J. Phys. 41 190 (1963).

Nuttall, J. (1965a) - Phys. Fluids 8 286 (1965).

(1965b) - J. Geophys. Res. 70 1119 (1965).

Shkarofsky, I.P., T.W. Johnston (1964) - Reports under NASA Contract NASw-957.

Sturrock, P.A. (1961) - Nature 192 58 (1961).

(1965) - Phys. Fluids 8, 88 (1965).

Wallis, G. (1965) - J. Geophys. Res. 70 1113 (1965).

OPTIONAL FORM NO. 10
MAY 1962 EDITION
GSA FPMR (41 CFR) 101-11.6

UNITED STATES GOVERNMENT

Memorandum

J. P. Heppner 612

TO : J. P. Heppner
Code 612

DATE: April 19, 1967

FROM : Don C. Hutchison, Chief
Technical Information Division

SUBJECT: NASW-957, "Satellite Cyclotron Harmonic Resonances," Report RCA-RR-7-801-35

The report listed on the attached form has been requested by the NASA Scientific and Technical Information Facility.

If it is appropriate to release this report, please sign the attached form and return to the Technical Information Division, Code 250, with two copies of the report.

Don C. Hutchison

Don C. Hutchison

Attachment

5010-108

Buy U.S. Savings Bonds Regularly on the Payroll Savings Plan